

**Sensing and data fusion opportunities for raw material characterisation in mining
Technology and data-driven approach**

Desta, F.S.

DOI

[10.4233/uuid:710856a6-4f0e-49f4-a9f2-b3b75cb72570](https://doi.org/10.4233/uuid:710856a6-4f0e-49f4-a9f2-b3b75cb72570)

Publication date

2021

Document Version

Final published version

Citation (APA)

Desta, F. S. (2021). *Sensing and data fusion opportunities for raw material characterisation in mining: Technology and data-driven approach*. [Dissertation (TU Delft), Delft University of Technology].
<https://doi.org/10.4233/uuid:710856a6-4f0e-49f4-a9f2-b3b75cb72570>

Important note

To cite this publication, please use the final published version (if applicable).
Please check the document version above.

Copyright

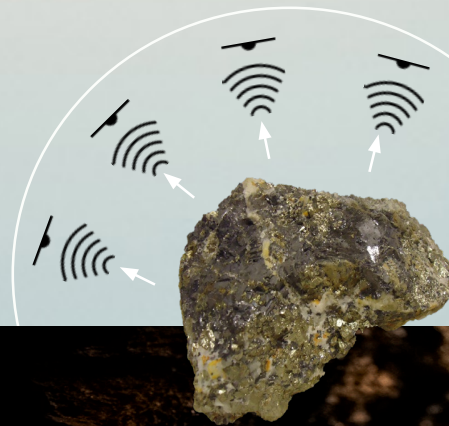
Other than for strictly personal use, it is not permitted to download, forward or distribute the text or part of it, without the consent of the author(s) and/or copyright holder(s), unless the work is under an open content license such as Creative Commons.

Takedown policy

Please contact us and provide details if you believe this document breaches copyrights.
We will remove access to the work immediately and investigate your claim.

SENSING AND DATA FUSION OPPORTUNITIES FOR RAW MATERIAL CHARACTERISATION IN MINING

Technology and data-driven approach



Feven Solomon Desta

SENSING AND DATA FUSION OPPORTUNITIES FOR RAW MATERIAL CHARACTERISATION IN MINING

TECHNOLOGY AND DATA-DRIVEN APPROACH

SENSING AND DATA FUSION OPPORTUNITIES FOR RAW MATERIAL CHARACTERISATION IN MINING

TECHNOLOGY AND DATA-DRIVEN APPROACH

Dissertation

for the purpose of obtaining the degree of doctor
at Delft University of Technology,
by the authority of the Rector Magnificus, Prof.dr.ir. T.H.J.J. van der Hagen,
chair of the Board for Doctorates,
to be defended publicly on
Tuesday 6 July 2021 at 10:00 o'clock

by

Feven Solomon DESTA

Master of Science in Geo-information Science and Earth Observation,
University of Twente, the Netherlands,
born in Arssi, Ethiopia

This dissertation has been approved by the promotor.

Composition of the doctoral committee:

Rector Magnificus,	chairperson
Dr. M.W.N. Buxton	Delft University of Technology, promotor
Prof.dr.ir. J.D. Jansen	Delft University of Technology, promotor

Independent members:

Prof.dr. G. Bertotti	Delft University of Technology
Prof.Dr.-Ing. J. Benndorf	Freiberg University of Mining and Technology, Germany
Prof.dr. P.C. Rem	Delft University of Technology
Dr. N. Zajzon	University of Miskolc, Hungary

Other members:

Dr. J.J. Jansen	Radboud University, the Netherlands
-----------------	-------------------------------------

This research was funded by the European Union's Horizon 2020 project "Real-Time Mining" (RTM), grant agreement No. 641989.

Copyright © 2021 by Feven Solomon Desta
All rights reserved.

Cover design by Feven Solomon Desta

The front and back covers show photographs of the Freiberg underground mine, Germany.

Photo credit: Frank Baldauf

Printed by ProefschriftMaken, the Netherlands
ISBN 978-94-6423-318-6

An electronic version of this dissertation is available at
<http://repository.tudelft.nl/>.

CONTENTS

CONTENTS	v
SUMMARY.....	xiii
SAMENVATTING	xv
LIST OF ABBREVIATIONS.....	xvii
PREAMBLE.....	1
INTRODUCTION.....	3
1.1. CONTEXT	4
1.2. RESEARCH HYPOTHESIS.....	7
1.3. RESEARCH OBJECTIVES.....	7
1.4. DISSERTATION STRUCTURE	10
REFERENCES.....	12
POTENTIAL APPLICATIONS FOR SENSOR TECHNOLOGIES FOR MATERIAL CHARACTERISATION IN MINING	15
2.1. OPPORTUNITIES FOR THE USE OF SENSORS IN MINING	16
2.2. USE OF SENSORS IN REAL-TIME MATERIAL CHARACTERISATION.....	18
2.3. POTENTIAL LOCATIONS FOR SENSORS IN MINING OPERATIONS.....	18
2.4. SENSOR-DERIVED DATA IN MINING.....	22
2.4.1. TYPES OF SENSOR DATA	22
2.4.2. DATA QUALITY PARAMETERS.....	24
2.4.3. KEY GEOLOGICAL ATTRIBUTES DERIVED FROM SENSOR DATA	24
REFERENCES.....	25
SENSOR TECHNOLOGY OPTIONS.....	27
3.1. INTRODUCTION.....	28
3.2. INFRARED SPECTROSCOPY.....	31
3.2.1. VISIBLE AND NEAR-INFRARED (VNIR).....	33
3.2.2. SHORT-WAVE INFRARED (SWIR).....	35
3.2.3. MID-WAVE INFRARED (MWIR)	36
3.2.4. LONG-WAVE INFRARED (LWIR).....	37
3.3. RAMAN SPECTROSCOPY	38
3.4. RGB IMAGING	40

CONTENTS

3.5. VALIDATION CHEMICAL ANALYSIS	41
3.5.1. X-RAY FLUORESCENCE (XRF)	41
3.5.2. INDUCTIVELY COUPLED PLASMA-MASS SPECTROMETRY (ICP-MS).....	41
3.5.3. X-RAY DIFFRACTION (XRD)	41
3.6. INSTRUMENTS USED IN THIS STUDY.....	42
REFERENCES.....	44
THE METHODOLOGICAL FRAMEWORK AND THE CASE STUDY SITE ...	51
MULTIVARIATE ANALYSIS TECHNIQUES AND DATA FUSION	53
4.1. INTRODUCTION.....	54
4.2. MULTIVARIATE ANALYSIS TECHNIQUES	54
4.2.1. PRINCIPAL COMPONENT ANALYSIS.....	56
4.2.2. K-MEANS.....	57
4.2.3. PARTIAL LEAST SQUARES REGRESSION (PLSR)	57
4.2.4. PARTIAL LEAST SQUARES – DISCRIMINANT ANALYSIS (PLS-DA)	58
4.2.5. PRINCIPAL COMPONENT REGRESSION (PCR)	58
4.2.6. SUPPORT VECTOR MACHINE (SVM)	58
4.2.7. SPECTRAL ANGLE MAPPER (SAM).....	59
4.2.8. MAXIMUM LIKELIHOOD	59
4.2.9. MINIMUM DISTANCE.....	60
4.3. EXPLORATORY DATA ANALYSIS.....	60
4.3.1. PATTERN RECOGNITION.....	60
4.3.2. OUTLIER DETECTION	60
4.4. DATA PRE-PROCESSING	61
4.5. DATA FUSION.....	62
4.5.1. LEVELS OF DATA FUSION.....	63
4.5.2. CONCEPTUAL FRAMEWORK	64
4.6. SOFTWARE AND PROGRAMS.....	67
REFERENCES.....	67
CASE STUDY SITE AND SAMPLE MATERIAL	73
5.1. INTRODUCTION.....	74
5.1.1. REGIONAL GEOLOGY	74
5.1.2. LOCAL GEOLOGY	75

5.2. TEST BLOCK AND SAMPLING STRATEGY.....	76
5.2.1. TYPES OF SAMPLES.....	79
5.2.2. GEOREFERENCING.....	82
5.2.3. SAMPLE PREPARATION.....	83
REFERENCES.....	86
APPLICABILITY OF THE INDIVIDUAL TECHNIQUES	87
RGB IMAGING FOR MINERALOGICAL FACE-MAPPING IN AN UNDERGROUND MINE.....	89
6.1. INTRODUCTION.....	90
6.2 DATA ACQUISITION.....	91
6.2.1. MINE FACE IMAGING.....	91
6.2.2. MUCK PILE IMAGING.....	92
6.3. METHODOLOGY.....	93
6.3.1. MINE FACE MAPPING.....	93
6.3.2. FRAGMENTATION ANALYSIS.....	95
6.4. RESULTS AND DISCUSSION.....	96
6.4.1. MINERAL MAPPING AND ORE-ZONE DELINEATION.....	96
6.4.2. FRAGMENTATION ANALYSIS.....	105
6.5. CONCLUSIONS	109
REFERENCES.....	110
VISIBLE-NEAR INFRARED AND SHORT-WAVE INFRARED HYPERSPSPECTRAL IMAGING FOR MATERIAL CHARACTERISATION IN A POLYMETALLIC SULPHIDE DEPOSIT	113
7.1. INTRODUCTION.....	114
7.2. INSTRUMENTATION AND DATA ACQUISITION.....	115
7.3. METHODOLOGY.....	115
7.3.1. PRE-PROCESSING	117
7.3.2. FEATURE EXTRACTION AND MAPPING	117
7.4. RESULTS AND DISCUSSION.....	118
7.4.1. MINERAL IDENTIFICATION USING VNIR.....	119
7.4.2. MINERAL IDENTIFICATION USING SWIR.....	121
7.4.3. COMPARISON OF THE VNIR AND SWIR DATA.....	124
7.5. CONCLUSIONS	126
REFERENCES.....	127

CONTENTS

MID-WAVE INFRARED AND LONG-WAVE INFRARED FOR SULPHIDE ORE DISCRIMINATION	129
8.1. INTRODUCTION.....	130
8.2. MATERIAL AND INSTRUMENTATION	131
8.2.1. MATERIAL.....	131
8.2.2. INSTRUMENTATION AND DATA ACQUISITION.....	131
8.2.3. CHEMICAL VALIDATION DATASETS.....	133
8.3. METHODOLOGY.....	133
8.3.1. DATA EXPLORATION.....	133
8.3.2. DATA PRE-PROCESSING.....	134
8.3.3. DATA MODELLING AND VALIDATION	136
8.4. RESULTS AND DISCUSSION	137
8.4.1 EXPLANATORY DATA ANALYSIS	137
8.4.2. DATA PRE-PROCESSING AND MODELLING	142
8.4.3. POTENTIAL APPLICATION FOR IN-SITU AND REAL-TIME MATERIAL CHARACTERISATION	145
8.5. CONCLUSIONS	145
REFERENCES.....	146
RAMAN SPECTROSCOPY FOR THE CHARACTERISATION OF A POLYMETALLIC SULPHIDE DEPOSIT	149
9.1. INTRODUCTION.....	150
9.2. METHODS.....	151
9.2.1. MATERIALS AND EXPERIMENTAL SETUP	153
9.2.2. IDENTIFICATION OF MINERALS	154
9.2.3. CLASSIFICATION OF MATERIALS.....	154
9.3. RESULTS AND DISCUSSION.....	155
9.3.1. INTERPRETATION OF RAMAN SPECTRA.....	155
9.3.2. SEPARATION OF ORE AND WASTE MATERIALS.....	160
9.4. CONCLUSIONS	163
REFERENCES.....	164
PERFORMANCE OF THE DATA FUSION APPROACHES	167
IMAGE AND POINT DATA FUSION FOR ORE–WASTE DISCRIMINATION	169
10.1. INTRODUCTION	170

10.2. DATASETS AND INSTRUMENTATION	171
10.3. METHODS.....	172
10.3.1. THEORETICAL CONCEPT FOR POSSIBLE IMAGE TO POINT DATA FUSION	173
10.3.2. IMAGE DATA CONVERSION	175
10.3.3. POINT SPECTRAL DATA PRE-PROCESSING.....	176
10.3.4. DATA MODELLING	177
10.3.5. DATA FUSION AND VALIDATION	178
10.4. RESULTS AND DISCUSSION.....	179
10.4.1. EXPLORATORY ANALYSIS	179
10.4.2. THE INDIVIDUAL DATA BLOCKS MODELS	180
10.4.3. FUSION OF THE VNIR AND SWIR DATA	183
10.4.4. IMAGE AND POINT DATA FUSION.....	185
10.4.5. THE OPPORTUNITIES AND LIMITATIONS OF THE APPROACH	188
10.5. CONCLUSIONS.....	190
REFERENCES.....	191
DATA FUSION FOR SEMI-QUANTITATIVE ANALYSIS OF MINERALS	193
11.1. INTRODUCTION	194
11.2. MATERIALS AND INSTRUMENTATION.....	195
11.2.1. MID-WAVE INFRARED AND LONG-WAVE INFRARED DATASETS.....	195
11.2.2. CHEMICAL ANALYSIS.....	196
11.3. METHODOLOGY	196
11.3.1. MULTIVARIATE ANALYSIS.....	196
11.3.2. MODEL PERFORMANCE ASSESSMENT.....	197
11.3.3. DATA PRE-PROCESSING	197
11.3.4. DATA FUSION.....	197
11.3.5. CALIBRATION AND VALIDATION DATASETS	201
11.4. RESULTS AND DISCUSSION.....	201
11.4.1. SPECTRAL FEATURES OF THE MINERALS	201
11.4.2. EXPLORATORY ANALYSIS	202
11.4.3. MWIR AND LWIR DATA MODELS	203
11.4.4. LOW-LEVEL FUSION WITHOUT FEATURE SELECTION.....	206

CONTENTS

11.4.5. LOW-LEVEL DATA FUSION WITH FEATURE SELECTION.....	207
11.4.6. DATA FUSION VS. INDIVIDUAL SENSORS	209
11.4.7. COMPARISON OF THE PROPOSED MODELS	209
11.4.8. BENEFITS AND LIMITATIONS OF THE PROPOSED APPROACH FOR MINING APPLICATIONS	209
11.5. CONCLUSIONS	210
REFERENCES.....	211
DATA FUSION FOR THE INDICATION OF ELEMENTAL CONCENTRATIONS	213
12.1. INTRODUCTION	214
12.2. MATERIALS AND INSTRUMENTATION	215
12.2.1. MATERIALS.....	215
12.2.2. MWIR AND LWIR DATASETS.....	215
12.2.3. CHEMICAL ANALYSES.....	215
12.3. METHODOLOGY	216
12.3.1. DATA EXPLORATION.....	216
12.3.2. DATA SPLITTING	216
12.3.3. PRE-PROCESSING	216
12.3.4. PREDICTION MODELS.....	219
12.3.5. MWIR AND LWIR DATA MODELS	219
12.3.6. LOW-LEVEL DATA FUSION	219
12.3.7. MID-LEVEL DATA FUSION.....	220
12.4. RESULTS AND DISCUSSION.....	220
12.4.1. EXPLORATORY DATA ANALYSIS AND PRE-PROCESSING	220
12.4.2. MWIR AND LWIR DATASETS.....	222
12.4.3. LOW-LEVEL DATA FUSION	224
12.4.4. MID-LEVEL DATA FUSION.....	227
12.4.5. DATA FUSION VERSUS INDIVIDUAL SENSORS	228
12.4.6. USE OF INFRARED REFLECTANCE SPECTRA FOR INDICATION OF ELEMENTAL CONCENTRATION	229
12.4.7. OPPORTUNITIES AND LIMITATIONS FOR IN-SITU APPLICATION.....	231
12.5. CONCLUSIONS	233
REFERENCES.....	234

EPILOGUE	237
DISCUSSION.....	239
13.1. SYNTHESIS.....	240
13.2. THE USE OF THE INDIVIDUAL TECHNIQUES FOR MATERIAL CHARACTERISATION	243
13.2.1. RGB IMAGING.....	243
13.2.2. VISIBLE AND NEAR-INFRARED	244
13.2.3. SHORT-WAVE INFRARED	247
13.2.4. MID-WAVE INFRARED	248
13.2.5. LONG-WAVE INFRARED.....	249
13.2.6. RAMAN SPECTROSCOPY	249
13.2.7. COMPARISON OF TECHNIQUES	250
13.2.8. POLYMETALLIC SULPHIDE DEPOSITS AND SENSOR TECHNOLOGIES.....	251
13.3. SENSOR DATA AND DATA QUALITY.....	252
13.4. DATA FUSION AND ANALYTICS.....	254
13.4.1. THE USE OF DATA FUSION	254
13.4.2. MODELS IN DATA FUSION	256
13.4.3. OPPORTUNITIES WITH FUSING OF DATA.....	257
13.4.4. CHALLENGES IN DATA FUSION	259
13.5. IMPLICATIONS OF THE RESULTS	261
13.5.1. IDENTIFICATION OF MINERALS.....	262
13.5.2. ORE-WASTE DISCRIMINATION	263
13.5.3. SEMI-QUANTITATIVE ANALYSIS OF MINERALS AND ELEMENTS.....	264
13.6. FEASIBILITY OF THE USE OF SENSORS AND DATA FUSION FOR MATERIAL CHARACTERISATION IN MINING.....	265
13.6.1. SENSOR-BASED MATERIAL CHARACTERISATION	265
13.6.2. PROSPECT FOR AUTOMATED (REAL-TIME) ANALYSIS OF MATERIAL.....	269
13.6.3. IN-SITU CHARACTERISATION OF MATERIALS.....	270
13.7. OPPORTUNITIES AND LIMITATIONS.....	271
13.7.1. INTERNET OF THINGS (IOT)	272
13.7.2. SOCIETAL RELEVANCE.....	272
13.7.3. LIMITATIONS.....	273

CONTENTS

REFERENCES.....	273
CONCLUSIONS AND RECOMMENDATIONS.....	279
14.1. CONCLUSIONS.....	280
14.1.1. THE USE OF SENSOR TECHNOLOGIES.....	280
14.1.2. DATA FUSION IN MATERIAL CHARACTERISATION.....	281
14.1.3. GENERAL CONCLUSIONS.....	281
14.2. RECOMMENDATIONS FOR FUTURE WORK.....	282
14.2.1. FURTHER EXPERIMENTS IN DIFFERENT GEOLOGICAL SETTINGS.....	283
14.2.2. ADDITIONAL EXPERIMENTS TO OPTIMISE THE DATA FUSION APPROACH.....	283
14.2.3. TOOLS FOR AUTOMATION.....	284
14.2.4. SENSOR DESIGN AND DEVELOPMENT.....	285
14.2.5. COPING WITH THE ENVIRONMENTAL FACTORS ON SENSOR MEASUREMENTS.....	285
14.2.6. EXTENDING THE APPROACH INTO SUBSURFACE (3D) INFORMATION.....	286
SPATIALLY CONSTRAINED DATA.....	287
PUBLICATIONS.....	289
MSC. AND BSC. THESES AND PROJECTS RELATED TO THIS RESEARCH	291

SUMMARY

The rising demands for mined products lead to the extraction of materials in geologically complex regions. This calls for mining process changes and interventions driven by technology and advanced data analytics. The dynamic development of state-of-the-art sensor technologies and their potential use in mining is projected to significantly reduce costs in the industry. However, despite rapid advances in sensor technologies, there is still a demand for novel data analytical approaches to enable accurate characterisation of material along the mining value chain, as advanced data analytics is key to gain knowledge from the complex sensor-derived data. Therefore, sensor technology, coupled with advanced data analytics is crucial for the rapid and accurate characterisation of material in mining operations. Access to rapid and accurate data on the key geological attributes (e.g., mineralogy and geochemistry) along the mining value chain has significant implications for the production process efficiency in commercial mines. Such data would greatly assist the improvement of deposit models, optimise ore processing, specify product quality and improve operational decision-making.

Sensor technologies operate over a specific range of the electromagnetic spectrum and provide information on certain aspects of material properties that are of potential interest for mining extraction. However, a single sensor might not provide a sufficiently comprehensive description of a material's composition. This introduces uncertainty into both resource estimation and requirements definition for mineral processing. Thus, it is necessary to utilise strategic sensor combinations to improve accuracy, minimise uncertainty, and enhance specific insights of material compositions. Combinations of sensors can be implemented using a data fusion approach. The fusion of sensed data can be realised at different levels: low-, mid-, and high-level, when the integration occurs at the data level, features level and decision level, respectively.

This research aims to develop methods for the characterisation of raw materials using multiple sensor technologies and sensor combinations concept (data fusion at different levels), that can be potentially applicable to mining operations. The study involved the multispectral and hyperspectral imaging techniques, such as red-green-blue (RGB) imaging, visible and near-infrared (VNIR) and short-wave infrared (SWIR) hyperspectral imaging, and point spectroscopic techniques, such as mid-wave infrared (MWIR), long-wave infrared (LWIR) and Raman spectroscopy to acquire spectral information over a wider range of the electromagnetic spectrum. First, an investigation was conducted on the usability of the individual sensor technologies coupled with data analytics for the characterisation of a polymetallic sulphide deposit at different levels. The different levels of material characterisation aimed to allow mineral mapping, ore-waste discrimination, fragmentation analysis, and semi-quantitative analysis of elements and minerals. The positive outcomes of the use of the individual techniques led to the development of a data fusion framework that enables data integration (including multi-scale and multi-resolution data) at different levels (e.g., low-level and mid-level). The developed data fusion concept was implemented and validated using different test scenarios.

This contribution demonstrates the potential benefits of and opportunities for the use of sensor technologies and data fusion for the discrimination of ore and waste materials, mineral identification, mineral mapping, and semi-quantitative analysis of mineralogical and

geochemical information in polymetallic sulphide deposit. The use of the individual sensor technologies resulted in the successful characterisation of materials. For example, the use of RGB imaging allowed mapping of minerals and ore geometry delineation at a mine face in-situ in an underground mine. Discrimination of ore–waste materials was achieved using the VNIR, SWIR, MWIR, and LWIR spectral data. This was done by direct detection of the signals from the sulphide minerals as well as the signals from the waste mineralogy. The MWIR and LWIR sensors are effective for semi-quantitative analysis of minerals (SiO_2 , Fe_2O_3 and Al_2O_3) and elements (the combined Pb–Zn and Fe). The fusion of data blocks at different levels allowed for improved predictability and classification of materials. For example, the low-level fusion of MWIR and LWIR resulted in better prediction of mineralogical concentrations than the individual techniques. Likewise, the fusing of the VNIR and SWIR spectral data resulted in an enhanced classification of ore and waste material than the individual techniques. The integration of the SWIR, MWIR and LWIR resulted in even better classification of the ore and waste materials.

Overall, the use of the individual techniques enabled the effective characterisation of the polymetallic sulphide deposit. Moreover, data fusion further enhanced the performance of the prediction and classification models. In this study, semi-quantification of elements was achieved using the infrared technologies; such elements are commonly analysed using the geochemical (elemental) techniques. The MWIR technique is the least-explored region of the electromagnetic spectrum, owing to the limited development of instrumentation. However, the use of MWIR in this study suggests the potential use of the technology for effective characterisation of materials in mining operations. The sulphide minerals exhibit weak spectral signals in the infrared data. However, the developed approaches enabled the establishment of a robust mathematical relationship between the spectra and material properties to provide useful information on the key geological attributes. Moreover, the fact that the study was conducted using a low-grade base metals deposit indicates the potential use for the characterisation of material in other deposit types, including sub-economic deposits. The proposed approach can serve as a baseline for the development of a software tool that enables on-line analysis of materials along the mining value chain (e.g., in mineral exploration, extraction and processing). Thus, it can greatly benefit the productivity and efficiency of mining operations and can contribute to sustainability in mining.

SAMENVATTING

De toenemende vraag naar uit mijnbouw afkomstige producten leidt tot de extractie van materialen in geologisch complexe gebieden. Dit vraagt voor veranderingen en interventies in het mijnbouwproces, gedreven door technologie en geavanceerde data-analyse. Van de dynamische ontwikkeling van de nieuwe sensortechnologieën en hun potentieel gebruik in mijnbouw wordt verwacht dat deze de kosten in de industrie in belangrijke mate zullen reduceren. Ondanks de snelle vooruitgang in sensortechnologieën, is er nog steeds een vraag naar data-analysebenaderingen die nauwkeurige karakterisatie van materiaal in de mining value chain mogelijk maken, omdat geavanceerde data-analyse essentieel is om kennis te verkrijgen uit complexe, door sensors bepaalde data.

Daarom is sensortechnologie, gekoppeld aan geavanceerde data-analyse, cruciaal voor de snelle en nauwkeurige karakterisatie van materiaal in mijnbouwoperaties. Toegang tot snelle en nauwkeurige data van de geologische sleutelkenmerken (bijvoorbeeld mineralogie en geochemie) in de mining value chain heeft belangrijke implicaties voor de efficiëntie van het productieproces in commerciële mijnen. Dergelijke gegevens zouden een grote ondersteuning kunnen zijn in de verbetering van modellen van afzettingen, in het optimaliseren van ertsverwerking, in het specificeren van productkwaliteit en in de verbetering van operationele besluitvorming.

Sensortechnieken werken over een specifieke range van het elektromagnetisch spectrum en verschaffen informatie over bepaalde materiaaleigenschappen, die potentieel van interesse zijn voor mijnbouwextractie. Echter, één enkele sensor verschaft mogelijk niet voldoende diepgaande beschrijving van de samenstelling van het materiaal. Dit leidt tot onzekerheid in zowel reserveschatting als de vaststelling van de vereisten voor mineraalverwerking. Het is dus noodzakelijk om strategische sensorcombinaties te gebruiken om nauwkeurigheid te verbeteren, onzekerheid te minimaliseren, en inzicht in specifieke materiaalsamenstellingen te vergroten. Combinaties van sensors kunnen worden ingezet wanneer hun gegevens worden samengevoegd. Deze versmelting van meetgegevens kan op verschillende niveaus worden gerealiseerd: laag, midden en hoog niveau, wanneer de integratie plaatsvindt op respectievelijk het gegevensniveau, het niveau van de kenmerken, en het beslissingsniveau.

Dit onderzoek beoogt het ontwikkelen van methoden voor de karakterisatie van grondstoffen met gebruikmaking van meerdere sensortechnologieën en een concept van sensorcombinaties (gegevensversmelting op verschillende niveaus), welke mogelijk toepasbaar zijn in mijnbouwoperaties. Deze studie bracht het gebruik van multi-spectrale en hyper-spectrale beeldvormende technieken met zich mee, zoals rood-groen-blauw (RGB) beeldvorming, zichtbaar licht en nabij-infrarood (VNIR), korte-golf infrarood (SWIR), hyper-spectrale beeldvorming en punt-spectroscopische technieken, zoals middengolf infrarood (MWIR), lange-golf infrarood (LWIR) en RAMAN spectroscopie, dit alles om spectrale informatie te verkrijgen over een groter bereik van het elektromagnetisch spectrum. Ten eerste werd een onderzoek uitgevoerd naar de toepasbaarheid van de individuele sensortechnieken, gekoppeld aan gegevensanalyse voor de karakterisatie van polymetallische sulfide-afzettingen op verschillende niveaus. De verschillende niveaus van materiaalkarakterisatie hadden als doel mineraalkartering, erts-afval onderscheiding, fragmentatie-analyse en semi-kwantitatieve analyse van elementen en mineralen mogelijk te

maken. De positieve uitkomsten van het gebruik van de verschillende technieken leidde tot de ontwikkeling van een gegevenscombinatie-netwerk, dat gegevensintegratie (inclusief multi-schaal en multi-resolutie gegevens) op verschillende niveaus mogelijk maakt. Het ontwikkelde gegevensversmeltingsconcept werd geïmplementeerd en gevalideerd onder gebruikmaking van verschillende testscenario's.

Deze bijdrage demonstreert de potentiële voordelen en mogelijkheden van het gebruik van sensortechnologieën en gegevenscombinatie voor de onderscheiding van erts en afval, mineraal-identificatie, mineraalkarteringen en semi-kwantitatieve analyse van mineralogische en geochemische informatie in polymetallische sulfide-afzettingen. Het gebruik van individuele sensortechnologieën resulteerde in de succesvolle karakterisatie van materialen. Bijvoorbeeld, het gebruik van RGB-beeldvorming maakte de kartering van mineralen en erts-geometrie afbakening in-situ aan een mijnfront in een ondergrondse mijn mogelijk. Onderscheid tussen erts en afvalmaterialen werd bereikt door middel van VNIR, SWIR, MWIR, en LWIR spectraal-gegevens. Dit werd uitgevoerd door directe detectie van de signalen van de sulfidemineralen zowel als signalen van de afval-mineralogie. De MWIR- en LWIR-sensors zijn effectief voor de semi-kwantitatieve analyse van mineralen (SiO_2 , Fe_2O_3 en Al_2O_3) en elementen (gecombineerd Pb-Zn en Fe). De combinatie van gegevensblokken op verschillende niveaus liet verbeterde voorspelbaarheid en classificatie van materialen toe. Bijvoorbeeld, de combinatie op laag niveau van MWIR en LWIR leidde tot een betere voorspelling van mineralogische concentraties dan de individuele technieken. Evenzo, de combinatie van VNIR en SWIR spectraal-gegevens resulteerde in verbeterde classificatie van erts en afvalmateriaal dan de individuele technieken. De integratie van SWIR, MWIR en LWIR resulteerde in een nog betere classificatie van erts en afvalmaterialen.

In het algemeen heeft het gebruik van individuele technieken de effectieve karakterisatie van de polymetallische sulfide-afzetting mogelijk gemaakt. Bovendien heeft gegevensversmelting de prestatie van de voorspellings- en classificatie-modellen verbeterd. In deze studie is semi-kwantificatie van elementen bereikt door middel van infrarood technologieën; normaal worden dergelijke elementen geanalyseerd met geochemische (element) technieken. Het MWIR-gebied is het minst onderzochte deel van het elektromagnetische spectrum, als gevolg van de beperkte ontwikkeling van instrumentatie. Echter, het gebruik van MWIR in deze studie suggereert het potentiële gebruik van de technologie voor effectieve karakterisatie van mineralen in mijnbouwoperaties. De sulfidemineralen tonen zwakke spectrale signalen in de infraroodgegevens. Echter, de ontwikkelde benaderingen maken een robuuste wiskundige relatie tussen spectra en materiaaleigenschappen mogelijk, welke bruikbare informatie over belangrijke geologische kenmerken kan verschaffen. Bovendien, is deze studie uitgevoerd op een laaggradige afzetting van base metals. Dit geeft aan dat het potentieel gebruikt kan worden voor de karakterisatie van materiaal in andere afzettingstypen, inclusief sub-economische afzettingen. De voorgestelde aanpak kan dienen als een uitgangspunt voor de ontwikkeling van een software-tool dat online analyse van materialen gedurende de mining value chain (bijvoorbeeld in exploratie, extractie en verwerking) mogelijk kan maken. Het kan dus grote voordelen bieden voor de productiviteit en efficiëntie van mijnbouwoperaties en het kan bijdragen aan de duurzaamheid van mijnbouw.

LIST OF ABBREVIATIONS

The following table describes the various abbreviations used throughout the thesis. The chemical formula of minerals and symbol of elements are not on this list.

Abbreviations	Meaning
ASEM	automated scanning electron microscopy
ATR	attenuated total reflectance
ATR-FTIR	attenuated total reflectance Fourier transform infrared
BB	blasting block
BIL	band-interleaved by layer
CCD	charge-coupled devices
CMOS	complementary metal-oxide-semiconductor
DE-XRT	dual-energy x-ray transmission
DoE	design of experiment
EDA	exploratory data analysis
EPMA	electron microprobe analyser
FIR	far-infrared
FOV	field of view
FTIR	Fourier-transform infrared spectrometer
GCP	ground control point
ICP-MS	inductively coupled plasma-mass spectrometry
IoT	Internet of things
ICA	independent component analysis
IP	induced polarization
LHD	load-haul and dump
LV	latent variable
LIBS	laser-induced breakdown spectroscopy
LIDAR	light detection and ranging
LOOCV	leave-one-out cross-validation
LWIR	long-wave infrared
MC	mean centring
MCR	Multivariate curve resolution
MD	minimum distance
ML	maximum likelihood
MLR	multiple linear regression
MNF	minimum (or maximum) noise fraction
MR	magnetic resonance
MSC	multiplicative scatter correction
MCR-ALS	multivariate curve resolution-alternating least squares
NaN	non-numeric values
NIR	near-infrared
PARAFAC	parallel factor analysis
PC	principle component
PCA	principle component analysis
PCR	principal component regression
PCC	Pearson correlation coefficient

LIST OF ABBREVIATIONS

Abbreviations	Meaning
PLS-DA	partial least squares – discriminant analysis
PLSR	partial least squares regression
PPI	pixel purity index
RBF	radial basis function
RGB imaging	red-green-blue imaging
RMSECV	root mean square error of cross validation
RMSEP	root mean square errors of prediction
ROI	region of interest
SAM	spectral angle mapping
SDBS	spectral database systems
SAM	spectral angle mapper
SNV	standard normal variate
SVs	support vectors
SVC	support vector classification
SVD	singular value decomposition
SVM	support vector machine
SVR	support vector regression
SWIR	short-wave infrared
SWOT	strengths, weaknesses, opportunities, and threats
VNIR	visible and near-infrared
WD-XRF	wavelength dispersive x-ray fluorescence
XRD	x-ray diffraction
XRF	x-ray fluorescence

I

PREAMBLE

1

INTRODUCTION

The first chapter of this dissertation provides the background information to address the research problem, the scope of the research, the proposed methodological framework, and addresses the relevance and potential benefits of the proposed approach. It also presents the general objective and the specific objectives of the study. The last part of the chapter presents an overview of the dissertation structure and contents.

1.1. CONTEXT

Global demand for mined products is increasing rapidly, because of population and economic growth. While accompanied by greater prosperity, the rise in demand for mineral resources requires a sustainable supply. However, the mining industry is challenged by various factors such as the overtime-declining trend of ore grade, discovery of new resources at deeper depths and increasing energy costs (Carvalho, 2017; Gordon et al., 2006; MinEx, 2017; Rogich and Matos, 2008; Rötzer and Schmidt, 2018; West, 2011). For example, as shown in Figure 1.1, the recent trend in the discovery of base metals shows the occurrence of moderate-to giant-sized new deposits in deeper depths. The extraction of resources from low-grade deposits or deeper mines causes challenges related to access to the resource, identification of the minerals, and more time is required to extract, process and market the minerals. Therefore, mining requires novel technologies and rapid analysis of data for the potential economic benefits and sustainable extraction of mineral resources.

In mining, sensors can allow selectivity in the extraction process, ore grade control, sorting of blasted materials, optimisation of mineral processing and automation. In recent years, innovative sensor technologies are being introduced at a fast pace. However, sensor technologies are still rarely utilised for the characterisation of material in the mining industry, due to various factors, including (i) inadequate sensor design, since most are intended for laboratory use, or are specific to a particular deposit type and operational environment; (ii) the need to demonstrate the sensors' utility in the mining industry; and (iii) the high initial cost related to purchasing and setting up the instruments, which may in some cases exceed the benefit to be realised. Despite the limited use of sensors, findings yielded by extant studies in this field (Aznar-Sánchez et al., 2019; Benndorf and Buxton, 2016; Buxton and Benndorf, 2013; Fox et al., 2017; Goetz et al., 2009; Lessard et al., 2014) show that the use of sensor technologies in the mining industry can improve efficiency, reduce operational cost, increase productivity, enhance safety and minimise environmental impact.

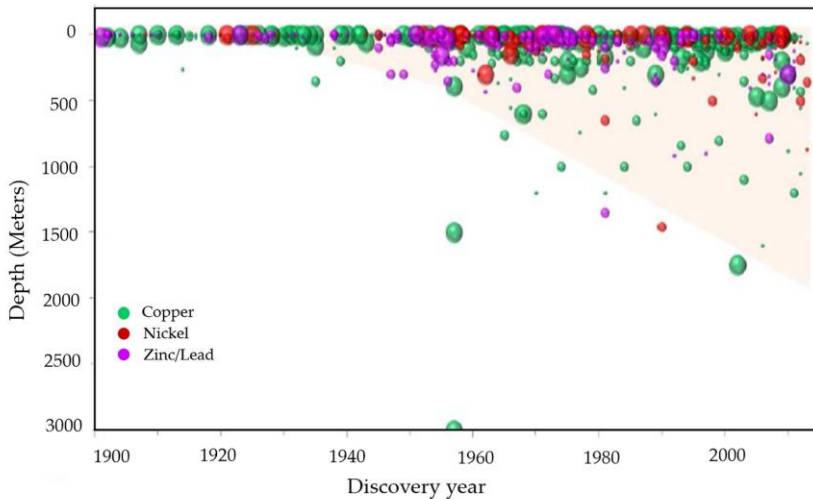


Figure 1.1: A graph that shows the depth and size of the newly discovered base metals in the world from the year 1990 to 2013. The size of the bubbles refers to “Moderate”, “Major”, and “Giant”- sized deposits (Source: MinEx, 2017).

Sensor technologies are as powerful as the information that can be derived from their spectral data. However, understanding the multivariate data is challenging for most of the sensor outputs. Therefore, despite the technological advancement, there is still a demand for advance in data analytics to extract knowledge from sensor data. The framework proposed in this study can enable resource efficiency and sustainability through technology and advanced data analytics (Figure 1.2).

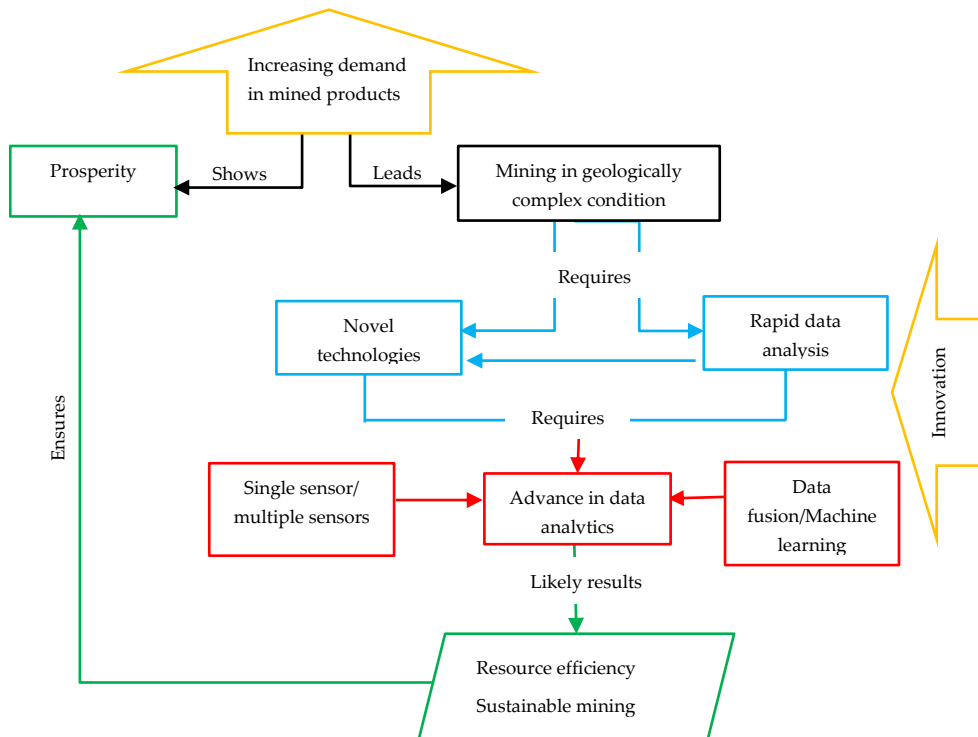


Figure 1.2: The proposed approach for addressing the rising demand in mined products through technology and advanced data analytics.

Sensor technologies provide qualitative, quantitative and semi-quantitative information on different aspects of material properties. Such information can be broadly categorized into geochemistry, mineralogy, and texture but is not limited to these attributes of materials. Each sensor technology operates over a specific range of the electromagnetic spectrum and provides chemical information that might be of potential interest in mining. The detection limit, sensitivity and material properties that the instrument detects and measures vary from sensor to sensor. Thus, a single sensor might not provide a sufficiently comprehensive description of material composition. Subsequently, it is necessary to utilise strategic sensor combinations to achieve a holistic view, improve accuracy, minimise uncertainty, and enhance specific inferences for raw material characterisation. Some of the potential benefits of data fusion in mining are presented in Figure 1.3.

Sensor technologies may be integrated physically or digitally (through data fusion). Physical integration is achieved when two or more sensors are combined on a single platform. Data fusion integrates data blocks from multiple sources or sensors into a single

comprehensive model (Cocchi, 2019; Hall and McMullen, 2004). It can be realised at three levels, designated as low-level, mid-level, and high-level fusion. Low-level data fusion involves the integration of multiple data sources by concatenating data blocks of different nature (Castanedo, 2013; Forshed et al., 2007; Silvestri et al., 2014). Mid-level or hierarchical data fusion is a feature-level fusion that involves variable screening (Borràs et al., 2015; Silvestri et al., 2014). High-level data fusion is a decision-level fusion that combines model outputs to produce a final fused response (Cocchi, 2019). The physical integration of multiple sensor technologies into a single platform is challenging, and in terms of practical implementation, it is expensive. Therefore, in this study, the data fusion approach was considered since it is an economic and practical alternative option.

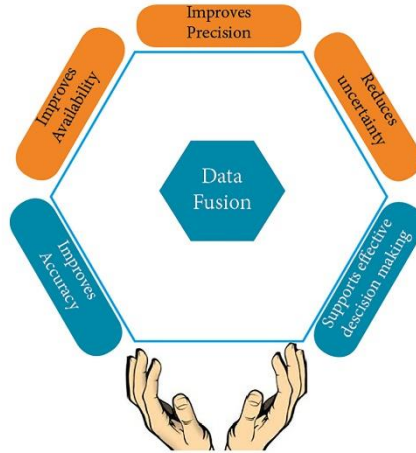


Figure 1.3: The potential benefits of data fusion in mining operations.

In mining, accurate and reliable resource estimation is required, as it is advantageous to be able to obtain more readily information on the potential economic and environmental operability of commercial mines. Sensor technologies can provide accurate data for the reliable estimation of resources and efficient extraction of materials. Sensors can be utilised along the mining value chain, starting from the exploration stage to the marketing of the mined products. Some of the potential sensor installation sites for sensor-based material characterisation along the mining value chain include mine face, drill core /drill hole logging, muck pile, load-haul and dump (LHD) and conveyor belts. The use of innovative technologies coupled with advanced data analytics at each potential sensor installation site offers the possibility for rapid, accurate and on-line analysis of materials in the mining process. Thus, it can contribute to the sustainable and cost-effective extraction of mineral resources.

1.2. RESEARCH HYPOTHESIS

This study was designed to validate or disprove the hypothesis that combinations of sensor enable improved accuracy, availability, predictability and quantification in raw material characterisation than individual sensor technologies. It is possible to use sensor technologies to characterise and define raw material properties in different applications such as in mining. However, such an approach requires the definition of combinations of sensor types to generate more accurate and reliable data, as this is beneficial for efficient process optimisation and effective decision-making in the mining industry.

1.3. RESEARCH OBJECTIVES

This research aimed to explore the opportunities and benefits of the use of sensor technologies for the characterisation of raw materials in a polymetallic sulphide deposit and investigate the comparative advantages of sensor combinations using a data fusion approach that integrates multi-source and multi-scale data. The sensor technologies explored in this study are red-green-blue (RGB) imaging, visible and near-infrared (VNIR), short-wave infrared (SWIR), mid-wave infrared (MWIR), long-wave infrared (LWIR) and Raman spectroscopy. The use of the individual sensor technologies for the qualitative and quantitative analysis of the geological attributes (e.g., geochemistry, mineralogy) in a polymetallic sulphide deposit was assessed using the different multivariate techniques. The outcomes of the technologies usability assessment guided the development of a concept for the combinations of sensor. The conceptual framework illustrates the potential sensor combination options using a data fusion approach and it demonstrates the opportunities of data fusion at different levels (low-level, mid-level and high-level). The developed data fusion concept was implemented and validated using different test scenarios.

To achieve the aim of the research, the following specific objectives and the corresponding research questions were formulated (Figure 1.4). The objectives are briefly discussed in the subsequent chapters. In this section, the three key objectives (the black boxes of Figure 1.4) are further elaborated.

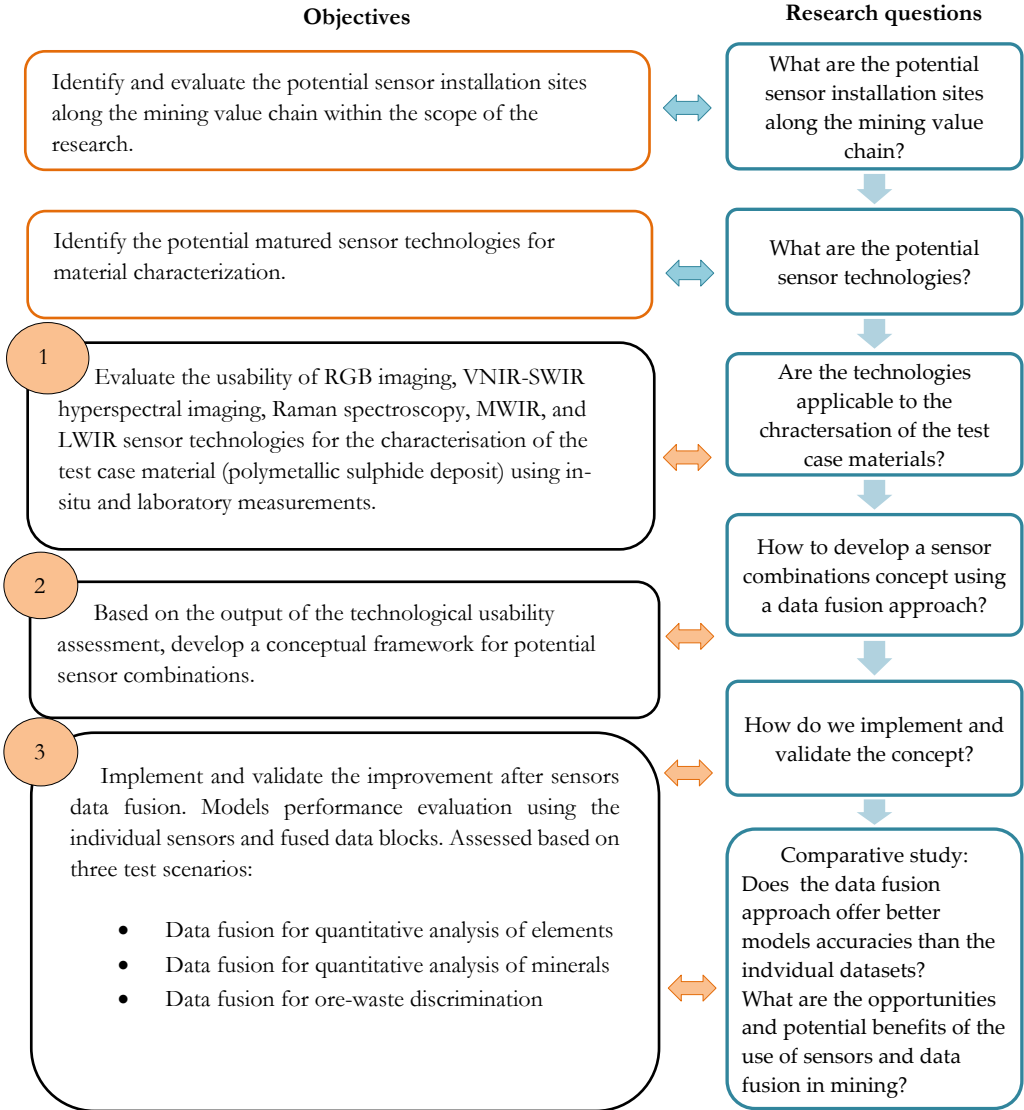


Figure 1.4: The specific objectives of the research and the corresponding tasks.

1. **Assessment of the applicability of the individual sensor technologies:** evaluate the usability of RGB imaging, VNIR-SWIR hyperspectral imaging, Raman spectroscopy, MWIR, and LWIR sensor technologies for the characterisation of material in a polymetallic sulphide deposit. Measurements were performed both in-situ and in the laboratory using the collected representative samples. Achieving this aim addressed the following specific objectives.
 - a. Identify the geological attributes that can potentially be acquired from each sensor output

- b. Assess the use of the individual technique for the detection, identification, ore–waste discrimination and quantitative analysis of elements and minerals
 - c. Evaluate the opportunities and benefits of the use of each sensor technology
 - d. Identify the optimum data pre-processing and the linear or non-linear data modelling algorithms required to maximise the information from each sensor output
2. **Develop a conceptual framework for sensor combinations:** based on the output of the technological usability assessment, develop a conceptual framework for the potential sensor combinations options using a data fusion approach. The framework specifies a multi-step methodological approach for the fusion of multiple data blocks at different levels of integration using multi-source and multi-scale data.
 3. **Validate the defined data fusion concept:** implement and validate the developed data fusion concept. Evaluate the performance of the prediction and classification models of the individual sensor data and fused data using three test scenarios.
 - Data fusion for quantitative prediction of elements (the combined Pb–Zn and Fe) using the mineralogical techniques (MWIR and LWIR)
 - Data fusion for quantitative analysis of minerals (SiO_2 , Fe_2O_3 , and Al_2O_3) using the linear and non-linear algorithms and the infrared technologies
 - Develop a conceptual framework for the integration of image (VNIR and SWIR) and point (MWIR and LWIR) data: evaluate the performance of the fused hyperspectral image and point data for the discrimination ore–waste.

The study focuses on the opportunities and potential benefits of the use of sensors and sensor combinations in mining operations. Techno-economic assessment of the feasibility of applying data fusion using multiple data sources is beyond the scope of this investigation. Further points that are out of the scope of this research are indicated in Table 1.1.

Table 1.1: The research scope statement.

In Scope	Out of Scope
Usability assessment of the RGB imaging, VNIR, SWIR, MWIR, LWIR, and Raman technologies in a polymetallic sulphide deposit	Validation of the approach in multiple geological settings
Development of methodological approaches for knowledge generation from each technique	Investigation of the influence of the environmental factors on sensor measurements
Design and development of a data fusion concept	Assessment of textural and hardness information
Implementation of the developed data fusion concept using multiple possible combinations	Assessment of the techno-economic benefits of the developed approaches
Evaluation of the results from the use of individual technique and fused data blocks	Modelling of the ore body in 3D
Indicate the benefits and possible limitations of the use of technologies and the developed methodological approaches in mining thus to indicate potential future research directions	

1.4. DISSERTATION STRUCTURE

The structure of this dissertation contemplates the outlined research objectives. It is divided into 14 chapters and organised into five parts (Table 1.2).

Table 1.2: Overview of the thesis structure.

Part	Chapter	Description
PART I - PREAMBLE	Chapter 1	Illustrates why there is a need for state-of-the-art sensor technologies and advanced data analytics for effective raw material characterisation in mining operations. The chapter introduces the proposed methodological framework and explains its significance, relevance and potential benefits. The research aim and specific objectives are explained. The chapter also presents an overview of the dissertation structure and contents.
	Chapter 2	Presents the potential applications and opportunities for the use of sensors in mining. It discusses the possible role and benefits of sensors in real-time material characterisation. It also describes the potential sensor location sites along the mining value chain.
	Chapter 3	Describes the state-of-the-art sensor technologies with particular emphasis on the technologies assessed in this study, the material properties the techniques detect and the type of data the sensors produce. It also presents the specification and set-up of the technologies used in this study.
PART II -THE METHODOLOGICAL FRAMEWORK AND THE STUDY SITE	Chapter 4	Elaborates the methodological approaches for the exploratory data analysis and data pre-processing. The chapter presents a review of the multivariate data analysis techniques used for the extraction of knowledge from the individual sensor data. It also explains the methodological approaches used for the fusion of sensor responses at multi-level.
	Chapter 5	Provides a brief explanation of the study site geological setting. It describes the regional and local geology. A detail description of the mineralisation at the defined study block is presented. The chapter finally describes the adopted sampling strategy and the different types of samples collected for this research.
PART III -APPLICABILITY OF THE INDIVIDUAL TECHNIQUES	Chapter 6	Demonstrates the usability of RGB imaging for mineralogical face mapping and ore zone delineation in an underground mine. The technique was further assessed for the analysis of fragmentation using the RGB images taken from small muck piles. The chapter discusses the methodological approach for image data acquisition, processing and knowledge extraction. It also shows the potential benefits and possible challenges of the use of the technique in operational mines.
	Chapter 7	Presents the use of the VNIR and SWIR hyperspectral images for the identification of the test case minerals and mineral mapping. The chapter also demonstrates the possibility of the techniques for the indication of ore zones using drill core and rock chips samples. It discusses the knowledge extraction processes and compares the outcomes of the two techniques.

Part	Chapter	Description
PART IV – PERFORMANCES OF THE DATA FUSION APPROACHES	Chapter 8	Presents the use of MWIR and LWIR techniques coupled with chemometrics for the discrimination of sulphide ore. This study aims to evaluate whether MWIR, the least explored region of the electromagnetic spectrum in terms of material characterisation, is capable of discriminating the sulphide ore. The chapter also compares the performance of the MWIR data model with the LWIR data model for the discrimination of ore–waste materials. The chapter starts with exploratory analysis. Thereafter, the methodological approach is briefly discussed. The chapter further provides the results with discussion and finally concludes with the overview of the outcomes and potential improvements.
	Chapter 9	Demonstrates the use of the Raman spectroscopy for the characterisation of material from the test case. The chapter compares the performances of two Raman spectrometers with excitation laser sources of 532 nm and 785 nm for the identification of minerals in powder, pellets and rock samples. It also assesses the use of Raman for ore and waste separation. The chapter further provides the results with discussion and finally concludes with the overview of the outcomes and potential considerations.
	Chapter 10	Evaluates the use of a fusion of hyperspectral image (VNIR and SWIR) and point data (MWIR and LWIR) for ore-waste discrimination. The chapter describes the different scenarios for the integration of image and point data. It also provides the results with discussion and finally concludes with the overview of the outcomes and potential improvements.
	Chapter 11	Evaluates the use of MWIR and LWIR data fusion for quantitative analysis of minerals. The chapter describes the developed methodological approaches for the fusion of MWIR and LWIR at low-level and low-level with features extraction. The results are discussed, and conclusions were drawn.
PART V – EPILOGUE	Chapter 12	Studies how the multi-level data fusion of MWIR and LWIR reflectance spectral data influences the prediction of elemental concentrations. The elemental prediction was performed using the mineralogical techniques, individual data blocks (MWIR and LWIR) and the fused data. The following questions are addressed to compare the performances of the prediction models developed using the different data blocks. (i) Can the MWIR be used to predict elemental concentration? (ii) Can the LWIR be used to predict elemental concentration? (iii) Does data fusion improve model performance? (iv) Does the multi-level fusion (low-level and mid-level) result in different prediction accuracies? The chapter provides an extensive discussion on the outcomes and concludes with a recommendation.
	Chapter 13	Discusses the opportunities for the use of sensor technologies for the characterisation of a polymetallic sulphide ore deposit. The chapter also discusses the opportunities with multi-level sensors data fusion for classification and prediction of materials in mining operations. The chapter further discusses the possibilities and limitations of the developed methodological approaches for automated in-situ applications.
	Chapter 14	Presents the general conclusions of this research. The chapter also provides a few recommendations for future work to improve further and automate the classification and prediction of the geological attributes.

REFERENCES

- Aznar-Sánchez, J. A., Velasco-Muñoz, J. F., Belmonte-Ureña, L. J. & Manzano-Agugliaro, F. (2019). Innovation and technology for sustainable mining activity: A worldwide research assessment. *Journal of Cleaner Production*, 221, pp. 38-54. doi: 10.1016/j.jclepro.2019.02.243
- Benndorf, J. & Buxton, M. (2016). Sensor-based real-time resource model reconciliation for improved mine production control – a conceptual framework. *Mining Technology*, 125, pp. 1-11. doi:10.1080/14749009.2015.1107342
- Borràs, E., Ferré, J., Boqué, R., Mestres, M., Aceña, L. & Busto, O. (2015). Data fusion methodologies for food and beverage authentication and quality assessment – A review. *Analytica Chimica Acta*. 891, pp. 1-14. doi: 10.1016/j.aca.2015.04.042
- Buxton, M. & Benndorf, J. (2013). The use of sensor derived data in optimization along the mine-value-chain: An overview and assessment of techno-economic significance. *Proceedings of the 15th International ISM Congress, Aachen, Germany*, pp. 324-336.
- Carvalho, F. P. (2017). Mining industry and sustainable development: time for change. *Food and energy security*, 6(2), pp. 61-77. doi: 10.1002/fes3.109
- Castanedo, F. (2013). A Review of Data Fusion Techniques. *The Scientific World Journal*, 2013, 19. doi:10.1155/2013/704504
- Cocchi, M. (2019). Chapter 1 - Introduction: Ways and Means to Deal with Data from Multiple Sources. In: M. Cocchi (Ed.), *Data Handling in Science and Technology*. Elsevier, pp. 1-26.
- Forshed, J., Idborg, H. & Jacobsson, S. P. (2007). Evaluation of different techniques for data fusion of LC/MS and 1H-NMR. *Chemometrics and Intelligent Laboratory Systems*, 85, pp. 102-109. doi: 10.1016/j.chemolab.2006.05.002
- Fox, N., Parbhakar-Fox, A., Moltzen, J., Feig, S., Goemann, K. & Huntington, J. (2017). Applications of hyperspectral mineralogy for geoenvironmental characterisation. *Minerals Engineering*, 107, pp. 63-77. doi: 10.1016/j.mineng.2016.11.008
- Goetz, A. F. H., Curtiss, B. & Shiley, D. A. (2009). Rapid gangue mineral concentration measurement over conveyors by NIR reflectance spectroscopy. *Minerals Engineering*, 22, pp. 490-499. doi: 10.1016/j.mineng.2008.12.013
- Gordon, R. B., Bertram, M. & Graedel, T. E. (2006). Metal stocks and sustainability. *The National Academy of Sciences of the United States of America*, 103(5), pp. 1209-1214. doi: 10.1073/pnas.0509498103
- Hall, D. L. & McMullen, S. A. H. (2004). *Mathematical Techniques in Multisensor Data Fusion*, 2nd ed., Artech House, Norwood, Massachusetts.
- Lessard, J., De Bakker, J. & Mchugh, L. (2014). Development of ore sorting and its impact on mineral processing economics. *Minerals Engineering*, 65, pp. 88-97. doi: 10.1016/j.mineng.2014.05.019
- MinEx. (2017). Challenges of Exploring Under Deep Cover [Online]. Available: <https://minexconsulting.com/challenges-of-exploring-under-deep-cover> [Accessed January 2021].
- Rogich, D. G. & Matos, G. R. (2008). The global flows of metals and minerals: U.S. Geological Survey Open-File Report 2008-1355. Available online: <https://pubs.usgs.gov/of/2008/1355/>
- Rötzer, N. & Schmidt, M. (2018). Decreasing Metal Ore Grades—Is the Fear of Resource Depletion Justified? *Resources*, 7(4), 88. doi: 10.3390/resources7040088

- Silvestri, M., Elia, A., Bertelli, D., Salvatore, E., Durante, C., Li Vigni, M. & Cocchi, M. (2014). A mid-level data fusion strategy for the varietal classification of Lambrusco PDO wines. *Chemometrics and Intelligent Laboratory Systems*, 137, pp. 181-189.
doi: 10.1016/j.chemolab.2014.06.012
- West, J. (2011). Decreasing metal ore grades: Are they really being driven by the depletion of high-grade deposits? *Journal of Industrial Ecology*, 15(2), pp. 165-168.
doi: 10.1111/j.1530-9290.2011.00334.x

2

POTENTIAL APPLICATIONS FOR SENSOR TECHNOLOGIES FOR MATERIAL CHARACTERISATION IN MINING

This chapter presents the potential applications and opportunities for the use of sensors in mining. It discusses the possible role and benefits of sensors in real-time material characterisation. It also describes the potential sensor location sites along the mining value chain.

2.1. OPPORTUNITIES FOR THE USE OF SENSORS IN MINING

Sensor technologies offer opportunities to address the essential parts of the mining process, such as ore grade control, mine planning and design, vehicle control, remote operation, and automation. Thus, various sensor systems can be used for different applications. For example, sensors for machine performance monitoring, collision avoidance, hazardous gas monitoring and raw material characterisation (Buxton and Benndorf 2013, Ehsan 2017, Ramjack 2019). Among the various potential use of sensors in mining, sensor-based material characterisation was the focus of this study. In mining, sensor-based material characterisation is beneficial for effective grade control, accurate delineation of lithological or mineralogical domains, the reduction of resources consumption, sorting of materials, quality control, optimisation of mineral processing, and can allow secondary recovery (Buxton and Benndorf, 2013; Lessard et al., 2016). Besides, technology can also permit the identification and discovery of new mineral reserves, mature new mines with the sub-economic deposit, increase the efficiency of the production process, and reduce waste volume. Therefore, it has a substantial contribution to the sustainability of mining.

The value or cost drivers for effective planning and predictability in mining operations include data accuracy, data availability, in-situ characterisation, automation and sample representativity. The potential benefits of the use of sensors in mining industries have a direct link to the most of cost drivers (Table 2.1). For example, high-end sensor technologies can enable the detection of minerals/elements of economic interest at very low concentrations. Accurate information on low-grade ore provokes the feasibility of mining in sub-economic deposits. The other important aspect of the use of sensors in mining is the tangible contribution of sensor-derived data for the digital transformation of the mining industry. As the digitalisation of mining is beneficial to lower operational costs, improve safety, and provide real-time data (Chaulay et al., 2016). Consequently, the use of sensors can potentially benefit the economic viability of mining operations and ensures environmental sustainability (Benndorf and Jansen, 2017; Benndorf et al., 2015; Buxton and Benndorf, 2013; Lessard et al., 2016). However, maximising these benefits requires well-developed sensor technologies, advanced data analytics, as well as well-calibrated software.

Broadly, there are two types of mining methods; surface mining and underground mining. Surface mining is a mining method used for the extraction of minerals from the surface (e.g., open-pit mining, placer). Whereas, underground mining is the mining of minerals from a certain depth when the deposit is too deep for surface mining. The two mining types differ in different aspects. For example, the depth of mining, ore recovery, the environmental conditions, and the volume of materials to be moved. The main advantages of surface mining over underground mining include enhanced ore recovery, operational flexibility, lower cost, better safety and higher productivity (National Research Council, 2002). Currently, most of the metallic, non-metallic and large portion of coal mines are surface mines (Hartman, 1987).

Mining begins with exploration, continues through extraction and production, and ends with mine closure and post-mining rehabilitation. Sensor technologies can be utilised at all stages of the mining life cycle and potentially benefit mining industries (Table 2.1 and Figure 2.1). This includes the use of sensors along the mining value chain, starting from the exploration stage to the marketing of the mined products. The main components of the mining life cycle and the potential use of sensors at each stage are indicated in Figure 2.1. For example, in the discovery of new deposits, a variety of sensing technologies can be

employed. Depending on the preferred exploration approach, sensors can be used for drill cores logging, mapping of the target area (commonly using air-borne or remote sensing techniques) and rock chips analysis (Figure 2.1). Likewise, during the extraction stage of the mining cycle, sensors can provide mineralogical information at the mine face and can be used for automated drill cores logging.

Table 2.1: Summary of some of the potential benefits of the use of sensors for raw material characterisation in the mining industries.

Potential benefits	
Sensors can provide real-time data	<ul style="list-style-type: none"> • Useful for a real-time updating of the resource models thus to promote continuous mining • Automation of material characterisation can be achieved • Minimises the time required for off-line analysis • Supports effective decision-making in mining
Accurate sensor - derived data can be used for	<ul style="list-style-type: none"> • Grade control applications • Requirement definition and optimisation of geometallurgical processes (e.g., the energy requirement, the floatation properties and the recovery of metal ores) • Requirement definition of the blasting parameters • To understand the spatial distribution of mineable materials e.g., ore geometry delineation at the mine face • Material tracking • Ensures quick visualisation of data (e.g., mineral maps form hyperspectral images or RGB images) • Product quality control during processing and marketing
In-situ measurements	<ul style="list-style-type: none"> • This is beneficial in reducing the time required for sampling, sample transport and off-line analysis in the laboratories • More samples can be analysed therefore the issue of samples representativeness can be minimised • Increase data availability (e.g., geochemical, mineralogical and textural)
Sensors for ore–waste sorting	<ul style="list-style-type: none"> • Dry separation of the ore and waste materials minimises the energy requirement at the later stage of mineral processing. Thus, ore–waste sorting sensors maximise the resource efficiency of mining operations
Promote the digital transformation of mining	<ul style="list-style-type: none"> • The digital transformation supports the transfer of the Industrial Internet of Things (IIoT) from other industries to the mining industry – thus improves productivity and safety • Promotes the development of comprehensive digital databases • Increase data availability (e.g., geochemical, mineralogical and textural)
Provide spatial coordinates	<ul style="list-style-type: none"> • Spatially constrained (georeferenced) data can be generated. Such kind of data is essential for resource model updating, understanding of the spatial distribution of minerals, and material tracking
Maximises safety through automation and data availability	<ul style="list-style-type: none"> • Identification of weak zones (e.g., at the mine face using image data) • Minimise human exposure to dangerous or unsafe conditions • Minimise the exposure to hazardous substances

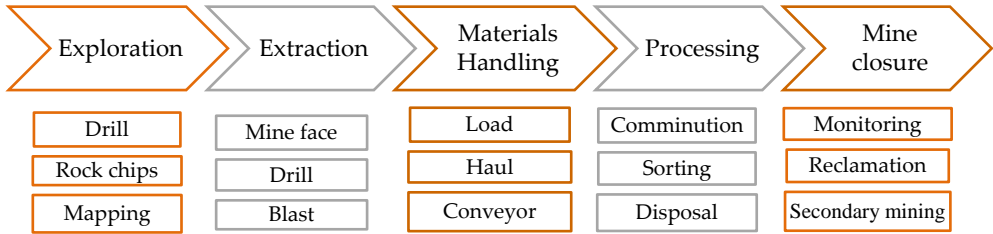


Figure 2.1: The major components of the mining life cycle and some of the potential sensor-based material characterisation options at each stage.

2.2. USE OF SENSORS IN REAL-TIME MATERIAL CHARACTERISATION

The demand for rapid, accurate and reliable resource estimation in mining operations is proliferating, as it is advantageous to be able to obtain more readily information on the potential economic and environmental operability of commercial mines. The use of sensors can allow rapid analysis of materials. Rapid and accurate data throughout the mining value chain permit automated material characterisation, prompt resource model updating, on-line ore quality control, prompt optimisation of mineral processing, enable sensor-based sorting, permits safety assurance, and allow material tracking (Benndorf et al., 2015; Benndorf and Jansen, 2017; Dalm, 2018). Thus, it benefits the mining industry through rapid process optimisation and control.

The growing interest in real-time information in the mining industry promotes the need for automated material characterisation along the mining value chain. The potential sensor locations (installation) sites along the mining value chain differ in terms of material flow, production environment, throughput and material type (form). Some of the sites are static with low speed of material flow such sites include mine face, drill core and muck piles. On the other hand, the dynamic sites that involve higher speed material flow include conveyor belt and material characterisation during transport (e.g., load-haul and dump—LHD)). Therefore, the time required for real-time material characterisation at the different potential sensor installation sites along the mining value chain varies. For example, mine face has intact material, no or slow material flow, the material can be analysed in undisturbed form and has excellent potential for in-situ analysis. Real-time mineral mapping at the mine face may require a time scale in the order of hours or days since mine face mapping can be performed after a new blast. In contrast, the sorting of materials at the conveyor belt requires information in the order of seconds. Therefore, real-time material characterisation at the potential sensor locations in the mining cycle may require different time scales. Besides, achieving a real-time material analysis is highly dependent on two factors. One is the competency of sensor technologies for rapid data acquisition, and the other key enabler is a well-calibrated software system that can promptly transfer the acquired data into usable information.

2.3. POTENTIAL LOCATIONS FOR SENSORS IN MINING OPERATIONS

Some of the potential sensor location sites during material extraction and transport include mine face, drill core/drill hole logging, muck pile, LHD and conveyor belts. Figure 2.2 and Figure 2.3 show the opportunities for sensor-based material characterisation in

open-pit and underground mines, respectively. This research focused on usability assessment of sensors at mine face, drill core and muck pile sites. Measurements of rock attributes were performed both in-situ and using rock samples collected from the sites. Figure 2.4 shows the investigated potential sensor installation sites and explored sensor technologies. The measurements were performed in-situ and in a laboratory; this is discussed in detail in Chapter 5. Sensors can be mounted at the three sites (mine face, drill core and muck pile) to acquire data on different material properties (geological attributes). However, the use of sensor at each potential sensor data acquisition sites along the mining value chain has also challenges. The potential benefits and possible challenges of the use of sensors at the mine face, drill core, and muck pile potential sensor data collection sites along the mining value chain are discussed and summarised in Table 2.2.

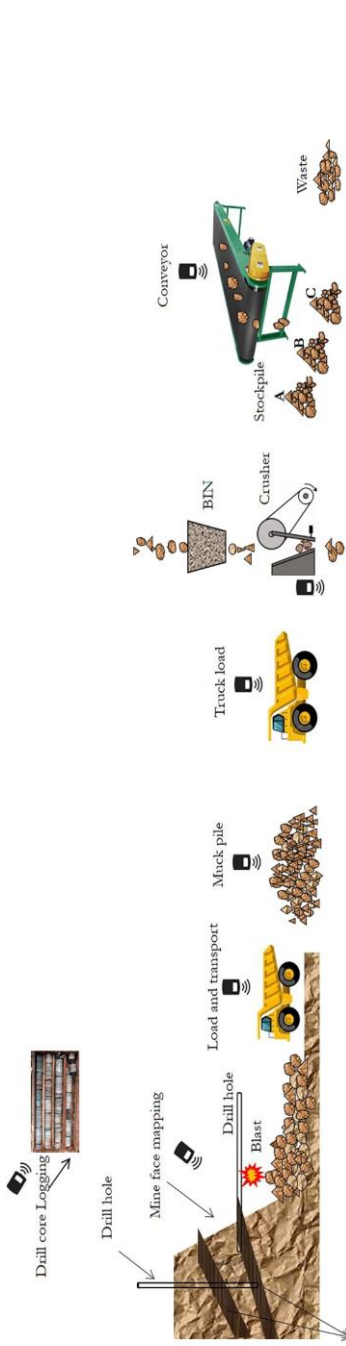


Figure 2.2: Schematic sketch that illustrates some of the potential sensor locations for sensor-based material characterisation in an open-pit mine.

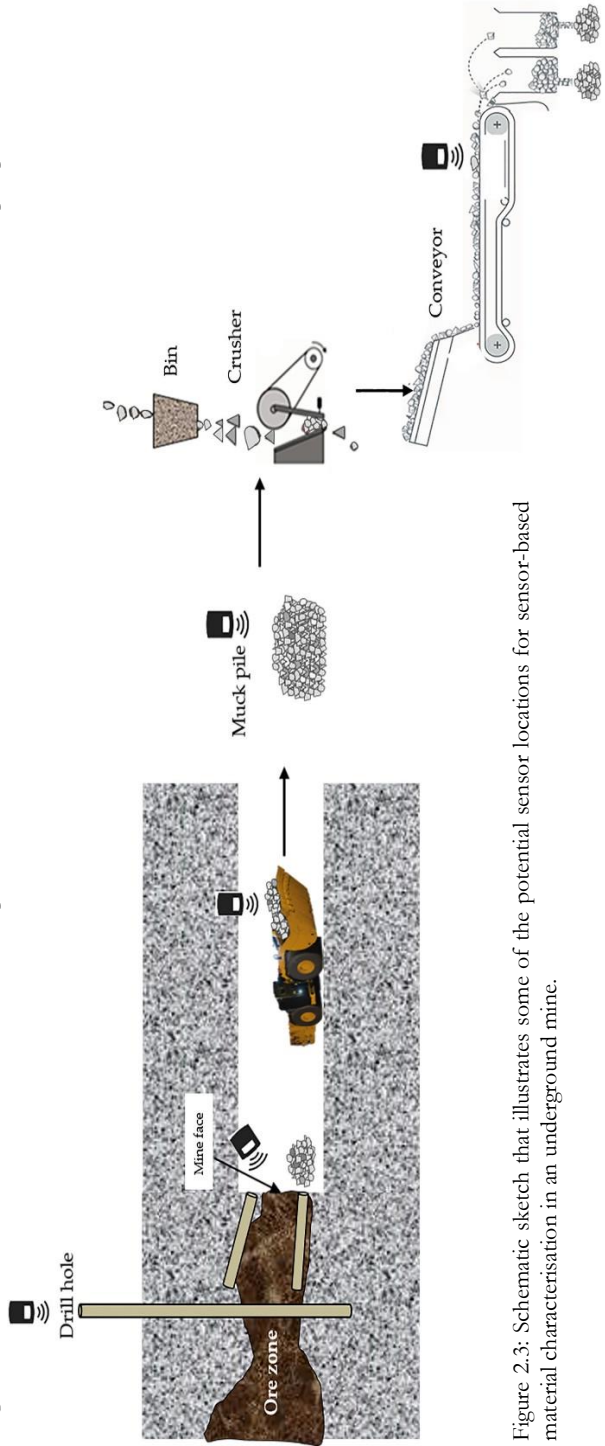


Figure 2.3: Schematic sketch that illustrates some of the potential sensor locations for sensor-based material characterisation in an underground mine.

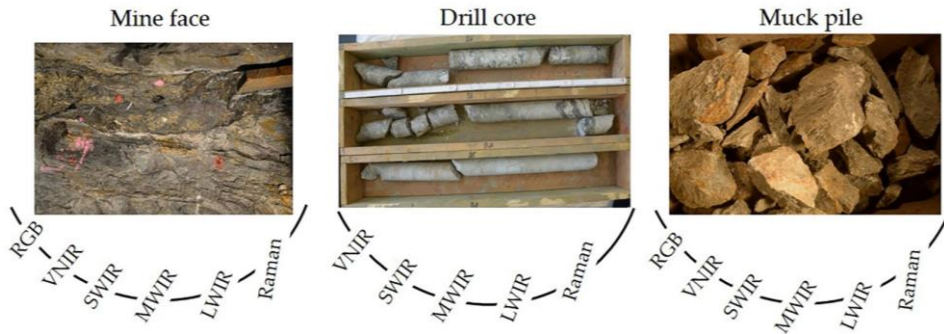


Figure 2.4: The explored potential sensor solutions for the characterisation of materials at (a) the mine face, (b) drill core, and (c) muck pile potential sensor installation sites in the mining value chain.

Table 2.2: The potential benefits and the possible challenges of the use of sensors at mine face, drill core and muck pile potential sensor installation sites along the mining value chains.

Sites	Potential benefits	Possible challenges
Mine face	<ul style="list-style-type: none"> • Ore geometry delineation • Block classification: as ore if above the cut-off grade • Blasting requirements definition • In-situ information (in its undisturbed original form) can be generated before/after blasting • Potentially allows for selective extraction of the material • Verification of the analysis results can be done on the same samples • No time pressure (the measurements will be taken between consecutive blasts) • There is no material flow • Enables to acquire georeferenced spatial data • Possible to combine with drill core and channel-cut samples • Having access to real-time information of the geometry and mineralogy of the mine face could give an estimate of the ore-grade and volume being excavated • Both point and image data can be acquired • Surface mounting of compact device possible • Static site no time pressure 	<ul style="list-style-type: none"> • Under realistic conditions (i.e. routine use in a mine) the sensors have to be semi-automated; this could require a complicated mechanical and optical layout depending on the surface conditions of the mine face • Operator required • Requires long (power) cables • Needs illumination source depending on the technology • Surface information (only the exposed part) • Requires mobile platform – rotating platform (e.g., translation, up and down) • Surface contamination (e.g., dust after blast, surface weathering)

Sites	Potential benefits	Possible challenges
Drill core	<ul style="list-style-type: none"> • Information of the material composition is available before crushing of the material • Multiple measurements at the same samples are possible • Validation of the analysis results can be done on the same samples (e.g., by wet chemical analysis) • Requires static sensor mounting platform (no time pressure) • Gives information about the unexposed surface geology (up to the depth of the drill core) • Remote (up to few cm) application possible (distance between sample and sensor) • Low scanning speed is acceptable • Compact device can be mounted 	<ul style="list-style-type: none"> • Information is available only after drilling • Mechanical sample handling system required • Operator required • Requires a large area to handle the drill cores
Muck pile	<ul style="list-style-type: none"> • Verification of the analysis results can be done on the same samples (e.g. by wet chemical analysis) • Multiple measurements at the same samples are possible (allows for relatively simple validation of the analysis results) • Principally no time pressure, planning and organisation of the measurements can be performed beforehand and integrated into the mining procedures for routine use in a mine • Remote application possible • Static site no time pressure for the sensor measurements 	<ul style="list-style-type: none"> • Intensive de-mixing of the material during storage • No representative analysis results possible if only the surface of the pile is measured • Sampling necessary • Mixed materials • Homogeneity of the material composition of the pile and hence the sampling procedure depend on the storage duration of the pile and the weather conditions during storage, the same holds for a potentially ongoing chemical and physical alteration of the bulk material that may influence the analysis results • Operator required • Slow data acquisition • Piling has effect

2.4. SENSOR-DERIVED DATA IN MINING

2.4.1. TYPES OF SENSOR DATA

Sensors measure the different aspects of material properties and record the measurements into signals. The signals are stored as data for use in the digital domain. Sensors produce various types of data, and understanding of the different data natures is crucial in many ways. Such as, it is beneficial to choose the required pre-processing techniques, data analysis methods, and programming languages or software. It is also advantageous to assess data quality and understand data storage requirements. Therefore, a data type can determine the data analysis works. Sensors can produce a point, image or volumetric data (Figure 2.5). This division is based on the number of data points per a single measurement and the depth of penetration of sensor measurements. The number of data

points (e.g., pixels) per a single measurement varies from technology to technology. Therefore, some techniques produce point data, while others produce image data.

The point techniques offer a discrete unit of information (a single data point) for the whole measured area per a single measurement. Typically, each point measurement covers a very small area or spot and produce point data (1D information). However, the spot size varies from instrument to instrument. Depending on the technology, a point datum can be a spectrum that consists of wavelength and reflectance or intensity information. Whereas, image data constitutes multiple pixels (data points) and covers a larger area of a target per a single measurement. Image data is a 2D data that provide spatial and spectral information about the entities under investigation. On the other hand, the volumetric data provide 3D details up to the depth the measuring instrument can penetrate the sample. These kinds of sensors are commonly used in geophysical studies. However, other sensors also produce volumetric data such as dual-energy x-ray transmission (DE-XRT) or gamma-ray technologies (Haefner et al., 2017; Kern et al., 2019; von Ketelhodt and Bergmann, 2010).

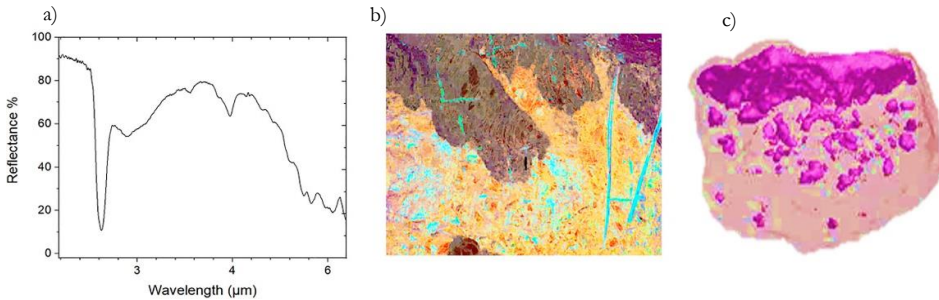


Figure 2.5: Example of data types: (a) point—represent a measurement at a single data point, (b) image—a 2D representation of multiple data points (pixels), and (c) volumetric—provide 3D information up to the penetration depth of the measuring system.

Sensors can also produce univariate, bivariate or multivariate data. Univariate data comprise one type of data (one variable) per observation. The bivariate data are data with two variables per observation. Whereas, multivariate data provide more than two variables for each observation. Types of data can be discrete or continuous. Discrete data can only take particular values, but it can be either numeric or categorical. Whereas, continuous data are not restricted to specific values, but can take any value within a range. Thus, continuous data are numeric. Sensors data can also be qualitative, semi-quantitative and quantitative. Qualitative data are categorical and quantitative data are numerical. Semi-quantitative data are numeric but less precise than quantitative data.

Data volume (the amount of data) has significant implications for data storage, processing, and visualisation. For example, the storage and analysis of big data require extensive data warehouse and computing systems with high computational power. Thus, the amount of data should be taken into account before any data analysis tasks. Data volume depends on the type of data and commonly expressed in bytes. The volume of data from the imaging spectrometers is usually higher than the point spectrometers. The data volume of image data depends on the spatial and spectral resolutions of the images. The higher the spatial and spectral resolutions, the larger the data volume. For example, the data size of a point SWIR reading is ~ 54 KB, whereas the SWIR hyperspectral image of a rock piece is ~ 215 MB. The various data types from sensors are stored in different data formats. The

common examples of data formats include integers, floating-point number, strings or arrays. Data volume also depends on the number of bits used to store data.

2.4.2. DATA QUALITY PARAMETERS

There are many definitions of data quality, but generally, it can be defined as the fitness for intended uses. For example, in the context of this research, fitness for the characterisation of materials, modelling (e.g., classification and prediction), and decision-making in mining operations. Data that is suitable for use with one application might not fit for use with another application. The fitness of data depends on the data quality parameters: accuracy, completeness, consistency, and precision of data (Veregin, 1999). Accuracy is the measure of the correctness of the information. Completeness refers to the comprehensiveness of the data (no missing values or complete information). Consistency means information from different data sources, but on the same entity does not contradict each other. Precision refers to the degree to which the measurement is reproducible. In other words, repeated measures give the same results. In this research, the quality of each sensor output was assessed based on the accuracy, completeness, consistency, and precision data quality parameters.

2.4.3. KEY GEOLOGICAL ATTRIBUTES DERIVED FROM SENSOR DATA

The crucial information derived from sensor outputs is application dependent. In mining, the essential material properties from the sensor readings are the geological attributes. These key geological attributes include mineralogy, geochemistry, fragmentation, hardness, and ore geometry. Information on the geological attributes can directly be derived from sensor data (e.g., mineralogy) or indirectly inferred from the primary data (e.g., hardness). Table 2.3 shows some of the geological parameters that can directly or indirectly be derived from sensor data. Of the various geological attributes, the parameters considered in this study are mineralogy, geochemistry, separation of ore and waste, ore geometry and fragmentation.

Table 2.3: Some of the geological attributes that can directly or indirectly be derived from sensor data.

Geological attributes	Direct methods	Indirect methods
Mineralogy	X	X
Geochemistry	X	X
Grade	X	X
Hardness	X	X
Ore/waste ratio	X	X
Texture	X	
Lithology		X
Fragmentation	X	
Density	X	X

Imaging or point technologies can provide mineralogical information via direct interpretation of the spectra or using data-driven approaches. Besides, information on minerals can also be indirectly derived from chemical composition data. The imaging techniques that provide mineralogical information include the RGB imagers and infrared

hyperspectral imagers. Likewise, the x-ray diffraction (XRD), infrared (e.g., ASD TerraSpec, FTIR 4300) and Raman spectroscopy (e.g., IRIS echelle) are among the point mineralogical techniques. Mineralogical investigation can describe minerals chemical structure and composition. Such kind of description can permit the analysis of the types and amounts of elements present in a mineral. Primarily, elemental information can directly be acquired using several chemical analysis techniques such as x-ray fluorescence (XRF) and laser-induced breakdown spectroscopy (LIBS). Imaging geologies are suitable techniques to define ore geometry at the mine face or outcrops. Likewise, analysis of rock fragmentation can be performed using the imaging techniques, or Radar reflectivity (this topic is discussed in detail in Chapter 6).

The applicability of sensor technologies for the characterisation of a specific deposit type depends on several factors. Such as, the nature of the deposit (material), the maturity of the techniques, the operational environment, and the material throughput. Deposit types define material properties that are relevant to sensors measurement that the kind of material profoundly influences sensor applicability. Technological readiness level is a crucial factor for the utilisation of the technology in in-situ or ex-situ applications. Matured technologies are desired to ensure rapid practical implementation in mining practices. The operational environment is essential in determining the need for ruggedized systems, especially for operations in harsh environmental conditions (e.g., underground mine). The data acquisition speed of sensor systems required for the analysis of material depends on the material throughput, a high material flow (e.g., conveyor) requires a rapid method that acquires and analyses data in few seconds. Thus depending on the aim of application, sensor choice is determined by the points as mentioned above, among others. Consequently, based on the applicability potential and maturity of the technologies, sensors used in this research are RGB imaging, VNIR hyperspectral imaging, SWIR hyperspectral imaging, MWIR, LWIR, and Raman Spectroscopy. The technologies are briefly described in the next chapter.

REFERENCES

- Benndorf, J., Buxton, M. W. N., Nienhaus, K., Rattmann, L., Korre, A., Soares, A., deJong, A., Jeanne, N., Graham, P., Buttgerreit, D., Gehlen, S., Eijkelkamp, F., Mischo, H., Sandtke, M. & Wilsnack, T. (2015). Real-time mining - Moving towards continuous process management in mineral resource extraction. Proceedings of the 3rd international future mining conference: AusIMM, Sydney, Australia, pp. 1-10.
- Benndorf, J. & Jansen, J. D. (2017). Recent Developments in Closed-Loop Approaches for Real-Time Mining and Petroleum Extraction. *Mathematical Geosciences*, 49, pp. 277-306. doi: 10.1007/s11004-016-9664-8
- Buxton, M. & Benndorf, J. (2013). The use of sensor derived data in optimization along the mine-value-chain: An overview and assessment of techno-economic significance. Proceedings of the 15th International ISM Congress, Aachen, Germany, pp. 324-336.
- Chaulya, S.K. & Prasad, G.M. (2016). Chapter 6 - Formation of Digital Mine Using the Internet of Things. In: S. K. Chaulya & G. M. Prasad (Eds.), *Sensing and Monitoring Technologies for Mines and Hazardous Areas*. Elsevier, pp. 279-350.
- Dalm, M. (2018). Raw material beneficiation in mining – sensor-based sorting opportunities for hydrothermal ore deposits, PhD thesis, Delft University of Technology. Available: <https://repository.tudelft.nl/islandora/object/uuid> [Accessed March 2020].
- Espid, E. (2017). Sensor Systems in Mining Industry. *Nanotechnology Letters*, 1(1): 2.

- Hartman, H. L. & Mutmanský, J. M. (2002). Chapter 1 - Introduction to mining. In: H.L. Hartman & J.M. Mutmanský (Eds.), *Introductory mining engineering*, 2nd ed., John Wiley & Sons, Hoboken, NJ, pp. 1-22.
- Haefner, A., Barnowski, R., Luke, P., Amman, M. & Vetter, K. (2017). Handheld real-time volumetric 3-D gamma-ray imaging. *Nuclear Instruments and Methods in Physics Research Section A: Accelerators, Spectrometers, Detectors and Associated Equipment*, 857, pp. 42-49. doi: 10.1016/j.nima.2016.11.046
- Kern, M., Tusa, L., Leißner, T., van den Boogaart, K. G. & Gutzmer, J. (2019). Optimal sensor selection for sensor-based sorting based on automated mineralogy data. *Journal of Cleaner Production*, 234, pp. 1144-1152. doi: 10.1016/j.jclepro.2019.06.259
- Lessard, J., De Bakker, J. & Mchugh, L. (2014). Development of ore sorting and its impact on mineral processing economics. *Minerals Engineering*, 65, pp. 88-97. doi: 10.1016/j.mineng.2014.05.019
- Lessard, J., Sweetser, W., Bartram, K., Figueroa, J. & Mchugh, L. (2016). Bridging the gap: Understanding the economic impact of ore sorting on a mineral processing circuit. *Minerals Engineering*, 91, pp. 92-99. doi: 10.1016/j.mineng.2015.08.019
- Lööw, J., Abrahamsson, L. & Johansson, J. (2019). Mining 4.0—the impact of new technology from a work place perspective. *Mining, Metallurgy & Exploration*, 36(4), pp. 701-707. doi: 10.1007/s42461-019-00104-9
- National Research Council. (2002). *Evolutionary and Revolutionary Technologies for Mining*. The National Academies Press, Washington, DC.
- Ramjack. (2019). Real-time mine monitoring [Online]. Available: <https://ramjacktech.com/fields-expertise/real-time-monitoring> [Accessed December 2019].
- Veregin, H. (1999). Chapter 12 - Data quality parameters. In: P.A. Longley, M.F. Goodchild, D.J. Maguire, & D.W. Rhind (Eds.), *Geographical Information Systems – principles and applications*, 2nd ed., John Wiley and Sons, New York, USA, pp. 177-189.
- von Ketelhodt, L. & Bergmann, C. (2010). Dual energy X-ray transmission sorting of coal. *Journal of the Southern African Institute of Mining and Metallurgy*, 110(7), pp. 371-378.

3

SENSOR TECHNOLOGY OPTIONS

This chapter describes the state-of-the-art sensor technologies with particular emphasis on the technologies assessed in this study, the material properties the techniques detect and the type of data the sensors produce. It also presents the specification and set-up of the technologies used in this study.

3.1. INTRODUCTION

Sensor technologies operate over a wide range of the electromagnetic spectrum and provide information on various aspects of material properties. As indicated in the previous chapters, the sensor technologies used in this research are RGB imaging, infrared spectroscopy (VNIR, SWIR, MWIR and LWIR), and Raman spectroscopy. The RGB imaging, VNIR, and SWIR hyperspectral imaging are among the imaging technologies that produce image data. Whereas, the point techniques are the MWIR, LWIR and Raman.

Spectroscopy studies the interaction between radiation and matter as a function of the radiation wavelength (λ). Spectroscopic analysis usually requires a source light (electromagnetic radiation), a disperser that separates the light into its component wavelengths and a detector that senses the dispersed light. Spectrometers are the apparatuses that produce spectrum in different forms such as absorption, reflection, emission, and scattering. For example, absorption spectroscopies measure the loss of electromagnetic energy due to its interaction with a sample. This permits the identification of material since the energy levels of most of the atoms and molecules are unique and identifiable. Examples of the interaction of electromagnetic energy with matter are presented in Figure 3.1. The recent development in spectroscopy resulted in state-of-the-art sensor technologies that enable rapid and accurate determination of material composition. The electromagnetic spectrum and the operating wavelength region of the sensor technologies assessed in this study are indicated in Figure 3.2.

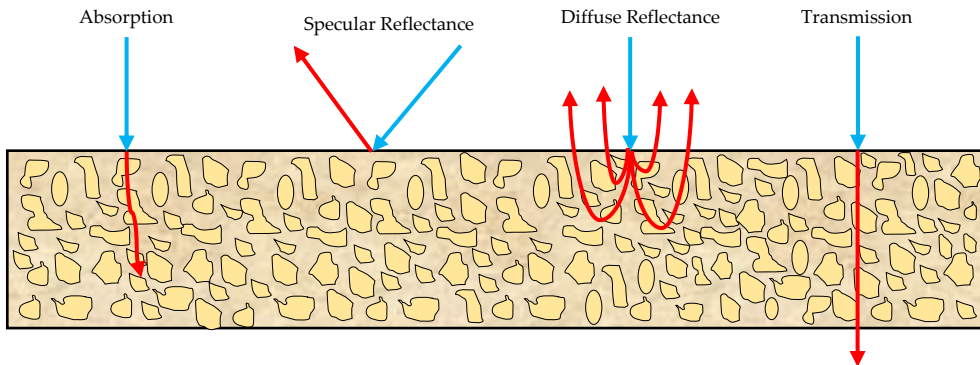


Figure 13.1: Examples of the different phenomena (the red lines) that result from the interaction of light with matter. The blue lines indicate the incident light.

Sensor technologies that produce high-throughput multivariate data are advancing (STEINERT, 2021; SPECTRAL Industries, 2021; TOMRA, 2019). Sensors-derived data are in current use in a wide range of applications. The characterisation of raw material in mining operations is one of the potential application areas. Sensor technologies measure different aspects of material properties. Material property is a broad term that includes optical, electrical, magnetic, mechanical and other physical properties. A fundamental understanding of material characteristics is crucial in selecting suitable sensor solutions for operational decision-making in raw material characterisation. Besides, the selection of sensors for a specific application requires knowledge of sensor parameters. These parameters include operating wavelength range, spatial resolution, spectral resolution, accuracy, precision, sensors field of view (spot size), robustness for environmental

conditions (such as vibration, humidity and dust), detection limit and depth of penetration (e.g., surface or volumetric measurements). The operating wavelength range of a sensor is the window of the electromagnetic spectrum over which the given sensor operates. The spatial resolution specifies the pixel size of an image that provide details or the smallest addressable element the image holds (the distinct detail in the image). The spectral resolution is a measure of sensor ability to resolve spectral features and bands into separate components (width of spectral band). Finer spectral resolutions enable the higher resolution spectral characteristics of the targets to be captured by the sensor. Accuracy is a measure of the closeness of a result to the true or known standard value. On the other hand, precision refers to the reproducibility of multiple measurements. Robustness of sensor systems for harsh environmental conditions (e.g., vibration, humidity and dust) is essential for in-situ applications (e.g., in underground applications). The detection limit of a sensor is the lowest quantity of a substance that can be detected by the system with a general confidence level of 99%. It is one of the important parameters for the use of sensors in low-grade mines since the concentration of minerals or elements of interest are lower in such deposits. Depth of penetration is the depth light, or electromagnetic radiation can penetrate a material. Whereas, the sensor field of view or measuring spot refers to the size of the measured area of a single measurement.

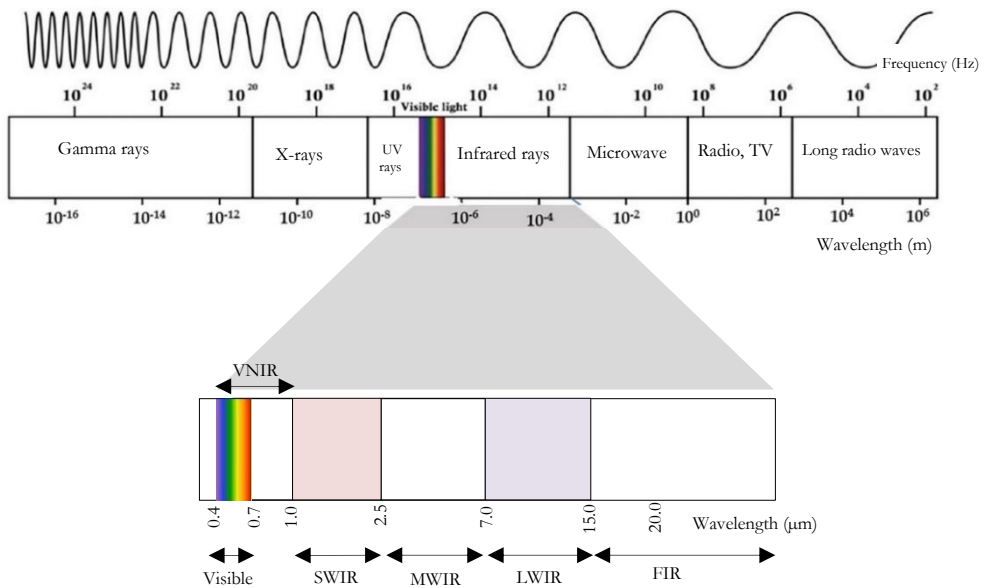


Figure 3.2: The electromagnetic spectrum and the different regions of the infrared range.

Sets of sensor solutions that are potentially applicable in raw material characterisation are available. These techniques include infrared technologies, LIBS, Raman spectroscopy, DE-XRT, and XRF. Previous studies indicated the use of sensor technologies for the characterisation of material in geological surveys and mining applications. For example, Death et al. (2008) showed the potential use of LIBS for on-line compositional determination of iron ore samples. Likewise, Kruse (1996) demonstrated the use of SWIR for rapid and enhanced production of drill logs and geological maps, as well as in the

definition of alteration zones. More recently, Culka et al. (2016) demonstrated the applicability of a handheld Raman spectrometer for in-situ detection and discrimination of arsenate minerals at outcrops. In another study, Wells and Ramanaidou (2015) assessed the utility of Raman spectroscopy in the automated in-situ mapping of iron ore and gangue mineralogy. Recent studies show, the use of XRF analysers for on-line in-situ elemental analysis of bulk materials (Orbit Technologies, 2017; ThermoFisher, 2017). On the other hand, Alov et al. (2010) used an XRF analyser over the conveyor belt to determine the quality of the iron ore mixture. These studies, among other numerous publications, indicate the potential benefits and opportunities of the use of sensors for raw material characterisation in mining operations.

In this research, the explored technologies (mentioned above) were assessed to address the different geological parameters that are crucial in mining. The rationales behind the choice of each technology for the analysis of the outlined geological attributes are presented in Table 3.1. The validation of the sensors measurements was performed using the conventional laboratory techniques namely XRD, XRF, and inductively coupled plasma-mass spectrometry (ICP-MS). A brief description of the investigated techniques and the validation technologies is presented in the sections that follow.

Table 3.1: Summary of the sensor technologies, the analysed geological attributes and the rationale for each sensor choice in this work.

Sensor Technology	The analysed geological	Why this sensor?
RGB Imaging	<ul style="list-style-type: none"> • Mineral mapping • Fragmentation analysis • Ore geometry definition 	It can be used for mapping of visually distinct minerals, edge detection, and geological structures identification.
VNIR	<ul style="list-style-type: none"> • Ore–waste discrimination • Minerals identification 	The VNIR exhibits weak spectral signals for most of the sulphide minerals. Thus, the technique was assessed for the identification of the minerals and separation of ore–waste materials in the polymetallic sulphide deposit. Besides, the VNIR region is ideal for the identification of iron oxides; in this study, the possibility of identifying the iron oxides in sulphide mineral mixture was assessed.
SWIR	<ul style="list-style-type: none"> • Ore–waste discrimination • Minerals identification 	The sulphide minerals do not exhibit spectral features in the SWIR region, the featureless nature of the minerals was used to discriminate the ore and waste materials. SWIR is an ultimate technique for the identification of alteration minerals; thus, it was also assessed for the identification of the alteration minerals in sulphide matrix.
MWIR	<ul style="list-style-type: none"> • Ore–waste discrimination • Elemental concertation indication • Quantitative mineralogical indication 	MWIR is an understudied region of the infrared spectra. Even though the sulphide minerals do not show particular absorption features in this region, the observed characteristic reflectance pattern of the minerals was assessed to establish a relationship between the MWIR spectra and the geological attributes (ore–waste separation, elemental indication, and quantitative mineralogical indication).
LWIR	<ul style="list-style-type: none"> • Ore–waste discrimination • Elemental concertation indication • Quantitative mineralogical indication 	The LWIR is suitable for the identification of rock-forming minerals and the carbonates. The possibility of detecting the waste material minerals (e.g., carbonates and silicates) were used for the separation of the ore and waste material. Besides the observed characteristic reflectance pattern of the sulphide minerals in the LWIR spectra were assessed to establish relationships between the LWIR spectra and the geological attributes (ore-waste separation, elemental indication, and quantitative mineralogical indication).
Raman	<ul style="list-style-type: none"> • Mineral identification • Ore–waste separation 	Raman is a well-established technique for the identification of a wide range of minerals, such as the sulphide, silicates, and carbonates minerals. Thus, the technique was assessed for the identification of minerals and separation of ore-waste materials.

3.2. INFRARED SPECTROSCOPY

Infrared spectroscopy is one of the most useful analytical techniques for the evaluation of organic and inorganic materials (Chukanov and Chervonnyi, 2016; Griffiths and Haseth, 2007; Smith, 2011). It is a well-established technique that provides rapid, relatively high

signal to noise ratio spectral data, and highly reproducible analytical measurements. Consequently, infrared is widely used in remote sensing, laboratories and field-based applications. The technique is a mineralogical technique that provides information on the functional groups (e.g., OH and CO₃). Then, the information on the functional groups is used to identify various type of minerals.

Infrared sensors can be passive or active (McGrath and Scanail, 2013). In the passive form, the sensors do not generate or radiate energy for detection; instead, they rely on heat detection or measures the infrared light radiated from the material of interest. On the other hand, active sensors employ an infrared light source to illuminate the sample. When infrared light interacts with a molecule, the bonds between molecule constituents selectively absorb the infrared radiation energy at specific wavelengths. The consequent changes in the vibrational energy level of the molecules can be observed through signals at particular wavelengths in the infrared spectrum. The infrared spectra can be measured as absorption, emission and reflection. The technique is also used in determining subtle molecular structure variations in a wide variety of minerals.

The infrared region of the electromagnetic spectrum extends from $\lambda = 0.7$ to $1000 \mu\text{m}$ with a corresponding wavenumber range from $14,285$ to 10.0 cm^{-1} (Smith, 2011; Stuart, 2004). The spectral range is subdivided into different regions, and defined as NIR (0.7 to $1.0 \mu\text{m}$), SWIR (1.0 to $2.5 \mu\text{m}$), and far-infrared (FIR: 15.0 to $1000 \mu\text{m}$) (Gupta, 2003; Kerekes, 2009; Patrice et al., 2009; Rogalski and Chrzanowski, 2014). Besides, the MWIR and LWIR are the subsets of the infrared that correspond to the wavelength ranges of 2.5 to $7.0 \mu\text{m}$ and 7.0 to $15.0 \mu\text{m}$, respectively (Gupta, 2003; Hackwell et al., 1996; Kerekes, 2009; Patrice et al., 2009; Rogalski and Chrzanowski, 2014). NIR sensors can provide accurate identification and an indication of iron oxides, and sulphide minerals (Spectral Evolution, 2015; Szalai et al., 2013). SWIR is one of the most widely used infrared technologies in the identification and discrimination of phyllosilicates, sulphates and carbonates (Sun et al., 2001). SWIR is commonly employed in the identification of alteration minerals associated with mineralization. On the other hand, LWIR permits the identification of rock-forming minerals, whereas FIR can be employed in the rare earth mineral analyses (Clark, 1999; Karr and Kovach, 1969). The measurable material properties using the explored sensor technologies are presented in Table 3.2.

Table 3.2: The operating wavelength range of the explored sensor technologies and measurable material properties in this work (based on Chukanov and Chervonnyi, 2016; Gupta, 2003; Hackwell et al., 1996; Kerekes, 2009; Patrice et al., 2009; Rogalski and Chrzanowski, 2014).

Sensor technology	Spectral range	Material property
RGB Imaging	0.4 to $0.7 \mu\text{m}$	Colour, Reflection, brightness, transparency
VNIR	0.4 to $1.0 \mu\text{m}$	Reflection, absorption
SWIR	1.0 to $2.5 \mu\text{m}$	Reflection, absorption
MWIR	2.5 to $7.0 \mu\text{m}$	Reflection, absorption
LWIR	7.0 to $15 \mu\text{m}$	Reflection, absorption, heat conductivity, emission
Raman	0.18 to $1.4 \mu\text{m}$	Scattering of radiation

The recent development of infrared technologies resulted in portable, rapid, sensitive, and versatile systems (Agilent, 2017; Malvern Panalytical, 2020). This dynamic advancement leads to an increased establishment of the technique in mining applications such as exploration studies, drill core logging, ore sorting, and mineral processing. The other main advantage of the infrared technology is its operability in a more extensive spectral range since this is essential to allow the characterisation of a great variety of minerals in different deposit types. The infrared spectroscopies offer both imaging and point infrared spectrometers. This permits the use of the technique in minerals profiling, fingerprinting, quantifying of minerals abundance, and mapping of the spatial distribution of minerals. Thus, the technique has great potential and benefits for material characterisation in mining operations. Some of the potential use of the infrared, RGB and Raman techniques in material characterisation are presented in Table 3.3. A detailed description of the characteristics of the infrared techniques, their potential applications and benefits in material characterisation is presented in the sections that follow.

Table 3.3: Some of the potential minerals that can be identified with different sensors (based on Haskin et al., 1997; TERRACORE, 2016; TOMRA, 2020; von Ketelhodt and Bergmann, 2010; Wang et al., 1995).

Sensor	Minerals that can be detected or identified
RGB Imaging	<ul style="list-style-type: none"> • Iron oxides e.g., hematite • Sulphide minerals e.g., galena and pyrite • Industrial minerals e.g., talc
VNIR	<ul style="list-style-type: none"> • Fe oxides e.g., hematite and goethite • Sulphides e.g., pyrite, galena • Silicate e.g., olivine and pyroxene
SWIR	<ul style="list-style-type: none"> • Clay minerals e.g., illite and kaolinite • Sulphate e.g., alunite and gypsum • Chlorite e.g., clinochlore • Mica e.g., muscovite • Amphibole e.g., actinolite
MWIR	<ul style="list-style-type: none"> • Sulphates e.g., alunite • Silicate e.g., chlorite and epidote
LWIR	<ul style="list-style-type: none"> • Silicate e.g., olivine, pyroxene and silica • Phosphate e.g., apatite • Carbonates e.g., calcite and dolomite • Sulphate e.g., gypsum and alunite
Raman	<ul style="list-style-type: none"> • Sulphides e.g., sphalerite, pyrite, chalcopyrite, arsenopyrite • Carbonates e.g., calcite and dolomite • Sulphate e.g., gypsum, anhydride • Silicate minerals • Iron oxides

3.2.1. VISIBLE AND NEAR-INFRARED (VNIR)

The VNIR sensor is a well-established technology that operates over the 0.4 to 1.0 μm wavelength range of the electromagnetic spectrum. VNIR combines the full visible region with the adjacent portion of the infrared. Visible light and near-infrared light is absorbed and emitted by molecules and atoms as the electrons move from one energy level to another (Clark, 1999; Hunt, 1977). The electronic molecular process produces the spectral features

within the VNIR range and allows the identification of minerals. VNIR technology provides highly repeatable analytical measurements, with an excellent spectral resolution. The current advancement of the VNIR technology resulted in rapid and portable systems that acquire data with nanoscale spatial resolution. Both point spectrometers and hyperspectral imagers that operate in the VNIR range of the electromagnetic spectrum are available from multiple manufactures. For example, Malvern Panalytical, (2020) and SphereOptics, (2019), manufacture portable point VNIR systems. Manufactures such as Specim offer hyperspectral imagers that operate in the VNIR range (Table 3.4). The portability of the available systems ensures the possibility of impeding the sensor in available platforms. VNIR is insensitive to smaller particles like dust and water in the air (Nienhaus et al., 2014). The technology has great potential for in-situ online analysis materials in mining applications.

The VNIR sensor operates over a limited spectral range of the electromagnetic spectrum; however, it provides valuable information about some of the minerals such as iron oxides. For example, Haest et al. (2015) and Szalai et al. (2013) used VNIR sensors to characterise Fe-bearing minerals. In another study, the technique was used in the separation of metal ores and waste materials (Shankar, 2015; Spectral Evolution, 2015). In another study, Bolin and Moon, (2003) showed the potential use of the technology for the identification of some of the sulphide minerals in ultramafic platinum-palladium ores. Besides, high-speed VNIR sensors are available for drill core scanning as well as sensor-based sorting applications. For example, researchers and manufacturers indicate the potential use of the technology for sorting of materials (Goetz et al., 2009; Robben and Wotruba, 2019; TOMRA, 2019).

Table 3.4: Examples of portable VNIR spectrometers and their specifications (Source: Malvern Panalytical, 2020; Specim, 2019).

Data type	Picture	Manufacture	Dimension	Weight	Operating wavelength range
Point spectrometer		Malvern Panalytical	90 x 140 x 215 mm	1.2 kg	0.32 - 1.07 μm
Imager		Specim	207 x 91 x 74 mm	1.3 kg	4.0 - 1.0 μm
Imager		Specim	150 x 71 x 85 mm	1.4 kg	0.4 - 1.0 μm



3.2.2. SHORT-WAVE INFRARED (SWIR)

SWIR sensors are well-established technologies that operate over the spectral range of 1.0 to 2.5 μm (Table 3.2). In SWIR spectroscopy, absorption features are mainly related to overtones of stretching vibrations and combinations of stretching and bending vibrations (Clark, 1999). These diagnostic overtones and combinations are used for fingerprinting of materials. In the spectral range of SWIR, the molecular bonds that produce characteristic absorption features include H_2O , OH , CO_3 , NH_4 , Al-OH , Fe-OH and Mg-OH (Thompson et al., 1999; AusSpec, 2008). Absorption in the SWIR region is related to the molecular bonds, whereas, the VNIR absorption is associated with sub-atomic transitions.

The SWIR is one of the most widely used infrared technologies that allow a rapid and non-destructive analysis of materials. The technique is applicable for the analysis of a wide range of minerals such as hydroxylated silicates, phyllosilicates, carbonates, sulphates, and ammonium-bearing minerals (AusSpec, 2008; Clark, 1999; Herrmann et al., 2001; Sun et al. 2001). It is mainly used for the investigation of the alteration minerals, therefore; it can also be used for the exploration of hydrothermal deposits through the detection of minerals resulted from hydrothermal alteration (Thompson et al., 1999). Numerous previous studies indicate the use of the technique for mineralogical studies, such as in mineral mapping (Harraden et al., 2013; Herrmann et al., 2001; Kruse and Perry, 2013), drill core logging (Kruse, 1996), the indication of mineralogical concentration on moving conveyor belt (Goetz et al., 2009), and separation of ore and waste materials (Dalm et al., 2017).

Multiple manufactures supply laboratory-based and mobile SWIR range imaging and point spectrometers. Some examples of portable point SWIR analysers include ASD TerraSpec and PSR+ 3500 (Malvern Panalytical, 2019; SphereOptics, 2019). On the other hand, Corescan, Photonics, and Specim manufacture the SWIR hyperspectral imagers (Corescan, 2019; Photonics Online 2019; Specim, 2019). Examples of portable point and imaging SWIR spectrometers are shown in Table 3.5. The SWIR imagers are mainly used for rock chip samples and drill cores scanning whereas the portable point SWIR analyser can be used for drill cores, rock chips, or in-situ analysis of materials. Thus, the technique has great potential for use along the mining value chain, such as in mine face mapping, drill core logging and material sorting (Haest et al., 2015). The dynamic development of the technique, together with its enormous applicability potential ensures its potential benefits in mining applications.

Table 3.5: Examples of SWIR point spectrometer that simultaneously acquire spectral data in VNIR and SWIR ranges, and SWIR imager (Source: Malvern Panalytical, 2019; Specim, 2019).




Data type	Picture	Manufacturer	Dimension	Weight	Operating wavelength range	Data acquisition speed
Point spectrometer TerraSpec Halo		Malvern Panalytical	100 x 300 x 310 mm	2.5 kg	0.35 – 2.5 μm	in seconds
Imager SWIR		Specim	470 x 176 x 178 mm	14 kg	1.0 – 2.5 μm	up to 450 frames per second

3.2.3. MID-WAVE INFRARED (MWIR)

The MWIR portion of the electromagnetic spectrum covers the wavelength region between 2.5 to 7.0 μm (Table 3.2). MWIR radiation triggers a change in the vibrational energy level of the molecules and causes molecular vibrations. The signals from the molecular vibrations are measured as the MWIR spectrum. Vibration mode is different for each molecule that the infrared spectrum can be analysed to get information on different functional groups (Hollas, 2004; El-Azazy, 2018). The functional groups can further be related to mineralogy. MWIR is the region in which many fundamental hydroxyl groups stretching vibration occurs (Li et al., 2015; Coates, 2000).

The MWIR is the least-explored region of the electromagnetic spectrum when compared to the other infrared techniques. This is mainly due to the limited historical instrumental development of the MWIR sensor. Most of the existing MWIR systems are designed integrated with the LWIR sensors. For example, Table 3.6 shows specifications of a point spectrometer that acquires MWIR and LWIR data simultaneously, and MWIR imagers, respectively. Recently, portable, rapid and non-destructive MWIR sensors that acquire both point and image data are emerging (Agilent, 2017; FLIR, 2019; Specim, 2019; SphereOptics, 2020; TELOPS, 2019). Recent studies indicated the potential use of the technique for the characterisation of organic and inorganic materials in different applications (Li et al., 2015, Guatame-Garcia et al., 2018; Yitagesu et al., 2011). However, in raw material characterisation, the MWIR is still an understudied region of the electromagnetic spectrum.

Table 3.6: Examples of MWIR and LWIR spectrometers and their specifications. The point spectrometer collects MWIR and LWIR data simultaneously. The imagers acquire data in MWIR region. (Source: Agilent, 2017; FLIR, 2019; Specim, 2019).

Data type	Picture	Manufacture	Dimension (L x W x H)	Weight	Operating wavelength range	Data acquisition speed
Point spectrometer FTIR 4300		Agilent	100 x 190 x 350 mm	2 kg	1.9 – 16.67 μm	30 s
Imager Specim FX50		Specim	280 x 202 x 169 mm	7 kg	2.7 – 5.3 μm	up to 380 frames per second
Thermal Imager FLIR Neutrimo LC		FLIR	74 x 46 x 61 mm	< 380 g	3.4 to 4.9 μm	Frame rate 60 Hz

3.2.4. LONG-WAVE INFRARED (LWIR)

The LWIR technologies operate over the 7.0 to 15 μm wavelength range of the electromagnetic spectrum (Table 3.2). The working principle of the LWIR is similar to the MWIR technique. Like other infrared technologies, LWIR is a molecular technique that provides information on the functional groups. It measures the reflectance, absorbance, transmittance and thermal emissivity of materials. These properties differ among various types of materials. Thus, the technique can be used for the characterisation of a wide range of materials. The wavelength range from 3 to 14 μm is also known as the thermal infrared region. Thus, the MWIR and LWIR regions are also referred to as the first and the second thermal imaging bands, respectively (Holst, 2000). MWIR and LWIR range thermal imagers that acquire emissivity of materials are available from multiple suppliers (FLIR, 2019; Quantum Design, 2019; SIERRA-OLYMPIC, 2019). The thermal imagers can be used for military applications (Andersson, 2017), food quality assessment (Teena and Manickavasagan, 2014) as well as mineral mapping (Aslett et al., 2018; Riley and Hecker, 2013).

The LWIR sensors are widely used for mapping of minerals in remote sensing applications (Ayling et al., 2016; Gordon et al., 2016; Hecker et al., 2019; McDowel et al., 2015; Notesco et al., 2016; Tanya et al., 2019). However, there are also laboratory-based

LWIR analysers (e.g., TELOPS's Hyper-Cam,), drill core loggers (e.g., HyLogger, Specim's AisaOWL) and field-based LWIR scanners such as TELOPS's Hyper-Cam (TELOPS, 2019; Specim, 2019; Schodlok et al., 2016). The recent development of the technology resulted in rapid and portable (point and imaging) LWIR spectrometers that can be used for in-situ analysis of materials (Agilent, 2017; Specim, 2019). An example of a portable LWIR analyser is shown in Figure 3.3.

The LWIR technique is a useful tool for the identification of rock-forming minerals (most of the silicates), carbonates, sulphates and phosphates (Clark, 1999; Lorenz et al., 2018; Tanya et al., 2019; TERRACORE, 2016). In LWIR spectra, the silicon-oxygen bond (Si–O) stretching vibrations is the dominant spectral features (Baldrige et al., 2009). This makes it suitable for the analysis of feldspars, quartz, as well as other silicates. Numerous studies indicated the usability of the techniques for mineralogical analysis. For example, Hecker et al., (2012) used LWIR to determine the minerals modes of granitoid rocks. Similarly, Kuosmanen et al. (2015) applied LWIR for the identification and prediction of minerals compositions in rock samples. In another study, the technique was used for mapping rock-forming minerals that are indicative of sedimentary and meta-sedimentary lithology (Aslett et al., 2018). The recent development of the technology coupled with greater applicability potential indicates the usability of the technique for in-situ on-line analysis of materials in mining operations.



Figure 3.3: An example of a LWIR imager (Source: Specim, 2019).

3.3. RAMAN SPECTROSCOPY

Raman spectroscopy is a well-established laser-based molecular technique for the analysis of both organic and inorganic materials. The technique can be used for the identification of chemical composition, determination of sample stress and characterisation of molecular structure (Heintz, 2014; HORIBA Scientific, 2015). The excitation wavelength (laser) for Raman spectroscopy ranges from ultra-violet through visible to near-infrared of the electromagnetic spectrum. The technique uses a monochromatic laser beam to irradiate a sample with a particular well-defined wavelength. The laser interacts with the functional groups of the sample molecules and originates a scattered light. Most of the scattered light has the same frequency as the incident laser, and this is called Rayleigh scattering. The scattered light with a frequency different from that of incident light is called Raman scattering (White, 2005). The Raman scattered light is detected by the spectrometer to produce the Raman spectrum. Thus, the peaks in the spectrum are the scattered light that is shifted from the Rayleigh peak. These shifts produced by Raman scattering are called Stokes and anti-Stokes shifts. Stokes peaks are those with wavelengths longer than the

incident light. Whereas, anti-stokes peaks are those peaks whose wavelengths are shorter than that of the incident light. The intensity of the stokes peaks is higher than that of the anti-Stokes peaks. Hence, the stokes peaks are used in Raman spectrometry (Bumbrah and Sharma, 2016). Figure 3.4 shows a schematic sketch of a Raman spectrum with the stokes and anti-stokes peaks. The width and intensity of the resulting Raman peaks are influenced by the arrangement, symmetry, and the strength of chemical bonds of atoms in the unit cell (White, 2005). Besides, the wavelength bands at which the Raman shift occur are used to identify materials using the characteristic fingerprinting pattern.

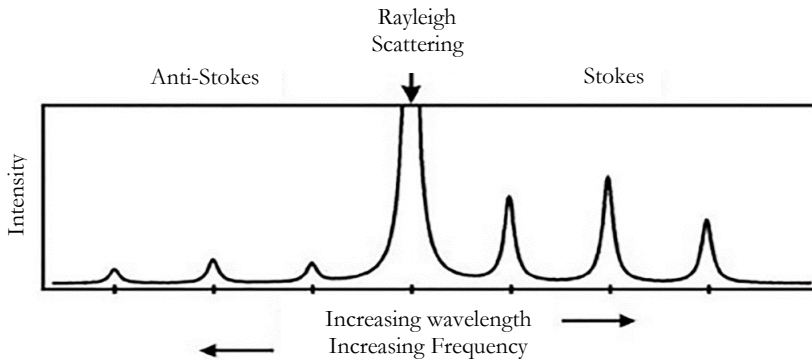


Figure 3.4: A schematic sketch of a Raman spectrum with the Stokes and anti-Stokes peaks (Source: White, 2005).

Raman spectra of minerals reveal sharp and mainly non-overlapping features. This makes Raman a powerful technique for mineralogical analysis, especially in the presence of a mixture (Gaft et al., 2005). The technique can be used for the identification of a wide range of minerals such as iron ore oxides, carbonates, silicate, sulphides and sulphate (Gaft et al., 2005; Griffith, 1975; Mernagh and Trudu, 1992; White, 1975). On the other hand, Raman has a weak signal than the infrared technologies. Thus, noise might obscure useful Raman peaks and results in a low signal-to-noise ratio. However, it is an excellent complementary technique that provides highly specific molecular fingerprints of material through non-destructive analysis. Raman spectroscopy can be used for remote analysis of materials (Gaft et al., 2005). The recent development of the technique offers portable high-resolution analysers that acquire reliable data at high speed. This shows the potential usability and benefits of the technique for rapid and in-situ analysis of materials in mining applications. For example, drill core and chip scanning Raman systems are currently in use in the iron ore industry (Ramanaidou et al., 2015). Figure 3.5 shows an example of a portable Raman system applicable in material characterisation.



Dimension: 220 x 195 x 80 mm (incl. CMOS camera)

Weight: 3 kg (incl. CMOS camera)

Data acquisition speed up to few seconds

Figure 3.5: An example of a portable IRIS echelle Raman spectrometer (Source: Spectral industries, 2020).

3.4. RGB IMAGING

The RGB imaging sensors operate in the visible range (0.4 to 0.7 μm) of the electromagnetic spectrum. RGB sensor is a multispectral sensor that provides RGB images (often called true colour images). The colour of each pixel of an RGB image is determined by the combination of the red, green and blue intensity values. RGB imagers characterise the reflectance property of a material and deliver three (red-green-blue) spectral band information often using three independent charge-coupled devices (CCD sensors). As an alternative, some cameras capture the three-band information using complementary metal-oxide-semiconductor (CMOS) technology. An RGB camera captures images using a line scan technique and a frame (area scan) sensor. For image capturing, frame cameras use a two-dimensional array of sensors. Line scan cameras have a 1-dimensional array of sensors. RGB images are stored as 24-bit images, where the red, green and blue components are 8 bits each. Therefore, RGB images can potentially show 16 million colours.

RGB sensors are matured and well-established technologies with rapid data processing capability. RGB imaging systems are easy to use, portable, fast, non-destructive, low-cost, and do not need complicated data analysis. Thus, its portability makes it ideal for embedding and surface mounting in different platforms. One potential such application is sidewall imaging at a mine face. Moreover, RGB sensors are robust to environmental conditions and have remote sensing capability that they can be used for in-situ applications in various environments. Multiple suppliers manufacture RGB sensors as consumer digital cameras. Therefore, commercial availability is not a concern.

The RGB imaging sensor is sensitive to colour differences or visual appearances. Thus, it has great potential for mapping visually distinct minerals. RGB cameras can be used for creating orthomosaic maps that show the entire area under investigation. This indicates the potential use of the technique for mapping minerals at mine faces or outcrops. The technology can be used for the mapping of minerals/lithological units. It produces images that can be seen by human eyes. The data becomes instantly understandable to viewers or operators, e.g., for quality control applications. In general, the technology can be directly applied in colour detection or indirectly for shape recognition of geological units.

The application of RGB images for material characterisation is very limited; so far, it is used in recycling, sorting and agricultural applications. TOMRA (2020) showed the use of a high-spatial-resolution and colour sensitive RGB camera for minerals (talc and calcite) sorting. Other studies showed the potential use of the RGB imagers for automatic detection, classification of plant leaf diseases and crop monitoring (Singh and Misra, 2017;

Lebourgeois, et al., 2008). The technology can be used for colour sorting of different material streams and surface inspection of natural material (LLA Instruments GmbH, 2017; STEINERT, 2020; REDWAVE, 2020; Richter et al. 2016).

3.5. VALIDATION CHEMICAL ANALYSIS

The conventional laboratory-based techniques namely XRF, ICP-MS and XRD were used for the validation of the material characterisation results from the investigated sensor technologies in this work. The ICP-MS and XRF measurements were performed using 115 and 60 samples, respectively. Whereas, the XRD measurements were performed using 56 samples. Descriptions of each of the validation techniques are presented in the sub-sections that follow.

3.5.1. X-RAY FLUORESCENCE (XRF)

XRF is a well-established analytical technique used to determine the elemental composition of materials. Easy of automation and versatility are the most important features of the technology. The recent development and commercialisation of the XRF analyser, offer portable and ruggedized systems that can be utilised in harsh environments (e.g., underground mining operations). The technology offers a wide range of applications within diverse fields. For example, in mineral exploration, ore grade control, mineral processing, mine waste characterisation, material recycling, and environmental soil screening. Portable and laboratory-based XRF analysers are available from multiple suppliers. XRF is also a standard geochemical analysis method in analytical laboratories that analyse multiple major and minor elements simultaneously down to the ppm level. In this research, a conventional laboratory-based Malvern PANalytical Axios mAX wavelength dispersive x-ray fluorescence (WD-XRF) system was used to acquire quantitative elemental information. Liborate fusion was used to achieve a high detection limit and upper limit. This method has no recovery issue that may exist with acid digestions, especially when the sulphide content is high within the sample.

3.5.2. INDUCTIVELY COUPLED PLASMA-MASS SPECTROMETRY (ICP-MS)

ICP-MS is the most widely used method for the determination of elemental concentrations in both organic and inorganic samples. It is a well-established laboratory-based technique capable of detecting most of the periodic table elements down to the ppm-level (Taylor, 2001; Thomas, 2008). The technique is used for the determination of elemental concentrations in broad subject areas, such as environmental monitoring, metallurgy, geochemical analysis, and clinical researches. In this research, a conventional laboratory-based ICP-MC was used to acquire quantitative elemental information. Aqua Regia partial digestion was used to enhance the detection limit and maximise the number of analysed elements. This method is recommended for multi-elemental analysis of base metal-sulphides.

3.5.3. X-RAY DIFFRACTION (XRD)

XRD is a conventional laboratory-based technique for qualitative and quantitative analysis of a wide range of materials. The technique provides detailed information about the chemical composition, grain size, and structure of crystalline materials. The recent development of the technology resulted in portable XRD systems that allow a rapid in-situ

analysis of major and minor mineral components, for example, Olympus's TERRA II Portable XRD analyser (OLYMPUS, 2019). In this research, qualitative and semi-quantitative mineralogical data were acquired using a laboratory-based XRD analyser. The XRD data were used to validate the analysis results of the explored sensor technologies.

3.6. INSTRUMENTS USED IN THIS STUDY

The specifications of the spectrometers used in this work and the types of data they produced are described in Tables 3.7 and 3.8, respectively. The RGB camera used in this study is a commercially available consumer Nikon camera (Figure 3.6). The raw data from RGB imagers are image data, with three bands of information (multivariate) and the R-G-B values are continuous. Whereas, the classified RGB images (the mineral maps) show qualitative categorical data (mineral types). Thus, RGB raw data is transformed into discrete information. The VNIR and SWIR hyperspectral images were acquired using a Specim's Lab Scanner. The VNIR and SWIR images were recorded using a single set-up but separate detectors. Pictures of the sensors and the specifications are presented in Figure 3.7 and Table 3.7, respectively. The SWIR hyperspectral imagers provide multivariate (288 bands) image data. Similarly, the VNIR hyperspectral camera provides multivariate (196 bands) image data. On the other hand, the point MWIR and LWIR data are continuous multivariate data with 5500 and 1691 variables, respectively. Two Raman spectrometers were investigated, one is the Bruker's Raman microscopy, and the other one is the IRIS echelle Raman spectrometer. The laser sources and other specification of the Raman systems are presented in Table 3.7. Raman spectroscopy provides a point continuous multivariate data and the Raman data used in this study has 2907 variables.

Table 3.7: An overview and specifications of the sensors used in this study.

	Sensor	Manufacturer	Spectral range	Spectral resolution	Image size (px)	Spatial resolution	Bands
RGB Imaging	D7100 digital camera	Nikon	0.4 to 0.7 μm	-	6000 x 4000 px frame	0.25 mm	3
Infrared	PFD-65-V10E	Specim	0.4 to 1.0 μm	3 nm	656 px per line	0.28 mm	196
	SWIR3	Specim	1.0 to 2.5 μm	12 nm	384 px per line	0.28 mm	288
	FTIR 4300	Agilent	1.9 to 16.67 μm (5200 to 600 cm^{-1})	4 cm^{-1}	Point measurement	~ 2.0 mm	-
Raman	Raman microscopy	Bruker	0.18 to 0.8 μm (785 nm and 532 nm laser sources)	3 cm^{-1}	Point measurement	1 mm	-
	IRIS echelle Raman spectrometer	SPECTRAL Industries	0.35 to 0.8 μm (532 nm laser source)	0.07 to 0.3 nm	Point measurement	1 mm	-

Table 3.8: Summary of the data types and data volumes of the sensor technologies used in this study.

Sensors	Operating Wavelength (μm)		Data types		Data volume per a single measurement
RGB Imaging	0.4 - 0.7	Image	Multivariate (3 bands)	Continuous	Per 1 x 1 m ² area ~ 13 MB
VNIR Hyperspectral Imaging	0.4 – 1.0	Image	Multivariate (196 bands)	Continuous	Per a rock chip sample ~ 239 MB
SWIR Hyperspectral Imaging	1.0 – 2.5	Image	Multivariate (288 bands)	Continuous	Per a rock chip sample ~ 215 MB
MWIR	2.5 - 7.0	Point	Multivariate 5500 variables	Continuous	Per a single measurement ~ 130 KB
LWIR	7.0 – 15.0	Point	Multivariate 1691 variables	Continuous	Per a single measurement ~ 50 KB
RAMAN	0.24 – 1.06	Point	Multivariate 2907 variables	Continuous	Per a single measurement ~ 124 KB



Dimension: 135.5 x 106.5 x 76 mm
 Weight: ~ 0.68 kg
 Data acquisition speed up to 2 seconds

Figure 3.6: Photograph of the Nikon RGB camera used in this study.

a)



Dimension: 231 x 80.5 x 78 mm
 Weight: 1.8 kg
 Data acquisition speed up to 150 fps

b)



Dimension: 470 x 176 x 178 mm
 Weight: 14 kg
 Data acquisition speed up to 450 fps

Figure 3.7: Specim's (a) VNIR, and (b) SWIR hyperspectral imagers used in this work, the cameras were mounted on LabScanner stage (Source: Specim, 2019).

A modern Fourier-transform infrared spectrometer (FTIR) has considerable advantages over other infrared spectrometers. For example; it has improved the quality of infrared spectra (a higher signal to noise ratio), short data acquisition time, higher accuracy, higher precision, wider scan range and high resolution (Agilent, 2017; Chemistry libretexts, 2017; Perkins, 1987; Smith, 2011; Stuart, 2004). Advances in technology now permit the development and application of portable instrumentation. This indicates that the technology

has the potential for real-time (in-situ) measurement of mineralogy (Agilent, 2017). In this study, Agilent FTIR 4300 handheld spectrometer was used to collect the MWIR and LWIR data, simultaneously. The instrument is depicted in Table 3.6, and the specification is presented in Table 3.7.

Overall, sensor data provide information about the different aspects of material properties. This information is crucial in diverse applications, including mining. However, not all-essential information can directly be interpreted from the spectral since the required information cannot directly be observed in the spectral data. Therefore, there is a need for ultimate methodological approaches for a better understanding and maximised analysis of sensor outputs. These methodological approaches could be the multivariate data analysis methods and data fusion approaches. The next two chapters describe the test case area and the methodological approaches developed in this study, respectively.

REFERENCES

- Agilent. (2017). FTIR Compact & Portable Systems [Online]. Available: <http://www.agilent.com/en/products/ftir/ftir-compact-portable-systems/4300-handheld-ftir> [Accessed February 2017].
- Aloy, N. V., Volkov, A. I., Ushero, A. I., Ishmets'ev, E. N. & Ushero, E. V. (2010). Continuous X-ray fluorescence analysis of iron ore mixtures in the production of agglomerate. *Journal of Analytical Chemistry*, 65(2), pp. 169-173. doi: 10.1134/S1061934810020127
- Andersson, K. (2017). Modelling the impact of surface emissivity on the military utility of attack aircraft. *Aerospace Science and Technology*, 65, pp. 133-140. doi: 10.1016/j.ast.2017.02.017
- AusSpec. (2008). G-MEX Spectral interpretation field manual (3 ed.). AusSpec International Ltd.
- Aslett, Z., Taranik, J. V. & Riley, D. N. (2018). Mapping rock-forming minerals at Boundary Canyon, Death Valley National Park, California, using aerial SEBASS thermal infrared hyperspectral image data. *International Journal of Applied Earth Observation and Geoinformation*, 64, pp. 326-339. doi: 10.1016/j.jag.2017.08.001
- Ayling, B., Huntington, J., Smith, B. & Edwards, D. (2016). Hyperspectral logging of middle Cambrian marine sediments with hydrocarbon prospectivity: a case study from the southern Georgina Basin, northern Australia. *Australian Journal of Earth Sciences*, 63(8), pp. 1069-1085. doi: 10.1080/08120099.2016.1204625
- Baldrige, A. M., Hook, S. J., Grove, C. I. & Rivera, G. (2009). The ASTER spectral library version 2.0. *Remote Sensing of Environment*, 113(4), pp. 711-715. doi: 10.1016/j.rse.2008.11.007
- Bolin, B. J. & Moon, T. S. (2003). Sulfide detection in drill core from the Stillwater Complex using visible/near-infrared imaging spectroscopy. 68(5), pp. 1561-1568. doi: 10.1190/1.1620630
- Bumrah, G. S. & Sharma, R. M. (2016). Raman spectroscopy – Basic principle, instrumentation and selected applications for the characterisation of drugs of abuse. *Egyptian Journal of Forensic Sciences*, 6(3), pp. 209-215. doi: 10.1016/j.ejfs.2015.06.001

- Clark, R. N. (1999). Chapter 1 - Spectroscopy of Rocks and Minerals, and Principles of Spectroscopy. In: A.N. Rencz (Ed.), *Remote Sensing for the Earth Sciences, Manual of Remote Sensing*, John Wiley & Sons, Hoboken, NJ, pp. 3-58.
- Chemistry libretexts. (2017). How an FTIR Spectrometer Operates [Online]. Available: https://chem.libretexts.org/Core/Physical_and_Theoretical_Chemistry/Spectroscopy/Vibrational_Spectroscopy/Infrared_Spectroscopy [Accessed February 2017].
- Chukanov, N. V. & Chervonnyi, A. D. (2016). *Infrared spectroscopy of minerals and related compounds*. Springer, Cham, Switzerland.
- Coates, J. (2000). Interpretation of Infrared Spectra, a practical approach. In: R. A. Meyers (Ed.), *Encyclopaedia of Analytical Chemistry*, John Wiley & Sons, Chichester, England, pp. 10821-10822.
- Culka, A., Kindlová, H., Drahotka, P. & Jehlička, J. (2016). Raman spectroscopic identification of arsenate minerals in situ at outcrops with handheld (532 nm, 785 nm) instruments. *Spectrochim Acta A Mol Biomol Spectrosc*, 154, pp. 193-199. doi: 10.1016/j.saa.2015.10.025
- Corescan. (2019). Automated mineralogy and texture [Online]. Available: <http://www.corescan.com.au> [Accessed December 2019].
- Dalm, M., Buxton, M. W. N. & van Ruitenbeek, F. J. A. (2017). Discriminating ore and waste in a porphyry copper deposit using short-wavelength infrared (SWIR) hyperspectral imagery. *Minerals Engineering*, 105, 10-18. doi: 10.1016/j.mineng.2016.12.013
- Death, D. L., Cunningham, A. P. & Pollard, L. J. (2008). Multi-element analysis of iron ore pellets by Laser-induced Breakdown Spectroscopy and Principal Components Regression. *Spectrochimica Acta Part B: Atomic Spectroscopy*, 63 (7), pp. 763-769. doi: 10.1016/j.sab.2008.04.014
- El-Azazy, M. (2018). Introductory Chapter: Infrared Spectroscopy - A Synopsis of the Fundamentals and Applications. In: *Infrared Spectroscopy - Principles, Advances, and Applications*. doi: 10.5772/intechopen.82210
- FLIR. (2019). Handheld Thermal Cameras [Online]. Available: <https://www.flir.eu/browse/industrial/handheld-thermal-cameras> [Accessed November 2019].
- Gaft, M., Reisfeld, R. & Panczer, G. (2005). *Modern Luminescence Spectroscopy of Minerals and Materials*, 2nd ed., Springer, Cham, Switzerland.
- Griffiths, P.R. & Haseth, J.A. (2007). *Fourier Transform Infrared Spectrometry*, 2nd ed., John Wiley & Sons, Hoboken, NJ.
- Griffith, W. (1975). Chapter 12 - Raman spectroscopy of terrestrial minerals. In: C. Karr (Ed.), *Infrared and Raman Spectroscopy of Lunar and Terrestrial Minerals*, Academic press, New York, USA, pp. 229-324.
- Goetz, A. F. H., Curtiss, B. & Shiley, D. A. (2009). Rapid gangue mineral concentration measurement over conveyors by NIR reflectance spectroscopy. *Minerals Engineering*, 22(5), pp. 490-499. doi: 10.1016/j.mineng.2008.12.013
- Gordon, G., McAvaney, S. & Wade, C. (2016). Spectral characteristics of the Gawler Range Volcanics in drill core Myall Creek RC1. *Australian Journal of Earth Sciences*, 63(8), pp. 973-986. doi: 10.1080/08120099.2016.1264475
- Guatame-Garcia, A. & Buxton, M. (2018). Prediction of Soluble Al₂O₃ in Calcined Kaolin Using Infrared Spectroscopy and Multivariate Calibration. *Minerals*, 8(4), 136. doi: 10.3390/min8040136

- Gupta, R.P. (2003). Chapter 3 - Spectra of minerals and rocks. In: R.P. Gupta (ed.), *Remote Sensing Geology*, 2nd ed., Springer, Berlin, Germany, pp. 33-52.
- Hackwell, J. A., Warren, D.W., Bongiovanni, R. P., Hansel, S. J., Hayhurst, T. L., Mabry, D. J., Sivjee, M. G. & Skinner, J. W. (1996). LWIR/MWIR imaging hyperspectral sensor for airborne and ground-based remote sensing. *Proceedings of SPIE's 1996 International Symposium on Optical Science, Engineering, and Instrumentation*, Denver, United States, Vol. 2819, pp. 102-107.
- Haest, M., Mittrup, D. & Dominguez, O. (2015). Reaping the first fruits – infrared spectroscopy: the new standard tool in BHP Billiton Iron Ore Exploration. *Proceedings of the iron ore conference: AusIMM*, Perth, Australia, pp. 277-284.
- Harraden, C. L., McNulty, B. A., Gregory, M. J. & Lang, J. R. (2013). Shortwave Infrared Spectral Analysis of Hydrothermal Alteration Associated with the Pebble Porphyry Copper-Gold-Molybdenum Deposit, Iliamna, Alaska. *Economic Geology*, 108(3), pp. 483-494. doi: 10.2113/econgeo.108.3.483
- Haskin, L. A., Wang, A., Rockow, K. M., Jolliff, B. L., Korotev, R. L. & Viskupic, K. M. (1997). Raman spectroscopy for mineral identification and quantification for in situ planetary surface analysis: A point count method, *Journal of Geophysical Research*, 102(E8), pp. 19293– 19306, doi: 10.1029/97JE01694.
- Hecker, C., Dilles, J. H., van der Meijde, M. & van der Meer, F. D. (2012). Thermal infrared spectroscopy and partial least squares regression to determine mineral modes of granitoid rocks. *Geochemistry Geophysics Geosystems*, 13(3). doi: 10.1029/2011gc004004
- Hecker, C., Van Ruitenbeek, F. J. A., Bakker, W. H., Fagbohun, B. J., Riley, D., Van Der Werff, H. M. A. & Van Der Meer, F. D. (2019). Mapping the wavelength position of mineral features in hyperspectral thermal infrared data. *International Journal of Applied Earth Observation and Geoinformation*, 79, pp. 133-140. doi: 10.1016/j.jag.2019.02.013
- Heintz, R. A. (2014). An Exceptional View of Geological Materials with Raman Imaging. *Proceedings of the 11th International GeoRaman Conference*, Madison, USA.
- Herrmann, W., Blake, M., Doyle, M., Huston, D., Kamprad, J., Merry, N. & Pontual, S. (2001). Short Wavelength Infrared (SWIR) Spectral Analysis of Hydrothermal Alteration Zones Associated with Base Metal Sulfide Deposits at Rosebery and Western Tharsis, Tasmania, and Highway-Reward, Queensland. *Economic Geology*, 96(5), pp. 939-955. doi: 10.2113/gsecongeo.96.5.939
- Holst, G. C. (2000). *Common sense approach to thermal imaging*. Copublished by SPIE Press and JCD Publishing, USA.
- HORIBA Scientific. (2015). *Raman Spectroscopy for Geological Materials Analysis* [Online]. Available: <http://www.horiba.com/scientific> [Accessed July 2015].
- Hollas, J.M. (2004). Chapter 2 - Electromagnetic radiation and its interaction with atoms and molecules. In: J.M. Hollas (Ed.), *Modern spectroscopy*, 4th ed., John Wiley & Sons, West Sussex, England, pp. 27-39.
- Hunt, G. R. (1977). Spectral signatures of particulate minerals in the visible and near infrared. *Geophysics*, 42(3), pp. 501-513. doi: 10.1190/1.1440721
- Karr, C. & Kovach, J. J. (1969). Far-infrared spectroscopy of minerals and inorganics. *Applied Spectroscopy*, 23(3), pp. 219-223. doi: 10.1366/000370269774380932

- Kerekes, J.P. (2009). Optical Sensor Technology. In: T. A., Warner, M.D. Nellis & G.M. Foody (Eds.), *The SAGE Handbook of Remote Sensing*, SAGE, London, UK, pp. 95-105.
- Kruse, F. A. (1996). Identification and mapping of minerals in drill core using hyperspectral image analysis of infrared reflectance spectra. *International Journal of Remote Sensing*, 17(9), pp. 1623-1632. doi: 10.1080/01431169608948728
- Kruse, F. & Perry, S. (2013). Mineral Mapping Using Simulated Worldview-3 Short-Wave-Infrared Imagery. *Remote Sensing*, 5(6), pp. 2688-2703. doi: 10.3390/rs5062688
- Kuosmanen, V., Arkimaa, H., Tiainen, M. & Bärs, R. (2015). Hyperspectral close-range LWIR imaging spectrometry—3 case studies. In: M.L. Airo (Ed.), *Geophysical Signatures of Mineral Deposit Types in Finland*. Geological Survey of Finland, Espoo, Finland, pp. 117-144.
- Lebourgeois, V. Bégue, A. Labbé, S. Mallavan, B. Prévot, L. & Roux, B. (2008). Can Commercial Digital Cameras Be Used as Multispectral Sensors? A Crop Monitoring Test. *Sensors*, 8(11), pp. 7300-7322. doi: 10.3390/s8117300
- Li, K., Liu, Q., Cheng, H., Deng, Y. & Frost, R. L. (2015). The molecular structure of chloritoid: a mid-infrared and near-infrared spectroscopic study. *Spectrochim Acta A Mol Biomol Spectrosc*, 145, pp. 604-609. doi: 10.1016/j.saa.2015.02.091
- LLA Instruments GmbH. (2017). Real-time color analysis for machine vision and sorting applications [Online]. Available: <https://www.lla-instruments.com/spectrometer-cameras/RGB-line-scan-camera.html> [Accessed February 2017].
- Lorenz, S., Kirsch, M., Zimmermann, R., Tusa, L., Möckel, R., Chamberland, M. & Gloaguen, R. (2018). Long-Wave Hyperspectral Imaging for Lithological Mapping: A Case Study. *Proceedings of IEEE International Geoscience and Remote Sensing Symposium: IGARSS, Valencia, Spain*, pp. 1620-1623.
- Malvern Panalytical. (2019). About ASD [Online]. Available: <https://www.malvernpanalytical.com/en/about-us/our-brands/asd-inc> [Accessed December 2019].
- Malvern Panalytical. (2020). Visible Near-infrared spectrometers (VNIR) [Online]. Available: <https://www.malvernpanalytical.com/en/products/category/near-infrared-spectrometers> [Accessed April 2019].
- McDowell, M. L. & Kruse, F. A. (2015). Integrated visible to near infrared, short wave infrared, and long wave infrared spectral analysis for surface composition mapping near Mountain Pass, California. *Proceedings of SPIE on Algorithms and Technologies for Multispectral, Hyperspectral, and Ultraspectral Imagery XXI*, Vol. 9472, Bellingham, USA.
- McGrath, M. J. & Scanaill, C. N. (2013). Sensing and Sensor Fundamentals. In: M.J. McGrath & C.N. Scanaill (Eds.), *Sensor Technologies: Healthcare, Wellness, and Environmental Applications*, Apress, Berkeley, CA, pp. 15-50.
- Mernagh, T. P., & Trudu, A. G. (1993). A laser Raman microprobe study of some geologically important sulphide minerals. *Chemical Geology*, 103(1), pp. 113-127. doi: 10.1016/0009-2541(93)90295-T
- Nienhaus, K., Pretz, T. & Wotruba, H. (2014). *Sensor Technologies: Impulses for the Raw Materials Industry*. Shaker Verlag GmbH, Aachen, Germany.
- Notesco, G., Kopačková, V., Rojík, P., Schwartz, G., Livne, I. & Dor, E.B. (2014). Mineral Classification of Land Surface Using Multispectral LWIR and Hyperspectral SWIR

- Remote-Sensing Data. A Case Study over the Sokolov Lignite Open-Pit Mines, the Czech Republic. *Remote Sensing*, 6(8), pp. 7005-7025. doi: 10.3390/rs6087005
- Orbit Technologies. (2017). Online XRF Analyzer [Online]. Available: <http://www.orbitindia.com/online-xrf-analyzer> [Accessed October 2017].
- OLYMPUS. (2019). TERRA™ Portable XRD analyser [Online]. Available: <https://www.olympus-ims.com> [Accessed October 2020].
- Patrice, A., Stephane, J., Stephane, R., Beatrice, V. & Herwig, W. (2009). Chapter 2 - Volatile compounds detection by IR Acousto-Optic Detectors. In: J. Byrnes (Ed.), *Unexploded Ordnance Detection and Mitigation*. Springer, Dordrecht, The Netherlands, pp 21-60.
- Perkins, W. D. (1987). Fourier transform infrared spectroscopy. Part II. Advantages of FT-IR. *Journal of Chemical Education*, 64(11), A269. doi: 10.1021/ed064pA269
- Photonics Online. (2019). SWIR camera [Online]. Available: <https://www.photonicsonline.com/solution/swir-cameras> [Accessed October 2019].
- Quantum Design. (2019). Products [Online]. Available: <https://qd-europe.com/nl/en/products> [Accessed October 2019].
- Ramanaidou, E., Wells, M., Lau, I., & Laukamp, C. (2015). Chapter 6 - Characterisation of iron ore by visible and infrared reflectance and, Raman spectroscopies. In: L. Liming (Ed.), *Iron Ore: Mineralogy, Processing and Environmental Sustainability*. Woodhead Publishing, Cambridge, UK, pp. 191-228.
- REDWAVE. (2020). REDWAVE sorting machine [Online]. Available: <http://www.redwave-us.com> [Accessed July 2020].
- Richter, M., Vieth, K., Langle, T. & Beyerer, J. (2016). Bag of visual words - A computer vision method applied to bulk material sorting. *Proceedings of sensor-based sorting and control conference, Aachen, Germany*, pp. 169-177.
- Riley, D.N. & Hecker, C.A. (2013). Mineral Mapping with Airborne Hyperspectral Thermal Infrared Remote Sensing at Cuprite, Nevada, USA. In: C. Kuenzer & S. Dech (Eds.), *Thermal Infrared Remote Sensing, Methods, Applications*. Springer, Dordrecht, The Netherlands, pp. 495-514.
- Robben, C. & Wotruba, H. (2019). Sensor-Based Ore Sorting Technology in Mining—Past, Present and Future. *Minerals*, 9(9), 523. doi: 10.3390/min9090523
- Rogalski, A. & Chrzanowski, K. (2014). Infrared devices and techniques (revision). *Metrology and Measurement Systems*, XXI (2014), pp. 565-618. doi: 10.2478/MMS-2014-0057
- Schodlok, M. C., Whitbourn, L., Huntington, J., Mason, P., Green, A., Berman, M., Coward, D., Connor, P., Wright, W., Jolivet, M. & Martinez, R. (2016). HyLogger-3, a visible to shortwave and thermal infrared reflectance spectrometer system for drill core logging: functional description. *Australian Journal of Earth Sciences*, 63(8), pp. 929-940. doi: 10.1080/08120099.2016.1231133
- Singh, V. & Misra, A. K. (2017). Detection of plant leaf diseases using image segmentation and soft computing techniques. *Information Processing in Agriculture*, 4(1), pp. 41-49. doi: 10.1016/j.inpa.2016.10.005
- Shankar, V. (2015). Field Characterisation by Near Infrared (NIR) Mineral Identifiers - A New Prospecting Approach. *Procedia Earth and Planetary Science*, 11, pp. 198-203. doi: 10.1016/j.proeps.2015.06.025
- SIERRA-OLYMPIC. (2019). All thermal cameras [Online]. Available: <https://sierraolympic.com/thermal-cameras> [Accessed October 2019].

- Smith, B.C. (2011). Chapter 1 - Fundamentals of Fourier Transform Infrared Spectroscopy. In: B.C. Smith (Ed.), *Introduction to infrared spectroscopy*, 2nd ed., CRC Press: New York, USA, pp. 1-17.
- Specim. (2019). Spectral Cameras [Online]. Available: <https://www.specim.fi/spectral-cameras> [Accessed October 2019].
- Spectral Evolution. (2015). UV-VIS-NIR Spectrometers [Online]. Available: http://www.spectralevolution.com/spectrometers_mining.html [Accessed June 2015].
- SPECTRAL Industries. (2020). IRIS Spectrometer [Online]. Available: <https://www.spectralindustries.com/products> [Accessed February 2020].
- SPECTRAL Industries. (2021). Conveyor belt sensor [Online]. Available: <https://www.spectralindustries.com/products> [Accessed January 2021].
- SphereOptics. (2019). Spectral Evolution Field spectrometers [Online]. Available: <https://sphereoptics.de/en/product/fieldspectrometers> [Accessed April 2019].
- SphereOptics. (2020). Multispectral infrared Cameras (MWIR and LWIR) [Online]. Available: <https://sphereoptics.de/en/product/multispec-ir-cams/> [Accessed April 2020].
- STEINERT. (2020). Sensor sorting units: colour sorting system [Online]. Available: <https://steinertglobal.com> [Accessed July 2020].
- STEINERT. (2021). Ore sorting [Online]. Available: <https://steinertglobal.com/mining/ore-sorting> [Accessed January 2021].
- Stuart, B. (2004). Chapter 1 – Introduction. In: J.A. David (Ed.), *Infrared Spectroscopy: Fundamentals and Applications*. John Wiley & Sons, Chichester, England, pp. 1-13.
- Sun, Y., Seccombe, P. K. & Yang, K. (2001). Application of short-wave infrared spectroscopy to define alteration zones associated with the Elura zinc–lead–silver deposit, NSW, Australia. *Journal of Geochemical Exploration*, 73(1), pp. 11-26. doi: 10.1016/S0375-6742(01)00167-4
- Szalai, Z., Kiss, K., Jakab, G., Sipos, P., Belucz, B. & Németh, T. (2013). The use of UV-VIS-NIR reflectance spectroscopy to identify iron minerals. *Astronomische Nachrichten*, 334(9), pp. 940-943. doi: 10.1002/asna.201211965
- Tanya, L. M., Timothy, J. J., Neal, B. G., Bruce, E. B., Toya, N. B., James, E. S., Russell, G. T., Ashley, M. B., Yin-Fong, S. & Tyler O. D. (2019). Hyperspectral imaging of minerals in the longwave infrared: the use of laboratory directional-hemispherical reference measurements for field exploration data. *Journal of Applied Remote Sensing*, 13(3), 034527. doi: 10.1117/1.JRS.13.034527.
- Taylor, H. E. (2001). Chapter 1 - Introduction. In: H. E. Taylor (Ed.), *Inductively Coupled Plasma-Mass Spectrometry*. Academic Press, San Diego, USA, pp. 1-5.
- Teena, M. & Manickavasagan, A. (2014). Thermal Infrared Imaging. In: A. Manickavasagan & H. Jayasuriya (Eds.), *Imaging with Electromagnetic Spectrum: Applications in Food and Agriculture*. Springer, Berlin Germany, pp. 147-173.
- TELOPS. (2019). High-speed MWIR cameras [Online]. Available: <https://www.telops.com/products/high-speed-cameras/mwir-cameras> [Accessed October 2019].
- TERRACORE. (2016). TERRACORE geospectral imaging [Online]. Available: <http://terracoregeo.com> [Accessed July 2016].
- ThermoFisher. (2017). X-Ray Fluorescence (XRF) [Online]. Available: <https://www.thermofisher.com> [Accessed August 2017].

- Thompson, A.J., Hauff, P.L. & Robitaille, A.J. (1999). Alteration mapping in exploration: application of short-wave infrared (SWIR) spectroscopy. Society of Economic Geologists newsletter, No.39.
- Thomas, R. (2008). Practical guide to ICP-MS. Marcel Dekker, New York, USA.
- TOMRA. (2019). Mining Sorting Equipment [Online]. Available: <https://www.tomra.com/en/sorting/mining/sorting-equipment> [Accessed March 2019].
- TOMRA. (2020). Quartz colour sorting [Online]. Available: <https://www.tomra.com> [Accessed July 2020].
- von Ketelhodt, L. & Bergmann, C. (2010). Dual energy X-ray transmission sorting of coal. Journal of the Southern African Institute of Mining and Metallurgy, 110(7), pp. 371-378.
- Wang, A., Jolliff, B. L. & Haskin, L. A. (1995). Raman spectroscopy as a method for mineral identification on lunar robotic exploration missions. 100 (E10), pp. 21189-21199. doi: 10.1029/95je02133
- Wells, M. A. & Ramanaidou, E. R. (2015). Raman spectroscopic core scanning for iron ore and BIF characterization. Proceedings of the 11th International Congress for Applied Mineralogy (ICAM), Mianyang, China, pp. 387-396.
- White, W.B. (1975). Chapter 13 - Structural interpretation of lunar and terrestrial minerals by Raman Spectroscopy. In: C. Karr Jr. (Ed.), Infrared and Raman Spectroscopy of Lunar and Terrestrial Minerals. Academic press, New York, USA, pp. 325-358.
- White, W.B. (2005). Identification of cave minerals by Raman spectroscopy: new technology for nondestructive analysis. International Journal of Speleology, 35(2), pp.103-107.
- Yitagesu, F. A., van der Meer, F., van der Werff, H. & Hecker, C. (2011). Spectral characteristics of clay minerals in the 2.5–14 μ m wavelength region. Applied Clay Science, 53(4), pp. 581-591. doi: 10.1016/j.clay.2011.05.007

II

THE METHODOLOGICAL FRAMEWORK AND THE CASE STUDY SITE

4

MULTIVARIATE ANALYSIS TECHNIQUES AND DATA FUSION

This chapter describes the general workflow in this research. It elaborates on the applied multivariate analysis techniques and the implemented exploratory data analysis. It also discusses the developed data fusion concept and provides some insight into the different levels of data fusion.

4.1. INTRODUCTION

The general methodological approach developed as a part of this research is a multi-step process that incorporates the design of experiments (the experimental scenarios), exploratory data analysis, data modelling and multi-block analysis using data fusion techniques. Possible experimental scenarios were formulated to address the main research objective. These scenarios are the specific objectives discussed in Chapter 1. The exploratory data analysis task includes pattern recognition, data pre-processing, outlier detection and data preparation. Following the exploratory data analysis, data modelling was performed to establish a relationship between the spectral signals from the different sensors and the key geological attributes. These include the use of linear and non-linear techniques for the prediction and classification of materials. The sensor data type and the objective of the analysis guided the choice of the analysis technique. Consequently, the usability assessment results from the individual sensors promoted the development of a data fusion concept that realizes a fusion of blocks at different levels (e.g., low- and mid-level). The concept was implemented and validated using multiple data sources and validation datasets. The details of the methodological approaches applied for the analysis of each sensor output are presented in the corresponding chapters. In this chapter, the general workflow, the multivariate analysis techniques, the exploratory data analysis and the data fusion approach are described (Figure 4.1 and 4.2).

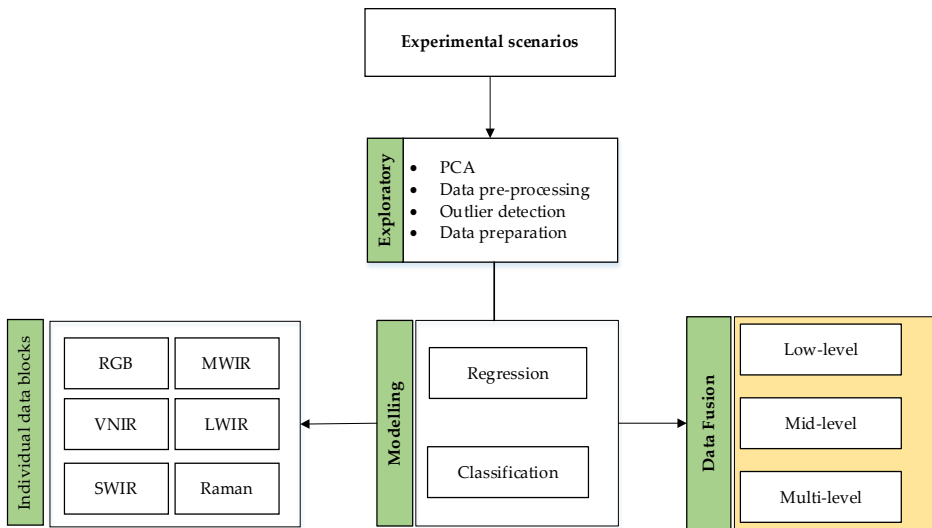


Figure 4.1: Simplified overview of the general research workflow. It includes four major steps: setting experimental scenarios, exploratory data analysis, modelling of the individual data blocks and multi-block analysis using a data fusion approach.

4.2. MULTIVARIATE ANALYSIS TECHNIQUES

Multivariate data analysis involves statistical and mathematical methods to process and evaluate large amounts of variables (Brereton, 2007; Mellinger, 1987; Miller and Miller, 2000; Roussel et al., 2014). These variables can be spectral data that are multivariate in nature. In

spectral data analysis, multivariate techniques correlate the physical properties of the material of interest to the spectral data. Thus, multivariate analysis is a useful technique that plays a significant role in material characterisation. For example, spectral interpretation or identification of minerals or elements using spectral data focuses on the analysis of each wavelength at which the diagnostic mineral features occur. However, attributed to various factors such as matrix effects or lower signals of the minerals, identification of the diagnostic features is sometimes challenging. In such cases, multivariate analysis can be the best alternative since it permits the use of the entire spectrum (much more information) at once to enable a better insight into the spectral data. Besides, multivariate analysis allows classification and quantitative analysis of materials. Thus, it is a useful method to understand the chemical composition of a material. Overall, multivariate techniques will enable the analysis of highly complex multivariate data to solve various real-world problems. Consequently, there is numerous application of the methods in a wide range of areas, such as, in material characterisation (Abedi et al., 2013; Death et al., 2008; Hecker et al., 2012; Zuo and Carranza, 2011), in petroleum reservoir characterisation (Scheevel and Payrazyan, 2001), and food quality analysis (Bro et al., 2002; Roussel et al. 2014).

Several multivariate data analysis techniques are available to allow classification analysis, multiple regression analysis, and principal component analysis (Mishra and Datta-Gupta, 2018; Roussel et al., 2014). These techniques can broadly be categorized into “supervised” or “unsupervised” learnings (Mishra and Datta-Gupta, 2018). In supervised learning, models are trained using labelled data that external supervision is required. The technique marks inputs to known output and can resolve both regression and classification problems. Whereas, unsupervised learning requires no prior information (no supervision) to train models. It identifies pattern and structures to solve classification and association problems. Thus, it discovers output based on trends. Hence, the classification techniques can be “supervised” or “unsupervised”. In the supervised classification techniques, the group membership is assigned to a given dataset based on a prior classification (Mishra and Datta-Gupta, 2018). Such kind of classification is also known as discriminant analysis. On the other hand, unsupervised classification techniques (i.e., commonly known as cluster analysis) partition or cluster the data into relatively similar entities based on the characteristics of the data. Therefore, such kind of classification techniques does not require prior information.

Multivariate techniques can also be linear or non-linear. Linear techniques handle the linear relationship between the dependent and independent variables. However, some complex real-world problems might not be defined using linear relationships. In such cases, non-linear techniques that take different forms are required. The other crucial multivariate analysis technique is a principal component analysis. This technique enables data dimensionality reduction to allow data visualisation and pattern recognition in a reduced dimensional space. The supervised and unsupervised classification techniques considered in this study are partial least squares – discriminant analysis (PLSR-DA), K-means, maximum likelihood (ML), minimum distance (MD), and spectral angle mapper (SAM) Figure 4.2. Whereas, the linear and non-linear regression techniques are the partial least squares regression (PLSR), support vector machine (SVM) and principal component regression (PCR) Figure 4.2. The types of data used in this work are image and point spectral data produced by the assessed technologies. A detail description of these data types is presented in Chapter 2. Consequently, the different data pre-processing and multivariate techniques applied for each data type are presented in Figure 4.2. The figure also shows the methods

used for the fusion of multiple data blocks. Detail descriptions of the above-mentioned techniques and the data fusion methodological approach are presented in the sub-sections that follow.

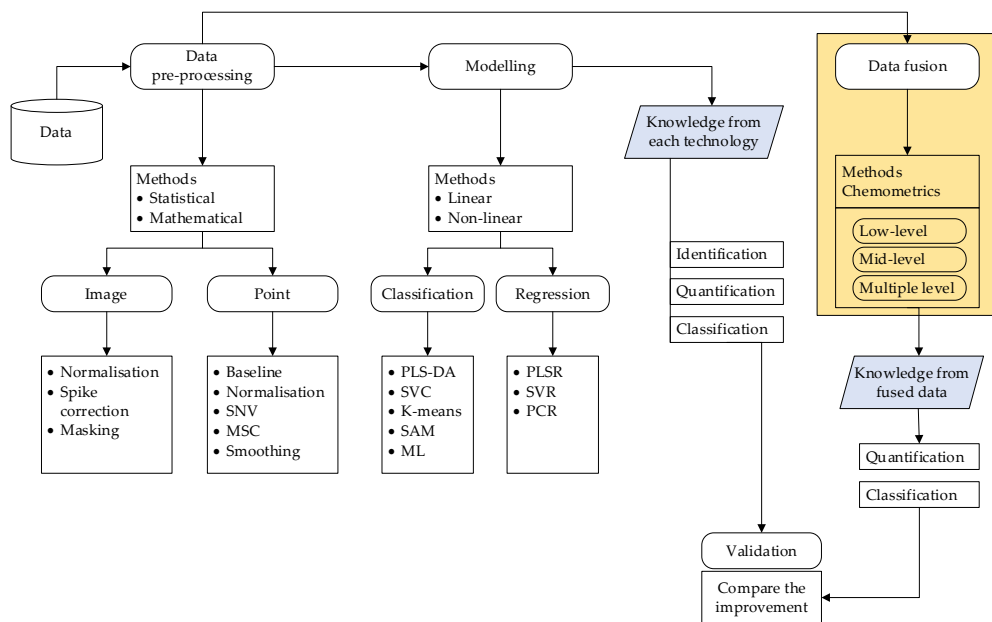


Figure 4.2: Overview of the pre-processing and multivariate techniques applied at the different methodological steps. The diagram also shows the methods used in the data fusion approach.

4.2.1. PRINCIPAL COMPONENT ANALYSIS

Principle component analysis (PCA) is a dimension-reduction tool that transforms multiple (possibly) correlated variables into a smaller set (uncorrelated variables) that still retains most of the important information (Eriksson et al., 2013; Esbensen and Geladi, 2009; Jolliffe, 2002; Yang, 2019). It reduces data dimensionality by computing new axes called principal components (PCs). PCs are linearly uncorrelated variables that are orthogonal to each other and describe complementary information. The first PC represents most of the variations in the data, and each succeeding component describes as much of the remaining variation in the original data. Thus, PCA is a feature extraction technique that expresses information as a set of PCs. It allows visualisation, data reduction, classification, trend analysis, outliers' detection and pattern recognitions of multivariate data. Thus, it is the most fundamental multivariate data analysis method for effective exploratory data analysis. The other important aspect of the technique is its flexibility for the analysis of datasets with missing values, multicollinearity, categorical data, and imprecise measurements (Howard et al., 2015).

4.2.2. K-MEANS

The K-means clustering is a one of the most commonly used and efficient unsupervised classification technique (Jain et al., 1999; McCool et al., 2012). It is used for clustering of unlabeled data (e.g., data without defined classes or groups) into k clusters. When applying this method, n observations are assigned to k clusters, using the centroid of the clusters and minimising the sum of squared errors (Jain et al., 1999; Kaufman and Rousseeuw, 2005) as shown below

$$J = \sum_{j=1}^k \sum_{i \in C_j} (x_i - m_j)^2,$$

where $m_j = \sum_{i \in C_j} x_i / n_j$ denotes the cluster centroid of C_j , n_j is the number of points in C_j and $(x_1, \dots, x_n) = X$ represents the data matrix.

The algorithm finds groups in the data based on feature similarity and the number of groups is determined by the variable k . It involves defining a target number of clusters (i.e., the number of centroids) required in the analysis and works iteratively to reassign each data point to one of the k groups. K-means is an iterative algorithm that allocates every data point to the nearest group by minimising the in-cluster sum of squares. The technique identifies non-overlapping subgroups (clusters) in the data using similarity measures, such as Euclidean-based distance. Thus, it is a useful tool that allows finding hidden patterns or grouping structures in data.

4.2.3. PARTIAL LEAST SQUARES REGRESSION (PLSR)

PLSR is a data prediction technique commonly applied in multivariate data analysis. It maximises the covariance between the predictor (X) and the response (Y) blocks, whereby the latent variables explain the variability of X with maximal Y correlation (Boucher et al., 2015). It also allows identifying new predictor variables, called PCs, and the optimal PCs for the proposed linear relationship (Noonan, 2017). Therefore, the latent variables in X can be used to predict the latent variables in Y. While PCA is utilised to extract PCs that describe variations in the data, PLSR allows PCs to be correlated with the response (Y) to compute latent variables (LVs). PLSR finds the multidimensional direction in the predictor (X) space that explains the maximum multidimensional variance direction in the response (Y) space. The technique is useful for reducing data dimension into LVs, thus reducing the complexity of multivariate data. A multivariate PLSR model is generally expressed as

$$X = TP^T + E,$$

$$Y = UQ^T + F,$$

where X denotes an $n \times m$ matrix of predictors, Y denotes an $n \times p$ matrix of responses; T and U represents $n \times l$ matrices that are, respectively, projections of X (the X score, factor matrix) and projections of Y (the Y scores); P and Q are, respectively, $m \times l$ and $p \times l$ orthogonal loading matrices; and matrices E and F are the error terms.

PLSR is a useful tool that can handle collinear (correlated) variables, noisy, missing variables (in both the response and predictor) and also simultaneously model several

response variables (Wold et al., 2001). It is one of the computationally efficient techniques for modelling of datasets with high number of variables to sample ratio.

4.2.4. PARTIAL LEAST SQUARES – DISCRIMINANT ANALYSIS (PLS-DA)

PLS-DA is a supervised classification method, used to optimise separation between different classes (Barker and Rayens, 2003; Lee et al., 2018; Christin et al., 2013). PLS-DA is a variant of PLS regression where the response variable is categorical. Development of the predictive PLS-DA model comprises two main steps: the first one is the construction of the PLS components (i.e., dimension reduction) and the second step is a construction of the prediction model (discriminant analysis). Therefore, it combines the dimensionality reduction and discriminant analysis into one algorithm that it is applicable for the modelling of multivariate data.

PLS-DA finds a linear regression model between the response and independent variables by projecting the predicted and the observed variables into a new space. In PLS-DA modelling, the categorical variables are internally recoded into continuous variables (dummy block matrix that records the membership of each observation). Therefore, it uses a binary encoding to assign one if the unknown measurement belongs to a specified class or zero if it belongs to other classes. Consequently, it uses one versus all approach and codes the response categories via an indicator variable. Once the classification model is developed, it can be used to assign unknown samples to the most probable class. Besides its use for classification problems, PLS-DA is a useful tool for identification of critical variables (feature selection) as well as for the understanding of differences among groups of samples (Christin et al., 2013).

4.2.5. PRINCIPAL COMPONENT REGRESSION (PCR)

PCR is a regression technique that relates the variance in a response variable (Y) to the variance in several predictors (X variables). As PCR is a two-step method, the X -matrix (comprising of X variables) is decomposed using PCA (Jolliffe, 2002; Lauter, 1988). In the second step, the PC scores (instead of the original X variables) are used as predictors to fit a multiple linear regression (MLR) model, aiming to establish a linear relationship between the predictor (X variables) and the response (Y variable) using the typical least squares procedure (Gauthier and Hawley, 2007). As the PCR is based on the orthogonal scores, the model does not suffer from collinearity effects. Unlike in the PLSR, the response variable in PCR plays no role in identifying the PCs directions.

4.2.6. SUPPORT VECTOR MACHINE (SVM)

SVM is a supervised learning algorithm for the analysis of classification (support vector classification—SVC) and regression (support vector regression—SVR) problems (Brereton and Lloyd, 2010; Deris et al., 2011). SVM maps the input data into a higher-dimensional feature space using kernel functions, which can take many forms, such as linear, polynomial, radial basis function (RBF), sigmoid, etc. Therefore, SVM is a powerful technique that can be applied to both linear and non-linear systems (Boucher et al., 2015). The SVC classification type used in this work is C-SVR with a polynomial kernel function, as this kernel type can be utilised to model non-linear systems of varying complexity. The SVC algorithm finds an optimal hyperplane (decision boundary) in a higher-dimensional feature space that distinctly classifies the data points using kernel functions. Data points that are

closer to the hyperplane influence the position and orientations of the decision surface. Such data points are referred to as support vectors (SVs). Thus, SVs are a subset of the analysed samples that are closest to the hyperplane. The key model parameters for the specification of C-SVC models are C value and gamma. The C value is a capacity (penalty) factor for the measure of models' robustness. It trades off the misclassification of data points against the simplicity of the hyperplane. The gamma parameter determines how far the influence of a single training example (single data sample) reaches and controls what is 'close' and what is 'far'. Thus, it adjusts the curvature of the hyperplane of the model. The SVM regression type used in this work is ϵ -SVR with RBF kernel function, as the RBF can be utilised to model non-linear systems of varying complexity. Detailed theoretical background on SVR can be found in pertinent literature (Awad and Khanna, 2015; Brereton and Lloyd, 2010; Deris et al., 2011; Kecman, 2005; Smola and Schölkopf, 2004). The key model parameters for the specification of ϵ -SVR models are C value and epsilon (ϵ), as they respectively determine the trade-off between the training error and the model complexity (flatness), and control the width of the band where the cost of errors in the epsilon-intensive loss function is zero. The value of ϵ can thus affect the number of SVs used to construct the regression function.

4.2.7. SPECTRAL ANGLE MAPPER (SAM)

SAM is a supervised classification method that uses an n-D angle to match pixel to the reference spectra. The algorithm considers the reference spectra (endmembers) and the unknown pixels as vectors in a space with dimensionality equal to the number of bands (Kruse et al., 1993; Richards and Jia, 2006). Then, for each unknown pixel, SAM calculates the spectral angle between the two spectra to identify the different classes in the image. Smaller angles represent closer spectral similarity to the reference spectrum (endmember), and angle bigger than the specified maximum angle threshold remains unclassified. SAM is a rapid mapping tool, which is relatively insensitive to illumination effects and other spectral artefacts (Kruse et al., 1993).

4.2.8. MAXIMUM LIKELIHOOD

Maximum likelihood (ML) is one of the most popular supervised classification methods in remote sensing. The algorithm computes the probability of each pixel belonging to a specific class that is represented in the signature file (endmembers) and assigns unknown pixel to the most probable class. ML is based on two principles: first, it assumes the distribution of the data within a given class obeys a multivariate normal distribution. The other principle is, it uses Bayes theorem to assign pixels to the corresponding classes, in which the unknown pixel with the maximum likelihood is classified into the corresponding class (Richards, 2013). The algorithm uses a sufficient number of pixels (e.g., greater than the number of bands in the respective images) for each training area (endmember), thus to allow the calculation of the covariance matrix. The model parameters can be adjusted to maximise the likelihood function of the ML method (Sisodia et al., 2014). For example, the probability threshold determines the number of pixels assigned to the class of the highest probability. The higher the threshold value than the highest computed probability, then pixel remains unclassified. However, without the probability threshold or with the probability values higher than the threshold, the algorithm assigns each pixel to the highest probable classes (Lillesand et al., 2004).

4.2.9. MINIMUM DISTANCE

The minimum distance algorithm (MD) is a supervised classification method that classifies pixels based on the Euclidean distance between the spectral signatures of image pixels and the reference (endmembers) spectral signatures. The algorithm uses the training data to determine the means of the classes and calculates the distance of every pixel to the mean vector of each class in multi-feature space. The distance indicates an index of similarity where the minimum distance corresponds to the maximum similarity. Therefore, based on the minimum Euclidean distance, it assigns each pixel to the nearest class (Richards, 2013; Richards and Jia, 2006). In MD classification, maximum distance criterion or distance thresholds can be set and pixels that do not meet the selected distance criteria remains unclassified.

4.3. EXPLORATORY DATA ANALYSIS

Exploratory data analysis (EDA) is an approach for data analysis that involves a variety of techniques to explore data characteristics. It is the first step in the data analysis process that employs visual and quantitative methods to get a sense of the data (or understand the data) on hand. EDA provides new insights into a dataset, uncover underlying data structure, identify the most important variables, detect outliers and identify optimal factors in the data. It can be used to test the underlying assumptions related to specific models and could lead to a formulation of new experiments. Therefore, EDA is an essential process to manipulate the available data in a maximised way. The EDA performed in this research are explained below.

4.3.1. PATTERN RECOGNITION

Pattern recognition is the automated recognition of regularities in data using different computer algorithms (Jain et al., 2000; Paolanti and Frontoni, 2020). It permits reliable and feasible decisions concerning the categories of the patterns. There are various pattern recognition frameworks used to design and develop systems that recognise a trend in data, such as, statistical methods, machine learning and deep learning approaches. Among the various pattern recognition techniques, PCA is the most widely applied method in different applications (e.g., spectral data analysis and image analysis). PCA is one of the most potent exploratory data analysis technique that can be applied to identify patterns in the samples, potential subtle outliers and informative variables (i.e., those responsible for the observed patterns). The scores and loading plots of the PCA models are used to investigate sample–variables relationships and the grouping structure (intra-sample relationships). The score plots show the grouping structure in the spectral data with respect to the analysed objectives (e.g., mineral concentrations or ore-waste classification). The loading plot thus reveals the most important (significant) variables within the spectral data that are responsible for the grouping observed in the score plots. Therefore, PCA improves the efficiency and accuracy of learning from multivariate data.

4.3.2. OUTLIER DETECTION

Outlier detection is one of the key steps for solving real-world problems using statistical analysis of sensor data. Outliers are inconsistent and differ from the other observations that a different mechanism likely arises them, e.g., due to measurement errors, (Hawkins, 1980; Rodrigues et al., 2019; Wang et al., 2019). However, outliers can also be unique values that

carry valuable and relevant information. Either way, outliers can affect the analyses of any modelling tasks that prior detection is crucial. Outlier detection is an essential and broad subject that needs careful study in many application areas. In this research, potential outliers were identified using the following outlier detection techniques: Hotelling's T^2 , residual map, influence plot and visual inspection of unique measurements.

Hotelling's T^2 is a useful outlier detection tool that describes the distance to the model centre, as spanned by the PCs (Jensen and Ramirez, 2017). It considers the inlier statistic (minimum Mahalanobis distance to the calibration samples) against Hotelling's T^2 statistic for each sample to identify the potential outliers. It also provides a critical limit (p-value) with different statistical confidence limits. For example, for the p-value of 5%, the 95% confidence ellipse can be included in the score plots of the PCA models to reveal potential outliers (i.e., data points located outside the ellipse contour). The influence plot shows the sample residuals' X-variance against Hotelling's T^2 and Leverage statistics. The residual statistics describe the sample distance to the model, whereas the Hotelling's T^2 and Leverage indicate how well the model describes the sample. Likewise, an influence plot is a useful tool for detecting influential samples and dangerous outliers. For example, samples with high residual variance and high leverage are deemed to contain the most dangerous outliers. Besides, variable residual plots (a map of residuals) are useful for determining whether samples have high residuals on few or all variables, and thus helps in outlier detection. Therefore, an integrated finding yielded by these inspections was considered in this study to identify measurements that are possible outliers.

4.4. DATA PRE-PROCESSING

Data pre-processing is an integral part of multivariate data analysis, irrespective of whether it is conducted for classification, exploration or prediction purposes (Engel et al. 2013). Sensor measurements include undesired variations (e.g., instrumental artefacts), which are generally compensated by data pre-processing, whereby unwanted variation within the data is removed to enhance the signal pertaining to the analytical information (Rinnan et al., 2009; Roussel et al. 2014). While several data pre-processing strategies are currently available, the choice of the optimal data pre-processing method for a particular application depends on the nature of the data and the ultimate goal of data analysis (Rinnan et al., 2009). Thus, the pre-processing technique is typically selected based on a systematic approach, the visual inspection of the spectra and quality parameters, such as Pearson correlation coefficient (PCC), which measures the linear correlation between two variables (Engel et al., 2013). As this is mostly a systematic approach, Design of Experiment (DoE) is required to identify the optimal data pre-processing techniques that yield the best results either for classification or prediction problems. This approach is advantageous when the aim is to analyse and understand the main effect and the interaction effect of the pre-processing techniques. Aiming to remove the most common artefacts of sensor measurements, the different scaling and signal correction methods considered in this research include mean centring (MC), baseline correction, standard normal variate (SNV), normalisation, multiplicative scatter correction (MSC) and smoothing (Gaussian filter smoothing). In spectroscopic data, the signal correction methods correct the influence of additive or multiplicative effects (Roussel et al. 2014). The additive effect can be a constant that depends on the wavelength location. Whereas, the multiplicative effect can be caused when a constant multiplies each element of the spectrum.

MC is a data scaling technique that subtracts the variable mean to each value, and it represents variation around a mean (Bro and Smilde, 2003). It removes offsets by subtracting the variable mean from each value (Bro and Smilde, 2003; Roussel et al., 2014). On the other hand, when baseline correction is performed, the unwanted “background signal” is subtracted from the main signal information (Roussel et al., 2014). SNV removes the spectrum mean value from each variable in the spectrum and divides them by the spectrum standard deviation (Fearn et al., 2009; Roussel et al., 2014). It normalises the spectrum data to itself and minimises the light scattering effect and particle size effects in the spectra data. Normalisation aims to divide each spectrum based on the estimation of its spectral intensity and remove undesired intensity variation due to the multiplicative effects (Roussel et al., 2014). MSC is used to reduce multiplicative scattering effects (Fearn et al., 2009). Smoothing is based on averaging the neighbourhood points, and it is used to minimise random noise (Roussel et al., 2014). It allows random noise to be removed from the dataset by averaging the neighbouring points (Roussel et al., 2014). The signal correction methods were performed on one sample at a time (row-wise), whereas for mean centring, the pre-processing is applied to individual columns. The pre-processing techniques used for the RGB and hyperspectral images are discussed in the subsequent chapters.

4.5. DATA FUSION

Accurate and comprehensive raw material characterisation is essential in mining operations. This can be achieved via the use of different sensor technologies. Each sensor technology operates over a specific range of the electromagnetic spectrum and provides information on a particular aspect of materials. Consequently, a single sensor might not offer a sufficiently comprehensive description of a material’s composition. This introduces uncertainty into both resource estimation and defining requirements for mineral processing. Therefore, it is necessary to utilise strategic sensor combinations to improve accuracy, minimise uncertainty, and enhance specific inferences for raw material characterisation.

Sensor technologies may be integrated physically or digitally (through data fusion). Physical integration is achieved when two or more sensors are combined on a single platform. For example, Sharma et al. (2009) integrated remote-laser-induced breakdown spectroscopy (LIBS) and Raman system for analysis of minerals (e.g., carbonates, sulphates, iron oxides) with a single 532 nm laser. The integrated system was capable of simultaneously providing elemental and mineralogical information. Fernández et al. (2013) physically integrated RGB and multispectral imagery sensors for improved classification of the Cabernet Sauvignon grapevine elements. Hoehse et al. (2009) demonstrated the utility of mapping heterogeneous minerals using a single unified LIBS and Raman set up for a combined analysis of molecular and elemental information that resulted in comprehensive material characterisation.

Data fusion is the term applied to the analysis of multiple data blocks from different data sources that can interact and inform each other (Cocchi, 2019). It is a process of integrating data blocks from multiple sources or sensors into a single comprehensive model (Hall and McMullen, 2004). The fusing of different data sources enhances the reliability of prediction or classification models owing to the synergy among the incorporated datasets. Data fusion can be implemented in different ways using various multivariate data analysis techniques. For example, data fusion can be implemented using probabilistic descriptions of observations and processes. One such method is the Bayes’ rule, which is the most commonly employed method in robotics (Thrun and Burgard, 2005) and military

applications (Hall, 1997). However, when probabilistic methods are employed, a large number of probabilities needs to be specified, thus introducing inconsistencies into the specification of a consistent set of beliefs in terms of probability and model precision. Even though these limitations can be partially mitigated using alternative techniques, such as fuzzy logic (Siciliano and Khatib, 2016), this approach was not considered in the present study due to its high complexity. Data fusion can also be implemented using chemometric techniques, which require the collected data to have a relatively high quality. Chemometrics is a discipline that uses data-driven approaches to extract relevant information from chemical (material) systems. This approach is widely applied in analytical chemistry and metabolomics (Biancolillo et al., 2014; Borràs et al., 2015; Doeswijk et al., 2011; Silvestri et al., 2013; Smilde et al., 2005).

4.5.1. LEVELS OF DATA FUSION

Data fusion can be achieved at multiple levels using various multivariate data analysis techniques. For example, data fusion using chemometrics can be realised at different levels, designated as low-level, mid-level, high-level and multiple-level fusion. Low-level data fusion involves the integration of multiple data sources by concatenating data blocks of different nature (Castanedo, 2013; Forshed et al., 2007; Silvestri et al., 2014). In this approach, correlations among all variables collected in the different data blocks are considered. This results in a single matrix, which yields a single classification or prediction model.

Mid-level or hierarchical data fusion is a feature-level fusion that involves two modelling steps (Borràs et al., 2015; Silvestri et al., 2014). First, the informative features (relevant information) of the different data blocks are separately extracted using suitable variable screening or selection methods (Cocchi, 2019; Li et al., 2018). In the second step, the extracted features are concatenated into a single matrix and are used to develop models (classification or regression) based on multivariate analysis techniques. In mid-level fusion, feature extraction can be accomplished using different strategies, such as data decomposition (multivariate curve resolution - MCR) and feature selection (PCA) methods. One of the advantages of mid-level data fusion is that it reduces data dimensionality, thereby allowing data blocks to be treated individually, avoiding the influence of other datasets. Mid-level data fusion, however, requires an optimal combination of extracted features that describe most of the variation in the data. Whereas both low- and mid-level data fusion methods combine the data sources at the data level, high-level data fusion is a decision-level fusion that combines model outputs to produce a final fused response. In high-level fusion, separate models are developed for each available block of data, and their individual responses are combined (e.g., by averaging) to produce a final fused response (Doeswijk et al., 2011). In multiple-level fusion, a combination of low- and mid-level fusions are used together to obtain a final output (Castanedo, 2013).

Data fusion approaches are now widely used in several disciplines, such as robotics (Thrun and Burgard, 2005), image processing (Westa and Resminib, 2009), food analysis (Biancolillo et al., 2019; Borràs et al., 2015; Hong and Wang, 2014) and metabolomics studies (Smilde et al., 2005). For example, low-level data fusion has been widely used to authenticate the origin of foods and beverages and assess their quality. Available evidence indicates that low-level data fusion results in better prediction and classification models than individual techniques. For example, low-level data fusion has been shown to improve the quality assessment of wines (Gil-Sánchez et al., 2011), the identification of the origin of olive

oils (Haddi et al., 2013), the predictive model accuracy of the quality parameters of soybean flour (Brás et al., 2005) and apples characterisation (Zude et al., 2006), as well as to enhance the robustness in the discrimination of coffee varieties (Downey et al., 1997).

Mid-level data fusion approaches have also been proven useful in a wide range of applications, such as in the identification of food fraud (Márquez et al., 2016), analysis of geographic traceability of soil samples (Silvestri et al., 2013) and discrimination of different types of beer (Aranda-Sanchez et al., 2009; Vera et al., 2011). To date, high-level fusion has mainly been applied to classification tasks pertaining to, for example, fruit quality assessment (Aranda-Sanchez et al., 2009; Li et al., 2007) and identification of food fraud (Márquez et al., 2016). Findings yielded by pertinent studies indicate that data fusion approaches can be highly beneficial for mineralogical applications (Chari et al., 2005; Khajehzadeh et al., 2017). However, at present, the application of data fusion for mineralogical investigations remains very limited.

4.5.2. CONCEPTUAL FRAMEWORK

A wide range of sensor technologies that are applicable for material characterisation in mining are rapidly emerging. The fusing of these different data sources likely enhances material characterisation owing to the synergy among the incorporated datasets. The imaging and point sensor technologies indicated in Figure 4.3 are among the various potential techniques applicable in mining. Taking into account these technologies, a general conceptual framework that deploys data fusion at multi-levels was developed (Figure 4.4). As shown in the figure, the workflow depicts the different steps required to achieve data fusion for improved and comprehensive characterisation of materials than that would have been possible by the use of the individual sensor outputs. The concept leads to an automated characterisation of material using a tool that links the combined sensor signals to material properties.

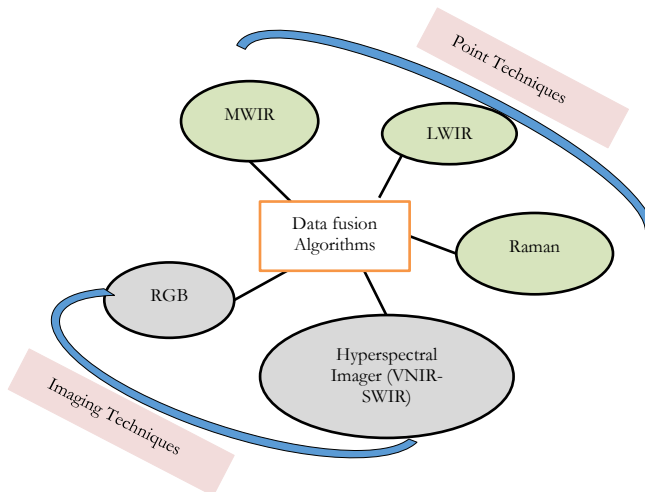


Figure 4.3: Some of the potential imaging and point sensor technologies applicable in raw material characterisation using data fusion.

Data fusion is mainly a data-driven approach that can be implemented using multiple data sources at multi-levels. Effective use of data fusion is highly reliant on the choice of the pre-processing techniques, levels of fusion, ultimate sensor choice, and algorithms (models). Therefore, characterisation of material using a data fusion approach requires an optimised solution. Consequently, DoE is proposed to test the possible scenarios for the optimal data pre-processing techniques, sensor combinations options, and the preferred level of data fusion (denoted as Block C of Figure 4.4). For example, in terms of practical implementation, integration of all the indicated sensors into the same platform might be challenging (e.g., due to a high data volume). Thus, the optimal sensor combinations should be selected in an optimised way. The data fusion task (indicated by Block B in Figure 4.4) includes the fusion of data blocks at low-, mid- and high-levels to address multiple classification and prediction problems using the models described in Section 4.2. The developed classification and regression models were validated using reference data acquired from conventional laboratory-based measurements. The details of the validation approach applied for each analysis are presented in the subsequent chapters. The validation results led to make choices for optimal pre-processing techniques and sensors combinations (represented by Block C in Figure 4.4). The preferred combined sensor signals can be used to develop a tool for an automated material characterisation (indicated by Block D in Figure 4.4). This sub-task is not performed in this work; however, within the framework of the proposed general concept, data fusion was realised. The implemented methodological approaches for the fusion of the different data sources are presented in the subsequent chapters (Chapter 10, 11 and 12).

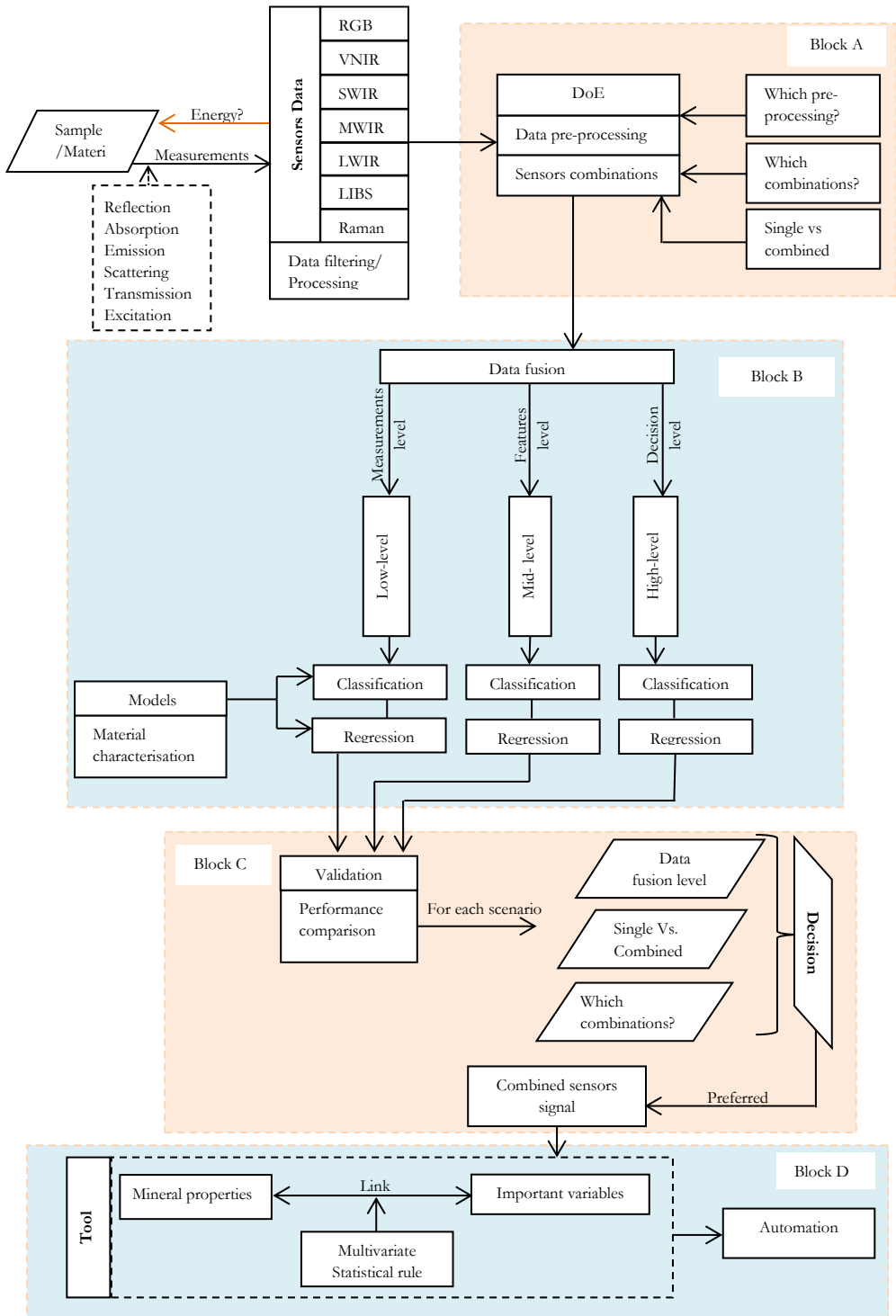


Figure 4.4: A concept for automated material characterisation using a data fusion approach.

4.6. SOFTWARE AND PROGRAMS

The software and programs used in this study include

- ArcGIS 10.6 (developed by Esri, California, United States)
- MATLAB R2018a (developed by The Mathworks, Massachusetts, United States)
- ENVI 4.5 (created by Harris Geospatial, Colorado, United States)
- The Unscrambler 10.5.1 (developed by CAMO Software, Oslo, Norway)
- R 3.5.0 (created by R Core Team, Vienna, Austria– an open-source software)
- Datamine Studio RM 1.3 (developed by Datamine software limited, Wells, United Kingdom)
- Split-Desktop 4.0 (created by Split Engineering LLC, Arizona, United States), and
- OriginPro 9.6 (developed by OriginLab Corporation, Northampton, United States)

The RGB images were analysed in ArcGIS. The hyperspectral images were pre-processed in MATLAB. ENVI software was used for features extraction and classification of the hyperspectral images. The point data analysis, modelling and data fusion, were performed using the Unscrambler and R programming. On the other hand, georeferencing of the RGB images in 3D and coordinate extraction from the point cloud was performed in Datamine Studio RM. Rock fragmentation was analysed using the Split Desktop image analysis software, and the OriginPro software was used for the processing of spectra and visualisation.

REFERENCES

- Abedi, M., Norouzi, G. H. & Torabi, S. A. (2013). Clustering of mineral prospectivity area as an unsupervised classification approach to explore copper deposit. *Arabian Journal of Geosciences*, 6(10), pp. 3601-3613. doi: 10.1007/s12517-012-0615-5
- Aranda-Sanchez, J. I., Baltazar, A. & González-Aguilar, G. (2009). Implementation of a Bayesian classifier using repeated measurements for discrimination of tomato fruit ripening stages. *Biosystems Engineering*, 102(3), pp. 274-284. doi: 10.1016/j.biosystemseng.2008.12.005
- Awad, M. & Khanna, R. (2015). Chapter 4 - Support Vector Regression. In: M. Awad & R. Khanna (Eds.), *Efficient Learning Machines: Theories, Concepts, and Applications for Engineers and System Designers*. Apress, Berkeley, CA, pp. 67-80.
- Barker, M. L. & Rayens, W. (2003). Partial Least Squares for Discrimination, *Journal of Chemometrics*, 17(3), pp. 166-173. doi: 10.1002/cem.785
- Biancolillo, A., Boqué, R., Cocchi, M. & Marini, F. (2019). Chapter 10 - Data Fusion Strategies in Food Analysis. In: M. Cocchi (Ed.), *Data Handling in Science and Technology*. Elsevier, pp. 271-310.
- Borràs, E., Ferré, J., Boqué, R., Mestres, M., Aceña, L. & Busto, O. (2015). Data fusion methodologies for food and beverage authentication and quality assessment - a review. *Analytica chimica acta*, 891, pp. 1-14. doi: 10.1016/j.aca.2015.04.042

- Boucher, T. F., Ozanne, M. V., Carmosino, M. L., Dyar, M. D., Mahadevan, S., Breves, E. A., Lepore, K. H. & Clegg, S. M. (2015). A study of machine learning regression methods for major elemental analysis of rocks using laser-induced breakdown spectroscopy. *Spectrochimica Acta Part B: Atomic Spectroscopy*, 107, pp. 1-10. doi: 10.1016/j.sab.2015.02.003
- Brereton, R. G. (2007). Chapter 1 - Introduction. In: R.G. Brereton (Ed.), *Applied Chemometrics for Scientists*. John Wiley & Sons, West Sussex, England, pp. 1-8.
- Brereton, R. G. & Lloyd, G. R. (2010). Support Vector Machines for classification and regression. *Analyst*, 135(2), pp. 230-267. doi: 10.1039/B918972F
- Brás, L. g. P., Bernardino, S. A., Lopes, J. A. & Menezes, J. C. (2005). Multiblock PLS as an approach to compare and combine NIR and MIR spectra in calibrations of soybean flour. *Chemometrics and Intelligent Laboratory Systems*, 75(1), pp. 91-99. doi: 10.1016/j.chemolab.2004.05.007
- Bro, R. & Smilde, A. K. (2003). Centering and scaling in component analysis. *Journal of Chemometrics*, 17(1), pp.16-33. doi: 10.1002/cem.773
- Bro, R., Berg, F., Thybo, A., Andersen, C., Jørgensen, B. & Andersen, H. (2002). Multivariate data analysis as a tool in advanced quality monitoring in the food production chain. *Trends in Food Science & Technology*, 13(6-7), pp. 235-244. doi: 10.1016/S0924-2244(02)00138-3
- Castanedo, F. (2013). A Review of Data Fusion Techniques. *The Scientific World Journal*, 2013, 704504. doi: 10.1155/2013/704504
- Chari, S., Fanning, J., Salem, S., Robinson, A. & Halford, C. (2005). LWIR and MWIR fusion algorithm comparison using image metrics. *Proceedings of SPIE 5784 on Infrared Imaging Systems: Design, Analysis, Modeling, and Testing XVI*, Vol. 5784, Florida, USA, pp. 16-26.
- Christin, C., Hoefsloot, H. C. J., Smilde, A. K., Hoekman, B., Suits, F., Bischoff, R. & Horvatovich, P. (2013). A Critical Assessment of Feature Selection Methods for Biomarker Discovery in Clinical Proteomics. *Molecular & cellular proteomics*, 12 (1), pp. 263-276. doi: 10.1074/mcp.M112.022566
- Cocchi, M. (2019). Chapter 1 - Introduction: Ways and Means to Deal with Data from Multiple Sources. In: M. Cocchi (Ed.), *Data Handling in Science and Technology*. Elsevier, pp. 1-26.
- Death, D. L., Cunningham, A. P. & Pollard, L. J. (2008). Multi-element analysis of iron ore pellets by Laser-induced Breakdown Spectroscopy and Principal Components Regression. *Spectrochimica Acta Part B: Atomic Spectroscopy*, 63(7), pp. 763-769. doi: 10.1016/j.sab.2008.04.014
- Deris, A., Zain, A. & Sallehuddin, R. (2011). Overview of Support Vector Machine in Modeling Machining Performances. *Procedia Engineering*, 24, pp. 308-312. doi: 10.1016/j.proeng.2011.11.2647
- Doeswijk, T. G., Smilde, A. K., Hageman, J. A., Westerhuis, J. A. & van Eeuwijk, F. A. (2011). On the increase of predictive performance with high-level data fusion. *Analytica Chimica Acta*, 705(1-2), pp. 41-47. doi: 10.1016/j.aca.2011.03.025
- Downey, G., Briandet, R., Wilson, R. H. & Kemsley, E. K. (1997). Near- and Mid-Infrared Spectroscopies in Food Authentication: Coffee Varietal Identification. *Journal of Agricultural and Food Chemistry*, 45(11), pp. 4357-4361. doi: 10.1021/jf970337t

- Engel, J., Gerretzen, J., Szymańska, E., Jansen, J. J., Downey, G., Blanchet, L. & Buydens, L. M. C. (2013). Breaking with trends in pre-processing? *TrAC Trends in Analytical Chemistry*, 50, pp. 96-106. doi: 10.1016/j.trac.2013.04.015
- Eriksson, L., Byrne, T., Johansson, E., Trygg, J. & Vikström, C. (2013). Chapter 3 - PCA. In: *Multi- and Megavariate data analysis: basic principles and applications*, 3rd ed., MKS Umetrics AB, Malmö, Sweden, pp. 33-53.
- Esbensen, K. H. & Geladi, P. (2009). Chapter 2 - Principal Component Analysis: Concept, Geometrical Interpretation, Mathematical Background, Algorithms, History, Practice. In: S.D. Brown, R. Tauler, & B. Walczak (Eds.), *Comprehensive Chemometrics*. Elsevier, pp. 211-226.
- Fearn, T., Riccioli, C., Garrido-Varo, A., & Guerrero-Ginel, J. E. (2009). On the geometry of SNV and MSC. *Chemometrics and Intelligent Laboratory Systems*, 96(1), pp. 22-26. doi: 10.1016/j.chemolab.2008.11.006
- Fernández, R., Montes, H., Salinas, C., Sarria, J. & Armada, M. (2013). Combination of RGB and Multispectral Imagery for Discrimination of Cabernet Sauvignon Grapevine Elements. *Sensors*, 13(6), pp. 7838-7859. doi: 10.3390/s130607838
- Forshed, J., Idborg, H. & Jacobsson, S. (2007). Evaluation of different techniques for data fusion of LC/MS and 1H-NMR. *Chemometrics and Intelligent Laboratory Systems - Chemometr Intell Lab Syst*, 85(1), pp. 102-109. doi: 10.1016/j.chemolab.2006.05.002
- Gauthier, T. D. & Hawley, M. E. (2007). Chapter 5 - Statistical Methods. In: B. L. Murphy & R. D. Morrison (Eds.), *Introduction to Environmental Forensics*, 2nd ed., Academic Press, Burlington, USA, pp. 129-183.
- Haddi, Z., Alami, H., El Bari, N., Tounsi, M., Barhoumi, H., Maaref, A., Jaffrezic-Renault, N. & Bouchikhi, B. (2013). Electronic nose and tongue combination for improved classification of Moroccan virgin olive oil profiles. *Food Research International*, 54(2), pp. 1488-1498. doi: 10.1016/j.foodres.2013.09.036
- Hall, D. L. & Llinas, J. (1997). An introduction to multisensor data fusion. *Proceedings of the IEEE*, 85, pp. 6-23.
- Hall, D. L. & McMullen, S. A. H. (2004). Chapter 1 - Introduction to Multisensor Data Fusion. In: D. L. Hall & S. A. H. McMullen (Eds.), *Mathematical Techniques in Multisensor Data Fusion*, 2nd ed., Artech House, Norwood, Massachusetts, pp. 1-32.
- Hawkins, D. (1980). Chapter 1 - Introduction. In: D. Hawkins (Ed.), *Identification of Outliers*, Springer, Dordrecht, The Netherlands, pp. 1-12.
- Hecker, C., Dilles, J. H., van der Meijde, M. & van der Meer, F. D. (2012). Thermal infrared spectroscopy and partial least squares regression to determine mineral modes of granitoid rocks. *Geochemistry, Geophysics, Geosystems*, 13(3), 3021. doi: 10.1029/2011GC004004
- Hoehse, M., Mory, D., Florek, S., Weritz, F., Gornushkin, I. & Panne, U. (2009). A combined laser-induced breakdown and Raman spectroscopy Echelle system for elemental and molecular microanalysis. *Spectrochimica Acta Part B: Atomic Spectroscopy*, 64(11), pp. 1219-1227. doi: 10.1016/j.sab.2009.09.004
- Hong, X. & Jun, W. (2014). Detection of adulteration in cherry tomato juices based on electronic nose and tongue: Comparison of different data fusion approaches. *Journal of food engineering*, 126, pp. 89-97. doi: 10.1016/j.jfoodeng.2013.11.008
- Howard, W. J., Rhemtulla, M. & Little, T. D. (2015). Using Principal Components as Auxiliary Variables in Missing Data Estimation. *Multivariate behavioral research*, 50(3), pp. 285-299. doi: 10.1080/00273171.2014.999267

- Jain, A. K., Murty, M. N. & Flynn, P. J. (1999). Data clustering: A review. *ACM Computing Surveys*, 31(3), pp. 264-323. doi: 10.1145/331499.331504
- Jain, A.K., Duin, R.P.W. & Jianchang, M. (2000). Statistical pattern recognition: a review. In *IEEE Transactions on Pattern Analysis and Machine Intelligence*, 22(1), pp. 4-37.
- Jensen, D. & Ramirez, D. (2017). Use of Hotelling's T²: Outlier Diagnostics in Mixtures. *International Journal of Statistics and Probability*, 6(6), pp. 24-34. doi: 10.5539/ijsp.v6n6p24
- Jolliffe, I.T. (2002). *Principal Component Analysis*, 2nd ed., Springer, New York, USA.
- Kaufman, L. & Rousseeuw, P. J. (2005). *Finding Groups in Data: An Introduction to Cluster Analysis*. John Wiley & Sons, Hoboken, New Jersey.
- Kecman, V. (2005). Chapter 1 - Support Vector Machines - Introduction. In: L. Wang (Ed.), *Support Vector Machines: Theory and Applications*. Springer-Verlag, Berlin, Germany, pp. 1-47.
- Khajehzadeh, N., Haavisto, O. & Koresaar, L. (2017). On-stream mineral identification of tailing slurries of an iron ore concentrator using data fusion of LIBS, reflectance spectroscopy and XRF measurement techniques. *Minerals Engineering*, 113, pp. 83-94. doi: 10.1016/j.mineng.2017.08.007
- Kruse, F. A., Lefkoff, A. B., Boardman, J. W., Heidebrecht, K. B., Shapiro, A. T., Barloon, P. J. & Goetz, A. F. H. (1993). The spectral image processing system (SIPS)—interactive visualization and analysis of imaging spectrometer data. *Remote Sensing of Environment*, 44(2), pp. 145-163. doi: 10.1016/0034-4257(93)90013-N
- Läuter, H. (1988). *Applied Linear Regression*, 2nd ed., John Wiley & Sons, New York, USA.
- Lee, L. C., Liong, C. Y. & Jemain, A. A. (2018). Partial least squares-discriminant analysis (PLS-DA) for classification of high-dimensional (HD) data: a review of contemporary practice strategies and knowledge gaps. *The Analyst*, 143(15), pp. 3526-3539. doi: 10.1039/c8an00599k
- Li, C., Heinemann, P. & Sherry, R. (2007). Neural network and Bayesian network fusion models to fuse electronic nose and surface acoustic wave sensor data for apple defect detection. *Sensors and Actuators B: Chemical*, 125(1), pp. 301-310. doi: 10.1016/j.snb.2007.02.027
- Li, Y., Zhang, J. Y. & Wang, Y. Z. (2018). FT-MIR and NIR spectral data fusion: a synergetic strategy for the geographical traceability of *Panax notoginseng*. *Analytical and bioanalytical chemistry*, 410(1), pp. 91-103. doi: 10.1007/s00216-017-0692-0
- Lillesand, T.M., Kiefer, R.W. & Chipman, J.W. (2004). *Remote Sensing and Image Interpretation*. John Wiley & Sons, Hoboken, NJ.
- Márquez, C., López, M. I., Ruisánchez, I. & Callao, M. P. (2016). FT-Raman and NIR spectroscopy data fusion strategy for multivariate qualitative analysis of food fraud. *Talanta*, 161, pp. 80-86. doi: 10.1016/j.talanta.2016.08.003
- McCool, M., Robison, A. D. & Reinders, J. (2012). Chapter 11 - K-Means Clustering. In: M. McCool, A. D. Robison & J. Reinders (Eds.), *Structured Parallel Programming*. Elsevier, pp. 279-289.
- Mellinger, M. (1987). Multivariate data analysis: Its methods. *Chemometrics and Intelligent Laboratory Systems*, 2(1), pp. 29-36. doi: 10.1016/0169-7439(87)80083-7
- Miller, J. N. & Miller, J.C. (2000). *Statistics and chemometrics for analytical chemistry*, 4th ed., Prentice Hall, Harlow, England.

- Mishra, S. & Datta-Gupta, A. (2018). Chapter 5 - Multivariate Data Analysis. In: S. Mishra & A. Datta-Gupta (Eds.), *Applied Statistical Modeling and Data Analytics*, Elsevier, pp. 97-118.
- Noonan, R. (2017). Chapter 1 - Partial Least Squares: The Gestation Period. In: H. Latan & R. Noonan (Eds.), *Partial Least Squares Path Modeling*, Springer, Cham, Switzerland, pp. 3-18.
- Paolanti, M. & Frontoni, E. (2020). Multidisciplinary Pattern Recognition applications: A review. *Computer Science Review*, 37, 100276. doi: 10.1016/j.cosrev.2020.100276
- Richards, J. A. (2013). Chapter 8 - Supervised Classification Techniques. In: J. A. Richards (Ed.), *Remote Sensing Digital Image Analysis*, Springer-Verlag, Berlin, Heidelberg, pp. 247-318.
- Richards, J. A. & Jia, X. (2006). Chapter 8 - Supervised Classification Techniques. In: J. A. Richards & X. Jia (Eds.), *Remote Sensing Digital Image Analysis*, 4th ed., Springer, Berlin, Heidelberg, pp. 193-247.
- Rinnan, Å., van den Berg, F. & Engelsen, S. B. (2009). Review of the most common pre-processing techniques for near-infrared spectra. *TrAC Trends in Analytical Chemistry*, 28(10), pp. 1201-1222. doi: 10.1016/j.trac.2009.07.007
- Rodrigues, R. D., Zhao, L., Zheng, Q. & Zhang, J. (2020). A tourist walk approach for internal and external outlier detection. *Neurocomputing*, 393, pp. 203-213. doi: 10.1016/j.neucom.2018.10.113
- Roussel, S., Preys, S., Chauchard, F. & Lallemand, J. (2014). Multivariate Data Analysis (Chemometrics). In: C.P. O'Donnell, C. Fagan & P.J. Cullen (Eds.), *Process Analytical Technology for the Food Industry*. Springer, New York, USA, pp. 7-59.
- Scheevel, J. R. & Payrazyan, K. (2001). Principal Component Analysis Applied to 3D Seismic Data for Reservoir Property Estimation. *SPE Reservoir Evaluation & Engineering*, 4(01), pp. 64-72. doi: 10.2118/69739-PA
- Sharma, S. K., Misra, A. K., Lucey, P. G. & Lentz, R. C. F. (2009). A combined remote Raman and LIBS instrument for characterizing minerals with 532nm laser excitation. *Spectrochimica Acta Part A: Molecular and Biomolecular Spectroscopy*, 73(3), pp. 468-476. doi: 10.1016/j.saa.2008.08.005
- Siciliano, B. & Khatib, O. (2016). *Handbook of Robotics*, 2nd ed., Springer: Berlin, German.
- Silvestri, M., Bertacchini, L., Durante, C., Marchetti, A., Salvatore, E. & Cocchi, M. (2013). Application of data fusion techniques to direct geographical traceability indicators. *Analytica Chimica Acta*, 769, pp.1-9. doi: 10.1016/j.aca.2013.01.024
- Silvestri, M., Elia, A., Bertelli, D., Salvatore, E., Durante, C., Li Vigni, Marchetti, A. & Cocchi, M. (2014). A mid-level data fusion strategy for the Varietal Classification of Lambrusco PDO wines. *Chemometrics and Intelligent Laboratory Systems*, 137, pp. 181-189. doi: 10.1016/j.chemolab.2014.06.012
- Sisodia, P. S., Tiwari, V. & Kumar, A. (2014). Analysis of Supervised Maximum Likelihood Classification for remote sensing image. Proceedings of the international conference on recent advances and innovations in engineering (ICRAIE-2014), Jaipur, India, pp. 1-4.
- Smilde, A. K., van der Werf, M. J., Bijlsma, S., van der Werff-van der Vat, B. J. C. & Jellema, R. H. (2005). Fusion of Mass Spectrometry-Based Metabolomics Data. *Analytical Chemistry*, 77(20), pp. 6729-6736. doi: 10.1021/ac051080y
- Smola, A., & Schölkopf, B. (2004). A tutorial on support vector regression. *Statistics and Computing*, 14, pp. 199-222. doi: 10.1023/B%3ASTCO.0000035301.49549.88

- Thrun, S., Burgard, W. & Fox, D. (2005). Chapter 1- Introduction. In: Probabilistic Robotics, MIT Press, Cambridge, MA, pp. 3-11.
- Vera, L., Aceña, L., Guasch, J., Boqué, R., Mestres, M. & Busto, O. (2011). Discrimination and sensory description of beers through data fusion. *Talanta*, 87, pp. 136-142. doi: 10.1016/j.talanta.2011.09.052
- Wang, C., Liu, Z., Gao, H. & Fu, Y. (2019). VOS: A new outlier detection model using virtual graph. *Knowledge-Based Systems*, 185, 104907. doi: 10.1016/j.knosys.2019.104907
- Westa, M. S. & Resminib, R. G. (2009). Hyperspectral imagery and LiDAR for geological analysis of Cuprite, Nevada. Proceedings of SPIE on Defense & Security, Algorithms and Technologies for Multispectral, Hyperspectral, and Ultraspectral Imagery XV, Vol. 7334, Orlando, USA.
- Wold, S., Sjöström, M. & Eriksson, L. (2001). PLS-regression: a basic tool of chemometrics. *Chemometrics and Intelligent Laboratory Systems*, 58(2), pp. 109-130. doi: 10.1016/S0169-7439(01)00155-1
- Yang, X. S. (2019). Chapter 5 - Logistic regression, PCA, LDA, and ICA. In: X.S. Yang (Ed.), *Introduction to Algorithms for Data Mining and Machine Learning*. Academic Press, pp. 91-108.
- Zude, M., Herold, B., Roger, J. M., Bellon-Maurel, V. & Landahl, S. (2006). Non-destructive tests on the prediction of apple fruit flesh firmness and soluble solids content on tree and in shelf life. *Journal of Food Engineering*, 77(2), pp. 254-260. doi: 10.1016/j.jfoodeng.2005.06.027
- Zuo, R. & Carranza, E. J. M. (2011). Support vector machine: A tool for mapping mineral prospectivity. *Computers & Geosciences*, 37(12), pp. 1967-1975. doi: 10.1016/j.cageo.2010.09.014

5

CASE STUDY SITE AND SAMPLE MATERIAL

This chapter provides a brief explanation of the geological setting of the study site. It describes the regional and local geology. A detail description of the mineralization at the defined study block is presented. The chapter finally describes the adopted sampling strategy and the different types of samples collected for this research.

5.1. INTRODUCTION

The Reiche Zeche underground mine located in the Freiberg district, eastern Erzgebirge, Germany, served as the case study area (Figure 5.1). Originating in 1168, it is one of the oldest mines in Europe and, during its operation it was mined for silver, copper, lead, arsenic, zinc and pyrite (Scheinert et al., 2009; Seifert and Sandmann, 2006). In 1863 and 1886, the elements indium and germanium were discovered, respectively at the local Freiberg district (Seifert and Sandmann, 2006). As the mine ceased operating in 1969, the “Reiche Zeche” and “Alte Elisabeth” shafts were reconstructed in 1976 and were reopened as a research and teaching mine.

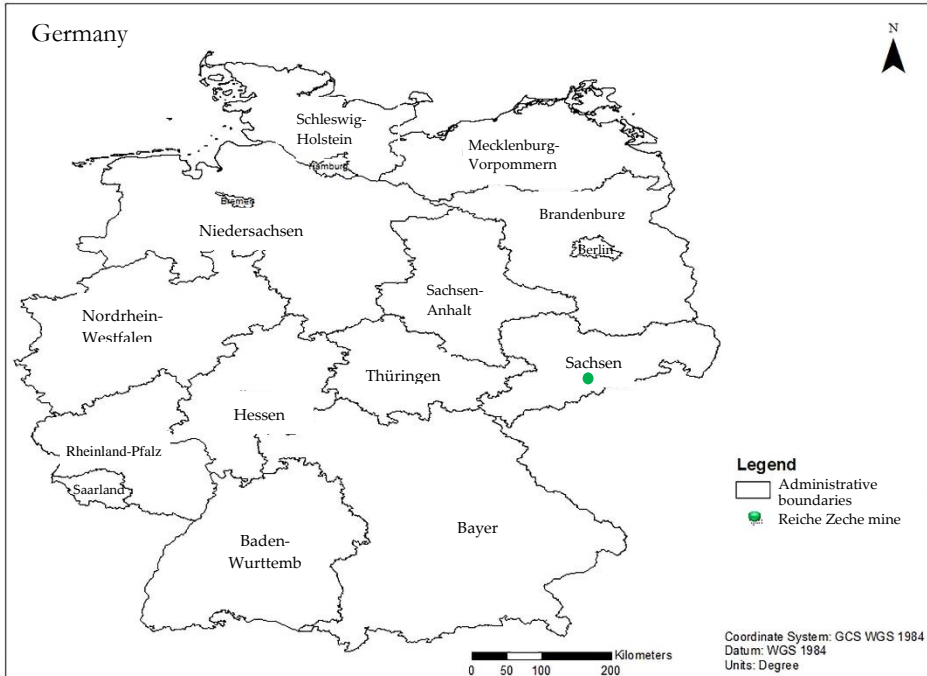


Figure 5.1: Location map of the Reiche Zeche underground mine.

5.1.1. REGIONAL GEOLOGY

The Erzgebirge is one of the major polymetallic mineral provinces in Europe. It is part of the internal Mid-European Variscides metamorphic basement and located along the NW-border of the crystalline Bohemian Massif core complex (Seifert and Sandmann, 2006; Ostendorf et al., 2019) (Figure 5.2). The Erzgebirge forms NE-SW trending antiformal megastructure that extends over 120 km in length and 45 km in width (Mingram, 1998). It comprises medium- to high- grade metamorphic rocks that are formed during the continent-to-continent collision processes during Variscan Orogeny (Kroner et al., 2007; Sebastian, 1995 as cited in Seifert and Sandmann, 2006; Seifert and Sandmann, 2006; Mingram, 1998). The Erzgebirge consists of five metamorphic units namely, low-grade unit, phyllite unit, garnet-phyllite unit, mica schist-eclogite unit and gneiss-eclogite units (Willner et al., 1997;

Rötzler et al., 1998). The metamorphic units are associated with numerous hydrothermal mineral deposits (Seifert and Sandmann, 2006).

Volcanic intrusions occur in the metamorphic core complex of the Erzgebirge region. The Variscan Orogeny and the subsequent crustal reorganisation triggered the magmatism process in the area. The hydrothermal deposits of the Erzgebirge are associated with intrusive bodies of Variscan and younger granite (Seifert and Sandmann, 2006). In the region, the polymetallic sulphide veins of the hydrothermal deposits are hosted by para- and orthogneisses, mica schists and subordinately by post-kinematic granites (Seifert and Sandmann, 2006). Two main gneiss units are identified in the eastern Erzgebirge region; the “red gneiss unit” and the “grey gneiss unit” (Tichomirowa et al., 2001; Willner et al., 1997). The grey gneiss unit is subdivided into two groups based on the textural differences: inner grey gneiss (orthogneiss) and outer grey gneiss (paragneiss). The inner grey gneiss is coarse to medium-grained texture, whereas the outer grey gneiss is mostly fine-grained (Tichomirowa et al., 2001; Willner et al., 1997). Mica schist is the main rock type of the mica schist–eclogite unit. It is subdivided into feldspar-free schist, graphite-bearing schist and albite-bearing schist (Mingram, 1998).

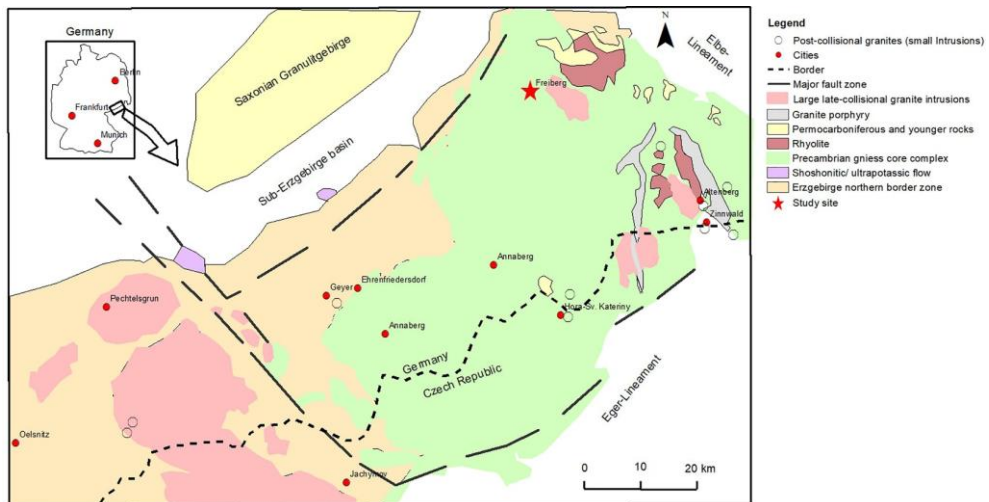


Figure 5.2: A simplified geological map of the Erzgebirge (Saxony, Germany; Bohemia, Czech Republic) (reproduced after Seifert and Sandmann (2006) with permission).

5.1.2. LOCAL GEOLOGY

The geologic setting of the Freiberg mining district is dominated by an orthogneiss dome (“inner grey gneisses”) surrounded by a paragneiss unit (“outer grey gneisses”). Red gneisses occur as elongated bodies in outer grey gneisses of the gneiss-eclogite metamorphic unit. The red gneisses are muscovite-bearing gneisses with variable textures (e.g., coarse-grained augen gneisses and medium-grained foliated gneisses) (Tichomirowa et al., 2001). The other rock types in the vicinity include mica schist, gabbro, granulites, variscan granites, variscan rhyolites and eclogites. In the area, the ore vein network is characterised by NNE-SSW to N-S and E-W to ENE-WSW trending shear systems (Scheinert et al., 2009; Kröner and Willner, 1998; Ostendorf et al., 2019). The ore veins in the district are associated with a system of dykes (Scheinert et al., 2009).

In the Freiberg district, the deposit is characterised by polymetallic vein-type mineralization formed by two hydrothermal mineralization events of Late-Variscan (late Carboniferous to early Permian) and Post-Variscan age (Seifert, 2008). The Late-Variscan mineralization event dominates in the central part of the mine and mineralization is rich in Pb, Zn, Fe, S, and Cu. Typical ore minerals include pyrite, galena, arsenopyrite, chalcopyrite and sphalerite, along with quartz and minor carbonate gangue. Ore minerals with a smaller Cu, Zn and Fe content characterise the Post-Variscan mineralization event. This mineralization event consists of a fluorite-barite-lead ore assemblage, mainly containing sphalerite, pyrite, galena, chalcopyrite and marcasite, as well as quartz, fluorite, carbonates, and barite, as gangue (Benkert et al., 2015; Seifert, 2008). The polymetallic sulphide veins of the Freiberg district are mainly hosted by orthogneiss. Red gneisses, rhyolites, lamprophyres, gabbros and Permo-Carboniferous granites, host minor occurrences of the veins. More than 1100 polymetallic ore veins run through the metamorphic core complex of the Freiberg district (Ostendorf et al., 2019).

5.2. TEST BLOCK AND SAMPLING STRATEGY

A mine face of approximately 22 m long and 2 m high was defined to test the research concept at the Reiche Zeche underground mine, as shown in Figure 5.3. The defined mine face is characterised by high material variability and located at the first level of Wilhelm Stehender North, at a depth of about 150 m. The northern part of the mine face has an ore vein of thickness ranging from 30 to 100 cm; the vein consists of galena, pyrite, chalcopyrite and sphalerite minerals hosted by gneiss rock. At the central part of the mine face, the ore is disseminated throughout the gneiss rock whereas weathering of the host rock and the ore materials is observed at different locations. Moreover, small circular pores filled with calcite and ore can also be noted. Within the defined ~ 22m long mine face, a blasting block (BB) of ~ 4m long and 2m high was delineated. Blasting was performed at the BB area and samples were acquired from the freshly exposed mine face as well as, from the mine face before the blasting (Figures 5.4 and 5.5). The BB is located in the northern part of the bigger block, and an ore vein of 30 to 100 cm characterises it. A simplified geological map of the freshly exposed BB mine face is shown in Figure 5.6.

In this study, in-situ measurements were performed using an RGB imager. Besides, representative samples were acquired and analysed ex-situ. A strategic sampling campaign was conducted to collect reliable and representative samples. A detail description of the collected sample types is presented in the section that follows.

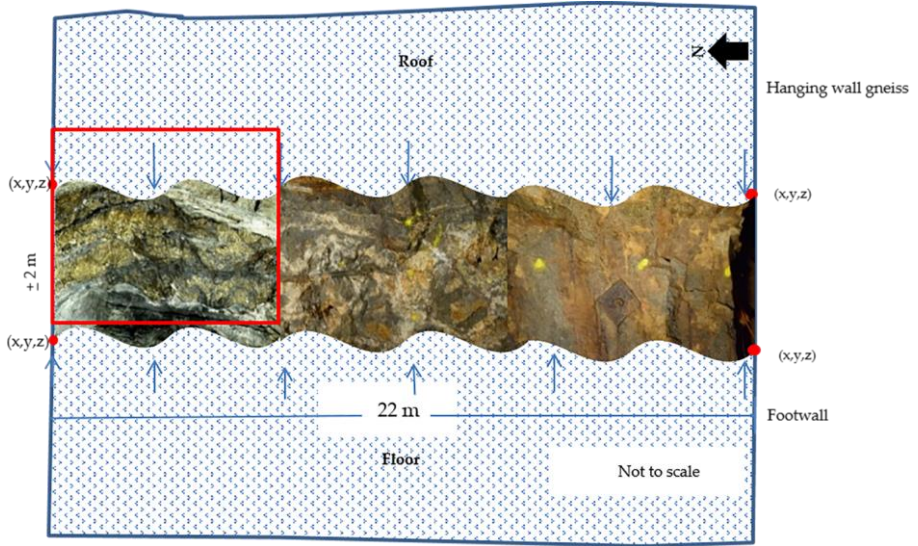


Figure 5.3: A sketch with sample photographs that illustrates the defined mine face having ~ 22 m lateral extent and ~ 2 m height. The red box shows the location of the blasting block having ~ 4 m length and ~ 2 m height.

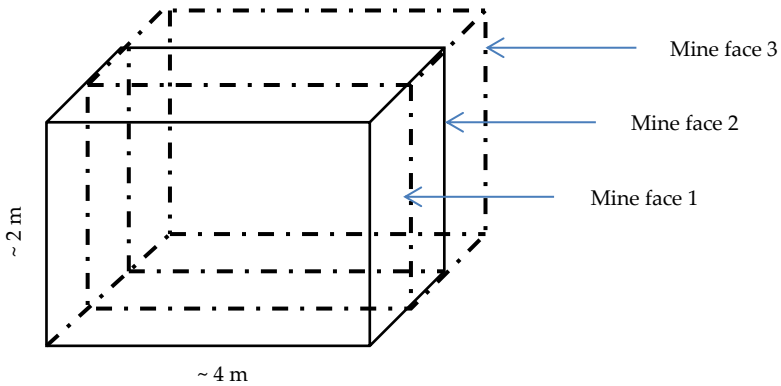


Figure 5.4: Schematic sketch to show the blasting block mine face advancement after each blast.

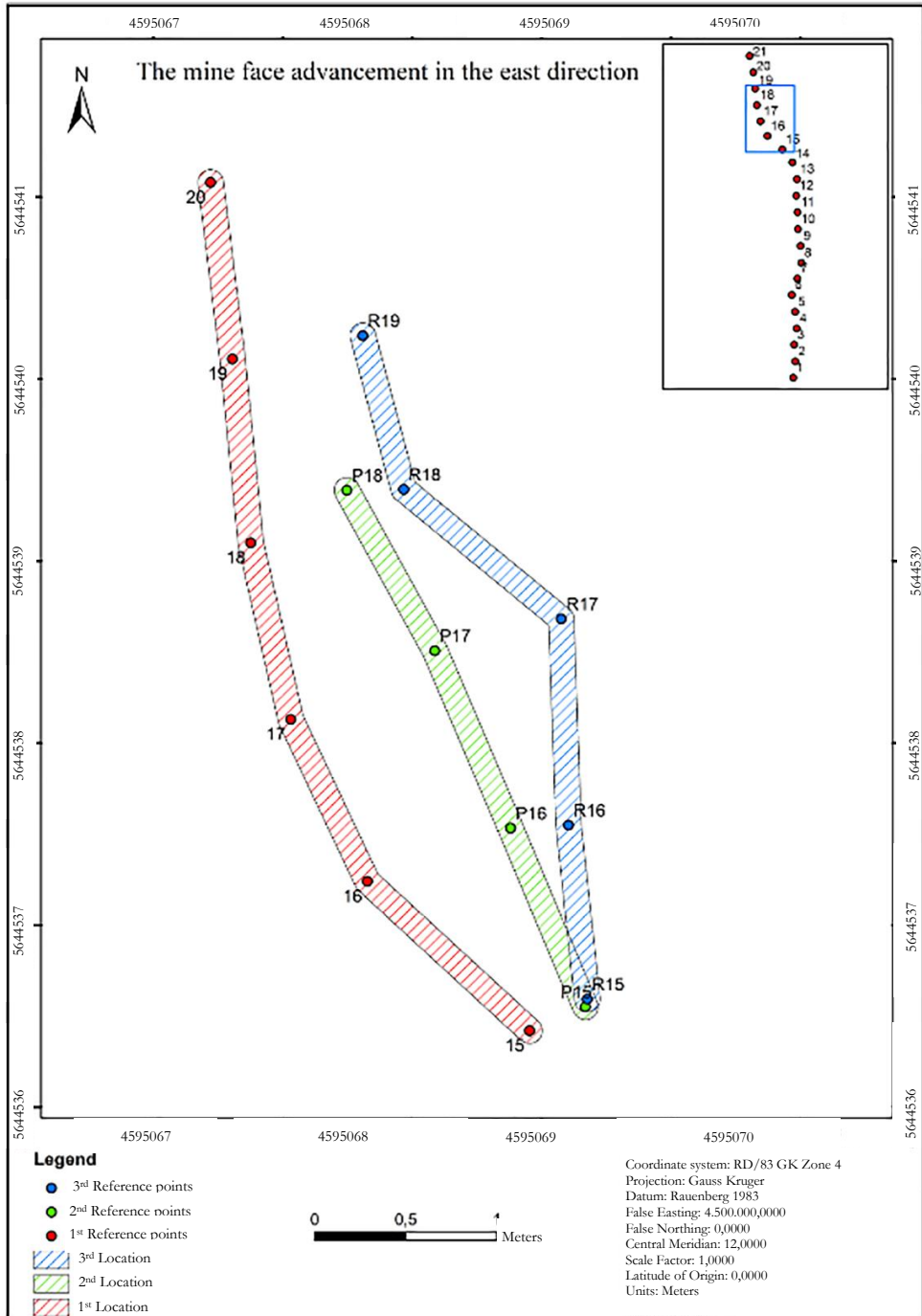


Figure 5.5: A map showing the mine face advancement in the east direction after each blast. The red patch shows the mine face location before the blast, the green patch shows the mine face location after the first blast, and the blue patch shows the mine face after the second blast.

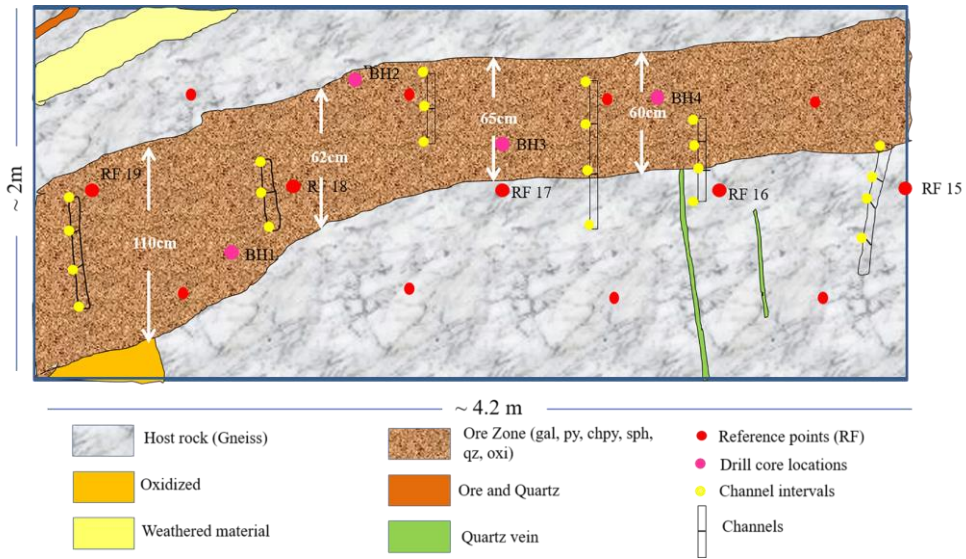


Figure 5.6: A simplified geological map of the blasting block showing the different lithotypes, reference points, drill hole locations, channel locations and channel intervals. This map shows the newly exposed mine face after the second blast.

5.2.1. TYPES OF SAMPLES

In mining, inference about a deposit is developed based on the analysed samples. Therefore, sampling is an essential component of material investigation in mining operations. Optimal sampling minimises the uncertainty of the inference to be made for non-sensed positions based on the information of sensed locations. For this research, different types of samples: channel, muck pile, and drill core were collected. The significance of analysing the different types of samples include: to ensure sample representativity, to understand the unexposed dimension of the study block (e.g., 3D information using drill core samples), and to comprehend the spatial distribution and variability of minerals. It is also beneficial in assessing the potential of the technologies for future material tracking applications along the mining value chain. The sample collection procedures took in to account the integrity of samples in the field. The entire sampling and assay process was monitored on a continuous basis. The description of the different types of samples is presented in the sub-sections that follow:

5.2.1.1. CHANNEL SAMPLES

Channel sampling is advantageous for capturing different lithotypes and variations in their abundance and distribution. It is an information-driven sampling strategy where the spacing of the channels and the intervals within each channel cut were determined based on the observed material variability. Channel samples were collected to address the observed spatial variability and ensure sample representiveness. At the ~ 22m long mine face, twenty-three channels spaced approximately 80 to 120 cm apart (depending on the material variability at each channel location) were cut, and 102 samples were acquired from the different intervals within each channel, as shown in Figure 5.7. The observed material variability determined the spacing between the channels. Besides, 12 channels spaced approximately 75 to 100 cm apart were cut at the newly exposed BB mine face following

the blasting, and 32 samples were collected from the different intervals of these channels. Therefore, a total of 134 channel samples were collected from the three batches.



Channel cut

Figure 5.7: A photograph that illustrate a channel cut at the defined mine face. The channel crosscuts four different intervals, each belonging to a different lithotype and sampled separately (the red boxes).

5.2.1.2. MUCK PILE SAMPLES

The blasted rock fragments (muck pile) are disturbed samples since the rock fragments moved from their original location (Figures 5.8 and 5.9). Forty muck pile samples were collected from the blasted fragments of the BB. The sampling strategy from the muck pile is random. However, to ensure material representativity, the sampling was done from each material type, based on the proportion of the observed material variability.

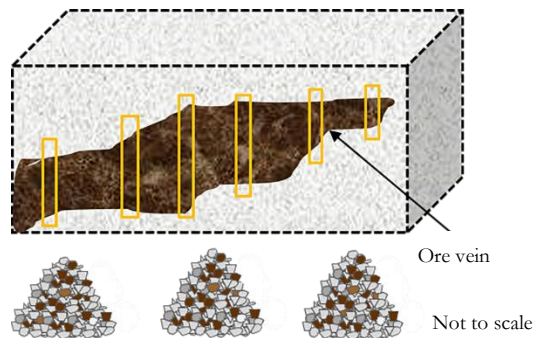


Figure 5.8: Schematic sketch to show the muck piles after blasting. The yellow boxes show the channel samples.



Figure 5.9: Images of the muck piles.

5.2.1.3. DRILL CORE SAMPLES

Drill core samples provide continuous information across the entire depth of the drill profile. Twelve 50 mm diameter drill cores each having a length of approximately 1.5 to 3 m were acquired at different locations of the defined mine face (Figures 5.10 and 5.11). The total length of the drill cores is ~ 23.3 m. The drill cores provide information in the x-direction (easting), thus crucial to have 3D information about the investigated block. Drill core logging was performed to identify the different lithotypes. Besides, the drill cores were analysed using sensor measurements.

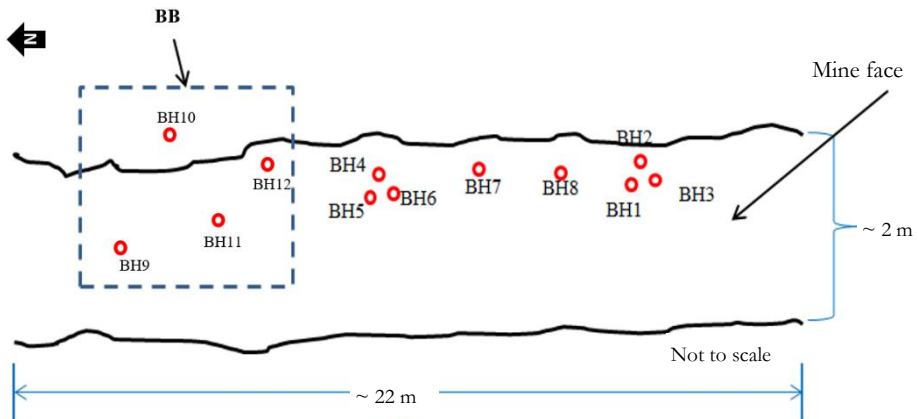


Figure 5.10: A sketch that illustrates the locations of the 12 drill holes at the ~ 22 m mine face. The blue square shows the blasting block site.



Figure 5.11: Images of drill core samples showing the different lithotypes at the drilled sites. The major lithotypes include the weathered materials (e.g., clay minerals), the ore that consists of the sulphide minerals and host rock (gneiss).

5.2.2. GEOREFERENCING

Ground control points (GCPs) were marked on the mine face and the geographic coordinates of the GCPs were collected using light detection and ranging (LIDAR) scan by Mine Surveying and Geodesy team of TUB Freiberg. The collected GCPs were used to georeference and mosaic the RGB images. Georeferencing and mosaicking of the RGB images provided a comprehensive view of mineral distribution over the imaged part of the mine face. Thus, it is advantageous in understanding the spatial distribution, the relative abundance of minerals (therefore to infer grade indirectly), and used to define target domain for further detail analysis. Coordinates of the channel centroids were computed using the surveyed points (GCPs) and the point cloud generated using LIDAR (Figure 5.12). The locations of the drill cores at the mine face were also measured using LIDAR. Therefore, spatially constrained chemical and mineralogical data were generated to demonstrate the possibility of producing georeferenced data from each sampling location. The benefits of the spatially constrained data include providing location-based sensor data for the resource model updating, and it can also be used to link information from the different data sources based on location. However, for the integration of sensors data based on location, further considerations are required. These include the sensors field of view, spatial resolution, positional accuracies and the material variability.

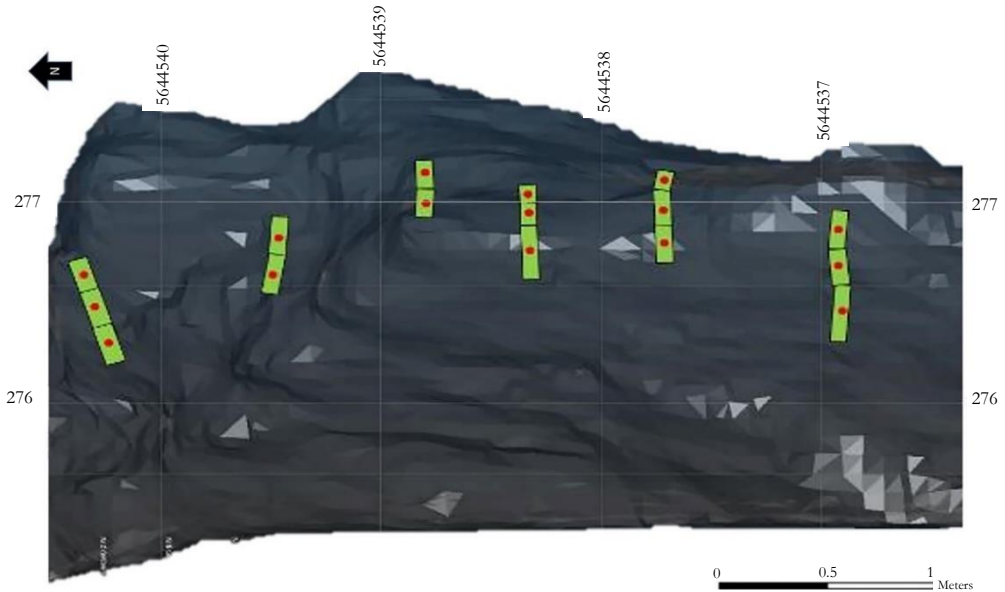


Figure 5.12: Meshed surface of the blasting block showing the channel intervals (green rectangles) and channel centroids (red dots). Mine Surveying and Geodesy team of TUB Freiberg generated the meshed surface.

5.2.3. SAMPLE PREPARATION

The nature (form) of samples analysed in this research were whole-rock, powder, and pellets samples. Analysing the different kinds of samples allows evaluating and maximising the usability of the sensor technologies in material characterisation. The powdering of samples reduces heterogeneity (ensures consistency) and minimises surface irregularities. The surface roughness of samples plays vital roles for sensor measurements that require actual contact with the sample. Without establishing good contact between the sample surface and sensor tip, a sensor detector might not collect all reflected lights from the surface. Therefore, powdering of the samples reduces the effect from the surface raggedness and can improve the analysing performances of sensors. Whole-rock samples preserve the natural condition (e.g., surface irregularities and sample heterogeneity) and require no sample preparation. Thus, analysing whole-rock samples is crucial to evaluate the competency of sensor technologies for in-situ applications. The other sample forms considered in this study are pellets. Pressed pellets can minimise the particle size effect and voids since particles come together uniformly by pressing at high loads. Thus, it provides greater consistency and can enhance the signal from sensors.

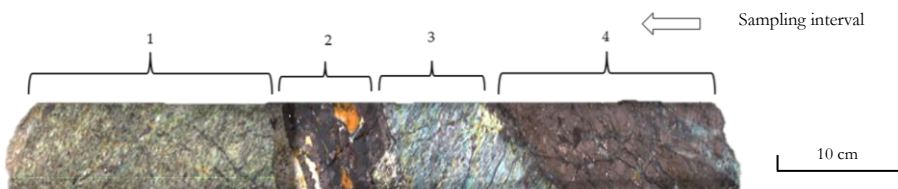


Figure 5.13: A drill core with different lithotypes. Each lithotype was sampled separately.

Following the collection, samples were prepared in the laboratory. The channel and muck pile samples split into two. One part of the split powdered and the other half left as rock sample. Likewise, the drill core samples were cut into two along the drill core length. The half split remained in the core tray. Whereas, the other half cut of the drill cores was used to systematically collect representative samples from each lithotype (Figure 5.13). Thus, the different lithotypes sampled separately and powdered. Sensor measurements were performed using the drill cores in rock forms as well as the powdered samples. For the analyses using the drill cores in the natural form, the imaging technologies capture the whole drill cores length. Whereas, the length of each unit and the observed material variability within each unit determined the number and location of point measurements. The powdered samples of the channel, muck pile and drill core samples were sub-sampled to prepare 50 pressed pellets. The powder mix used to make the pellets was CEREON wax, and the ratio of sample to the wax mix is 4:1. Sensor measurements using the different sample forms enabled the assessment of the preferred sample form for technology. Besides, it allowed comparison and validation of sensor outputs (e.g., whole-rock measurements were validated using the analysis from the powder samples).

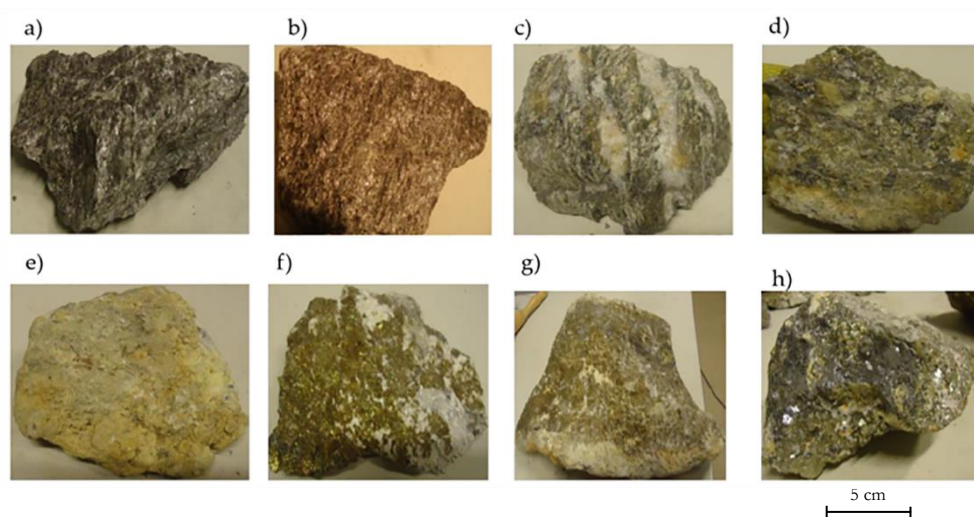


Figure 5.14: Photographs of some of the samples collected from the test site. The samples (a), (b) and (c) were collected from the host rock (gneiss and banded gneiss), samples in ((d), (f) and (h)) were collected from ore that consists of the sulphide minerals (e.g., galena, pyrite and sphalerite), and the pictures (e) and (g) show samples acquired from the weathered materials (e.g., clay minerals).

This research is based on 134 channel samples, 45 samples that were systematically collected from the different lithotypes of the drill cores, 12 drill cores each having a length of approximately 1.50 to 3 m, as well as 40 muck pile samples. The forms of samples analysed in this study were rock, powdered, and pellet samples. In each study, different sets of samples were used. Thus, the type and form of samples used in each study are described in the chapters. The collected samples represent different lithotypes in the vicinity. For example, Figure 5.14 shows some of the samples acquired from the ore, host rock and weathered materials. For this research, ore refers to the sulphide minerals such as galena, sphalerite, pyrite and chalcopyrite. These minerals are the main sources of Zn, Pb and Cu, which are of primary economic interest. Arsenic is a penalty element in mineral processing,

and its presence in the dust is a health concern; therefore, it is of importance as well. In the context of the current investigation, waste refers to the gangue materials, including the carbonates, quartz and the host rock (gneiss). The sensor technologies explored in this research (RGB imaging, VNIR/SWIR hyperspectral imaging, MWIR, LWIR, and Raman) and the forms of samples used for the analysis by each technology are indicated in Figure 5.15. The target domain and sampling locations were determined using RGB imaging. Following this, samples were collected, and each sample was split into two. One part of the split powdered and the other half left as rock sample. Moreover, pellets samples were prepared using half split of the powdered samples. The rock samples were used for measurements using the hyperspectral imagers. The MWIR, LWIR and Raman measurements were performed using both the rock and powder samples. Besides, the Raman analysis was also performed using the pellets samples. On the other hand, the measurements using the validation techniques (ICP-MS, XRF and XRD) were performed using powder samples.

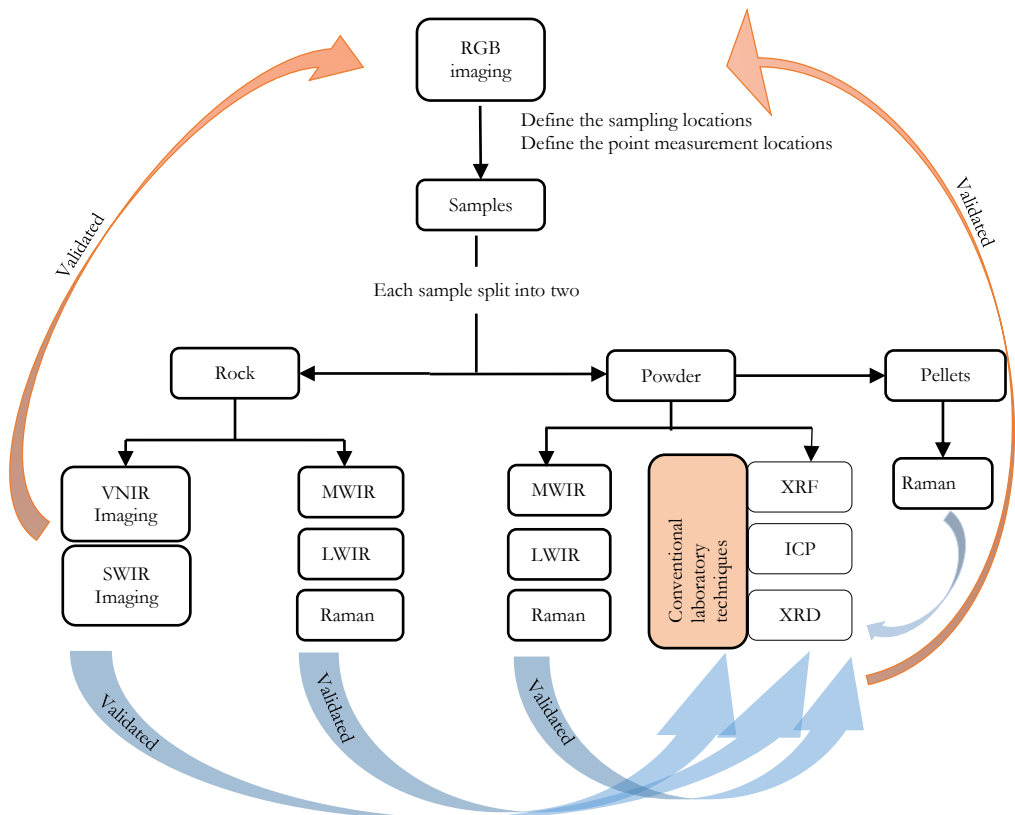


Figure 5.15: The technique used for the definition of sampling locations, and the types of samples used for the analysis using the investigated technologies and the validation techniques.

REFERENCES

- Benkert, T., Dietze, A., Gabriel, P., Gietzel, J., Gorz, I., Grund, K., Lehmann, H., Lowe, G., Mischo, H., Schaab, H., Schreiter, F. & Stanek, K. (2015). First step towards a virtual mine - generation of a 3D model of Reiche Zeche in Freiberg. Proceedings of the 17th Annual Conference of the International Association for Mathematical Geosciences (IAMG), Vol. I and II, Freiberg, Germany, pp. 1350-1356.
- Kröner, A. & Willner, A.P. (1998). Time of formation and peak of Variscan HP-HT metamorphism of quartz-feldspar rocks in the central Erzgebirge, Saxony, Germany. *Contrib Mineral Petrol*, 132(1), pp. 1-20. doi: 10.1007/s00410005040
- Kroner, U., Hahn, T., Romer, R. & Linnemann, U. (2007). The Variscan orogeny in the Saxo-Thuringian Zone - Heterogenous overprint of Cadomian/Palaeozoic Peri-Gondwana crust. *Geological Society of America Special Paper*, 423, pp. 153-172. doi: 10.1130/2007.2423 (06)
- Mingram, B. (1998). The Erzgebirge, Germany, a subducted part of northern Gondwana: geochemical evidence for repetition of early Palaeozoic metasedimentary sequences in metamorphic thrust units. *Geological Magazine*, 135(6), pp. 785-801. doi: 10.1017/S0016756898001769
- Ostendorf, J., Henjes-Kunst, F., Seifert, T. & Gutzmer, J. (2019). Age and genesis of polymetallic veins in the Freiberg district, Erzgebirge, Germany: constraints from radiogenic isotopes. *Mineralium Deposita*, 54(2), pp. 217-236. doi: 10.1007/s00126-018-0841-1
- Rötzler, K., Schumacher, R., Maresch, V. W. & Willner, A. P. (1998). Characterisation and geodynamic implications of contrasting metamorphic evolution in juxtaposed high-pressure units of the Western Erzgebirge (Saxony, Germany). *European Journal of Mineralogy*, 10(2), pp. 261-280.
- Scheinert, M., Kupsch, H. & Bletz, B. (2009). Geochemical investigations of slags from the historical smelting in Freiberg, Erzgebirge (Germany). *Chemie der Erde - Geochemistry*, 69(1), pp. 81-90. doi: 10.1016/j.chemer.2008.03.001
- Seifert, T. (2008). *Metallogeny and Petrogenesis of Lamprophyres in the Mid-European Variscides - Post-Collisional Magmatism and Its Relationship to Late-Variscan Ore Forming Processes in the Erzgebirge (Bohemian Massif)*. IOS Press BV, Amsterdam, The Netherlands.
- Seifert, T. & Sandmann, D. (2006). Mineralogy and geochemistry of indium-bearing polymetallic vein-type deposits: Implications for host minerals from the Freiberg district, Eastern Erzgebirge, Germany. *Ore Geology Reviews*, 28(1), pp. 1-31. doi: 10.1016/j.oregeorev.2005.04.005
- Tichomirowa, M., Berger, H. J., Koch, E. A., Belyatski, B. V., Götze, J., Kempe, U. & Schaltegger, U. (2001). Zircon ages of high-grade gneisses in the Eastern Erzgebirge (Central European Variscides) - constraints on origin of the rocks and Precambrian to Ordovician magmatic events in the Variscan foldbelt. *Lithos*, 56(4), pp. 303-332. doi: 10.1016/S0024-4937(00)00066-9
- Willner, A. P., Rötzler, K. & Maresch, W. V. (1997). Pressure-Temperature and Fluid Evolution of Quartzo-Feldspathic Metamorphic Rocks with a Relic High-Pressure, Granulite-Facies History from the Central Erzgebirge (Saxony, Germany). *Journal of Petrology*, 38(3), pp. 307-336. doi: 10.1093/ptroj/38.3.307

III

APPLICABILITY OF THE INDIVIDUAL TECHNIQUES

6

RGB IMAGING FOR MINERALOGICAL FACE-MAPPING IN AN UNDERGROUND MINE

This chapter demonstrates the usability of RGB imaging for mineralogical face mapping and ore zone delineation in an underground mine using RGB images taken at the defined mine face. It discusses the methodological approach for image data acquisition, processing and knowledge extraction. It also presents the applicability of the technique for fragmentation analysis using the RGB images taken from small muck piles. The last part of the chapter discusses the potential benefits and possible challenges of the use of the technique in operational mines.

Parts of this chapter have been published in:

Destá, F. S. & Buxton, M. W. N. (2017). The use of RGB Imaging and FTIR Sensors for Mineral Mapping in the Reiche Zeche Underground Test Mine, Freiberg. Proceedings of the Real-Time Mining International Raw Materials Extraction Innovation Conference, Amsterdam, The Netherlands, pp. 103-127.

6.1. INTRODUCTION

Mineralogical maps provide essential information in the exploration of new mineral deposits as well as during subsequent mining. This information indicates the type and distribution of minerals, ore-zone boundaries, and host rocks description. Mapping can be done at different stages of the mine-life cycle, such as during exploration (at a regional scale or local scale), mine planning (ore-reserve definition), and extraction (mine face mapping). Thus, accurate mineral mapping can lead to improved efficiency of mine development and operations.

Mineralogical maps can be produced using sensor-derived image data. Such images include the multispectral and hyperspectral images that are acquired from space-based, ground-based or laboratory-based platforms. Sensor-derived images are increasingly in use in a wide range of applications. One such application is mineral mapping. The use of images in geological studies is not limited to mineralogical mapping; instead, it extends to the identification of geological structures, textural analysis and ore-zone delineation. In remote sensing, mapping of minerals is commonly performed using hyperspectral images that provide up to hundreds of spectral channels or bands information at different spatial resolutions. For example, numerous studies show the use of hyperspectral images in mineral exploration (Beiranvand et al., 2019; Bishop et al., 2011; Kruse and Perry, 2013; Neville et al., 2003; Rajan and Mayappan, 2019). On the other hand, one of the most common laboratory-based imaging is drill core logging using hyperspectral images (Dalm et al., 2018; Kruse et al., 2012; Tusa et al., 2019).

Mine face mapping can be done using ground-based close-range multispectral or hyperspectral imaging. Studies show the use of ground-based imaging techniques for mineralogical face mapping. For example, the VNIR and SWIR sensors were used for the mapping of minerals (clay, iron oxide, carbonate, and jarosite) at vertical exposure in Carlin Style sediment-hosted gold deposit (Krupnik and Khan, 2019). Similarly, Krupnik and Khan, (2019) used VNIR and SWIR to map alteration minerals that correspond to the occurrence of ore in the copper porphyry deposit. In another study, Beckert et al. (2017) applied VNIR and SWIR to distinguish carbonate phases with slight compositional differences at quarry cliff faces. Mapping of minerals at higher resolution provides a good insight into the understanding of mineral types and their spatial distributions. Moreover, the digital mapping of minerals improves the efficiency of mapping and enable automation. Thus, mineralogical mapping using sensor-derived data plays a significant role in supporting effective decision-making in mining operations.

As discussed in Chapter 3, RGB imaging is one of the imaging sensor technologies that have potential in material characterisation. The RGB imaging operates in the 0.4 to 0.7 μm range of the electromagnetic spectrum and delivers 3-bands (red-green-blue) information. The technique is sensitive for colour differences and has a great potential in distinguishing ores consisting of visually distinct minerals. The use of RGB imaging in material characterisation is very limited. However, promising results were obtained in mineral sorting (TOMRA, 2020; STEINERT, 2020; Robben and Wotruba, 2019) and recycling applications (REDWAVE, 2020). Portable, high-resolution and high-speed RGB sensors are available from multiple suppliers. This allows rapid and accurate data acquisition, besides its portability permits embedding and surface mounting of the sensors on different platforms. Such applications include sidewall imaging at a mine face and muck pile imaging.

The fragmentation of rock is an essential step in the mining process that prepares material for excavation and transportation. The fragmentation of rock through blasting

influences the crushing and grinding operations. Thus, it is crucial information in mineral processing that has an economic significance (Singh et al., 2016; Workman and Eloranta, 2003). The degree of fragmentation can be determined using direct (e.g., sieve analysis) or indirect methods (e.g., image processing) (Tavakol and Hosseini, 2017). Thus, RGB imaging can be deployed for the analysis of rock fragmentation. This approach is advantageous since there is no limitation on the mass size and volume of materials that can be analysed at once. The other advantage is that the data can be acquired and processed rapidly. Thus, it does not disrupt the production process and the blast parameters can be optimised using online data. Nevertheless, there are also some limitations of this method such as particle size can be underestimated or overestimated, it gives 2D information and the pilling effect since spatial size distribution of fragmented materials can vary (Kemeny et al., 1993). However, these effects can be minimised by selecting appropriate sampling location, suitable image scales and high-quality images (with high spatial and spectral resolution).

RGB imaging can create new data and knowledge in real-time that would be of great interest in mining. However, mapping of minerals at mine face using RGB images in underground mine has not been conducted. This gap in the current mineralogical mapping approach motivated this study. The purpose of this chapter is hence two-fold: (1) to explore the usability of the RGB imaging for the mapping of minerals and delineation of ore-zone (definition of target domains) at a mine face in an underground mine, and (2) to investigate the use of the technique for the determination of rock fragmentation size of small muck piles in the underground mine.

6.2 DATA ACQUISITION

Image data were acquired in-situ from the mine face and muck pile sites using an RGB sensor (Nikon D7100 digital camera). The instrument used in this study is described in Chapter 3. Different imaging procedures were followed to obtain usable data from the two sites. These procedures are described in the sub-sections that follow.

6.2.1. MINE FACE IMAGING

Reference points (GCPs) were marked at the 22 m long by 2 m height study block (Figure 6.1). These points have 50 cm spacing. The geographic coordinates of the GCPs were acquired using LIDAR technology by the Mine Surveying and Geodesy team of TUB Freiberg. As it is described in Chapter 5, a BB of ~ 4 m long and 2 m high was delineated within the bigger block. Thus, the same procedure was followed to acquire images at the mine face of the BB after each blast. Therefore, in this study, two sets of images were used; one is from the ~ 22 m long mine face, and the other one is from the newly exposed mine faces of the BB.

RGB sensor field of view varies depending on the distance between the camera and the mine face. Therefore, an attempt was made to maintain the same distance between the camera and the target. The same camera setting was used to acquire images from two vertical reference points (Figure 6.1 and 6.2). This allowed capturing the full defined mine face both laterally and vertically. Variation in illumination has a significant effect on image analysis. So, halogen lamps were used to ensure constant illumination throughout the mine face. Most importantly, each image ensures to cover at least three reference points, and the photos have about a 40% overlap. This is beneficial in providing full coverage of the mine face as well as the three GCP points of each image can be used to tie the images together (georeference and mosaic). Besides, the photographs were taken in front of the face (~ 90°);

this is beneficial in minimising distortion. At each reference point, multiple images were taken to minimise errors that can be associated with the photographing process (e.g., distortion and illumination related issues).

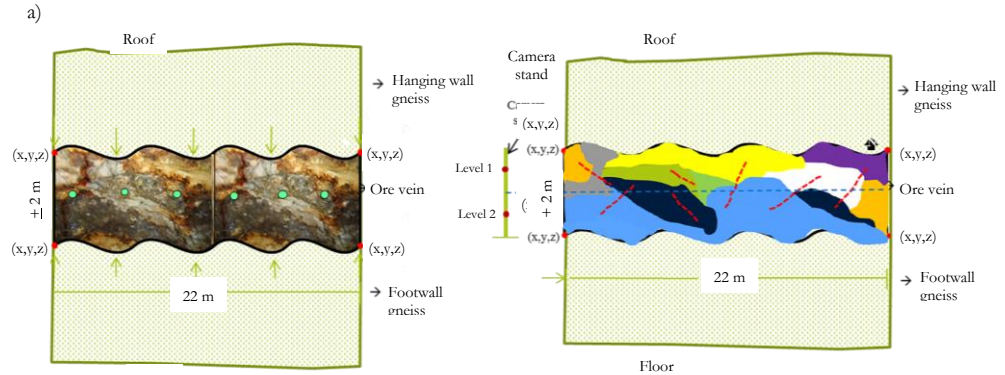


Figure 6.1: (a) Floor etch illustrating the reference points at the mine face, and (b) illustrates the two vertical camera standpoints for image data acquisition.

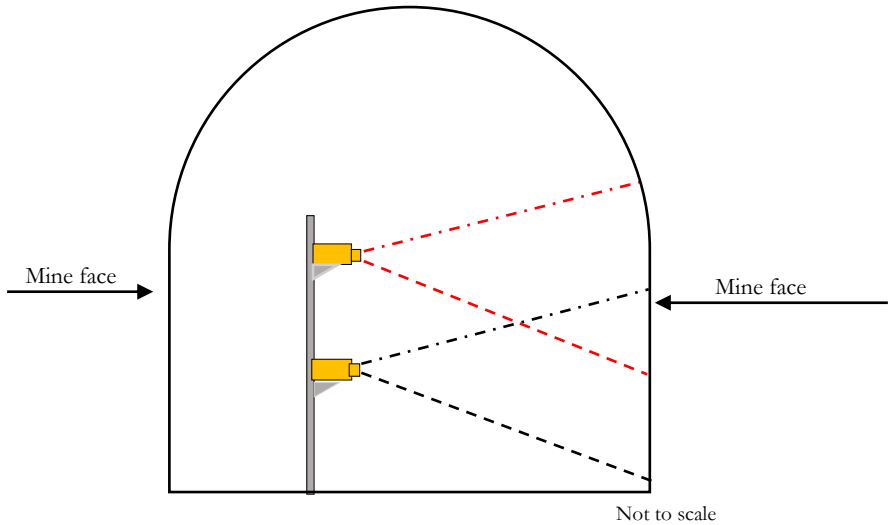


Figure 6.2: A sketch to illustrate the mine face cross-section and the two vertical camera standpoints.

6.2.2. MUCK PILE IMAGING

After the blast of the BB, small muck piles were placed in the underground mine. The following procedures were followed to acquire RGB images at the muck piles. Halogen lamps were used to maintain the same illumination and minimise the shadow of bigger rock fragments. A known scale was placed at the muck pile; later, the scale was used to calibrate the fragment size analysis model. Besides, multiple pictures were acquired at each location; thus, images with better qualities can be chosen. Figure 6.3 illustrates the two-camera orientations for the acquisition of image data from the small muck piles.

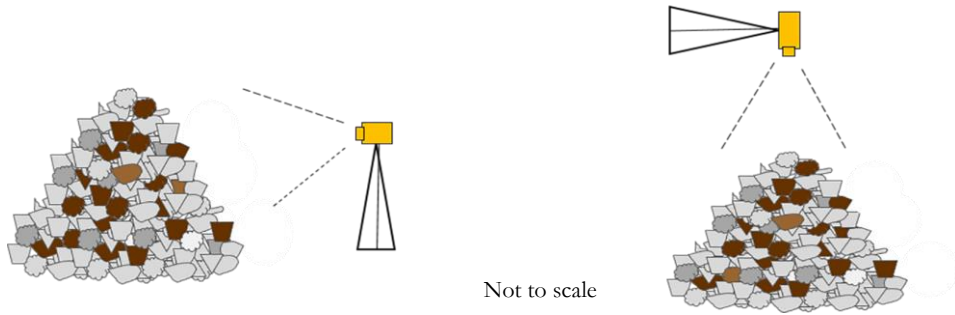


Figure 6.3: A sketch to illustrate two of the camera orientation for the acquisition of image data from the muck piles.

6.3. METHODOLOGY

As illustrated in Figure 6.4, the methodological approach developed for mapping of minerals using RGB images comprises a multi-step process that commences with data preparation, followed by features extraction and classification, and culminates with model validation. The data preparation task (denoted as Block A in Figure 6.4) includes data exploration, data pre-processing, georeferencing and mosaicking. The classification of the processed images was performed using both the unsupervised and supervised classification techniques (represented by Block B in Figure 6.4). The classification models were validated using independent datasets (indicated by Block C in Figure 6.4). This section also discusses the methodological approach for the fragmentation analysis using RGB images taken from small muck piles. The details of each step are described below.

6.3.1. MINE FACE MAPPING

A total of 42 images were used to cover the defined 22 x 2 m block mine face both laterally and vertically. A low-pass filter was applied to enhance the distinct identification of feature types. A low-pass filter is an image filtering technique that reduces local variation and removes noise by averaging the neighbourhood high and low pixel values. The nearest resampling technique was used to resample the pixels of the images to the same cell size. The nearest resampling technique is the fastest interpolation technique that performs a nearest neighbour assignment. The mosaicked images were used to perform exploratory data analysis. The pre-processed images were georeferenced and mosaicked using the geographic coordinates of the GCPs (denoted as Block A in Figure 6.4). Image classification was performed using both unsupervised and supervised classification techniques (represented by Block B in Figure 6.4). First, unsupervised classification using K-means methods were applied to assess any clustering or grouping of pixels based on their grey level. A detail explanation of the K-means method is presented in Chapter 4. K-means was applied with no prior knowledge about the different classes; however, the number of cluster centres was specified.

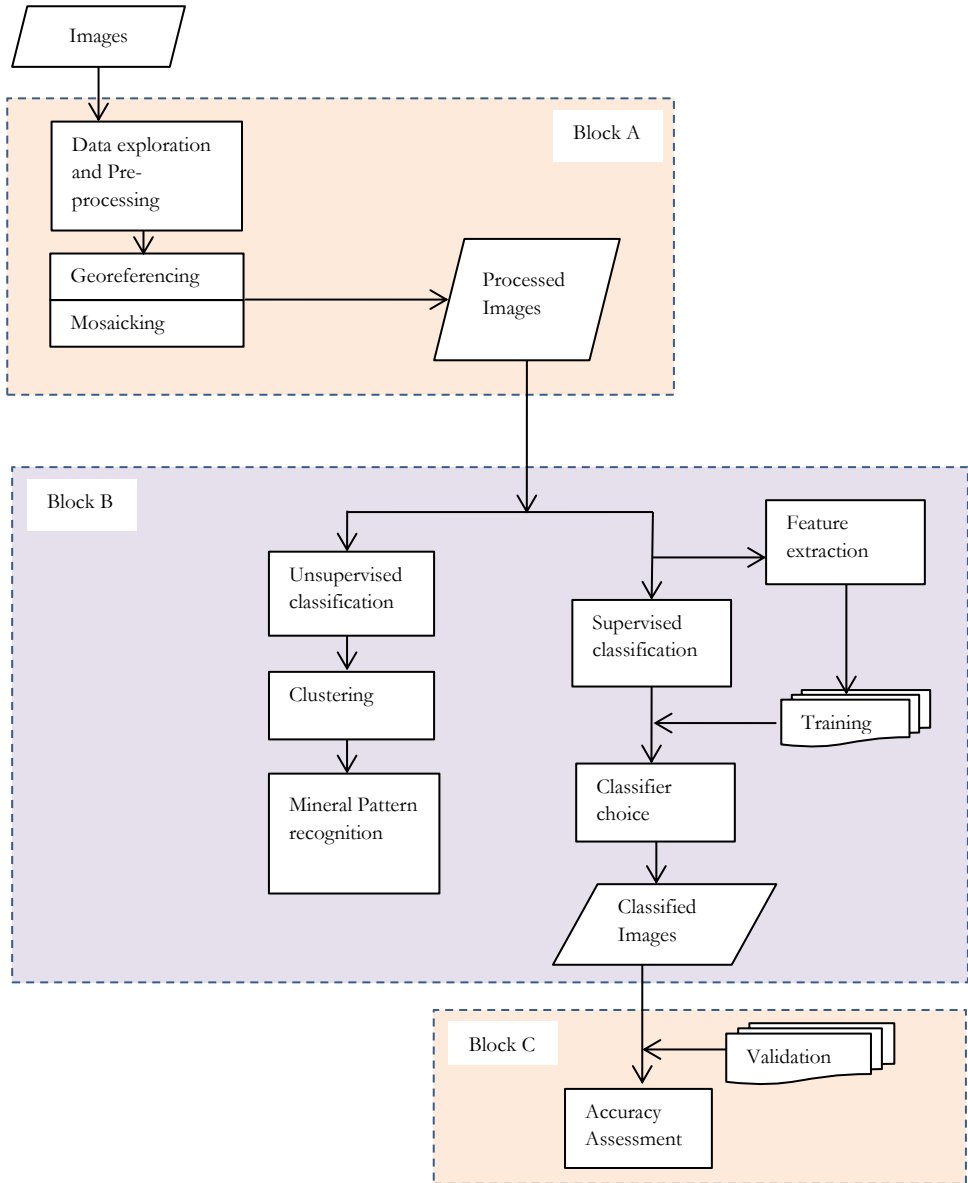


Figure 6.4: A workflow diagram depicting the steps of the mineral mapping using the RGB images.

Supervised classification requires a labelled training set for the classifier. The classifier uses a training set of spectral signatures to identify similar signatures in the remaining pixels of the images. It labels all the image pixels as per the trained parameters (Kaufman and Rousseeuw, 2005). Prior knowledge of the different classes is crucial since the training set selection affects the classification accuracy. A large number of supervised classification algorithms are available for image classification and the choice of the classifier algorithm is based on classification accuracy (Kaufman and Rousseeuw, 2005; Kotsiantis, 2007). For this

study, the classification performance of ML, MD and SAM algorithms were compared. A detail description of the algorithms is presented in Chapter 4.

Visual interpretation of the RGB images was conducted to identify the main mineral classes within the defined mine face. The visual inspection of the images was supported by the geological map, which was generated during the sampling campaign and the unsupervised classification results. Training sets (groups of pixels) were generated to represent five broad classes in a supervised classification. The feature selection is based on the visual appearance (colour difference) of the designated material classes. The number of mineral types, which can be identified, depends on different factors, such as the presence of the minerals at a certain location, their clear appearance, the freshness of the exposure so that oxidation or other weathering processes will not lower the visibility of the minerals and the resolution of the camera. Thus, for some of the pictures more than five mineral classes are identified.

To ensure reliable prediction of the class membership, training area uniformity and representability of the same class over the whole image was taken into account. In addition, the separability of the classes in the multidimensional attribute space was checked using histograms. Overlapping classes were merged and five broad classes were identified for the classification. Some of the minerals are combined together (e.g., quartz and calcite) since distinguishing the minerals based on their colour and the utilised camera is limited. Following the selection of training areas, a signature file was generated and the whole image was classified using the signature file of the training sets. The output multiband raster is a classified image that shows the mineral distribution at the defined mine face. The classification work is validated using a separate validation sample set (represented by Block C in Figure 6.4). Classification accuracy was assessed by comparing ground truth classes with the predicted or classified pixel class at each ground truth location. The results are expressed in an error matrix (confusion matrix) which shows the overall and class accuracies. For this study, the ground truth classes (pixels) were collected using the raw RGB images. The choice of the pixels was based on the geological map produced for this study, close up RGB images taken in-situ (better resolution), visual inspection and using physical samples collected from the mine face. Using extract values to points geoprocessing tool, the value of the ground truth and the predicted (classified) pixels values at each ground truth location was extracted separately. A frequency table was created to generate a summary table of every class classification accuracy. To arrange it into confusion matrix form, a pivot table geoprocessing tool was used. The overall accuracy was calculated by dividing the correct predictions by the total predictions. The classes' accuracy was calculated by dividing the number of correctly classified pixels of a class by the total number of ground truth pixels of the same class.

6.3.2. FRAGMENTATION ANALYSIS

The rock fragmentation analysis was performed using multiple RGB images taken from two muck pile locations. The better quality images were imported into the Split desktop software and scaled using known scale references. The scale of each image was indicated during the image acquisition process using scale references; an example is presented in Figure 6.5. The rock fragments of each image were automatically delineated using the software. Following this, the delineation parameters were edited; for example, the fine areas were assigned or introduced as fine material. This task can be automated from the software; however, for improved performance, manual editing was also performed. Part of the images

that show other features than the rock fragments were masked. Likewise, the over delineated and under delineated fragments were edited to ensure better results. Once the preferred delineation was achieved, the size distribution of the delineated rock fragments of each image was calculated and reported in graphical and tabular forms.



Figure 6.5: An example of an RGB image of a muck pile with known scale reference. This image shows the size of rock fragments at one of the muck pile site.

6.4. RESULTS AND DISCUSSION

This section consists of two parts. In the first part, the mineral mapping results of the three models (ML, MD and SAM) are presented. It also discussed the application of the RGB images for the delineation of ore-zone. In the second part, the rock fragmentation analysis results are described in detail. The section also discusses the benefits and limitations of the approach for in-situ underground applications.

6.4.1. MINERAL MAPPING AND ORE-ZONE DELINEATION

The use of unsupervised classifiers prior to any image classification tasks is beneficial in discovering unknown but useful classes (Roussel et al., 2014). Accordingly, a k-means classifier was applied to understand the general pattern or groups of the different classes. As shown in Figure 6.6, the general pattern or groups of the different classes that have a minimum degree of heterogeneity within a class were generated. This output of the unsupervised classifier was used as an additional input for the definition of the training set.

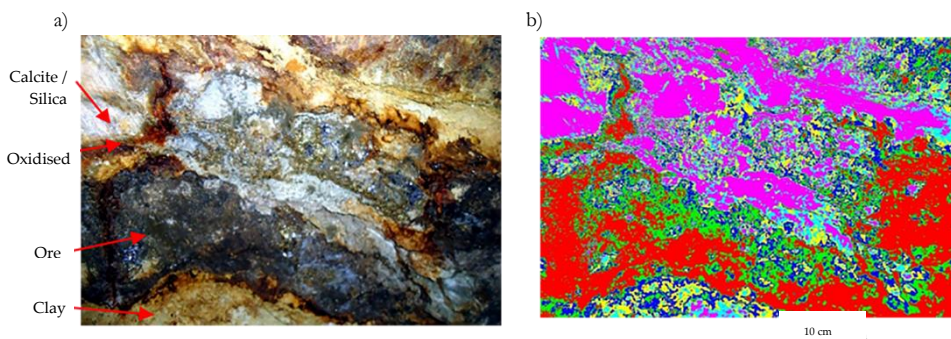


Figure 6.6: (a) RGB image taken at the mine face, and (b) thematic map produced by k-means classifier. The thematic map shows the identified pattern or groups of the different minerals.

The same training set was used to compare the classification performances of the ML, MD and SAM classifiers. The classification results of the algorithms were examined visually

using a pattern match approach. As shown in Figure 6.7, a better pattern match between the original RGB image and the classified image was achieved using the ML algorithm. For example, comparing the SAM classifier to ML, the chalcopyrite/pyrite class, which is clearly observed in the RGB images, is misclassified as clay on the SAM image (Figure 6.7 (a) and (d)). Whereas, it is correctly classified using the ML classifier. The optimal classifier choice was optimised using one photograph at a time; however, it was tested on multiple images. Following this ML was selected as the preferred classifier, and it was applied to the mosaicked images.

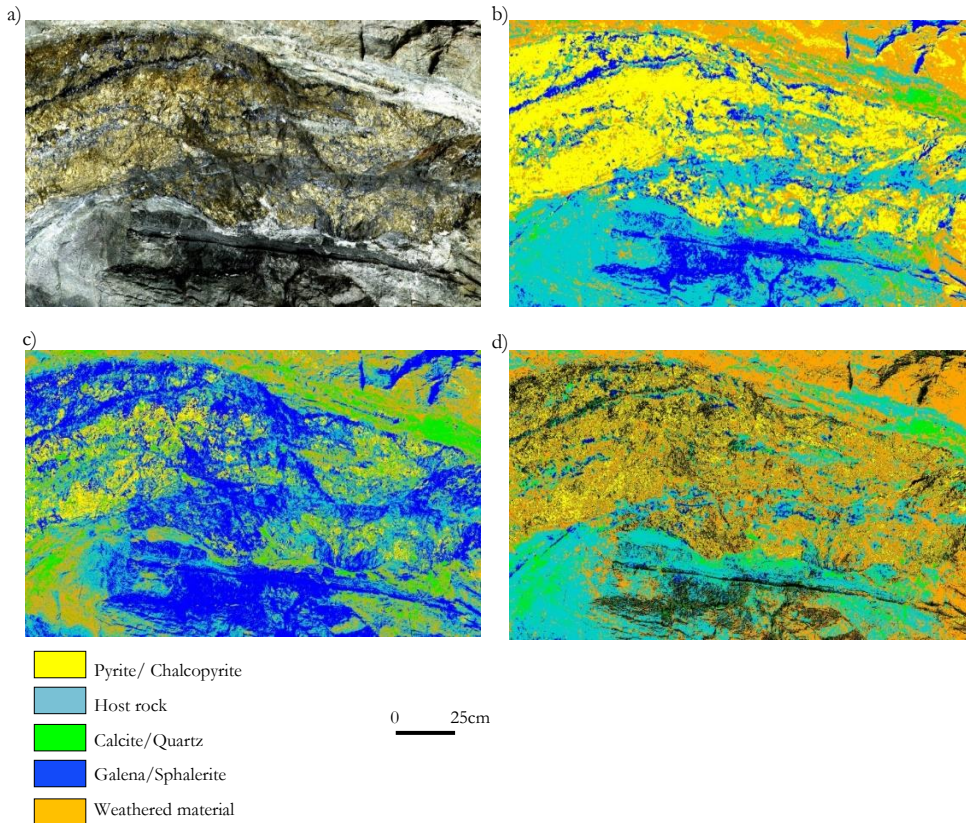


Figure 6.7: (a) RGB image taken at the mine face. Mineral mapping results produced by three classifiers (b) MD (c) ML and (d) SAM.

The facts that most of the sulphide minerals show sufficient variation in colour and mainly have medium-to-coarse grains allow the use of RGB imaging for mapping of minerals and delineation of ore-zones in the case study site. However, minerals (e.g., quartz) can have different visual appearances depending on their mixtures. Therefore, the definition of the training set should take into account the visual appearance of the minerals in specific deposit types. Consequently, the colours of the typical minerals from the test case were inspected prior to the selection of features (training set). In the area, arsenopyrite has a silvery/golden colour, pyrite has a golden appearance, galena has a grey colour, sphalerite is dark grey to black and quartz is white. This colour difference is the essential property of the minerals that enable RGB imaging to provide useful information on the minerals distribution and

ore-zone boundaries. For example, Figure 6.8 shows the RGB and classified images of a mine face, respectively. The ML classifier identified six main classes (mineral types). The classification algorithm performance was assessed using a validation set. Based on the confusion matrix results, the acquired overall accuracy is 78%, and the class accuracy ranges from 61% (e.g., galena/sphalerite class) to 94% (e.g., silica/calcite class). Joints and surface irregularities at some parts of the mine face can cause shadow (darker areas). These darker areas can be misclassified as galena/sphalerite mineral types since the minerals in the area also exhibit a dark grey colour. This is the likely reason for the obtained lower classification accuracy of the galena/sphalerite class.

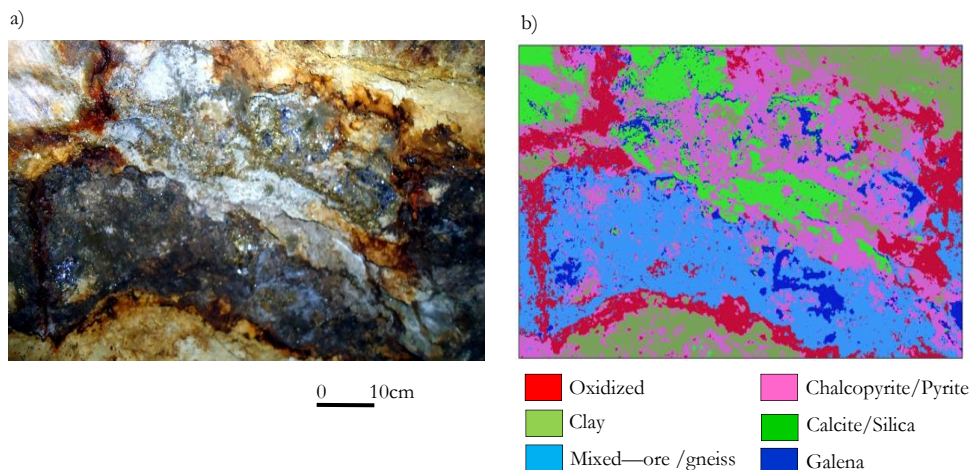


Figure 6.8: a) shows an RGB face image taken from polymetallic ore at the Freiberg mine b) mineral map produced from RGB image.

The georeferencing and mosaicking of the RGB images are essential to comprehend the full spatial distribution (i.e., spatial variability) of minerals on a single image and can cover the entire area of a mine face. Besides, it is beneficial to generate spatially constrained image data that can further be linked to other sensor outputs based on location. The ML classifier was applied for the different sets of georeferenced and mosaicked images. For example, Figure 6.9 and 6.10 show mosaicked RGB images and the classified mineral maps, respectively. The classified images show the distribution of the minerals and the location of the images at the ~22 m long block is indicated in the inset of Figure 6.10. The RGB images were not taken immediately after the blasting of the mine face, consequently weathering occurs and reduced the visibility of some of the sulphide minerals. This hinders differentiation among sulphide minerals. However, the image pixels were successfully classified into five mineral classes, namely weathered material, ore, quartz/ calcite, ore disseminated in gneiss and gneiss. This classification result is sufficient to indicate high-grade, medium-grade and low-grade ore zones. Therefore, it is beneficial in providing usable information in mining operations.

Depending on the visibility of material (or spatial distribution of minerals) along the defined mine face the training set (the extracted minerals or classes) might vary from region to region. Nevertheless, the classification results show the mineral distribution that exists in the actual condition that the information can be combined and presented on a single image.

Imaging is advantageous since it covers a wider areal extent and gives information at each specific point on the image. Whereas point spectrometers such as LIBS or infrared (e.g., ASD point analyser) gives point data at specific locations. Compared to other techniques such as hyperspectral imaging, acquisition of RGB images are a low cost, low data volume and low computational intensity technique. For the same deposit type, if the illumination is kept constant over the imaged mine face, the same training set can be used to automate the classification process. In addition, an RGB imager is a rapid, easily repeatable data acquisition system and it has a good potential for automation. Moreover, the use of a base map is essential for geological or mineralogical mapping; however, a base map for sidewall mapping might be challenging to obtain due to the rapid (continuous) change of the mine face after each blast. Geological mapping without a base map might raise a scale issue for the mapping of different lithological and structural units. Therefore, mineral mapping using RGB imaging can be an alternative solution.

The environmental conditions in deeper mines might not be favourable to stay longer to undertake extensive geological mapping. RGB imaging with suitable illumination systems can offer a potential automated solution for mapping in such deeper or other hazardous environments. The other possible application of RGB imaging is its capability in providing safety information in an open-pit as well as in underground mines. The fragmented or unstable ground in an open-pit and underground mines creates hazardous conditions that endanger lives. Thus, early identification of weak zones is essential. Monitoring of risk zones at the mine face can be achieved using sensor technologies. The different geological attributes (e.g., mineralogical and structural data) that can be generated from sensors may further be linked to indicate hazard (weak) zones. For such applications, one of the potential sensor technologies is the RGB sensor. For example, the RGB images can indicate high-risk, medium-risk and low-risk zones; thus can be applied in risk zones ranking. Besides, the technique can support surveying sample locations. In this study, the mine face was imaged after the channels were cut, and each channel location was digitalised (Figure 6.9). This allowed the production of georeferenced data. Spatially controlled data is beneficial to integrate sensor data based on location, it enables providing location-based sensor data for a resource model, and it is valuable for the understanding of the spatial distribution of minerals. The test case is a low-grade shallow underground mine that is characterised by vein-type mineralisation. In deeper mines, the use of RGB imaging might be challenging due to the harsh environmental condition and narrow nature of the cross-section. However, robust RGB imagers integrated with other scanning technologies (such as LIDAR) can enable scanning and imaging of a mine face under deeper level mining conditions.

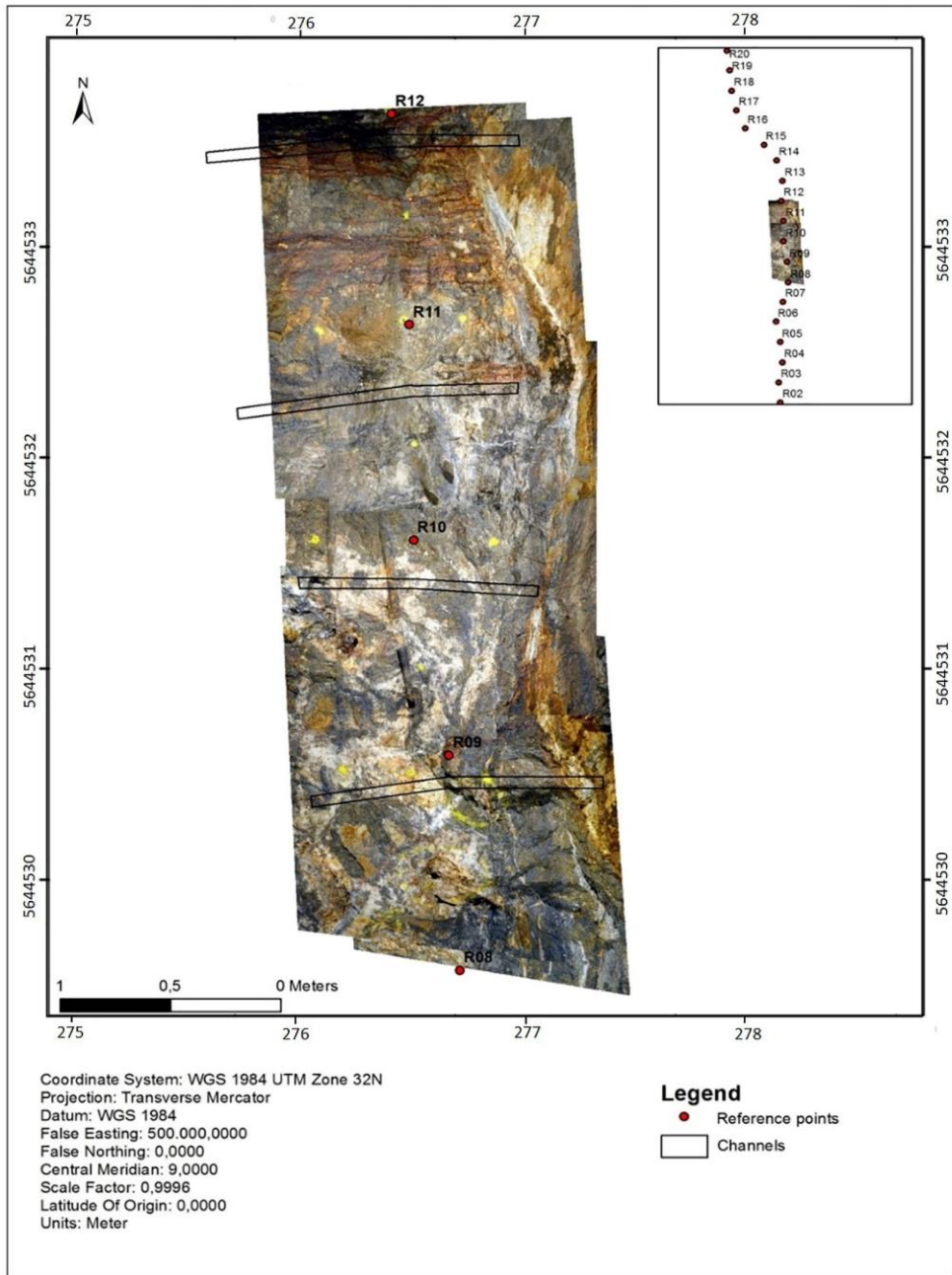


Figure 6.9: Mosaicked RGB images showing the position of the channel samples superimposed. The channels have ~ 75 cm to 120 cm spacing.

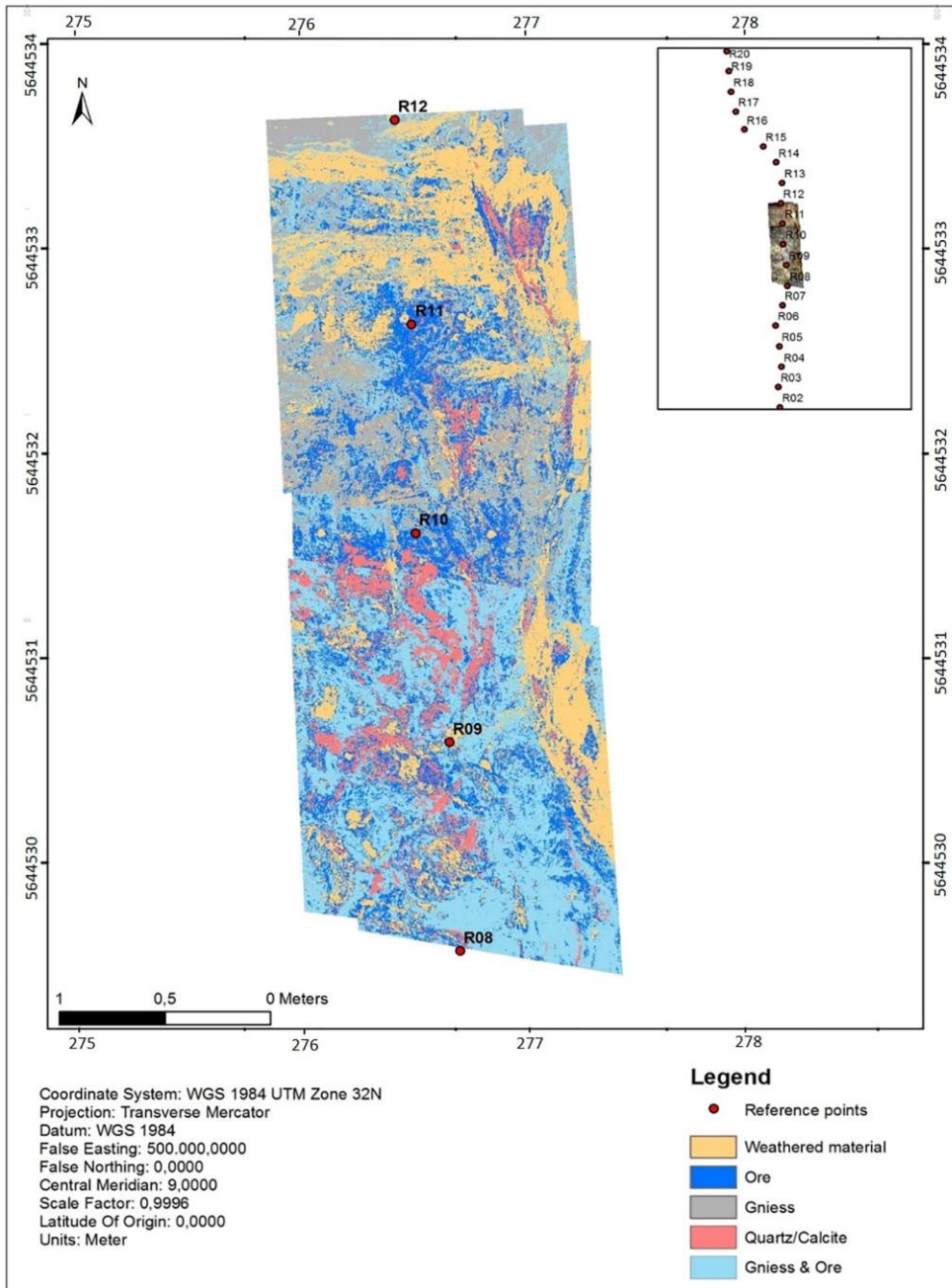


Figure 6.10: The corresponding thematic map of the mosaicked images. The relative location of the classified images with respect to the 22 m mine face is indicated in the inset map.

A mineral map was also produced using the RGB images taken from the BB (Figure 6.11 and 6.12). The map shows three mineral classes within the ore vein of the block (Figure 6.12). To enhance the classification result, the ore zone was digitized and defined as processing extent. Thus, the mineral types within the ore zone can be clearly identified.

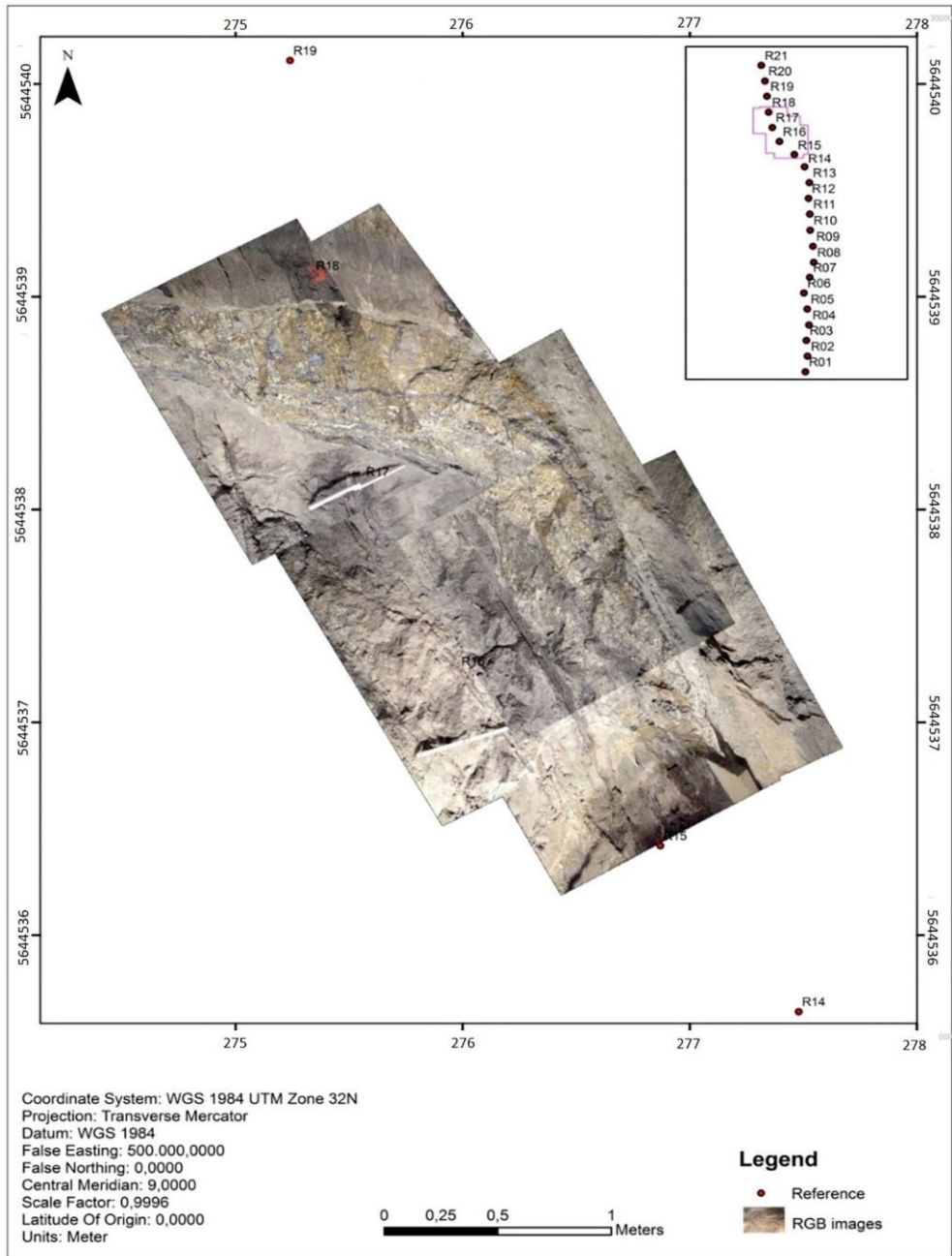


Figure 6.11: Mosaicked RGB images showing the ore zone in the northern part of the ~ 22 m block.

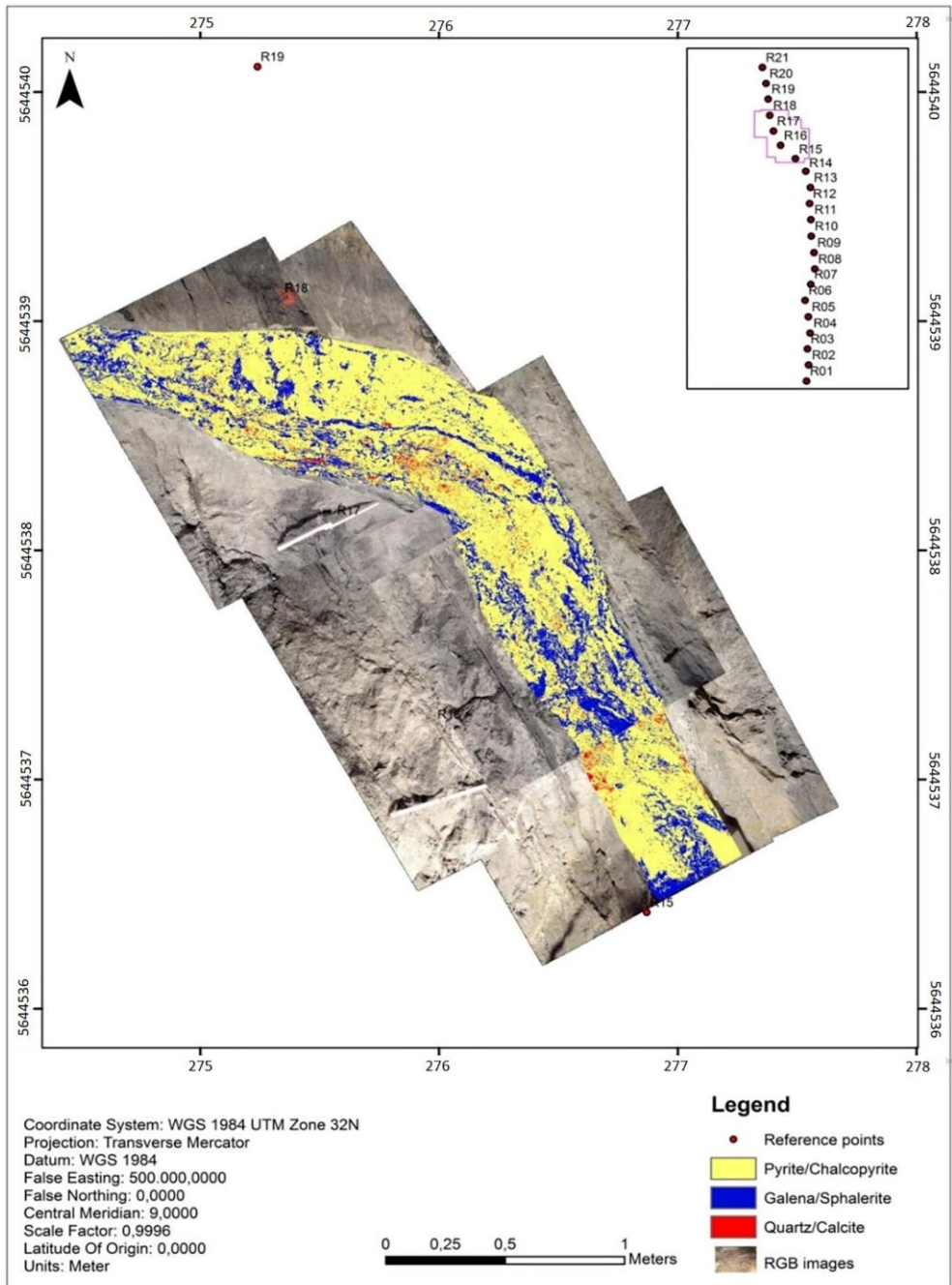


Figure 6.12: The corresponding thematic map of the mosaicked images. The relative location of the classified is indicated in the inset map.

Overall, the RGB images, coupled with the ML method, allowed the classification of materials into different groups (mineral types). The RGB images classification results were further compared to the results from other sensor technologies (such as SWIR and LWIR). The results show a close much in terms of indication of ore-waste regions as well as for the indication of some of the minerals. Comparing the approach with conventional mapping methods, RGB imaging gives objective, reproducible results and an expandable database. The fact that state-of-the-art RGB sensor that can rapidly scan a large area (e.g., mine face) are emerging and the promising results from this study ensure the great potential of the technique for material characterisation in mining applications. However, the test case has easy access and exhibits almost constant environmental conditions; for example, minimal dust, no vibration and no disturbance. Therefore, the influence of environmental factors is minimal. However, the use of the technique in operational underground mines might be challenged from disturbance due to vibration, dust and other factors. Therefore, to ensure the applicability of the technique under such conditions, sound approaches are required to reduce the effects of the different environmental factors on sensor measurements.

6.4.2. FRAGMENTATION ANALYSIS

The test case area is characterised by heterogeneous materials, and the heterogeneity causes the size distribution of fragmented rocks in the blasting. Consequently, variation in the particle size was observed in the fragmented rocks. Figure 6.13 (a) and (b) show the RGB images taken from the first muck pile and the delineation generated for the fragmentation analysis, respectively. The red patches on the figure show the fine areas. The size distribution graph of the rock fragments shows 100% of the rock fragments are below the size of 8 in (~ 20 cm). On the other hand, the percentage of fine fragments that passes 0.08 in (0.2 cm) is 2.22% (Figure 6.14). The same muck pile was imaged from different sides. For example, the analysis result of another image taken from the different side of the same muck pile shows a higher fine percentage (i.e., about 50% of the material passes through 0.75 in (~ 1.9 cm) (Figure 6.15). Figure 6.16 also shows the fragmentation analysis result of an image taken from the first muck pile. The percentage of fine fragments that passes 0.08 in (0.2 cm) is 0.35%. This shows the need for an integrated analysis of multiple images taken from different sides of a muck pile, thus to understand the size distribution of the rock fragments comprehensively.

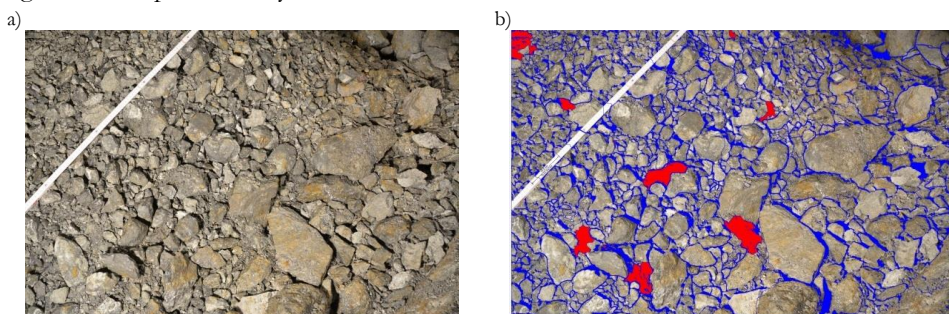


Figure 6.13: a) RGB image taken at the first muck pile b) delineated image. The red patches show the fine areas.



Figure 6.14: The corresponding (a) size distribution curve, and (b) table of the image in Figure 6.13.

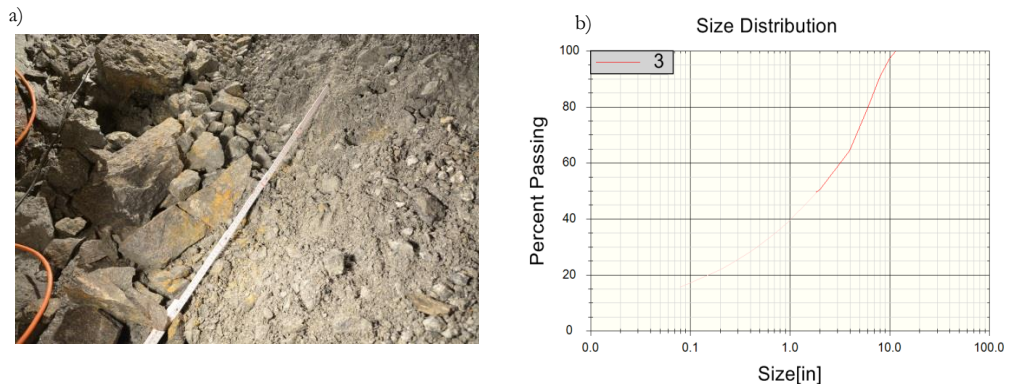


Figure 6.15: (a) RGB image taken at a different side of the muck pile, and (b) the corresponding size distribution curve.

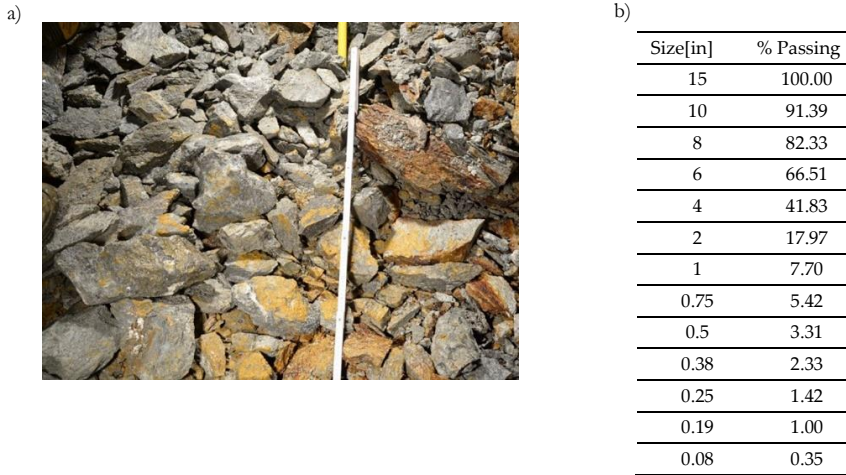


Figure 6.16: (a) RGB image taken at the first muck pile, and (b) the corresponding size distribution table.

Figure 6.17 (a) and (b) show an RGB image taken at the second muck pile and the delineated image, respectively. The red patches show the fine areas or the areas introduced as fine, whereas the cyan colour patch shows the masked area that was excluded from the grain size calculation. In this image, the masked area is part of the sidewall since the muck piles were located next to the mine face (sidewall). The grain size calculation shows about 29.69% of the rock fragments are below 0.75 in (1.9 cm) and 100% of the rock fragments are below the size of 4 in (~ 10 cm) (Figure 6.17 and 6.18). Likewise, another image was taken from the different side of this muck pile; bigger size rock fragments dominate this side of the muck pile (Figure 6.19). For example, only 2.78% of the rock fragments are below the size of 2 in (~ 5 cm).

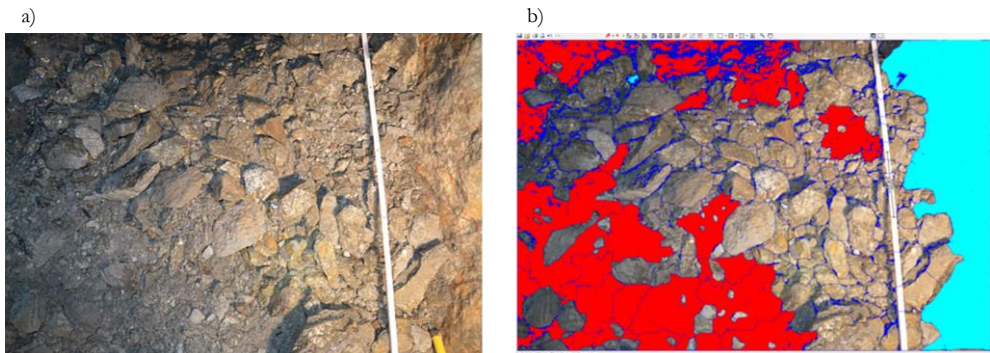


Figure 6.17: (a) RGB image taken at the second muck pile, and (b) the delineated rock fragments (the red patches show the fine areas and the cyan patch shows the masked areas).

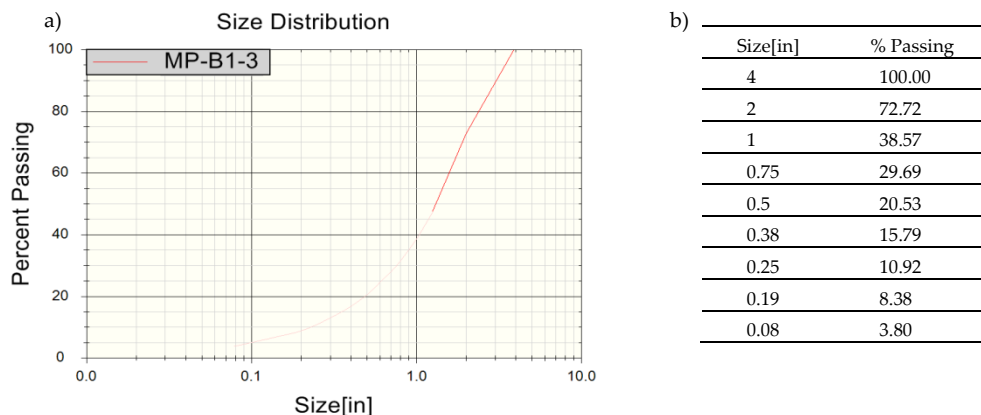


Figure 6.18: The corresponding (a) size distribution curve, and (b) table of the image in Figure 6.17.

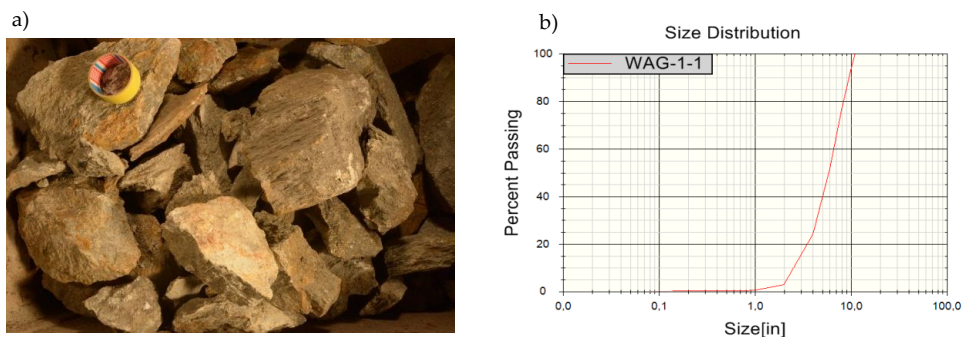


Figure 6.19: (a) RGB image, and (b) the corresponding size distribution curve.

The size of the rock fragments of the two muck piles ranges from fine (less than 2 mm) to boulder size materials (~ 30 cm). The percentage of the fine materials varies from image to image, thus pictures taken from the same muck pile showed different fine portions (Figure 6.15 and 6.16). Multiple images were acquired from the different sides of the muck piles in order to capture the observed grain size variability. Different factors determine the size of rock fragments such as material composition, geological structures (e.g., joints, fractures, minor faults) and blasting parameters. For example, one of the main reasons for the observed size distribution of the rock fragments in the study area is the composition of materials. Consequently, bigger rock fragments (boulders) mainly characterise the host rock. Whereas, the ore material is relatively weaker (softer) in strength and resulted in smaller rock fragments size.

Knowledge of material composition and fragmentation has high importance in mining. For example, technical decisions, blasting costs, productivity, and operational efficiency can all be related to optimum fragmentation. Thus, a reliable estimation of rock fragmentation is crucial in mining operations to improve waste productivity, mill throughput and wall stability. Different direct and indirect techniques can be applied to determine the size of rock fragments. For example, Drebenstedt and Ortuta, (2012) used radar reflectivity to measure fragments of flying stones during blasting. However, there are some open questions (e.g., the analysis assume spherical shapes for all fragments) to be addressed to understand,

measure, and then estimate fragmentation using radar reflectivity. On the other hand, the sieve analysis is a direct and the most accurate method for the determination of rock fragments size distribution. Nevertheless, this method is time-consuming and expensive. Therefore, the determination of rock fragments size using image analysis is considered a rapid and economical option. As discussed in the introduction, the rock fragment size analysis using image data has some limitations (e.g., pilling has an effect, it gives 2D information and particle size can be underestimated or overestimated). In this study, the accuracy of the calculated rock fragment size was not validated using an independent data source. However, to maximise the results, appropriate sampling locations were chosen, suitable image scales and better quality images were used, and manual editing supported the automated delineation of the rock fragments. The algorithm can detect clast sizes up to 2 mm, and everything below 2 mm is categorised in the same grain size class. Besides, the precision of the fragment size calculation was evaluated by analysing each image multiple times.

In this study, the use of RGB images taken from small muck piles located in the underground mine resulted in reproducible and consistent estimations of fragment sizes. Taking into account the blasting parameters, the result can further be used for the development of models that can better predict fragmentation in the test case. Rock fragmentation analysis using image data can be maximised by selecting appropriate sampling (imaging) locations, suitable image scales, and high-quality multiple images (high resolution). Besides, the delineation algorithm can be calibrated to automate the analysis of rock fragments. Therefore, the determination of rock fragments can be performed in a real-time application in underground mines (such as at LHD). The lower cost of the RGB sensor and the already existing software tool ensure rapid practical implementation.

6.5. CONCLUSIONS

This study assessed the use of RGB imaging for the characterisation of a polymetallic sulphide deposit in an underground mine. The technique was tested at the mine face and muck pile sites for mineralogical mapping, ore-zone delineation, and fragment size analysis. RGB images were acquired at the mine face following a well-defined imaging procedure. The images were georeferenced, mosaicked, and mineral maps were produced using three supervised image classification techniques (ML, MD and SAM). Likewise, images from the two small muck piles were used to calculate the size of rock fragments after the blast.

The results reported in the preceding sections show that the RGB images include relevant information that can be used for mapping of minerals, delineation of ore zones, and analysis of fragment sizes. Different mineral types were identified and mapped. Comparing the classification algorithms, the results from the ML technique is superior to the SAM and MD techniques. The acquired overall classification accuracy (78%), spatial resolution (0.25 mm), and easy interpretability of the classification results make RGB imaging a potential technique for material characterisation in mining operations. Besides, the use of RGB images taken at small muck piles in underground mine resulted in a reproducible and reliable estimation of fragment sizes. Moreover, the delineation algorithm can be calibrated to automate the analysis of rock fragments. Therefore, fragmentation analysis can be performed in real-time in underground mines (such as at LHD).

The RGB sensor has excellent potential for in-situ material characterisation via colour detection or shape recognition of geological units or rock fragments. The technique can be used to create new data (e.g., minerals distribution and ore-zone boundaries) and knowledge

in real-time that would be of great interest in mining. Overall, the acquired results are promising and can likely be improved by using better quality images and image enhancement techniques (such as radiometric corrections that minimise the radiometric distortion related to camera optics and environmental conditions). The outcomes suggest that the technique is efficient and provides acceptable success for the characterisation of a polymetallic sulphide deposit in an underground mine. Therefore, it can be considered as a complementary technique.

RGB sensors with a well-defined imaging procedure and suitable illumination system can provide automated, reproducible and objective results for the mapping of visually distinct minerals. It offers the possibility of mapping minerals at a high spatial resolution. Moreover, RGB imaging systems are easy to use, portable, rapid, low-cost, have high data storage capability, and robust to environmental conditions. The technique also allows quick data access and visualisation, thus can improve the efficiency of mapping and support effective decision-making in mining operations. However, the future practical implementation of the approach requires ultimate resampling and co-registration techniques to enable automated image registration and mineral mapping.

REFERENCES

- Beckert, J., Vandeginste, V., McKean, T., Alroichdi, A. & John, C. (2017). Ground-based hyperspectral imaging as a tool to identify different carbonate phases in natural cliffs. *International Journal of Remote Sensing*, 39(12), pp. 4088-4114. doi: 10.1080/01431161.2018.1452068
- Beiranvand, P. A., Park, S. T. Y., Park, Y., Hong, J. K., Muslim, A. M, Läufer, A., Crispini, L., Pradhan, B., Zoheir, B., Rahmani, O., Hashim, M. & Hossain, M. S. (2019). Landsat-8, advanced spaceborne thermal emission and reflection radiometer, and worldview-3 multispectral satellite imagery for prospecting copper-gold mineralization in the northeastern Inglefield Mobile Belt (IMB), Northwest Greenland. *Remote Sensing*, 11(20), 2430. doi: 10.3390/rs11202430
- Bishop, C. A., Liu, J. G. & Mason, P. J. (2011). Hyperspectral remote sensing for mineral exploration in Pulong, Yunnan Province, China. *International Journal of Remote Sensing*, 32(9), pp. 2409-2426. doi: 10.1080/01431161003698336
- Dalm, M., Buxton, M. W. N. & van Ruitenbeek, F. J. A. (2018). Ore–waste discrimination in epithermal deposits using near-infrared to short-wavelength infrared (NIR-SWIR) hyperspectral imagery. *Mathematical Geosciences*, 51, pp. 849-875. doi: 10.1007/s11004-018-9758-6
- Drebenstedt, C. & Ortuta, A. J. (2012). Use of radar reflectivity as possibility for measurements of fragmentation during the blasting. *Proceedings of the 10th international symposium on rock fragmentation by blasting*, New Delhi, India, pp. 105-110.
- Neville, R. A., Levesque, J., Staenz, K., Nadeau, C., Hauff, P. & Borstad, G. A. (2003). Spectral unmixing of hyperspectral imagery for mineral exploration: Comparison of results from SFSI and AVIRIS. *Canadian Journal of Remote Sensing*, 29, pp. 99-110. doi: 10.5589/m02-085
- Kaufman, L. & Rousseeuw, P. J. (2005). *Finding Groups in Data: An Introduction to Cluster Analysis*. John Wiley & Sons, Hoboken, NJ.

- Kemeny, J., Devgan, A., Hagaman, R. & Wu, X. (1993). Analysis of Rock Fragmentation Using Digital Image Processing. *Journal of Geotechnical Engineering*, 119(7), pp. 1144-1160. doi: 10.1061/(ASCE)0733-9410
- Kotsiantis, S. B. (2007). Supervised Machine Learning: A Review of Classification Techniques. *Informatica*, 31, pp. 249-268.
- Krupnik, D. & Khan, S. (2019). Close-range, ground-based hyperspectral imaging for mining applications at various scales: Review and case studies. *Earth-Science Reviews*, 198, 102952. doi: 10.1016/j.earscirev.2019.102952
- Kruse, F. A. & Perry, S. L. (2013). Mineral Mapping Using Simulated Worldview-3 Short-Wave-Infrared Imagery. *Remote Sensing*, 5(6), pp. 2688-2703. doi: 10.3390/rs5062688
- Kruse, F. A., L Bedell, R., Taranik, J. V., Peppin, W. A., Weatherbee, O. & Calvin, W. M. (2012). Mapping alteration minerals at prospect, outcrop and drill core scales using imaging spectrometry. *International Journal of Remote Sensing*, 33(6), pp. 1780-1798. doi: 10.1080/01431161.2011.600350
- Rajan Girija, R., & Mayappan, S. (2019). Mapping of mineral resources and lithological units: a review of remote sensing techniques. *International Journal of Image and Data Fusion*, 10(2), pp. 79-106. doi: 10.1080/19479832.2019.1589585
- REDWAVE. (2020). REDWAVE sorting machine [Online]. Available: <http://www.redwave-us.com> [Accessed July 2020]
- Roussel, S., Preys, S., Chauchard, F. & Lallemand, J. (2014). Chapter 2 - Multivariate Data Analysis (Chemometrics). In: C. P. O'Donnell, C. Fagan & P. J. Cullen (Eds.), *Process Analytical Technology for the Food Industry*. Springer, New York, USA, pp. 7-59.
- Robben, C. & Wotruba, H. (2019). Sensor-Based Ore Sorting Technology in Mining—Past, Present and Future. *Minerals*, 9(9), 523. doi: 10.3390/min9090523
- Singh, P. K., Roy, M. P., Paswan, R. K., Sarim, M., Kumar, S. & Ranjan J. R. (2016). Rock fragmentation control in opencast blasting. *Journal of Rock Mechanics and Geotechnical Engineering*, 8(2), pp. 225-237. doi: 10.1016/j.jrmge.2015.10.005
- STEINERT. (2020). Sensor sorting units - colour sorting system [Online]. Available: <https://steinertglobal.com> [Accessed July 2020].
- Tavakol Elahi, A. & Hosseini, M. (2017). Analysis of blasted rocks fragmentation using digital image processing (case study: limestone quarry of Abyek Cement Company). *International Journal of Geo-Engineering*, 8(1), 16. doi: 10.1186/s40703-017-0053-z
- TOMRA. (2020). Quartz colour sorting [Online]. Available: <https://www.tomra.com> [Accessed July 2020].
- Tusa, L., Andreani, L., Khodadadzadeh, M., Contreras, C., Ivascanu, P., Gloaguen, R. & Gutzmer, J. (2019). Mineral Mapping and Vein Detection in Hyperspectral Drill-Core Scans: Application to Porphyry-Type Mineralization. *Minerals*, 9, 122. doi: 10.3390/min9020122
- Workman, L. & Eloranta, J. (2003). The effects of basting on crushing and grinding efficiency and energy consumption. Proceedings of the 29th Conference on Explosives and Blasting Techniques, International Society of Explosives Engineers, Cleveland, USA.

7

VISIBLE-NEAR INFRARED AND SHORT- WAVE INFRARED HYPERSPECTRAL IMAGING FOR MATERIAL CHARACTERISATION IN A POLYMETALLIC SULPHIDE DEPOSIT

This chapter demonstrates the usability of VNIR and SWIR hyperspectral imaging for material characterisation in the polymetallic sulphide deposit using drill core, channel and muck pile samples collected from the defined block in the test case. The chapter compares the performance of the two techniques for the identification of minerals and ore–waste discrimination. The chapter also discusses the potential benefits and possible challenges of the use of the techniques in operational mines.

7.1. INTRODUCTION

Hyperspectral imaging combines spectroscopy and imaging to provide a continuous spectrum of each pixel in the image. Thus, it provides both spectral and spatial information. Hyperspectral imaging sensor collects a digital image in hundreds of narrow adjacent spectral bands resulting in a stack of two-dimensional images referred to as a “data cube”. Hyperspectral images can be acquired over a wide range of the electromagnetic spectrum. The most popular hyperspectral imaging sensors operate in the VNIR, SWIR, and LWIR regions. Nevertheless, other types of hyperspectral imagers are also emerging, such as Raman and x-ray spectroscopies. Infrared-based hyperspectral imaging is mainly used in airborne or spaceborne remote sensing applications. However, a remarkable number of laboratory-based and field-based imaging systems are also available. Such as Specim FX10, Specim’s SWIR, and Specim OWL are some of the examples that operate in the VNIR, SWIR and LWIR regions of the electromagnetic spectrum, respectively (Specim, 2020).

Hyperspectral imaging sensors are non-destructive and do not require actual contact with a sample or material under the scene. These sensors can be used in a broad area of applications. One such application is the raw material characterisation in mining operations. For example, hyperspectral imaging is advantageous in analysing a large number of cores rapidly than the traditional logging methods. In mining, hyperspectral imaging can be used for on-line investigation of materials, thus has notable benefits in increasing the throughput and yield of the production process. Hence, it allows maximising the production capacity and efficiency of key operational areas in the mining industries. Therefore, it can offer a significant financial benefit in mining operations.

The sensor type and set-ups determine the spatial and spectral resolutions of the hyperspectral images. Therefore, the choice of suitable hyperspectral sensors is application dependent. In mineral mapping, the most commonly used hyperspectral imagers are sensors that operate in the VNIR and SWIR regions of the electromagnetic spectrum. The working principle and the current state-of-the-art of these sensors are discussed in Chapter 3. The VNIR and SWIR sensors are commonly utilised for the mapping of minerals during the exploration and extraction phases of the mining value chain. For example, Murphy and Monteiro, (2013) used VNIR hyperspectral imagery to map ferric iron minerals on the vertical mine face of an open-pit mine. Likewise, Baissa, (2011) applied SWIR images for the identification and mapping of minerals in carbonate rocks. Similarly, Dalm et al., (2017) utilise SWIR hyperspectral images for the separation of ore and waste materials in porphyry copper deposit. In another study, Mathieu et al., (2017) used SWIR image data to map alteration minerals as a pathfinder for uranium related deposit. Studies by Feng et al., (2018) and Sabins, (1999) indicated the usability of the VNIR and SWIR hyperspectral image data for mapping of geological units and geological structures in remote applications.

Numerous researchers showed the usability of the VNIR and SWIR sensors for the mapping of minerals at different scales and in diverse deposit types. However, the use of these techniques for mapping of minerals and separation of ore–waste in polymetallic sulphide deposit was not investigated. In this chapter, the use of the VNIR and SWIR hyperspectral images for the characterisation of polymetallic sulphide ore was explored using rock chips and drill-core samples. The techniques were assessed for the identification and mapping of minerals. Besides, the usability of the sensors for the discrimination of ore and waste materials was investigated.

7.2. INSTRUMENTATION AND DATA ACQUISITION

The VNIR and SWIR hyperspectral images were acquired using a Specim ‘Lab Scanner’. The instrument consists of two push-broom line scanners that acquire hyperspectral imagery in the VNIR and SWIR spectral ranges using separate detectors. The bush-broom scanners build an image one line at a time when the samples move on a sample tray. The models of the VNIR and SWIR cameras are PFD-65-V10E and SWIR3, respectively. The manufacturer of the sensors is Specim spectral imaging Ltd. (Oulu, Finland). These sensors are described in detail in Bakker et al., 2019. The VNIR hyperspectral images were recorded in the spectral range of 0.4–1.0 μm and consist of 196 bands, and 656 samples. The SWIR hyperspectral images were acquired in the spectral range of 1.0–2.5 μm and consist of 288 bands and 384 samples. The number of bands indicates the number of spectral channels and samples represents the number of spatial pixels per image line for each band. The specifications of the VNIR and SWIR systems used in this study are presented in Chapter 3. Specim’s diffuse line illumination unit was used to illuminate the sample surface under the scene. This illumination unit provides diffused line-illumination on the sample, thus optimising the imaging of various surfaces (Specim, 2020). The focusing prior to the imaging procedure was performed manually by adjusting the lens with the help of a focusing grid mounted on the tray. Before each sample scan, a reference measurement was carried out using both white and dark internal standard references. Thus, each sample measurement was referenced to account for the background spectral responses of the instrument (the instrumental noise) and illumination. The material used as a white reference is spectralon and the dark reference is a closed shutter (no material). The acquisition rate per sample measurements is about 1 min. There is no averaging involved in the post-processing; the binning was done in the hardware. For VNIR measurements, the spatial binning was two (meaning 2×2 sensor pixels averaged for each pixel saved), and spectral binning was four (four bands were averaged for each wavelength saved). For the SWIR, no spatial or spectral binning was applied. The Lumo recorder software (developed by Specim Spectral Imaging Ltd., Oulu, Finland) was used to set camera parameters, visualise the images in real-time, acquire and save data in the hard disk, and control the scanner system. The data is received in band-interleaved by layer (BIL) data format. The BIL format allows easy access to both spectral and spatial information. Thus, it is recommended for multivariate classification (Yoon and Park, 2015). In addition, the BIL format is compatible with several commercial software packages. Hyperspectral images were acquired using 50 rock chips samples and 8 drill-cores.

7.3. METHODOLOGY

As shown in Figure 7.1, the usability assessment of the VNIR and SWIR hyperspectral images for the identification of minerals and ore–waste discrimination in polymetallic sulphide deposit involves multiple steps that incorporates data-pre-processing, feature extractions (endmember selection), and mineral identification and mapping. The data acquisition and data pre-processing approaches are denoted as Block A in Figure 7.1. Minerals were identified using mineral spectral libraries and mineral maps were produced using a supervised classification technique (represented as Block B in Figure 7.1). Besides, the endmembers from the ore and waste materials were used to produce maps that show the ore and waste regions in drill-core samples. The details of each step are described below.

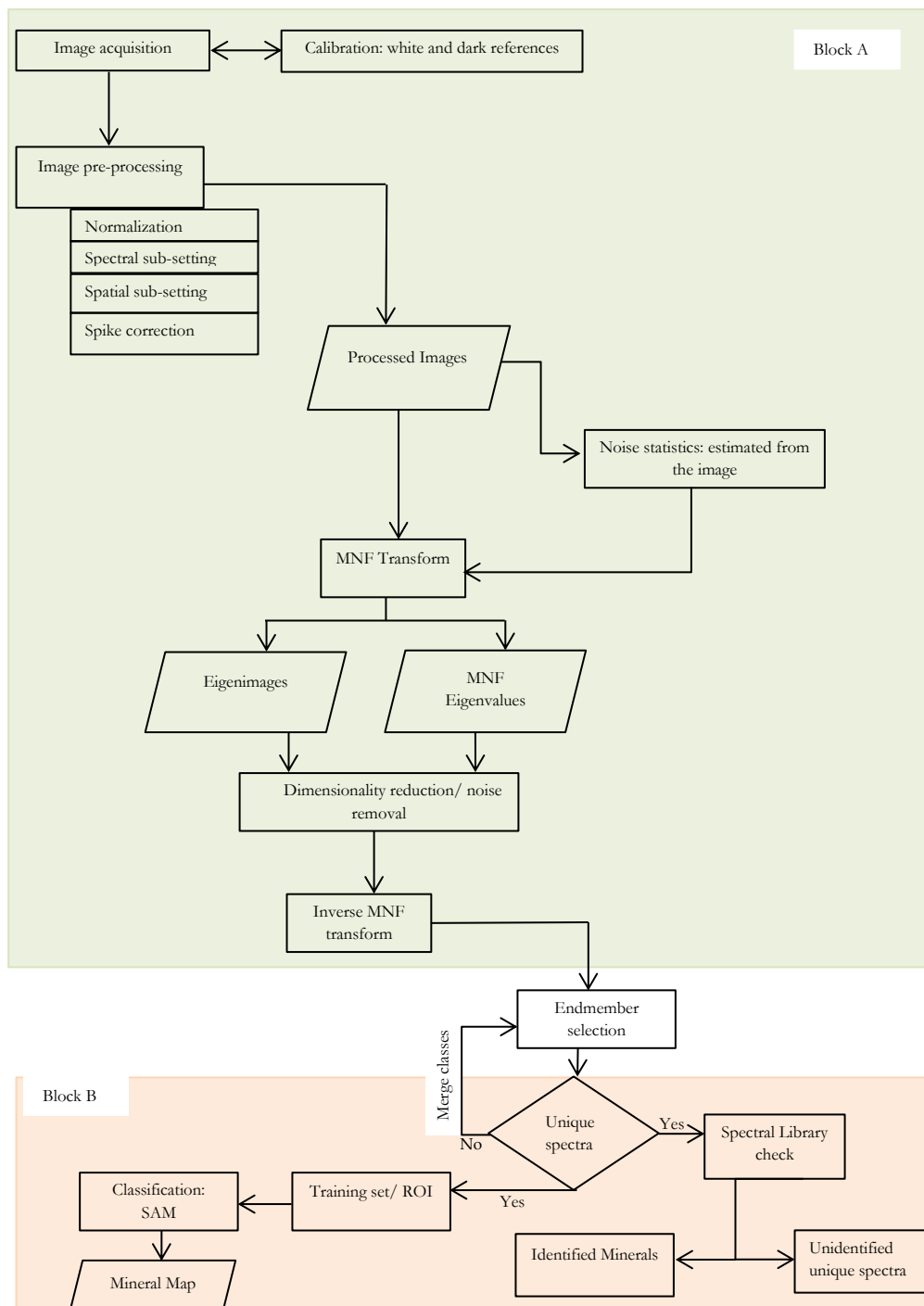


Figure 7.1: Workflow diagram depicting the steps of the mineral identification and mapping process using the VNIR and SWIR hyperspectral images.

7.3.1. PRE-PROCESSING

The raw VNIR and SWIR hyperspectral images were pre-processed prior to data analysis and information extraction. The pre-processing techniques applied were normalisation to reflectance, spectral subsetting, masking (spatial subsetting), and spike correction (Figure 7.1). The normalisation technique converts the irradiance data to reflectance using the white and dark references for the calibration. The white reference is the measurement with almost 100% reflection over the entire wavelength range, whereas the dark reference was captured with no light entering the sensor. Thus, the relative reflectance of the images is calculated by dividing the measured image by the white reference image after subtracting the dark reference image from both measurements. The raw hyperspectral images were acquired with more bands than the indicated range (e.g., the SWIR data were acquired from 0.98 μm to 2.53 μm ; however, for the test case materials, the spectral ranges from 0.98 to 1.0 μm and 2.5 to 2.53 μm yielded noisy results). Thus, spectral subsetting was performed to eliminate the noisy bands. Likewise, spatial subsetting was performed to remove unnecessary (e.g., pixels that do not represent a sample) parts of the acquired images. This was performed by a manual spatial subsetting. Spikes are intensity values that differ significantly from their neighbouring pixels. The spikes were identified by finding the local maxima and minima and setting a threshold. Consequently, the intensity values of spikes were removed and replaced using a linear interpolation of the surrounding wavelength bands.

7.3.2. FEATURE EXTRACTION AND MAPPING

The minimum (or maximum) noise fraction (MNF) transformation was applied for each processed image in order to isolate noise from the signal. The MNF transform is implemented in two cascaded principal component transformations (Figure 7.1). The first transformation estimates the noise from the data and, based on the estimated noise covariance matrix, the transformation decorrelates (no band-to-band correlations) and rescales (unit variance) the noise in the data. The data dimensionality was determined using the eigenvalues and the MNF images (eigenimages). The informative MNF components (with larger eigenvalues and coherent eigenimages) were used to inversely transform the MNF data to relatively noise-free spectral images that have the same number of bands as the original dataset (Green et al., 1988).

The inverse transformed MNF images were used to generate 2D scatter plots using the most informative MNF components (usually the first two components). These scatter plots were used to identify spectrally unique pixels (endmembers). The extracted features (selected endmembers) checked for their uniqueness and similar endmembers that show the same spectral information were merged (or combined) by computing the average. Moreover, the endmembers of the spectra were also assessed by computing the pixel purity index (PPI). PPI is the most popular endmember extraction algorithm (spectral unmixing method) that uses the spectral information of the hyperspectral data to find spectrally unique pixels. It is usually performed on MNF data that have been reduced to coherent images (Boardman, 1993; Kiran, 2015). The PPI is computed by continually projecting n-dimensional scatterplots onto a random vector. The extreme pixels for each projection are recorded and the total number of hits is stored in an image. These pixels are excellent candidates for selecting endmembers, which can be used in subsequent processing. Consequently, the pure endmembers of the VNIR and SWIR hyperspectral images were extracted separately.

The collected unique spectra were interpreted to identify minerals using spectral databases such as the USGS digital spectral library (Clark et al., 2003), the spectral interpretation field manual (AusSpec, 2008) and the ECOSTRESS spectral library (Groves et al., 1992). The identification of minerals was based on the wavelength location of distinctive features, the shape of the main absorption features of each spectrum, reflectance intensity and depth of diagnostic absorption bands, in comparison to reference spectra. As the illumination condition of the mineral libraries spectra and the acquired spectra differ, the intensity of reflectance value was not solely considered for direct comparison. However, it was used to supplement the interpretation process. Consequently, some of the unique spectra were identified using the available spectral libraries. However, there are also unidentified unique spectra, possibly due to factors such as mineral mixtures, physical matrix effects or weak spectral responses. The identified minerals were also validated using the XRD and LWIR (e.g., in the identification of carbonates and quartz) data. In addition, visual inspection using RGB images was also performed to validate the identification of the sulphide minerals (since most of the test case sulphide minerals are visually distinct).

The endmembers (including the unique unidentified unique spectra) were used to generate a training set (region of interest - ROI) for each inverse transformed MNF images. The ROI's were used to produce mineral maps that show minerals distribution and pixel abundances using SAM supervised classification technique. Besides, SAM was used to produce ore versus waste maps using the spectra from the ore minerals and other associated minerals. A description of the SAM technique is presented in Chapter 4. The advantages of the SAM classifier include its insensitiveness to illumination and albedo effects, besides it has a significant performance in hyperspectral data with few training sets (Yoon and Park, 2015).

7.4. RESULTS AND DISCUSSION

Inspecting the spectral variation of minerals using a false colour image gives a general and quick idea on the spectral behaviour of the minerals. However, minerals can show the same colour in one 3-band composite image that it is essential to examine multiple 3-band combinations. Consequently, the colour composite images of the VNIR and SWIR data show the minerals spectral variation within each sample (Figure 7.2). Moreover, the MNF images produced using the first three MNF components were used to examine the spectrally distinct minerals in the samples (Figure 7.3).

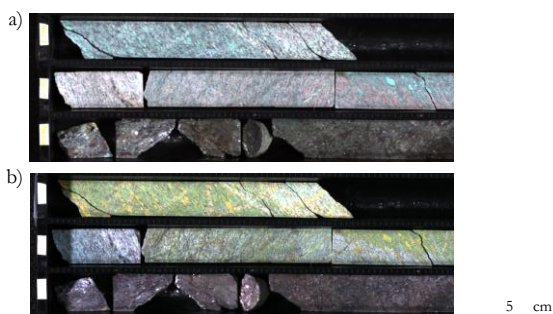


Figure 7.2: Colour composite image of a drill core showing the spectral variation of minerals (a) VNIR image, and (b) SWIR image.

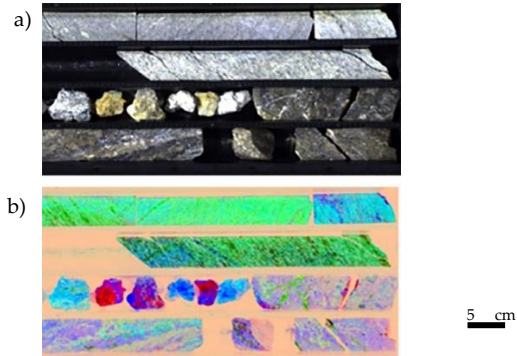


Figure 7.3: (a) An RGB image (true colour) of a drill core, and (b) the first three MNF components of the VNIR image.

7.4.1. MINERAL IDENTIFICATION USING VNIR

The unique endmembers of the VNIR and SWIR data were interpreted to identify the minerals using spectral reference databases. The interpretation is based on the distinctive features of minerals in specific spectral regions. In the VNIR region, the wavelength location of the ferric iron absorptions was taken into account to identify hematite and goethite minerals. These minerals show distinctive spectral features at $\sim 0.46 \mu\text{m}$, $\sim 0.65 \mu\text{m}$ and $\sim 0.85 - 0.95 \mu\text{m}$ (Townsend, 1987 as cited in Murphy and Monteiro, 2013; AusSpec, 2008). On the other hand, the sulphide minerals do not show absorption features in the VNIR region; thus, identification of the sulphide minerals could not be based on diagnostic absorption features. Instead, the reflectance pattern (e.g., higher reflection points) and the intensity of the VNIR data were matched to the reference spectral to identify some of the sulphide minerals in the analysed samples. The VNIR and SWIR reference spectra of some of the sulphide minerals are shown in Figure 7.4. Most of the VNIR data endmembers were interpreted. For example, Figure 7.5 shows the identified VNIR spectra of the pyrite and goethite minerals. However, there are also some mineral mixtures or unique spectra that could not be interpreted using the available spectral databases.

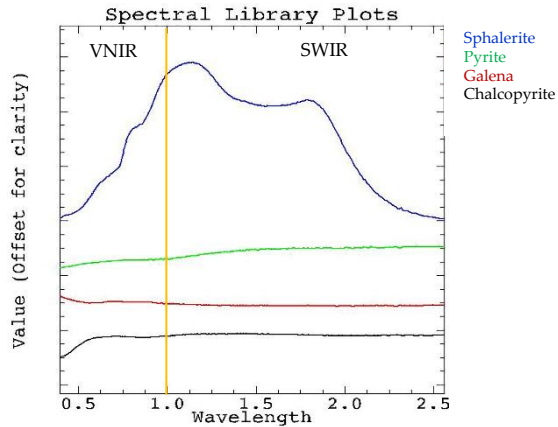


Figure 7.4: The VNIR and SWIR spectral signatures of some of the sulphide minerals based on USGS, 2020).

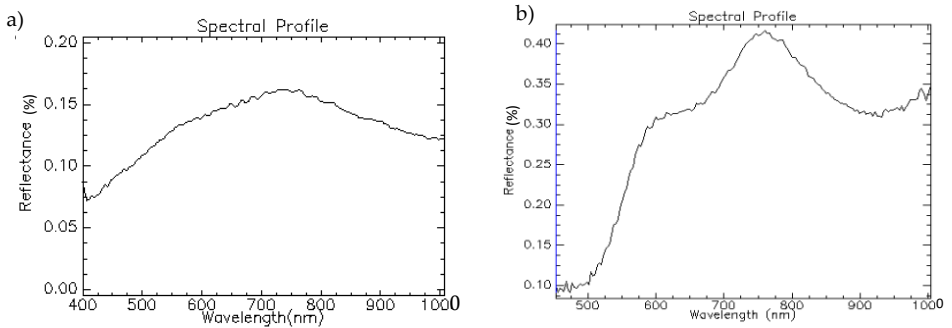


Figure 7.5: The VNIR spectra of (a) pyrite (b) goethite minerals.

The identified minerals using the VNIR data include the sulphides (e.g., pyrite, galena, sphalerite and chalcopyrite), the ferric iron minerals (e.g., hematite and goethite) and carbonates (e.g., siderites). Besides, the endmembers of the VNIR data and a SAM classifier were used to produce mineral maps. Examples of the mineral maps produced using the VNIR data are shown in Figure 7.6. The mineral maps show the minerals distribution and the pixel abundance of minerals in the sample. Therefore, it is beneficial for the indication of mineral proportions in the analysed samples.

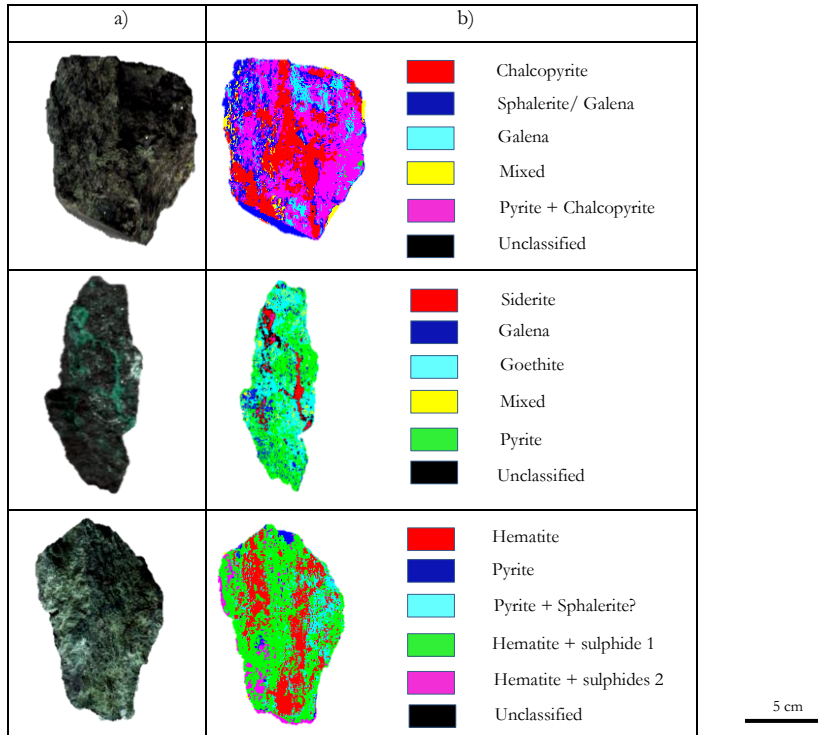


Figure 7.6: VNIR images of rock chip samples (a) colour composite images, and (b) classified images.

7.4.2. MINERAL IDENTIFICATION USING SWIR

In the SWIR region, most minerals show diagnostic absorption features between 1.3 to 2.5 μm , mainly in the wavelength region between 2.05 to 2.45 μm most minerals have major characteristics absorption features (AusSpec, 2008; Clark et al., 1990; USGS, 2020). The main absorption features in the SWIR region are indicated in Table 7.1. The functional groups OH, water, Al-OH, Fe-OH, Mg-OH, and CO_3 are major components of some of the minerals (such as phyllosilicates, sulphate, carbonates and Al-bearing minerals). Thus, the spectral information of these functional groups and a combination of the absorption features were used to identify those minerals that are active in SWIR. On the other hand, the sulphide minerals do not show spectral features in the SWIR region. Nevertheless, the featureless nature of the minerals was used to indicate the minerals. This approach enables the discrimination of ore and waste materials in polymetallic sulphide deposit using SWIR data.

Table 7.1: The main absorption features in the SWIR region of the electromagnetic spectrum based on AusSpec, (2008), Hauff, (2008) and USGS, (2020).

Functional groups	Diagnostic absorption features location	Mineral groups
OH	~1.4 μm (also ~1.55 μm and ~1.75 - 1.85 μm in some minerals)	Clays, sulphates, hydroxides
Water	~ 1.4 μm and ~ 1.9 μm	Clays, sulphates, hydroxides, smectite
Al-OH	~ 2.16 - 2.23 μm	Clays, sulphates, micas
Fe-OH	~ 2.23 μm	Fe-clays
Mg-OH	~2.3 - 2.37 μm	Mg-clays, chlorites
CO ₃ ²⁻	~ 2.3 - 2.37 μm (and also at 1.87 μm , 1.99 μm and 2.16 μm)	Carbonates

The minerals identified using the SWIR data include mica (e.g., muscovite), clay minerals (e.g., montmorillonite and illite), carbonates (e.g., siderite), tectosilicate (e.g., quartz), sulphide ores (no features and results with featureless line) and mineral mixture (e.g., muscovite + sulphides). For example, the distinctive features of illite are the OH absorption at ~1.41 μm , the water absorption at ~ 1.91 μm , Al-OH absorption which varies in wavelength from 2.18 – 2.23 μm depending on the composition of the sample (Figure 7.7). The minerals illite and muscovite share most of the absorption features; however, water absorption at 2.2 μm is more pronounced in illite than muscovite. Thus, the two minerals were identified accordingly.

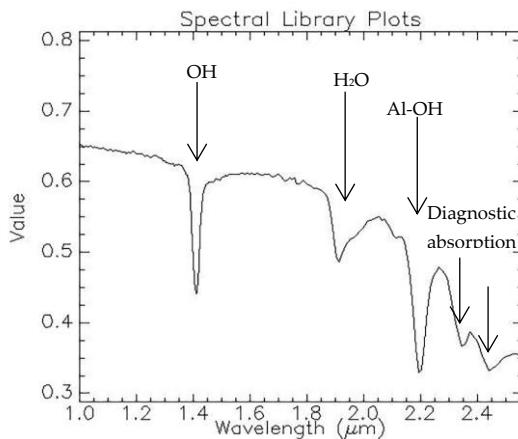


Figure 7.7: The distinctive features of illite in SWIR spectrum.

Figure 7.8 shows the mineral maps of three samples produced using the SWIR data and training data (endmembers). As shown in the figure, the identified minerals include siderite, muscovite, illite, illite sulphide mixture and muscovite sulphide mixture. However, there are also unclassified pixels as well as unidentified unique spectral signatures. The unclassified pixels could be the unrepresented signature in the endmember or outliers. Whereas, the unidentified unique spectra are spectral signatures that could not be interpreted using the existing mineral databases. This can be due to minerals mixtures or unidentified mineral

response. Interpretation of mixed spectra is not a straightforward procedure as minerals can mix with different proportions and compositions. Mixed spectrum can be characterised by additional absorption features, wavelength shifts and deeper depth than the actual (AusSpec, 2008). In some instances, the presence of certain minerals might lower the spectral responses of some of the minerals. For example, the occurrence of sulphide minerals in the proportion of > 5-10% has a significant effect in reducing the reflectance value and weakening the diagnostic absorption features of the SWIR active minerals (AusSpec, 2008). Consequently, these effects were taken into account for the identification of the sulphides mixture as well as other mineral mixtures.

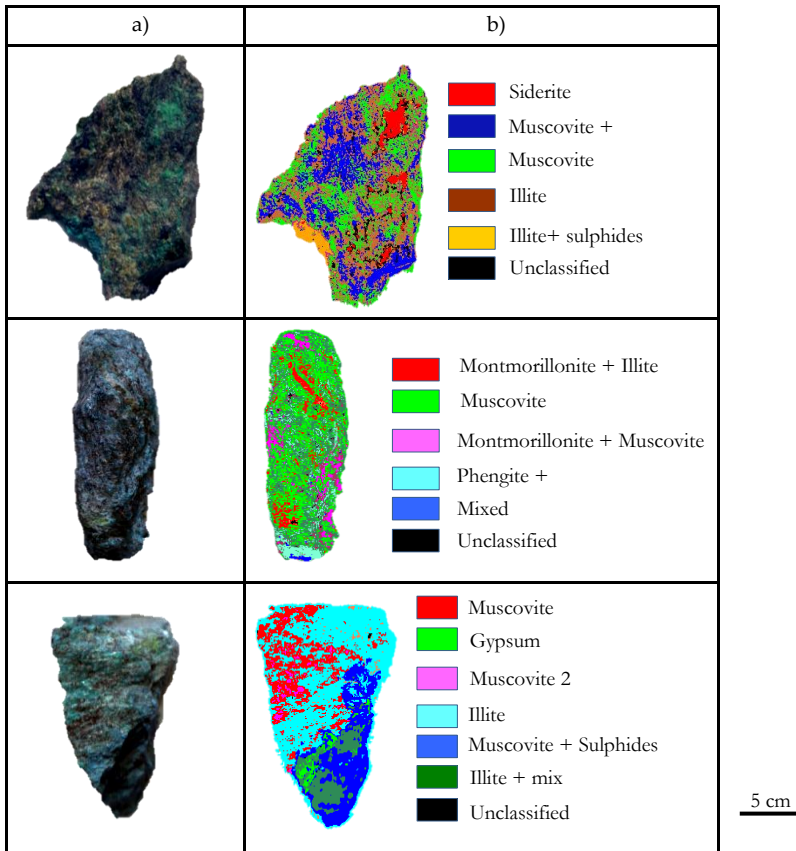


Figure 7.8: SWIR images of the rock chips samples (a) colour composite images, and (b) classified images.

The spectral differences between the sulphide minerals and the associated minerals are sufficiently distinct to allow the classification of ore and waste mineralogy using the SWIR images. An example of a drill-core SWIR image with some of the identified minerals is indicated in Figure 7.9. As shown in the figure, the response from the sulphide minerals is featureless. However, this featureless nature of the minerals in the SWIR spectra was used as a characteristic value to map ore versus waste materials (Figure 7.10). Despite the limitation related to the absence of prominent spectral features of the sulphide minerals in SWIR data, a mineral map that shows ore and waste zone could be generated.

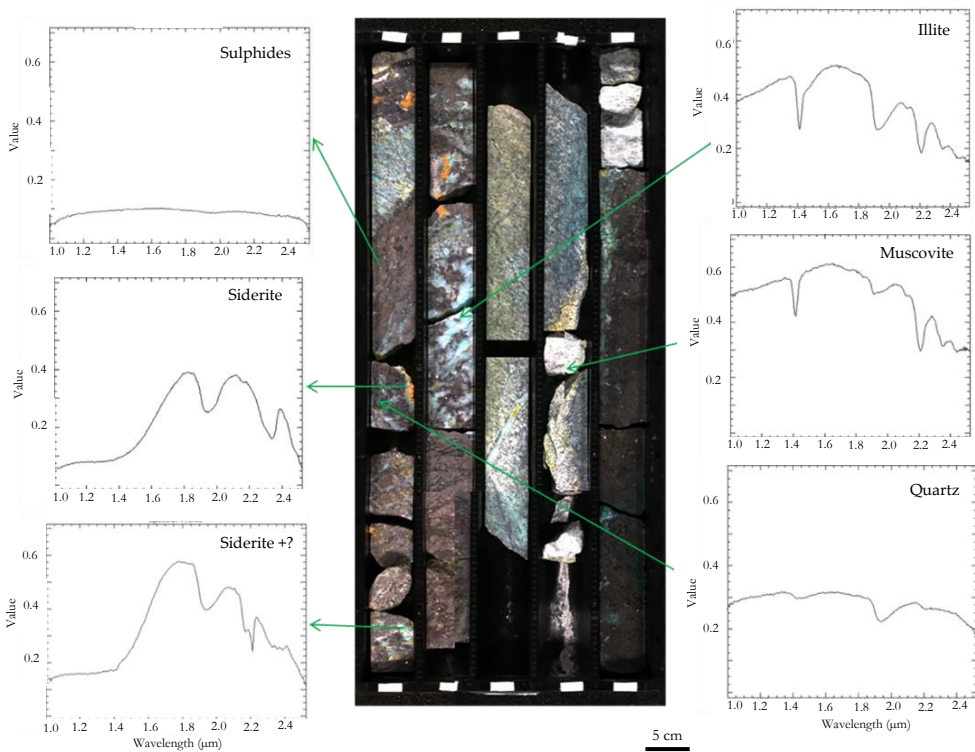


Figure 7.9: A false colour SWIR image of a drill core and some of the identified minerals.

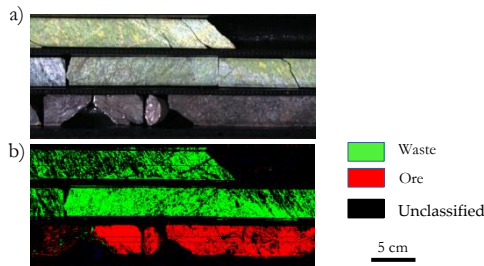


Figure 7.10: SWIR image (a) a false colour image, and (b) a classified image that shows the ore and waste materials of the drill core.

7.4.3. COMPARISON OF THE VNIR AND SWIR DATA

As shown in Figure 7.11 and 7.12, different minerals were identified using the VNIR and SWIR data. The identified minerals using the VNIR data include sulphides, siderite and mixture. Whereas, minerals such as muscovite, illite, quartz and mixtures were identified using the SWIR data. Minerals that do not exhibit characteristics spectral features in one region can have useful spectral signals in the other areas of the electromagnetic spectrum. For example, as shown in Figure 7.11, the mineral illite could not be identified in the VNIR data; however, it was detected in the SWIR data. Similarly, quartz could not be distinguished in the VNIR data, while it has essential spectral information in SWIR data. This shows that

the integrated analysis of the VNIR and SWIR data can allow the identification of more minerals than that can be achieved using one of the sensors. Thus, the combined analysis is beneficial for an enhanced characterisation material in different deposit types.

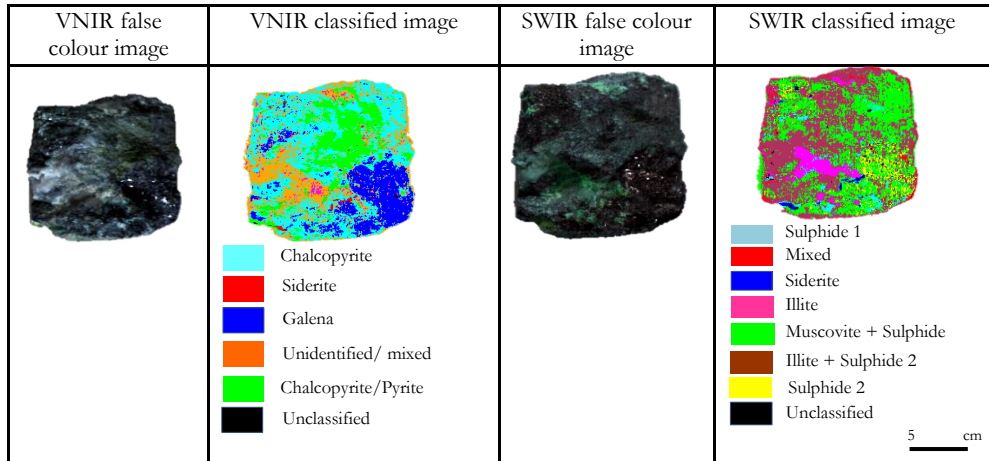


Figure 7.11: The VNIR and SWIR images of one of the samples showing the identified minerals in both regions.

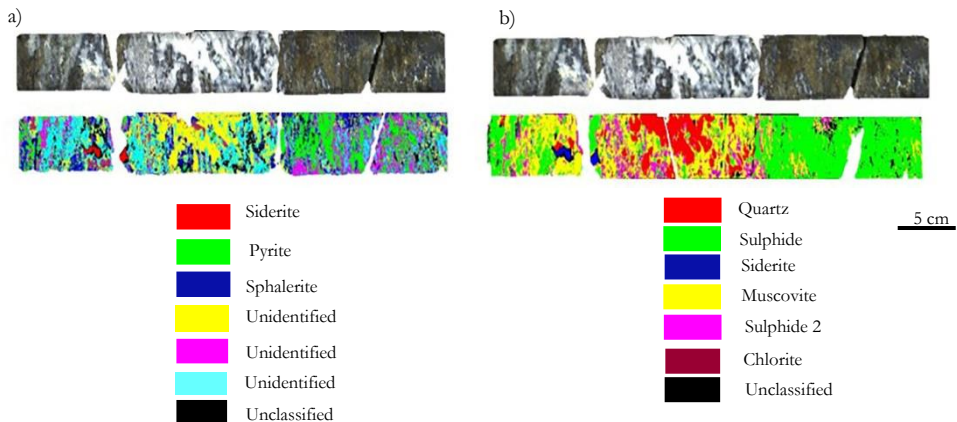


Figure 7.12: The RGB image and classified (a) VNIR, and (b) SWIR images of a drill core.

In this study, the minerals identified using the VNIR data include sulphides (e.g., pyrite, galena, sphalerite and chalcopyrite), the ferric iron minerals (hematite and goethite) and carbonates (siderites). Furthermore, mixed spectra were also observed. Likewise, the minerals identified using the SWIR data include mica (muscovite), sulphate (gypsum), clay minerals (montmorillonite and illite), carbonates (siderite), tectosilicate (quartz), phyllosilicate (Mg + Fe chlorite), sulphide ores (with no particular absorption features), and minerals mixture (e.g., muscovite + siderite). Some of the sulphide minerals were differentiated using the VNIR data without particular absorption features of the minerals in the region. This is also in line with a recent study that showed the potential use of the VNIR

technique for the identification of the sulphide minerals that are associated with platinum/palladium (Brock et al., 2003). Likewise, the sulphide minerals do not show characteristic spectral features in SWIR spectral data (Clark et al., 1993). However, the sulphide minerals exhibit sufficiently distinct spectral signatures from the associated minerals that the technique is promising for ore–waste discrimination and can allow indication of ore zones in mining operations. Besides, the use of the SWIR data can permit automated mapping of the ore and waste zones using comprehensive training data (endmembers).

The VNIR data showed promising results in the detection and identification of some of the sulphide minerals. However, it needs careful analysis and validation since the sulphides do not show any particular absorption features. The SWIR data is mainly known for mapping of alteration minerals since it detects most of the functional groups of these minerals (e.g., OH and Al-OH). However, the results in this study show the potential use of the technique for the separation of ore and waste materials in polymetallic sulphide deposits. There are also some limitations of the techniques. For example, the VNIR and SWIR techniques are surface techniques; as a result, surface material (or contamination) can influence the measurements. Fresh surface measurements (no weathering), surface cleaning and information from other sensors can minimise the effect of surface contamination. In general, the VNIR and SWIR techniques resulted in promising results for the characterisation of materials in polymetallic sulphide deposit. The promising results achieved coupled with the recent development of portable hyperspectral cameras (e.g., Specim IQ developed by Specim, 2020) can allow the use of the technique for in-situ mapping of minerals. Besides, a robust imaging system with the already existing field set-up and a suitable illumination source can allow mapping of minerals at the mine face in underground mines. Likewise, the availability of high-speed hyperspectral sensors allows on-line analysis of materials at the conveyor belt (Goetz et al., 2009; TOMRA, 2019). Thus, the technologies have significant potential for the characterisation of materials in mining and can significantly assist effective decision-making in the mining process.

7.5. CONCLUSIONS

This study assessed the applicability of the VNIR and SWIR hyperspectral images for the characterisation of materials in a polymetallic sulphide deposit. The VNIR and SWIR data were acquired from rock chips and drill core samples. The images were pre-processed, and spectrally distinct endmembers were extracted. The extracted unique spectra were interpreted using spectral reference databases. Besides, training sets were generated using the extracted endmembers, and mineral maps were produced using a SAM classifier. The results reported in the preceding sections show that both VNIR and SWIR datasets include relevant information that can be employed for the characterisation of polymetallic sulphide materials. The minerals identified using the VNIR data include the sulphides (pyrite, galena, sphalerite and chalcopyrite), the ferric iron minerals (hematite and goethite) and carbonates (siderites). Likewise, the minerals identified using the SWIR data include mica (muscovite), clay minerals (montmorillonite and illite), carbonates (siderite), tectosilicate (quartz), phyllosilicate (Mg + Fe chlorite), sulphide ores (with no particular absorption features), and minerals mixture (e.g., muscovite + siderite). Mixed spectra were also observed in both VNIR and SWIR spectral data. The use of individual VNIR and SWIR techniques resulted in a useful analysis of the materials. However, minerals that do not exhibit characteristic spectral features in the VNIR region can have useful spectral signals in the SWIR region.

Therefore, the use of both techniques is beneficial for an enhanced characterisation material in different deposit types.

The sulphide minerals do not have particular absorption features in the VNIR and SWIR regions. However, the featureless nature of the minerals was used as a characteristic value to map ore and waste materials using the SWIR data. Consequently, the use of SWIR data resulted in promising results for the separation of ore and waste materials in the polymetallic sulphide deposit. Overall, the VNIR and SWIR technologies are commonly used for the identification of minerals that have diagnostic absorption features. In this study, the use of the techniques for the characterisation of materials without diagnostic absorption features resulted in promising results. The VNIR data show a great potential to detect and identify among the sulphide minerals. However, it needs careful analysis and validation since the sulphides do not show any particular absorption features. Likewise, the use of SWIR allowed the identification of various minerals and classification of ore and waste materials in a polymetallic sulphide deposit. Therefore, the techniques have a significant potential for an automated indication of mineralised zones in polymetallic sulphide deposits. This will be beneficial in supporting effective decision-making in the mining process.

REFERENCES

- AusSpec. (2008). G-MEX Spectral interpretation field manual (3rd Ed.). AusSpec international publications.
- Baissa, R., Labbassi, K., Launeau, P., Gaudin, A. & Ouajhain, B. (2011). Using HySpex SWIR-320m hyperspectral data for the identification and mapping of minerals in hand specimens of carbonate rocks from the Ankloute Formation (Agadir Basin, Western Morocco). *Journal of African Earth Sciences*, 61(1), pp. 1-9. doi: 10.1016/j.jafrearsci.2011.04.003
- Bakker, W., Werff, H. V. & Meer, F. V. (2019). Determining Smile and Keystone of Lab Hyperspectral Line Cameras. *Proceedings of the 10th Workshop on Hyperspectral Imaging and Signal Processing: Evolution in Remote Sensing (WHISPERS)*, Amsterdam, The Netherlands, pp. 262-266.
- Boardman, J. (1993). Automating Spectral Unmixing of AVIRIS Data using Convex Geometry Concepts. *Proceedings of the 4th Annual JPL Airborne Geoscience Workshop: AVIRIS*, Vol. 1, Washington, DC, USA, pp. 11-14.
- Brock J. B. & Thomas S. M. (2003). Sulfide detection in drill core from the Stillwater Complex using visible/near-infrared imaging spectroscopy. *Geophysics*, 68, pp.1561-1568. doi: 10.1190/1.1620630
- Clark, R. N., King, T. V. V., Klejwa, M. & Swayze, G. A. (1990). High spectral resolution reflectance spectroscopy of minerals. *Journal of Geophysical Research*, 95, pp. 12653-12680. doi: 10.1029/JB095iB08p12653
- Clark, R. N., Swayze, G. A., Gallagher, A. J., King, T. V. V. & Calvin, W. M. (1993). The U. S. Geological Survey, Digital Spectral Library: Version 1: (0.2 to 3.0 μm). Open File Report 93-592. Available online: <http://pubs.er.usgs.gov/publication/ofr93592>
- Clark, R. N., Swayze, G. A., Wise, R. K., Livo, E., Hoefen, T. M., Kokaly, R. F. & Sutley, S. J. (2003). USGS Digital Spectral Library splib05a, Open-File Report 2003-395. Available online: <http://pubs.er.usgs.gov/publication/ofr03395>
- Dalm, M., Buxton, M. W. N. & van Ruitenbeek, F. J. A. (2017). Discriminating ore and waste in a porphyry copper deposit using short-wavelength infrared (SWIR)

- hyperspectral imagery. *Minerals Engineering*, 105, pp.10-18.
doi: 10.1016/j.mineng.2016.12.013
- Feng, J., Rogge, D. & Rivard, B. (2018). Comparison of lithological mapping results from airborne hyperspectral VNIR-SWIR, LWIR and combined data. *International Journal of Applied Earth Observation and Geoinformation*, 64, pp. 340-353.
doi: 10.1016/j.jag.2017.03.003
- Goetz, A. F. H., Curtiss, B. & Shiley, D. A. (2009). Rapid gangue mineral concentration measurement over conveyors by NIR reflectance spectroscopy. *Minerals Engineering*, 22(5), pp. 490-499. doi: 10.1016/j.mineng.2008.12.013
- Green, A. A., Berman, M., Switzer, P. & Craig, M. D. (1988). A transformation for ordering multispectral data in terms of image quality with implications for noise removal. In *IEEE Transactions on Geoscience and Remote Sensing*, 26(1): pp. 65-74.
- Grove, C. I., Hook, S. J. & Paylor, E. D. (1992). Laboratory reflectance spectra for 160 minerals 0.4 to 2.5 micrometers. Jet Propulsion Laboratory, Open-File Report 92-2. Available online: <http://hdl.handle.net/2014/40148>
- Hauff, P. (2008). An overview of VIS-NIR-SWIR field spectroscopy as applied to precious metals exploration. Spectral International Inc., Arvada, USA.
- Kiran Raj, S., Ahmed, S. A., Srivatsav, S. K. & Gupta, P. K. (2015). Iron oxides mapping from EO-1 hyperion data. *Journal of the Geological Society of India*, 86(6), pp. 717-725. doi: 10.1007/s12594-015-0364-7
- Mathieu, M., Roy, R., Launeau, P., Cathelineau, M. & Quirt, D. (2017). Alteration mapping on drill cores using a HySpex SWIR-320m hyperspectral camera: Application to the exploration of an unconformity-related uranium deposit (Saskatchewan, Canada). *Journal of Geochemical Exploration*, 172, pp. 71-88.
doi: 10.1016/j.gexplo.2016.09.008
- Murphy, R. J. & Monteiro, S. T. (2013). Mapping the distribution of ferric iron minerals on a vertical mine face using derivative analysis of hyperspectral imagery (430–970nm). *ISPRS Journal of Photogrammetry and Remote Sensing*, 75, pp. 29-39.
doi: 10.1016/j.isprsjprs.2012.09.014
- Sabins, F. F. (1999). Remote sensing for mineral exploration. *Ore Geology Reviews*, 14(3), pp. 157-183. doi: 10.1016/S0169-1368(99)00007-4
- Specim. (2020). Spectral Cameras [Online]. Available: <https://www.specim.fi/spectral-cameras> [Accessed March 2020].
- Specim. (2020). Accessories [Online]. Available: <https://www.specim.fi/accessories> [Accessed November 2020].
- TOMRA. (2019). Mining Sorting Equipment [Online]. Available: <https://www.tomra.com/en/sorting/mining/sorting-equipment> [Accessed March 2019].
- USGS. (2020). The USGS Spectral Library [Online]. Available: <http://speclab.cr.usgs.gov/spectral-lib.html> [Accessed March 2020].
- Yoon, S. C. & Park, B. (2015). Chapter 4 - Hyperspectral Image Processing Methods. In: B. Park & R. Lu (Eds.), *Hyperspectral Imaging Technology in Food and Agriculture*. Springer, New York, USA, pp. 81-101.

8

MID-WAVE INFRARED AND LONG-WAVE INFRARED FOR SULPHIDE ORE DISCRIMINATION

This chapter presents the use of the mid-wave infrared and long-wave infrared technologies for the discrimination of ore and waste in polymetallic sulphide ore deposit. The chapter also compares the performance of the MWIR data model with the LWIR data model for the discrimination of ore–waste materials. This study was conducted using the channel samples collected from the mine face of the defined study block.

Parts of this chapter have been published in:

Destá, F.S. & Buxton, M.W.N. (2018). Chemometric Analysis of Mid-Wave Infrared Spectral Reflectance Data for Sulphide Ore Discrimination. *Mathematical Geosciences*. 51(7), pp. 877-903. doi: 10.1007/s11004-018-9776-4

Despite significant recent advancements in the sensor technologies, the use of sensors for raw material characterisation in the mining industry remains limited. The aim of the present study was to assess the utility of applying the MWIR and LWIR reflectance data acquired by the use of a handheld FTIR spectrometer, combined with PLS-DA, for the characterisation of a polymetallic sulphide ore deposit. In achieving the study objectives, focus was given to the MWIR portion of the FTIR dataset, as it is the least explored region of the infrared spectrum in mineral characterisation studies. Three datasets—covering different wavelength ranges—were generated from the FTIR spectral data, namely the full FTIR range (2.5 to 15 μm), MWIR (2.5 to 7 μm) and LWIR (7 to 15 μm), in order to investigate the associated information level of each defined wavelength region separately. DoE was developed to determine the optimal data filtering techniques. Using the processed data and PLS-DA, a series of calibration and prediction models were developed for ore and waste materials separately. As the models applied to the MWIR data showed a successful classification rate of 86.3% for sulphide ore-waste discrimination, similarly using the full spectral FTIR dataset, a correct classification rate of 89.5% was achieved. This indicates that MWIR spectral range includes informative signals that are sufficient for classifying the material into ore or waste. The proposed approach could be extended for automating the sulphide ore-waste discrimination process, thus greatly benefiting marginally economical mining operations.

8.1. INTRODUCTION

The metal ore grades have been declining over the last decades. This leads mining to move to the extraction of resources in lower-grade deposits. The extraction of low-grade ore bodies is challenging and typically have substantial portions of waste materials. Thus, haulage and processing costs become extremely expensive. This shows the need for efficient mechanisms to provide comprehensive mineral sorting solutions that can potentially minimise the costly issues in the processing of low-grade ores. One such tool can be a technology-driven physical separation of materials into different material streams. Sensor-based sorting provides an innovative solution for the dry separation of ore and waste materials in mining operations. It has a substantial contribution in increasing productivity, lowering energy consumption, reducing greenhouse gas emissions and minimising water losses (Bamber et al., 2004; Batterham and Fleming, 2006; Robben and Wotruba, 2019; Wotruba, 2006). Thus, it can enable a significant increase in the efficiency and lifetime of mining operations.

Sensor-based sorting relies on measuring material properties to distinguish valuable and waste materials using sensor technologies. The sensor technologies that are currently in use for sensor-based ore sorting include VNIR, DE-XRT, XRF, magnetic resonance (MR), and RGB (Duffy et al., 2015; Robben and Wotruba, 2019; STEINERT, 2020; TOMRA, 2020). However, these technologies are only used in limited applications such as in the processing of industrial minerals, diamonds and gemstones. Therefore, there is still a demand for state-of-the-art sensor technologies for the separation ore and waste materials in various deposit types.

The objective of this study was to develop classification and prediction models using chemometric techniques that are capable of discriminating sulphide ore and waste materials in economically suboptimal mining operations, using spectral data acquired by a handheld FTIR spectrometer. The acquired FTIR spectral data were processed to produce three datasets, namely full FTIR spectra (2.5 to 15 μm), as well as MWIR (2.5 to 7 μm) and LWIR (7 to 15 μm). This approach was adopted in order to evaluate the information level associated with each wavelength region (MWIR and LWIR) separately. In particular, as the MWIR part of the electromagnetic spectrum has been under-investigated to date due to historically limited instrument development, it was the focal point of this study.

8.2. MATERIAL AND INSTRUMENTATION

8.2.1. MATERIAL

As a part of this study, channel samples were collected to address the observed spatial variability and ensure sample representativeness. For this purpose, twenty-three channels spaced approximately 80 to 120 cm apart (depending on the material variability at each channel location) were cut, and 102 samples were acquired from different intervals within each channel, as shown in Figure 8.1.

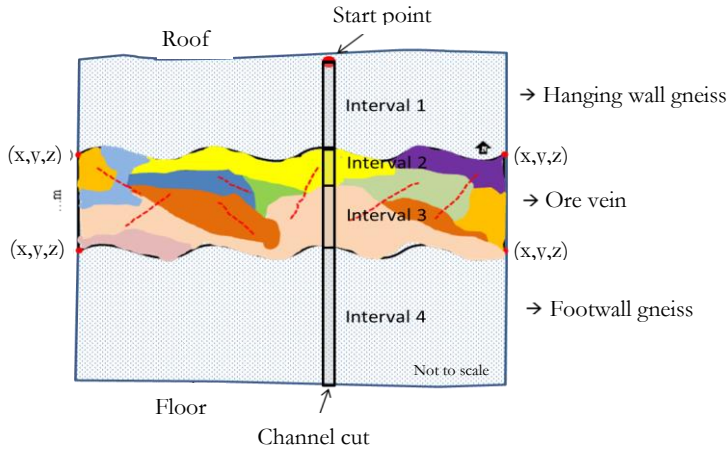


Figure 8.1: Sketch that illustrates a channel cut at the defined mine face. The channel cross-cuts four different intervals, each belonging to a different lithotype and sampled separately.

8.2.2. INSTRUMENTATION AND DATA ACQUISITION

An FTIR spectrometer simultaneously collects data in a wide spectral range in the time domain, whereby the resulting time-domain graph shows a signal changes over time. In the next step, a signal processing technique (Fourier transform) is used to convert the time-domain information to data in the frequency domain, which allows distinguishing the amount of signal within each specified frequency band over a range of frequencies (Ismail et al., 1997). Such frequency domain representation is necessary to convert the input signal into a full spectrum, which can be used to identify or quantify different materials. A FTIR spectrometer has considerable advantages over grating-based IR spectrometers. For example, it produces spectra of higher quality relative to the infrared equivalents (a higher signal-to-noise ratio). Its other benefits include short data acquisition time, higher accuracy, higher precision, wider scan range and high resolution (Agilent, 2017; Chemistry libretexts, 2017; Perkins, 1987; Smith, 2011; Stuart, 2004). Moreover, owing to the rapid technological advances, portable FTIR spectrometers can be produced, permitting their use in real-time (in-situ) applications (Agilent, 2017).

The FTIR 4300 analyser used in this study has three interchangeable sampling interfaces, namely external reflectance, attenuated total reflectance (ATR) and diffuse reflectance (Agilent, 2017). It provides point data at a high data acquisition speed (less than 30 s). FTIR obtains full-wavelength spectra over a wide range of the electromagnetic spectrum (1.9 to 15 μm). Thus, it has a great potential for identification of various materials. The instrument is depicted in Figure 8.2, and is a portable handheld device, powered by two 100/120/240

V batteries. Its compact dimensions and relatively lightweight (under 2.2 kg) ensure its effective use in a wide range of in-situ applications in real-time. However, due to the harsh environmental conditions in the mine that served as the study site, in-situ underground measurements were not attempted. Instead, samples were collected and analysed in a laboratory.



Figure 8.2: Handheld FTIR 4300 spectrometer and the three sampling interfaces.

The FTIR measurements were optimised by considering different instrument setups. This was done by interchanging the three sampling interfaces, varying the number of sample scans, modifying instrument calibration time and adjusting resolution. The external reflectance interface allows a mirror-like reflection (specular reflection) from the sample surface to be captured and is thus typically used for smooth surfaces. The ATR measures the internal reflection of the sample as the infrared radiation beam passes through an ATR element in contact with the sample. Finally, the diffuse reflectance interface allows internal and external reflection to be measured simultaneously and it is usually applicable for rough surfaces. The working principles behind all three setups are shown in Figure 8.3.

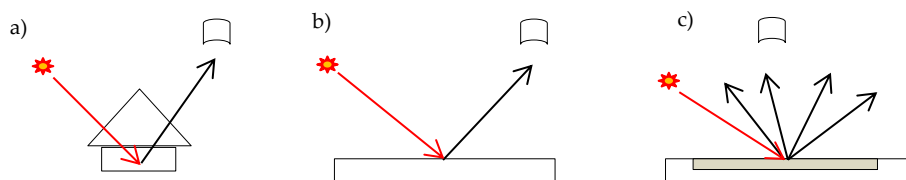


Figure 8.3: The three FTIR spectrometer interfaces: (a) ATR, (b) specular reflectance, and (c) diffuse reflectance.

The performance of each of the three sampling interfaces was assessed using homogenized powdered samples to remove artefacts due to surface texture and compositional intergrowth. To obtain optimal sample scans, the influence of changing the number of sample scans on the measurement results was evaluated. The instrument was calibrated at different time intervals and the measurement results were compared. To evaluate the significance of the spectral differences, FTIR measurements were collected at 4 cm^{-1} , 8 cm^{-1} and 18 cm^{-1} resolutions and the results were compared. The resultant optimised instrument setup comprised of 64 sample scans, 126 background scans, 4 cm^{-1}

resolution, 15-minute instrument calibration time and diffuse reflectance sampling interface. The FTIR spectroscopy data were collected over the ~ 1.9 to ~ 15 μm wavelength range. However, for the test case materials, the spectral range from 1.9 to 2.5 μm yielded noisy results and was excluded from further analyses. Three sub-datasets were prepared prior to modelling: the full FTIR data (excluding the range from 1.9 to 2.5 μm), the MWIR (2.5 to 7 μm) data and the LWIR (7 to 15 μm) data. To accommodate sample heterogeneity, multiple spectra were collected from each sample, the analysis results pertaining to 605 measurements collected using 102 samples are discussed in the sections that follow.

8.2.3. CHEMICAL VALIDATION DATASETS

The conventional data acquisition techniques namely XRD, XRF and ICP-MS were used to obtain the data that were employed in the validation of the material discrimination results. The ICP-MS and XRF measurements were performed using 50 samples, while XRD measurements were carried out using 34 samples. The XRD data used for this study provide semi-quantitative mineralogical information, whereas the XRF and ICP-MS data provide quantitative elemental information.

8.3. METHODOLOGY

As illustrated in Figure 8.4, the material discrimination approach developed as a part of the present study is a multi-step process that incorporates data exploration, data pre-processing, data modelling and model validation. The data exploration task (denoted as Block A in Figure 8.4) includes pattern recognition, material identification and data splitting (e.g., into calibration and validation datasets). DoE was developed to find the optimal data pre-processing techniques (represented by Block B in Figure 8.4 and 9.5). Using the pre-processed data, a series of calibration and prediction models were developed (indicated by Block C in Figure 8.4). All prediction models were validated using independent datasets. The aforementioned approach was independently applied to three datasets, namely the full FTIR spectra, MWIR and LWIR. Therefore, the use of these three datasets for the discrimination of the test case materials was evaluated (Block D in Figure 8.4). The details of each step are described below.

8.3.1. DATA EXPLORATION

8.3.1.1. UNSUPERVISED CLASSIFICATION

To identify a pattern and points of interest in the spectral data, descriptive statistics, cluster analysis and PCA were performed. Descriptive statistics, including box plots and histograms, were used to describe the basic data features. The unsupervised classification technique was applied to assess any natural patterns or groupings in the FTIR data. One of the highly efficient and the most commonly used unsupervised classification methods is K-means. Thus, K-means with Euclidian distance was applied to examine any clustering in the spectral data.

Using the full-range FTIR reflectance data and the K-means technique, the spectral data were classified into two classes. The unsupervised classification was implemented with no a priori knowledge about potential mineral groupings. However, the number of clusters was specified in advance and two distinct classes were distinguished. The geochemical difference between the two classes was investigated using validation data (XRF, ICP-MS and XRD). The two classes exhibited variations in elemental concentrations of Cu, Zn, Pb, As and Fe.

Thus, the class with a higher concentration of these elements was identified as ore, whereas the class with a lower concentration was considered as waste. In addition, the unsupervised classification results were compared with the hand specimen classification into the ore and waste classes. The comparison results revealed a very good agreement, confirming that the unsupervised classification method can be a practical alternative to a hand specimen description for ore–waste discrimination, as the former can be automated and the latter might be subjective. Subsequently, a category variable that indicates samples belonging to ore or waste classes was appended to the full FTIR data table. Once the category variable was added to the FTIR spectral data, three datasets (the full FTIR, MWIR and LWIR) were prepared.

8.3.1.2. PCA MODELS

In the present study, PCA models were developed using the three aforementioned datasets separately. The potential for using each dataset for separation of the two classes was assessed and compared. The loading plots of the PCA models were interpreted to identify the important (informative) variables.

8.3.1.3. OUTLIER DETECTION AND DATA SPLITTING

The outlier detection techniques considered in this study are Hotelling's T^2 , residual map, influence plot and visual inspection of unique measurements. Using the Hotelling's T^2 technique, a critical limit (p -value) of 5% with 95% confidence limits was used to reveal potential outliers. The observed possible outliers were labelled, and the influence plots and residual map were inspected. The potential outliers identified using the Hotelling's T^2 , influence plot and residual map were visually inspected and compared. Based on the integrated findings yielded by these inspections, fifteen measurements that are possible outliers were identified and were excluded from the datasets. Subsequently, each of the three datasets was split into calibration and validation sets, ensuring approximately equal representation of each class within the two datasets (Block A of Figure 8.4). To avoid introducing systematic errors, the datasets were split randomly, whereby measurements from the same samples were assigned to either validation or calibration dataset, but not both. The calibration and validation sets included 466 and 124 measurements, respectively.

8.3.2. DATA PRE-PROCESSING

As shown in Figure 8.5, baseline correction, SNV, MSC, smoothing (such as Gaussian filter smoothing), normalization and data scaling were the pre-processing methods considered for this study. The upper box of Fig 6. (labelled 1) shows the independent pre-processing techniques and the lower box (labelled 2) shows the combined pre-processing techniques. The choice of these methods was based on the fact that they are the most common artefacts of infrared data (e.g., baseline shift). In addition, the most prominent data artefacts (e.g., baseline, scatter and noise) were identified from the line plots of the reflectance spectra. With the exception of raw data, mean centering was performed in combination with each independent and combined techniques. The selected pre-processing methods were employed to develop a DoE that incorporates both independent and combined pre-processing techniques. The DoE was applied to the three datasets individually and sets of pre-processed data were generated.

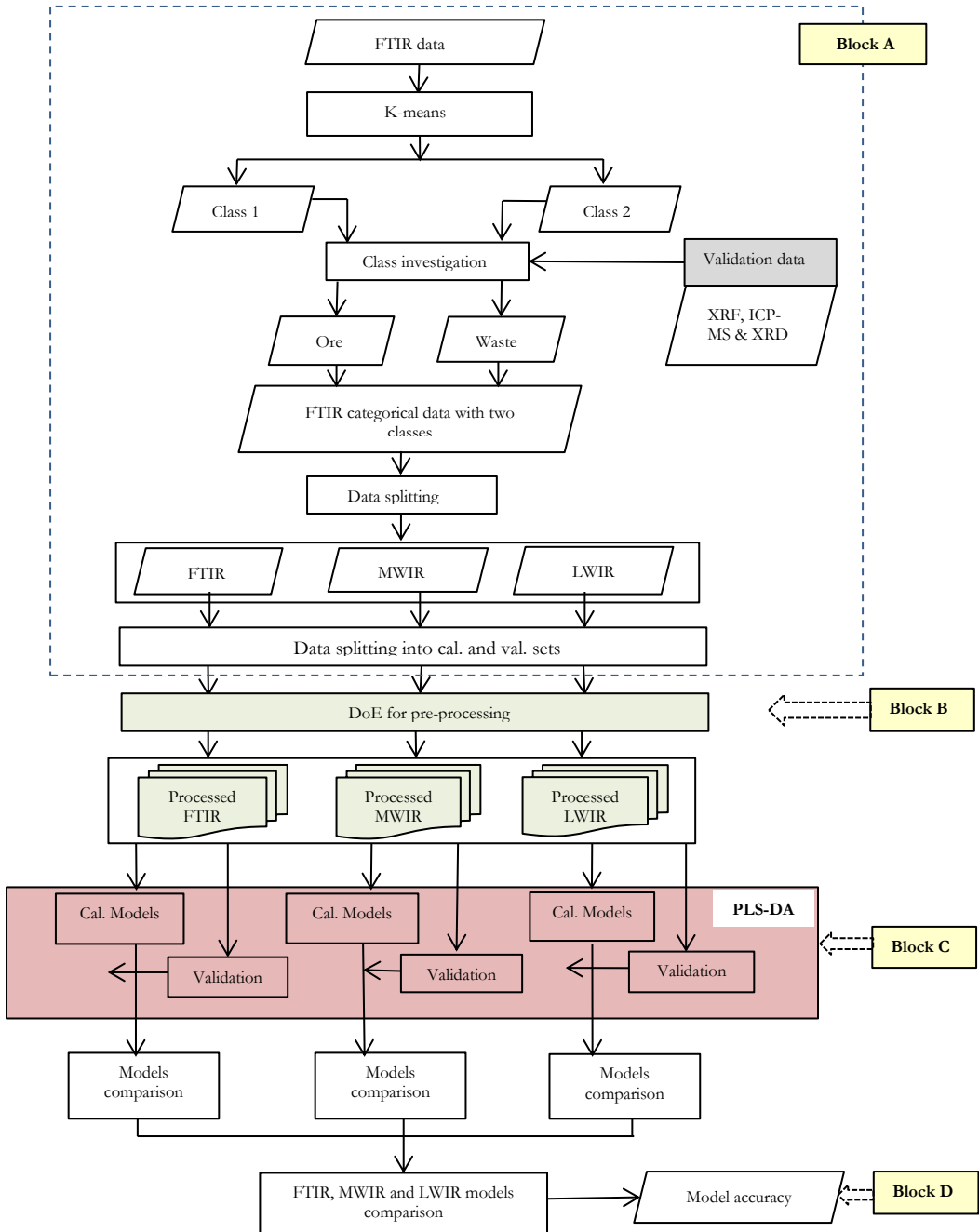


Figure 8.4: Overview of the research workflow. It includes four major steps: data exploration and preparation (Block A), data pre-processing (Block B), data modelling and model validation using independent datasets (Block C) and model comparison (Block D).

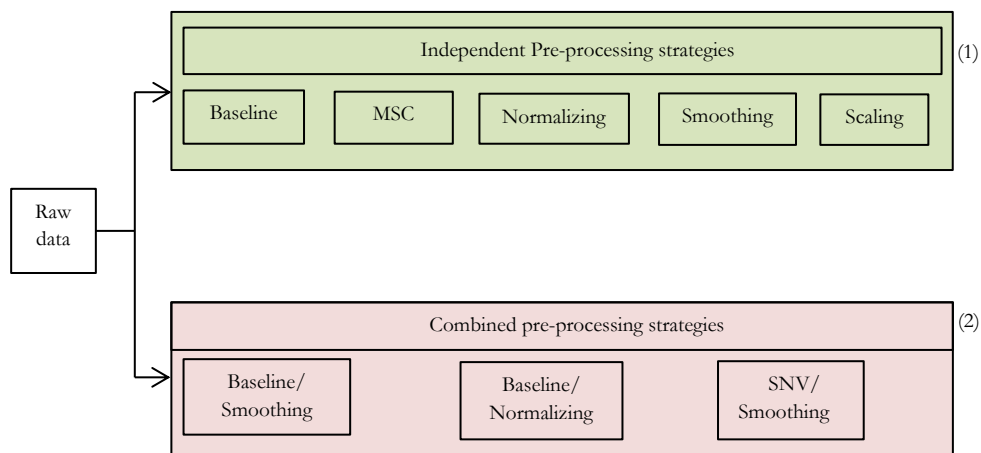


Figure 8.5: The independent (Box 1) and combined (Box 2) pre-processing methods that were applied to the spectral data of the full FTIR, MWIR and LWIR datasets.

8.3.3. DATA MODELLING AND VALIDATION

In the present study, to establish a discrimination rule of the two classes (ore and waste materials), PLS-DA classification models were developed using the pre-processed data of the three datasets. PLS-DA was implemented in two steps, whereby PLS regression was followed by prediction. In PLS regression, the categorical data (in this case, the ore and waste classes) as treated as a response variable and the spectral data at each wavelength is represented as the independent variables. As shown in Block C of Figure 8.4, the pre-processed calibration data were used to develop a series of calibration models that were applicable to each of the two classes (ore and waste). The prediction model parameters were estimated using the calibration datasets and were subsequently validated using the independent (validation) datasets.

The performance of the calibration and prediction models when applied to the same dataset (e.g., MWIR data) after incorporating each of the previously described data filtering techniques was evaluated. The optimal data pre-processing methods were selected based on the calibration, validation and prediction statistics of the classification and prediction models, whereby lower error terms and higher predicted R^2 value were deemed advantageous. In addition, confusion matrices were generated to assess the correct classification rates of individual models. The correct classification rates were computed by adding the number of true positives and true negatives and dividing their sum by the total number of the predicted samples. This approach was applied to the full FTIR, MWIR and LWIR datasets, and the material discrimination competencies of the three datasets were also assessed and compared.

8.4. RESULTS AND DISCUSSION

8.4.1 EXPLANATORY DATA ANALYSIS

8.4.1.1. K-MEANS

Application of the K-means method resulted into two separate classes indicating a natural pattern or grouping in the reflectance spectral data. The observed natural groupings are based on the correlation or similarity among the measured variables (spectral data). The obtained results were reproducible for the same clustering method. To elucidate any patterns in the spectral data, ascertaining the composition of the two classes (mineral groupings) is essential. Therefore, the geochemical compositional differences between the two classes were investigated using the validation data (obtained through XRF, ICP-MS and XRD measurements). As summarised in Table 8.1, the two classes differ in elemental concentration of Cu, Zn, Pb and Fe, all of which are of interest for the present study due to their economic value. In addition, they also differed with respect to As, which is also of interest, since it is a penalty element in mineral processing. Thus, its early identification would be highly beneficial for optimising product quality and eliminating risks, yielding saleable mineable material. In the material sampled from the study area for the test case, the primary sources of these elements are the sulphide ore minerals (chalcopyrite, pyrite, arsenopyrite, galena and sphalerite). Therefore, a higher/lower concentration of the elements signifies that the material is an ore/waste.

The class threshold value of each element concentration was set based on the value sequence observed in the classes and a relatively large change in elemental concentration. For example, the Cu content of 94% in the samples classified as Class 1 indicates greater than 250 ppm, as shown in Table 8.1. On the other hand, the Cu content of 93% in Class 2 samples indicates less than 250 ppm. Similarly, the Fe concentration of 89% in the samples categorized in Class 1 signifies greater than 60,000 ppm (6%), otherwise they are categorized as Class 2. Even though Fe has many mineral sources (e.g., sulphides, oxides and silicates), for the test case materials, Fe shows moderate to strong correlation with sulphide minerals, indicating that the main Fe sources are likely the sulphide minerals. Likewise, the Zn, Pb and As concentrations are higher in Class 1 than in Class 2 (Table 8.1). Therefore, based on the elemental concentration difference, Class 1 is denoted as ore, while Class 2 represents waste. In addition, the ICP-MS and XRF measurement data were used to compute the correlation coefficients of the elemental dependencies. As shown in Table 8.2, there is a moderate positive relationship between Cu and Zn, Cu and Pb, and Pb and Zn. Moreover, while Zn-As correlation is strong, no Pb-As correlation was observed in the data. The acquired correlation coefficients (except for a few exceptions) indicate that the elements co-occur. Therefore, a higher concentration of target elements is observed in one class than in the other.

Table 8.1: Summary of the XRF and ICP-MS data showing concentrations of the indicated elements above and below the specified threshold value of the two classes. The % shows the proportion of samples in a given class below or above the specified threshold.

Class	Cu		Pb		Zn		As		Fe	
	Above	Below	Above	Below	Above	Below	Above	Below	Above	Below
	250 ppm	250 ppm	10,000 ppm	10,000 ppm	10,000 ppm	10,000 ppm	1,000 ppm	1,000 ppm	60,000 ppm	60,000 ppm
Class 1	94%	6%	94%	6%	97%	3%	89%	11%	89%	11%
Class 2	7%	93%	22%	78%	6%	94%	0%	100%	0%	100%
Minimum value	274 ppm	28 ppm	10,082 ppm	245 ppm	12,215 ppm	159 ppm	1,033 ppm	57 ppm	61,400 ppm	22,500 ppm
Maximum value	90,142 ppm	235 ppm	208,000 ppm	7,014 ppm	96,400 ppm	7,474 ppm	22,049 ppm	792 ppm	313,900 ppm	59,600 ppm

Elemental concentration varied across samples, as shown in Table 8.1, where the minimum and maximum content of the indicated elements is given for both classes. The qualitative XRD measurement results show that most of the minerals assigned to the two classes are the same. This is likely due to the fact that, even though their concentration varies, these minerals occur in both classes. This assertion is also supported by the XRD measurement semi-quantification results, indicating that a higher concentration of the sulphide minerals (ore minerals) was observed in Class 1 than in Class 2. It is highly likely that the acquired reflectance spectra are mixed spectra that are influenced by combined mineral signals or matrix effects. This is one of the possible reasons for not assigning 100% of the samples into one of the classes. However, with the indicated level of confidence (the % of samples in a class), samples containing the elements in quantities that are above or below the indicated value can be categorized into the two classes. Separation of the two classes based on the elemental concentration signifies presence of a signal in the spectral data that can be linked to mineralogy and hence to economic value.

Table 8.2: Elemental correlation coefficient computed using 50 samples.

Element pairs	Correlation coefficient
Cu–Zn	0.55
Cu–Pb	0.43
Pb–Zn	0.48
Mg–As	-0.01
Ca–As	0.17
Pb–As	-0.06
Cu–As	0.11
Zn–As	0.69

The cut-off grade of a commodity is a variable that changes due to fluctuations in metal prices and mining costs. Compared to the typical current mining cut-off grades, the materials from the test case contain lower concentrations of the target elements. For example, the typical average cut-off grade for Cu in underground mining operations is above 5,000 ppm (0.5%) (Calvo et al., 2016; Lundin mining, 2018). However Cu content exceeded 5,000 ppm (0.5%) in only two of the measured samples. Similarly, while the average cut-off grade for

Zn in underground mining operations is above 5.5% (Canadian Zinc Corporation, 2018; Lundin mining, 2018), in 85% of the measured samples Zn content was below this value. Therefore, for the test case materials, the cut-off grade based on the current underground mining operations cannot directly be used to generically classify the ore and the waste materials. However, even when using sampled material containing elements of economic interest in low concentrations, discrimination of materials into two mineral groupings (ore and waste) was still achieved. This experimental classification result is consistent with the manual specimen classification into ore and waste. However, to avoid subjective sample classification and automate the process, application of the K-means technique was considered. Therefore, for the present study, the Cu, Zn, Pb, Fe and As concentration in the class specified as ore (waste) is above (below) the threshold value indicated in Table 8.1.

8.4.1.2. PCA MODELS

Figure 8.6 shows the PCA model score plots of the full FTIR, LWIR and MWIR datasets. A score plot provides valuable visual information on potential patterns in the samples. It depicts the relationship between sample differences or similarities and the data structure. As shown in Figure 8.6 (a) to (c), when the models are applied to the full FTIR dataset, the two classes are better distinguished than when the individual LWIR and MWIR datasets are used, most likely because the full FTIR incorporates more informative variables that can accommodate variations in the data. The PCA models were applied to transform the spectral data of the three datasets into PCs. The loading plots of the PCs were subsequently interpreted to identify the important or informative variables.

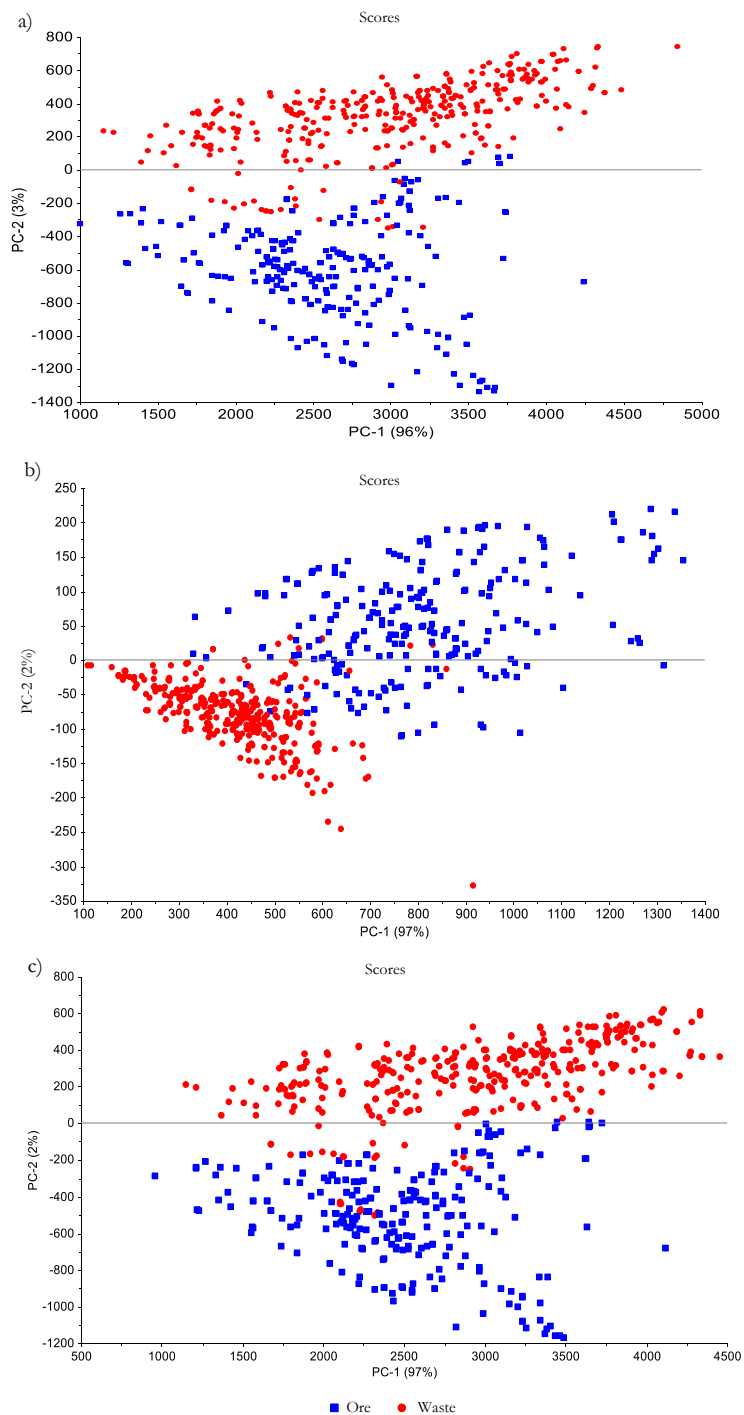


Figure 8.6: PCA models computed using raw (a) full FTIR data, (b) LWIR data, and (c) MWIR data. The three datasets can be separated into two classes.

Figure 8.7 shows the loading plot of the full-range FTIR, revealing that large loading coefficients or most variations are observed at different wavelength locations denoted by orange rectangles, such as at 2.5 to 2.6 μm , 3.3 to 3.8 μm , 7 μm , 7.5 to 7.9 μm , 8.8 to 9 μm , 10.0 μm and 10.7 μm (note that, for the purpose of clarity, not all informative variables are indicated on the plots). As such variations are highly informative, they indicate that these variables are responsible for the separation of the two classes. When the wavelength locations of the informative variables are compared with the data contained in spectral libraries (NASA, 2017), it is evident that most of the sulphide minerals show higher reflection at the identified wavelength locations. Thus, it is likely that the class separation is based on reflection signals from the sulphide minerals. For example, relatively higher reflection of galena is around 3.5 μm (NASA, 2017). These 3.3 to 3.8 μm wavelengths are identified as important variables for class separation.

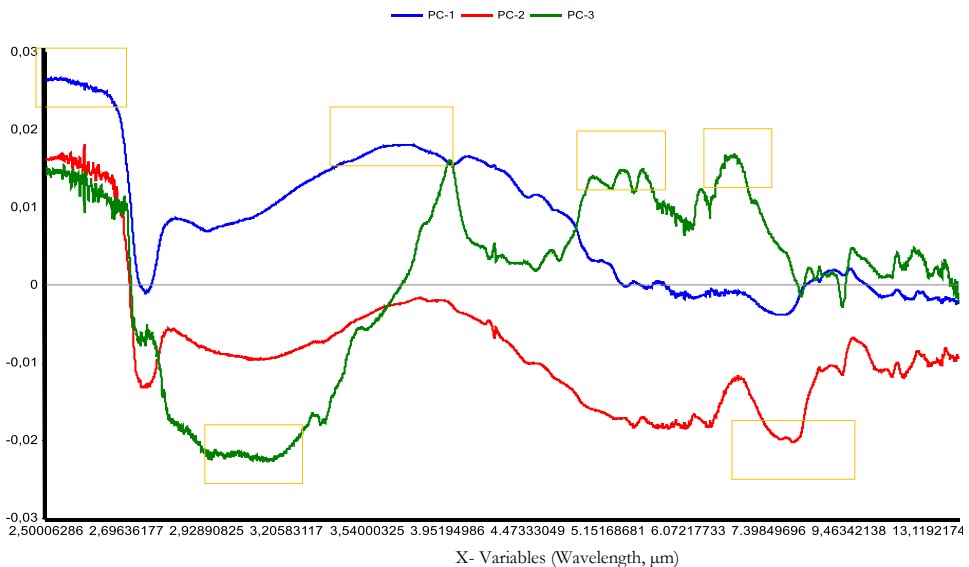


Figure 8.7: The loading plot of the first three PCs of the full FTIR dataset.

8.4.1.3. DETECTION OF OUTLIERS

Outliers can be unique sample measurement results or noise, or might arise due to measurement errors. As mentioned in Sect. 3.1, in the present study, outliers were detected using an integrated inspection of Hotelling's T^2 , residual map, influence plot and visual inspection. Figure 8.8 shows the possible outliers that were excluded using Hotelling's T^2 and influence plots. Measurements located outside the Hotelling's T^2 ellipse are potential outliers. The top right quadrant of the influence plot shows samples with higher leverage and higher residual, which are denoted as dangerous samples (as they are most likely outliers, as previously discussed). Samples in the lower right quadrant of the influence plot are influential, whereas those in the top left quadrant are poorly described by the model. Therefore, all samples in these two quadrants were carefully assessed using the Hotelling's T^2 and residual map to identify those that are potential outliers (i.e., samples that are poorly described by the developed models). Therefore, to ensure proper variable description,

fifteen measurements that are possible outliers were identified and excluded from the datasets.

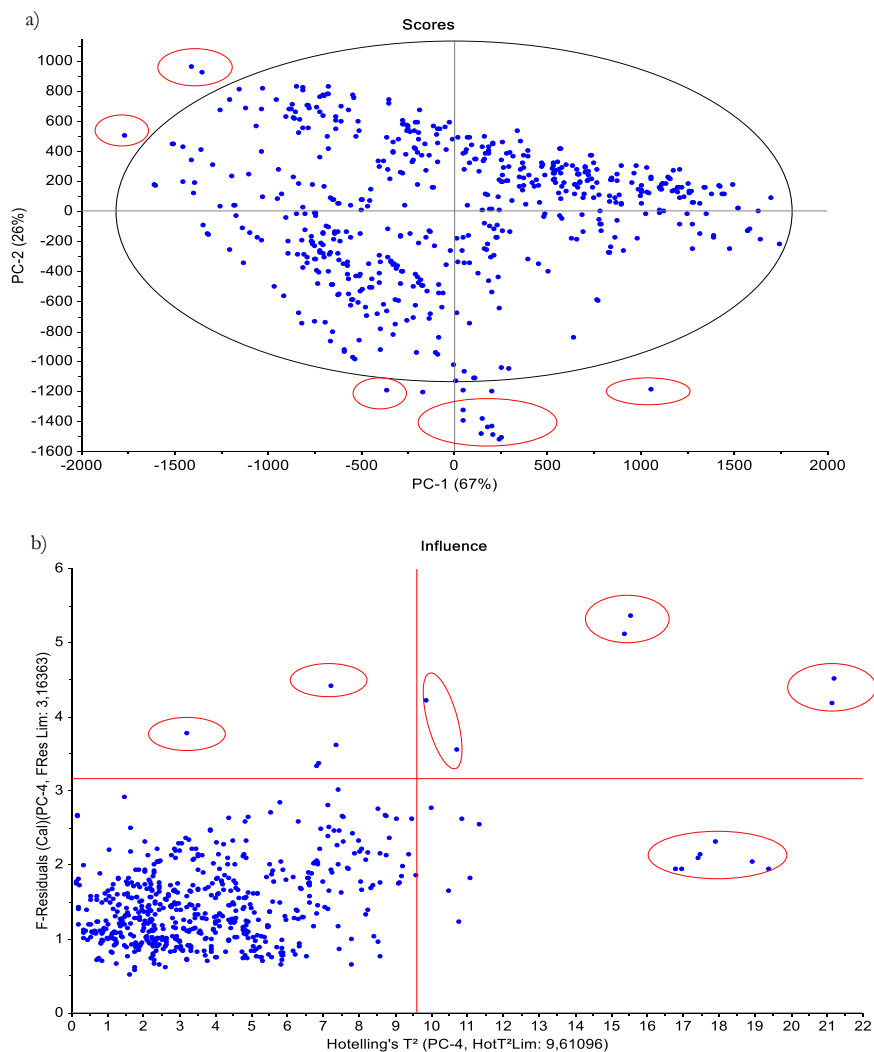


Figure 8.8: (a) A score plot with Hotelling's T² limit (α -value of 5%) (b) Influence plot with Hotelling's T² on the x-axis and F-residuals on the y-axis. Samples within red circles are potential outliers that were excluded from the datasets.

8.4.2. DATA PRE-PROCESSING AND MODELLING

Figure 8.9 (a) and 10(b) show the score plots of the PLS models of the LWIR and the full FTIR dataset, respectively, after application of the previously described data filtering techniques. The first two latent variables (Factor 1 and Factor 2) of the PLS regression explain most of the variations in the data. For example, 94% of the variation in the LWIR data is explained by the first two factors. Moreover, the first two factors explain 94% and

73% of the variation in the spectra and the class category, respectively. This finding indicates presence of an unstructured variation in the spectral data that is not related to the class category. The difference in the variation is likely due to other mineralogical information that has not been considered in the classification process. For example, sub-clustering was observed within the ore class, which could potentially be attributed to the different mineral groups that occur within the ore. Therefore, there is a high potential for further discrimination of the materials into additional classes.

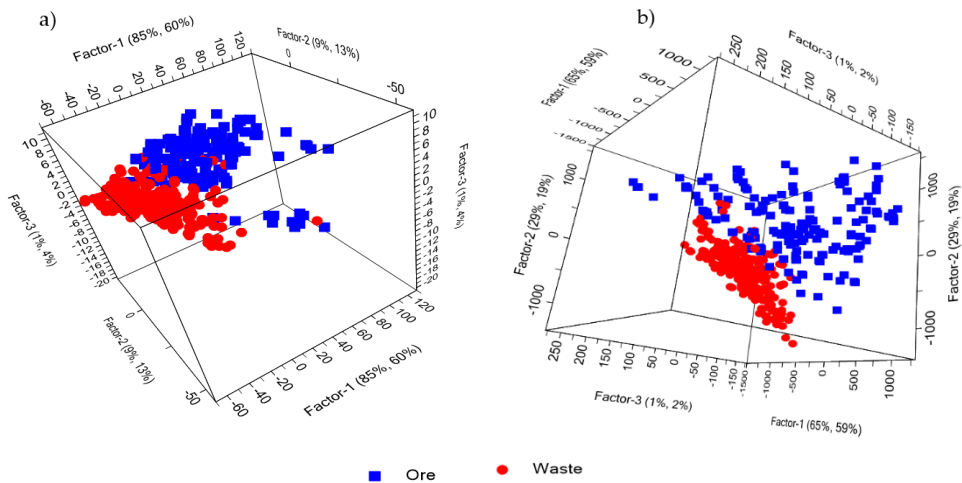


Figure 8.9: Score plots of PLS models after data smoothing (Gaussian filter) is applied to (a) the LWIR and (b) the full FTIR dataset.

Table 8.3 shows the correct classification rates of models applied to the three datasets, after each dataset has been subjected to individual data pre-processing techniques. It is evident that an enhanced prediction was obtained by applying the data pre-processing techniques to all three datasets. For example, for the full FTIR raw data, a correct classification rate of 83.1% was obtained. However the correct classification rate increased to 89.5% after the FTIR dataset was treated with the SNV data filtering technique. Conversely, not all data filtering techniques necessarily improved model performance. For example, the MSC filtering technique did not improve the model performance when applied to the MWIR data, most likely because the multiplicative effect is not pronounced in the spectral data. For the given datasets, combining the pre-processing techniques did not result in a better prediction than that obtained when these techniques were applied individually. Therefore, the results are not reported in this study. Moreover, the pre-processing technique that was most optimal differed for the three datasets. For example, when applied to the MWIR data, model performance improved (86.3% correct classification rate) after baseline correction (Table 8.3). On the other hand, the best results were achieved when the LWIR data were subjected to SNV (84.7% correct classification rate). This finding implies that, in the LWIR dataset, the undesired intensity variation was more pronounced than in the MWIR data. These results also concur with the empirical evidence indicating that the choice of most optimal pre-processing technique is data dependent and requires a trial and error

approach (Engel et al. 2013). Therefore, DoE is a crucial step in determining the most optimal data filtering technique.

Comparing the three datasets, the full FTIR data resulted in better prediction performance than the MWIR and LWIR data alone (Table 8.3), likely because the former covers a wider wavelength region. Thus, the full FTIR dataset includes more informative variables to adequately explain the variation in the reflectance spectra than the individual MWIR or LWIR data. Overall, the three datasets showed a good potential for discrimination of the test case materials into ore and waste. Moreover, after baseline correction, SNV and normalization, the correct classification rates were higher when the MWIR, rather than the LWIR dataset, was utilised (Table 8.3). This is an interesting finding, since MWIR is the least explored infrared region in lithological material characterisation. Overall, the maximum correct classification rates achieved for the full FTIR, MWIR and LWIR datasets after data filtering were 89.5%, 86.3% and 84.7%, respectively. Owing to the limited information level in the infrared spectra of the sulphide minerals and the intermediate values that obscure clear class boundaries (and thus bias model performance), the obtained accuracies are sufficient to discriminate the materials into ore and waste.

Table 8.3: Summary of the correct classification (ore–waste discrimination) rates when different models are applied to the full FTIR, MWIR and LWIR datasets.

Model	FTIR	MWIR	LWIR
Raw	83.1%	75.8%	79.8%
Normalised	87.1%	85.5%	84.7%
Baseline	83.9%	86.3%	79.8%
SNV	89.5%	85.5%	84.7%
Gaussian	86.3%	79.0%	80.6%

Figure 8.10 shows representative spectra of ore and waste material samples. Using spectral libraries (NASA, 2017) and evidence reported by other authors (Ji et al., 2009; Schodlok et al., 2016), different minerals—including dolomite, muscovite, quartz and calcite—were identified. The sulphide minerals exhibit very weak spectral features in the infrared reflectance data that a direct interpretation of target minerals spectra is challenging. However, they have a higher and lower reflection points at different wavelengths. Hence, this sulphide minerals property can be transformed into valuable information using the approach proposed in this study.

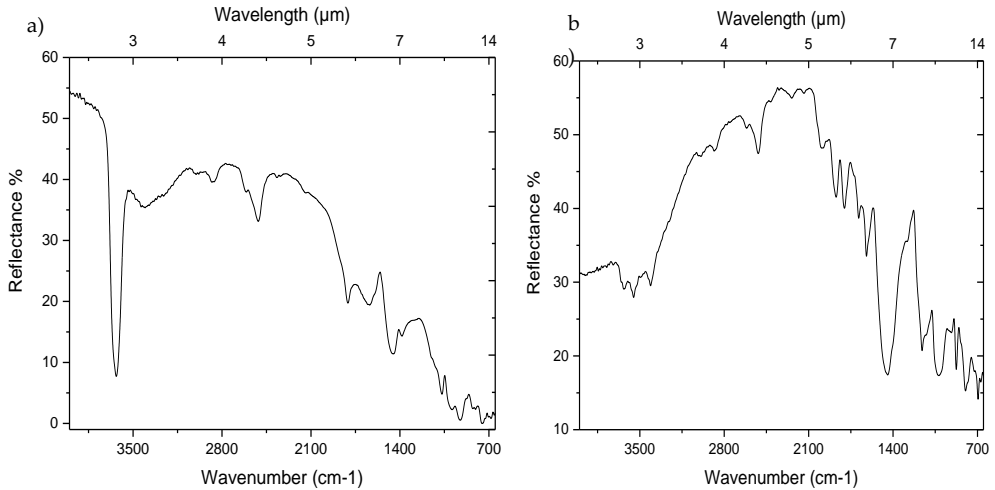


Figure 8.10: Representative spectra of the two classes denoting (a) waste material (b) ore material.

8.4.3. POTENTIAL APPLICATION FOR IN-SITU AND REAL-TIME MATERIAL CHARACTERISATION

In-situ real-time material characterisation requires both appropriate instrument design and software development. The current technological advancements have enabled design and implementation of portable instrumentation, making in-situ spectroscopy possible. However, for underground mining applications, care must be taken to avoid or minimise the effect of moisture and dust. With respect to software design, the findings reported in this work demonstrated the potential of using a FTIR spectrometer for distinguishing ore from waste, which is of particular relevance for marginally economical mining operations. A prediction model was developed to classify unknown spectra into ore and waste classes. The acquired results are promising and can be improved by the inclusion of additional samples into the calibration models. Thus, a test case-specific mineral library can be developed for automated online discrimination of ore–waste materials.

The present study was carried out using powdered homogenized samples. However, the approach can be extended for whole rock applications by developing customized sampling strategies to account for inherent material variability and heterogeneity. The ongoing depletion of mineral resources, accompanied by increasing societal demand, suggests that it is likely that increasingly lower-grade ores will be extracted in future mining operations. The work presented here has demonstrated the potential of utilizing the MWIR and LWIR data for ore–waste discrimination, which could assist in greater selectivity during extraction and pre-processing, thus maximising use of the resources while increasing economic viability.

8.5. CONCLUSIONS

Infrared spectra collected using an FTIR spectrometer were analysed and classified using chemometric analytical methods. The utility of the obtained results for the characterisation of sulphide ore and waste minerals from the selected test site was investigated. Three datasets spanning different wavelength ranges were prepared, namely the full FTIR spectra, as well as MWIR and LWIR spectra. Without a priori knowledge of

the material types, the well-known K-means method was implemented to separate the datasets into two classes, whereby two distinct classes were identified. The mineralogical composition of the two classes was investigated using the conventional XRF, ICP-MS and XRD measurement techniques. The two classes exhibited differences in the elemental concentrations of Cu, Pb, Zn, As and Fe, and were thus defined as ore and waste. The identified categorical variables (the two classes) were inserted into the spectral data of the three datasets.

DoE was implemented to identify the optimal independent and combined data-filtering techniques for discriminating the two classes using the three aforementioned datasets. The processed data were used to make predictions about the composition of unknown samples. A series of prediction models were developed using the processed data combined with PLS-DA. Model performance was evaluated using the calibration, validation and prediction statistics in the form of an estimated prediction error. In addition, the correct classification rate was calculated for each model. The same procedure was applied for the three (FTIR, MWIR and LWIR) datasets. In general, the results showed a good agreement in model performance when applied on the three datasets. However, when the full-wavelength FTIR dataset was employed, lower prediction errors and higher correct classification rates were obtained compared to those pertaining to the MWIR or LWIR data.

Even though not all data pre-processing techniques necessary improved model performance, baseline correction, normalization and smoothing improved the classification and prediction performance of the developed models. For example, when the models were applied to the full-range FTIR dataset, 89.5% correct classification rate was achieved after subjecting the data to the SNV technique. When models were applied to the MWIR dataset, the prediction improved to 86.3% after baseline correction. Finally, after normalization of the LWIR data, an enhanced correct classification rate of 84.7% was obtained. The MWIR data alone provides sufficient information to successfully classify the samples into ore and waste. Thus, it can be posited that this region offers great potential for rock and mineral characterisation. In this work, FTIR spectroscopy was successfully used to discriminate the ore and waste materials of the test case. For future research in this field, FTIR should be combined with PLS-DA to explore the potential for rapid automated online discrimination of ore and waste material. In sum, with accurate model calibration, the material discrimination process can be automated.

REFERENCES

- Agilent. (2017) FTIR Compact & Portable Systems [Online]. Available: <http://www.agilent.com/en/products/ftir/ftir-compact-portable-systems/4300-handheld-ftir> [Accessed February 2017].
- Bamber, A. S., Klein, B., Morin, M. & Scoble, M. J. (2004). Reducing selectivity in narrow vein mining through the integration of underground pre-concentration. Proceedings of the IV International Symposium on Narrow Vein Mining Techniques, Val d'Or, Canada.
- Batterham, R. B. & Fleming, R. (2006). Sustainability and Mineral Processing. Proceedings of the XXIII International Mineral Processing Congress, Istanbul, Turkey.
- Calvo, G., Mudd, G., Valero, A. & Valero, A. (2016). Decreasing ore grades in global metallic mining: A theoretical issue or a global reality? *Resources*, 5(4), 36. doi: 10.3390/resources5040036

- Canadian Zinc Corporation. (2018). Mineral resources and reserves [Online]. Available: <http://www.canadianzinc.com/projects/prairie-creek/resources> [Accessed March 2018].
- Chemistry libretexts. (2017). How an FTIR Spectrometer Operates [Online]. Available: https://chem.libretexts.org/Core/Physical_and_Theoretical_Chemistry/Spectroscopy/Vibrational_Spectroscopy/Infrared_Spectroscopy [Accessed February 2017].
- Duffy, K. A., Valery, W., Jankovic, A. & Holtham, P. (2015). Integrating Bulk Ore Sorting into a Mining Operation to Maximise Profitability. Proceedings of the MetPlant, Perth, Australia, pp. 273-287.
- Ismail, A. A., van de Voort, F. R. & Sedman, J. (1997). Chapter 4 - Fourier transform infrared spectroscopy: Principles and applications. In: J. R. J. Paré & J. M. R. Bélanger (Eds.), Techniques and Instrumentation in Analytical Chemistry. Elsevier, pp. 93-139.
- Ji, J., Ge, Y., Balsam, W. & Chen, J. (2009). Rapid identification of dolomite using a Fourier Transform Infrared Spectrophotometer (FTIR): A fast method for identifying Heinrich events in IODP Site U1308. *Marine Geology*, 258(1), pp. 60-68. doi: 10.1016/j.margeo.2008.11.007
- Lundin mining. (2018). Reserves and Resources [Online]. Available: <https://www.lundinmining.com/operations/overview> [Accessed March 2018].
- NASA. (2017). ECOSTRESS spectral library [Online]. Available: <https://speclib.jpl.nasa.gov/library> [Accessed September 2017].
- Perkins, W. D. (1987). Fourier transform infrared spectroscopy. Part II. Advantages of FT-IR. *Journal of Chemical Education*, 64(11), A269. doi: 10.1021/ed064pA269
- Robben, C. & Wotruba, H. (2019). Sensor-Based Ore Sorting Technology in Mining—Past, Present and Future. *Minerals*, 9, 523. doi: 10.3390/min9090523
- Schodlok, M. C., Green, A. & Huntington, J. (2016). A reference library of thermal infrared mineral reflectance spectra for the HyLogger-3 drill core logging system. *Australian Journal of Earth Sciences*, 63(8), pp. 941-949. doi: 10.1080/08120099.2016.1234508
- Smith, B. C. (2011). Chapter 1 - Fundamentals of Fourier Transform Infrared Spectroscopy. In: B. C. Smith (Ed.), *Introduction to infrared spectroscopy*, 2nd ed., CRC Press: New York, USA, pp. 1-17.
- Stuart, B. H. (2004). *Infrared spectroscopy: fundamentals and applications*. John Wiley & Sons, Ltd. Chichester, England.
- STEINERT. (2020). Ore sorting [Online]. Available: <https://steinertglobal.com/mining> [Accessed March 2020].
- TOMRA. (2020). Benefits of sensor based sorting [Online]. Available: <https://www.tomra.com/en/sorting/mining> [Accessed March 2020].
- Wotruba, H. (2006). Sensor Sorting Technology-is the minerals industry missing a chance? Proceedings of the XXIII International Mineral, Processing Congress, Istanbul, Turkey, pp. 21-29.

9

RAMAN SPECTROSCOPY FOR THE CHARACTERISATION OF A POLYMETALLIC SULPHIDE DEPOSIT

This chapter demonstrates the usability of Raman spectroscopy for the characterisation of material in a polymetallic sulphide deposit using channel and muck pile samples collected from the defined block in the test case. Two Raman systems with 532 nm and 785 nm excitation laser sources were compared. The chapter also discusses the opportunities and limitation of the technique in material characterisation.

Parts of this chapter have been published in:

Destá, F.S. & Buxton, M. W. N. (2019). Evaluation of Sensor Technologies for On-line Raw Material Characterisation in "Reiche Zeche" Underground Mine - outcomes of RTM implementation. Proceedings of the Real Time Mining - 2nd International Raw Materials Extraction Innovation Conference, Freiberg, Germany, pp. 32-48.

9.1. INTRODUCTION

Accurate mineralogical information is crucial along the mining value chain from exploration and extraction, to mineral processing and environmental management after mine closure. It is beneficial to understand geological processes (e.g., hydrothermal alteration), optimise extraction (e.g., blasting) and understand the geometallurgical properties of a deposit. Thus, it has a substantial significance for the efficiency of a mining process. Various advanced laboratory-based and portable sensor technologies that provide mineralogical information are available, such as XRD, SWIR, and LWIR. However, most of these techniques might not offer a comprehensive description of some deposit types. Consequently, Raman technology can be considered as a complementary or in some cases, a substitutionary technique for the detection of Raman active minerals through vibrations of the mineral bonds. Raman is a well-established, non-destructive technique that provides mineralogical information. The method can be used to fingerprint each detected mineral. Raman is often used to complement infrared spectroscopy. However, in some applications, Raman may be preferred over other vibrational spectroscopies because it is less affected by water — i.e., water is a weak Raman scatterer (Li et al., 2014). Besides, some minerals that do not exhibit spectral features in infrared could produce Raman signals (e.g., some of the sulphide minerals). The working principle and the current state-of-the-art of the technique are discussed in Chapter 3.

The intensity of the Raman signal depends on the specific bond of a molecule and the excitation laser wavelength. However, the Raman signal is fundamentally very weak in nature. Laser-induced fluorescence is the most common source of noise in Raman measurements. The fluorescence interference in the spectra may result from the analysed material or fluorescent impurities in the sample. It occurs when the electron in a molecule returns from an excited state to a ground state (Gaft et al., 2005). This entails the emission of a photon as fluorescence. The detection of the Raman signals of highly fluorescent compounds might be challenging due to the intense fluorescence signal. Therefore, the characterisation of material using Raman requires mechanisms to minimise this effect and increase the signal-to-noise ratio of a spectrum. One possible strategy to reduce the effect of fluorescence is to select a suitable laser excitation wavelength. The low-energy (longer-wavelength) laser sources can minimise the strong fluorescence; on the other hand, high-energy (shorter-wavelength) laser sources can produce a more vigorous Raman signal intensity. Thus, the Raman intensity is not solely based on the molecular characteristics of materials but also strongly depend on the choice of the excitation laser source (Chryssikos and Gates, 2017). Consequently, different laser wavelengths ranging from ultra-violet through visible to near-infrared are utilised in Raman spectroscopy.

Raman technique can be used for the identification, quantification, and classification of minerals. It can be applied for the analysis of a wide range of minerals such as iron ore oxides, rock-forming minerals, carbonates, silicate, sulphides and sulphate (Haskin et al., 1997; Gaft et al., 2005; Griffith., 1975; White., 1975; Mernagh and Trudu, 1993). Numerous studies show the usability of the technique for the characterisation of materials in different deposit types. For example, Pani et al., (2016) compared XRD, Raman and infrared systems for the analysis of minerals in manganese oxide ore. The results demonstrate the Raman as a complementary technique. Likewise, Escarate et al. (2010) showed the use of Raman for a quantitative indication of calcite in copper ore. Similarly, Ho et al., (2015) used Raman coupled with multivariate analysis techniques for the classification of uranium ore concentrates. In another study, Uusitalo et al., (2020) applied Raman for the identification

and indication of valuable mineral levels of sulphide minerals during froth flotation. Various studies show the greater applicability of the technique in material characterisation. However, the usability of the method is highly dependent on the deposit type, the form of material and the choice of the excitation laser source that Raman measurements require an optimised approach.

In view of the preceding discussions, the objective of this study was to assess the usability of two Raman spectrometers with 532 nm and 785 nm excitation laser sources for the identification and classification of minerals in a polymetallic sulphide deposit. The collected Raman spectra were pre-processed and interpreted. In addition, classification models were developed to evaluate the relevant information in the Raman signals that can be related to the characterisation of sulphide minerals.

9.2. METHODS

As illustrated in Figure 9.1, the assessment of the usability of the Raman technique for the characterisation of polymetallic sulphide ore involves multiple steps that incorporates data-pre-processing, minerals identification, and classification. Two Raman spectrometers with 532 and 785 nm excitation laser sources were compared using samples in the form of rock, pellet and powder. Minerals were interpreted using comprehensive mineral spectral libraries and published works. The Raman signals, coupled with supervised and unsupervised classification techniques, were assessed for the separation of ore and waste materials (Figure 9.1). The details of each step are described below.

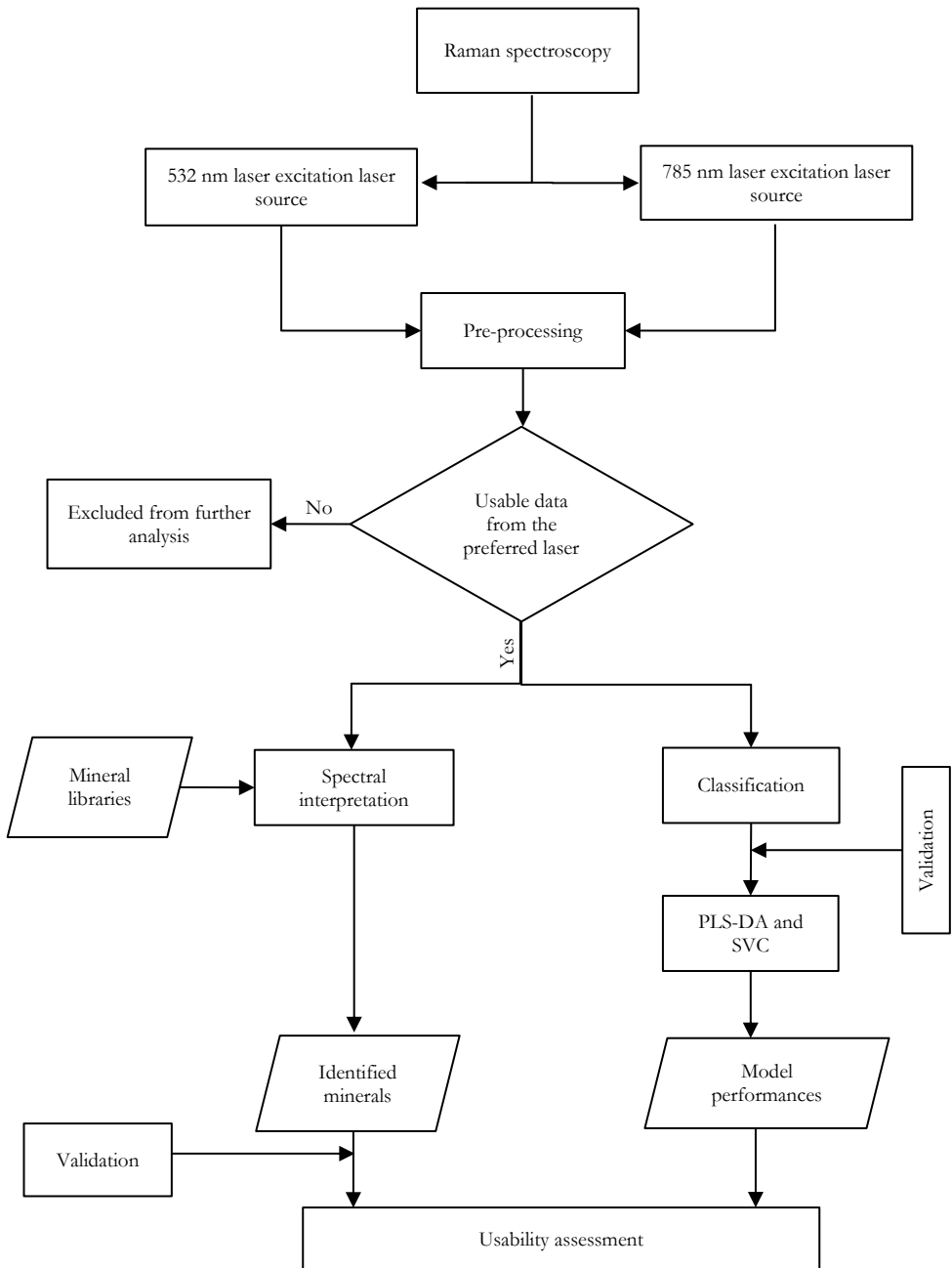


Figure 9.1: The general workflow depicting the different steps.

9.2.1. MATERIALS AND EXPERIMENTAL SETUP

A commercially available hand-held Raman instrument (IRIS echelle spectrometer) and laboratory-based Raman spectrometer (Bruker Senterra Raman Microscope) were used to analyse 40 samples from the polymetallic sulphide deposit. Studies indicate that Raman measurements are dependent on grain size and samples degree of compaction (Chen et al., 2012; Pellow-Jarman et al., 1996; Wang et al., 2002). Consequently, the Raman measurements were performed using the samples in three forms; rock, powder and pellet. The rock samples are in the natural form, the powder samples are ground into the finer grain, and the pellets are compacted samples.

The excitation laser sources used for the IRIS echelle spectrometer and Bruker Senterra Raman Microscope are 532 nm and 785 nm, respectively. The specifications of the two Raman systems used in this study are presented in Chapter 3. The set-ups for the IRIS echelle spectrometer were camera exposure of 1 second, frequency of 0.5 Hz and a camera gain of 20. The wavelength range recorded for an excitation wavelength of 532 nm was from 535 – 695 nm. The calibration was checked periodically using a paracetamol sample and compared to the reference spectrum. The software used for the data acquisition was SPECTRAL software and the measurements were performed at the Spectral Industry’s laboratory. Multiple measurements were performed at different spots using each sample to ensure the coverage of material variability. Besides, up to 30 measurements were taken at the same spot and summed to increase the signal-to-noise ratio. On the other hand, the specified parameters for the Bruker Raman microscope were laser power of 10 mw, the integration time of 2 seconds, 10 co-additions per spot measurement, and a Raman shift range of 78 - 1531 cm^{-1} . The software used for the data acquisition was OPUS and the measurements were performed at the University of Twente laboratory. For the Raman measurements using the 785 nm excitation laser source, multiple measurements were taken for each analysed sample using 10 co-additions. An example of the location of the measured points with the corresponding Raman spectra is shown in Figure 9.2.

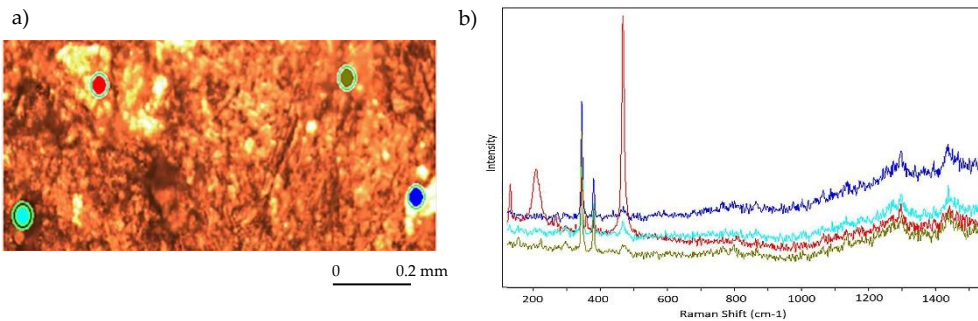


Figure 9.2: (a) Raman image showing the locations of the measured spots at the surface of one of the samples, and (b) the corresponding raw Raman spectra of each point. The colour of the points on the image shows the corresponding spectra.

The conventional laboratory techniques XRD, ICP-MS and XRF were used to validate the Raman measurements. The interpretation results of the Raman spectra were validated using the XRD data. The ICP-MS and XRF quantitative elemental information were used to assess and validate the performances of the classification models developed using the Raman spectral data.

9.2.2. IDENTIFICATION OF MINERALS

The Raman spectra recorded using the Bruker Senterra Raman Microscope is in Raman shift. However, the spectra collected using the IRIS echelle spectrometer is in wavelength that was converted to Raman shift. The formula used to convert the wavelength to the Raman shift is

$$\Delta w = \left(\frac{1}{\lambda_0} - \frac{1}{\lambda_1} \right) \times 10^7$$

where Δw is the Raman shift (cm^{-1}), λ_0 is the excitation laser wavelength (nm) and λ_1 is the Raman spectrum wavelength (nm).

Smoothing and baseline correction were performed to reduce the noise and remove the background from the raw Raman spectra. After the data were pre-processed, the spectra with no relevant information were excluded from further analysis (Figure 9.1). On the other hand, the RRUFF mineral spectral database and published literature were used to interpret the peaks in the usable Raman spectra. The interpretation results were validated using the XRD and other sensors (e.g., SWIR and LWIR) outputs.

9.2.3. CLASSIFICATION OF MATERIALS

The Raman signals, coupled with supervised and unsupervised classification techniques, were assessed for the separation of ore and waste materials. First, PCA was performed to evaluate the grouping structure in the Raman spectra. Following this, K-means with Euclidian distance was applied to examine any clustering in the spectral data. Two cluster centroids were specified, and the classification results of the K-means were assessed for the separation of ore and waste materials. The sum of the concentration of the combined Cu-Pb-Zn was used to designate the ore and waste materials. The elemental quantitative data were acquired using ICP-MC and XRF techniques. Cut-off grades (2% and 5%) were used to assign the samples into ore and waste classes. Besides, the supervised linear (PLS-DA) and non-linear classification techniques (SVC) were used to assess the use of the Raman spectra for the separation of ore and waste materials in polymetallic sulphide deposit. The PLS-DA model was developed using the material type (ore and waste) as dependent variables (the response), and the independent variables (the predictors) are the Raman spectra.

The model was validated using a leave-one-out cross-validation (LOOCV). LOOCV ensures that every observation from the original dataset has the chance of appearing in the training and test set. At each iteration of the algorithm, one sample was left out at a time from the calibration data, and the models were built using the remaining data in the training set. The performances of each of these resulting models were validated using the left-out sample. The algorithm repeatedly runs until each sample in the calibration dataset serves as the test. Thus, LOOCV provides an estimate of model performance as each sample measurement is allowed to represent in the validation dataset. The SVC model was developed using the polynomial and RBF kernel functions. The SVC classification type used in this work is C-SVC. The key model parameters for the specification of C-SVC models are C value and Gamma, which were optimised using a grid search approach with a LOOCV. The C-SVC model developed as a part of this work use the Raman spectra as the

input vector and material types (the ore and waste categorical data) as the response vector. Both the PLS-DA and SVC models were evaluated based on the correct classification rates. Detailed theoretical background on PLS-DA and SVC can be found in Chapter 4.

9.3. RESULTS AND DISCUSSION

This section presents and discusses the interpretation results of the Raman spectra from the two 532 nm and 785 nm excitation laser sources. The section compares the performances of the two laser sources for the characterisation of the polymetallic sulphide deposit. It also presents the use of the Raman spectra for the separation of ore and waste materials in the analysed samples.

9.3.1. INTERPRETATION OF RAMAN SPECTRA

The Raman spectra obtained using the 532 nm excitation laser source show a low signal-to-noise ratio. As a result, the Raman peaks could not be identified from the pellets and powder samples since the signal strength was not significantly high to allow the detection of minerals above the noise level. To amplify the Raman peaks 30 measurements were taken at the same spot and summed. However, no clear peaks could be discovered in the pellets and powder samples spectra. On the other hand, the Raman signal obtained using the rock sample showed relatively better signals. For example, Figure 9.3 shows the Raman spectrum of a calcite mineral. Calcite was identified based on its intense Raman peaks at 195 cm^{-1} , 317 cm^{-1} and 1117 cm^{-1} . Thus, comparing the sample forms the result acquired from the rock measurements are better than the pellets or powder samples measurements. This is likely due to the high fluorescence of the homogenised material that resulted in the drowning of the Raman peaks in the background fluorescence.

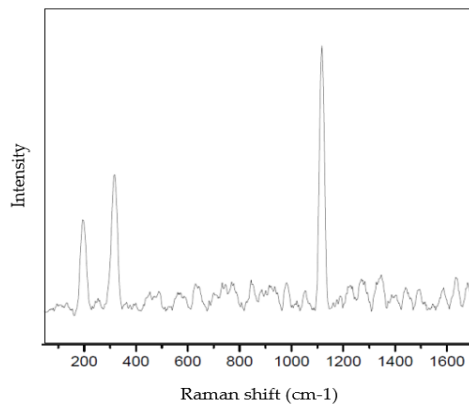


Figure 9.3: Raman spectrum of calcite obtained with the 532 nm excitation laser source.

The Bruker Senterra Raman microscope has the option to switch between the 532 nm and 785 nm excitation laser sources. Thus, the measurements were performed using both excitation laser sources. However, the results from the 532 nm were not usable and similar to the IRIS echelle spectrometer 532 nm laser measurements that they were excluded from further analysis. Multiple Raman spectra were obtained using the samples and the 785 nm laser sources. It should be noted that the location of the spot is not the same for each spectrum as multiple measurements were performed for each sample to capture the

observed sample heterogeneity. Thus, for most of the sample measurements, some minerals were analysed. For example, Figure 9.4 shows the different peaks of the three spots measurements of a pellet sample. The minerals identified using the 785 nm laser sources include pyrite, quartz, calcite, sphalerite, kaolinite, marcasite and siderite. The minerals peaks were consistently observed in all spectra of the samples that compose the same mineralogy. However, slight variation (a few wavenumbers) of the peak positions were observed for some of the samples. This variation could be due to the slight compositional differences in the samples.

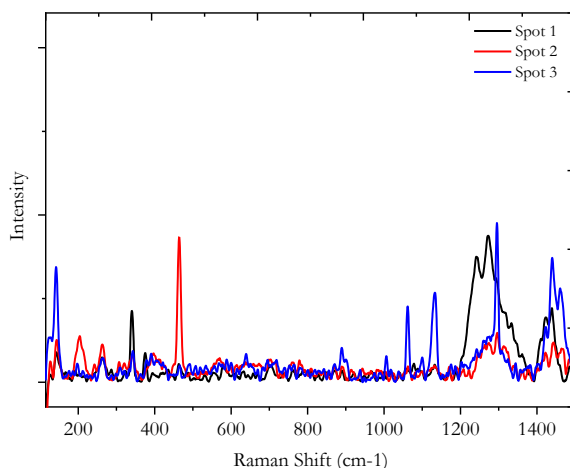


Figure 9.4: The Raman spectra of three measurements taken at different spots of a pellet sample using the 785 nm laser source.

Quartz was identified based on its intense Raman peak at 464 cm^{-1} and other peaks at 127 cm^{-1} , 205 cm^{-1} (Figure 9.5 (a)). The mineral pyrite shows Raman peaks at 342 cm^{-1} and 378 cm^{-1} (Figure 9.5 (b)). Likewise, kaolinite is detected in some of the samples. This mineral shows an intense Raman peak at 142 cm^{-1} and other peaks at 515 cm^{-1} and 640 cm^{-1} (Figure 9.6). The Raman peaks of siderite are found less often in the samples, and the peaks are not always easily distinguished from other mineral peaks such as calcite and dolomite, since the minerals co-occur together and the siderite peaks have a slight deviation. The peaks of pure siderite are found at Raman shift 290 cm^{-1} and 1090 cm^{-1} . When the siderite contains magnesium and manganese, peaks appear at 190 cm^{-1} . As shown in Figure 9.7, the peak at 190 cm^{-1} is from siderite and the peak at 171 cm^{-1} is from calcite.

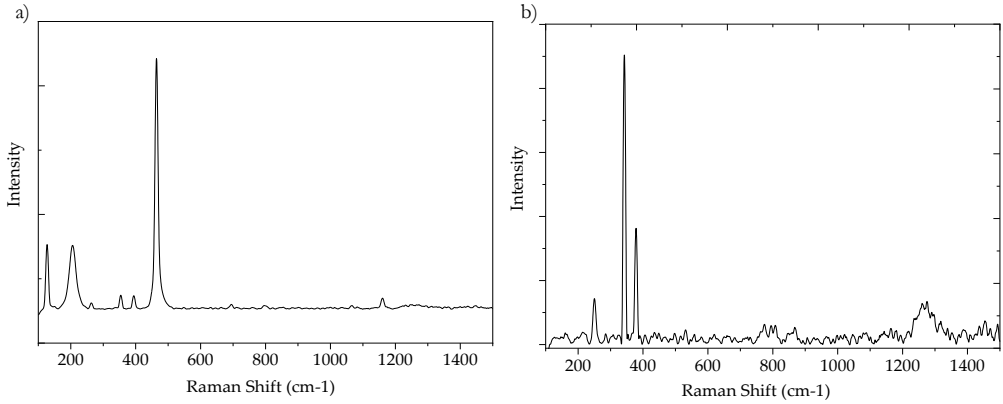


Figure 9.5: The Raman spectra of (a) quartz and (b) pyrite minerals obtained with the 785 nm excitation laser source.

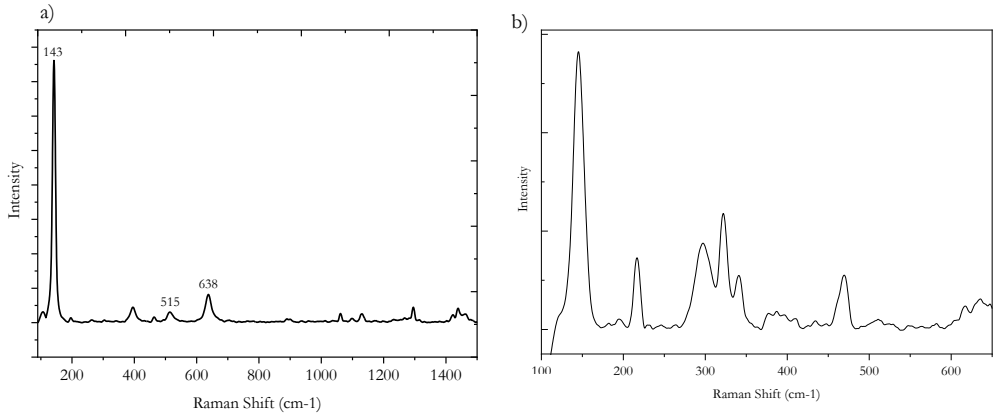


Figure 9.6: The Raman spectra of (a) kaolinite and (b) sphalerite minerals obtained with the 785 nm excitation laser source.

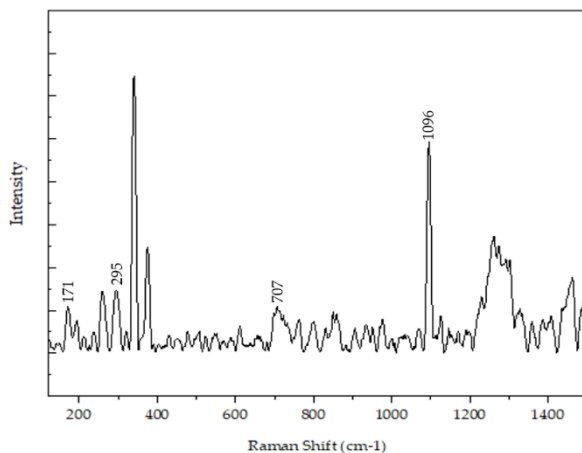


Figure 9.7: The Raman spectra of calcite and siderite minerals obtained with the 785 nm excitation laser source.

Depending on the iron content, sphalerite shows different Raman peaks. Consequently, sphalerite with high iron content has peaks at 295 cm^{-1} and 320 cm^{-1} , whereas sphalerite with lower iron content has peaks at 295 cm^{-1} and 345 cm^{-1} . When the mineral has iron content between high and low, the peaks can be shown at 295 cm^{-1} , 320 cm^{-1} and 345 cm^{-1} (Buzatua et al., 2013; Kharbish, 2007). In this study, sphalerite was detected in some of the samples. An example of a Raman spectrum of sphalerite is presented in Figure 9.6. The missing peak at 380 cm^{-1} indicates that the 342 cm^{-1} peak is not from pyrite but belongs to sphalerite with medium iron content. The rock samples were used to target the galena mineral. However, the acquired Raman signal was noisy and very weak (Figure 9.8). Galena exhibit a very weak Raman signal and this is in line with previous works (Mernagh and Trudu, 1993; RRUFF, 2020).

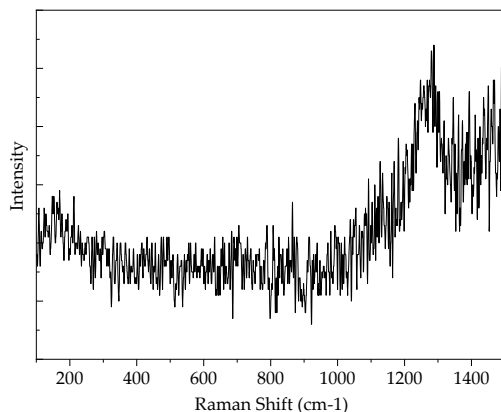


Figure 9.8: Raw Raman spectrum of galena obtained with the 785 nm excitation laser source using a rock sample.

The effect of fluorescence was observed in some of the Raman measurements. Mainly, in the measurements taken from the powder samples. The Raman spectra of some of the samples do not show Raman peaks due to the high levels of fluorescence in the signal. An example is shown in Figure 9.9 (b). The source of the high fluorescence in some of the Raman spectra can be the presence of fluorescent minerals such as calcite or fluorite in the analysed samples. Fluorescence was observed in the Raman spectra collected using both the 532 nm and 785 nm excitation laser sources. However, the effect was more pronounced in the spectra collected using the 532 nm than the 785 nm. The level of fluorescence emission can be reduced and the signal-to-noise ratio of a Raman spectrum can be maximised using suitable excitation laser sources (Chryssikos and Gates, 2017; Haskin et al., 1997). For example, the use of longer excitation wavelengths (lower energy lasers) reduces the fluorescence emission since photon could not have sufficient energy to induce molecular fluorescence. The other challenge in the interpretation of Raman spectra is that the occurrence of overlapping peaks. Some minerals exhibit one or multiple Raman peaks in common thus, when the minerals co-occur, interpretation becomes difficult. In such cases, the decomposition of the overlapping peaks into pure components using decomposition techniques such as multivariate curve resolution-alternating least squares (MCR-ALS) can be a good solution to understand the peaks from the different minerals.

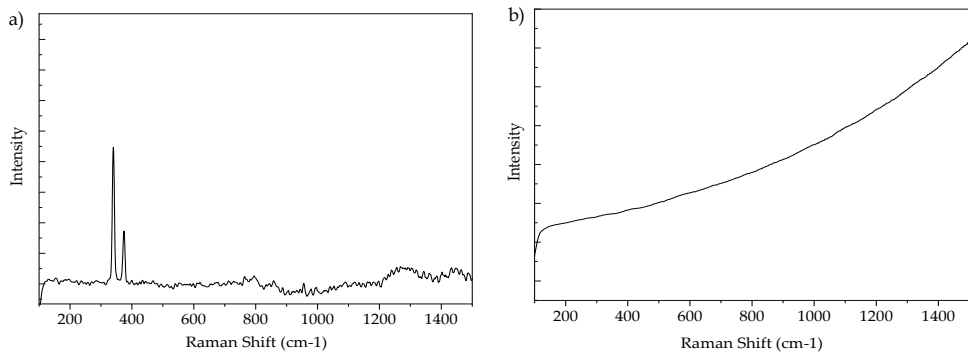


Figure 9.9: Raman spectra of one of the sample obtained with the 785 nm excitation laser source (a) in pellet form (b) in a powder form.

Overall, the 785 nm laser Raman measurements resulted in good Raman signal intensities for the three sample forms (rock, pellets, and powder samples). However, the results obtained from the analysis of the rock samples were superior to the powder and pellet samples measurements. Similarly, the 532 nm laser Raman measurements resulted in a better signal for the measurements of rock samples than powder and pellets samples. Comparing the two excitation laser sources for the characterisation of the polymetallic sulphide materials, the 785 nm laser source outperforms the 532 nm laser source. This is likely due to the fact that longer excitation wavelengths are known to give less fluorescence than shorter excitation wavelength (Bumbrah and Sharma, 2016). The other possible reason can be for non-transparent samples (such as the sulphide minerals) the longer excitation laser sources penetrate deeper into the samples and provide a better signal than the shorter wavelengths (Tuschel, 2016).

The semi-quantitative mineralogical XRD data were used to validate the interpretation results of the Raman spectra. This allowed a comparison of the Raman peak intensities with

the concentrations of the minerals. Although the intensities difference was not that significant due to the weak Raman response, it was observed that the lower the concentrations of the minerals, the lower the peak intensities. This is in line with other researchers that indicate the proportionality of the Raman intensity to minerals concentration (Foucher et al., 2017). Factors that influence Raman measurements include particle size, sample compaction, material type, and the choice of excitation laser sources (Chen et al., 2012; Pellow-Jarman et al., 1996; Wang et al., 2002). In this study, the Raman measurements were assessed using different forms of samples and excitation laser sources. The results show that the 785 nm laser source is the preferred laser choice and the measurement performed using the rock samples was superior to the pellet and powder sample forms. The variation in the physical properties of samples such as particle size and compactness influences the Raman intensities. For example, increased sample compaction can enable the more effective penetration of laser light into a sample. This can lead to enhanced light scattering in the direction of the incident light, thus causes light absorption by the sample (i.e., enhanced Raman scattering). However, the compactability of (powder) samples depends on different factors such as the composition of the material, the crystal structure and grain size (Heigl et al., 2012). Likewise, particle size determines the intensity of the scattered Raman signal. Therefore, future studies are recommended to assess the influence of grain size and degree of sample compactness for the quantitative analysis of minerals in polymetallic sulphide powder samples using Raman.

9.3.2. SEPARATION OF ORE AND WASTE MATERIALS

The usability assessment of the Raman spectra for the characterisation of material from the test case was extended to the applicability assessment in ore–waste separation using the chemical fingerprints of the minerals. Even though the Raman measurements were performed using 40 samples, the results of some of the samples were dominated by the noise that they were excluded from further analysis. Consequently, the number of samples used in the classification analysis was 27. The grouping structure in the Raman spectra was assessed using a PCA model. As shown in Figure 9.10, the PCA of the Raman spectra shows not a good distinction between classes or clustering based on the concentration of the combined Cu-Zn-Pb. Besides, K-means unsupervised classification was applied to the Raman spectra. The K-means results were compared to the concentration of the elements from the ICP-MS and XRF data. However, the classification results show no significant relationship with the concentration of the elements.

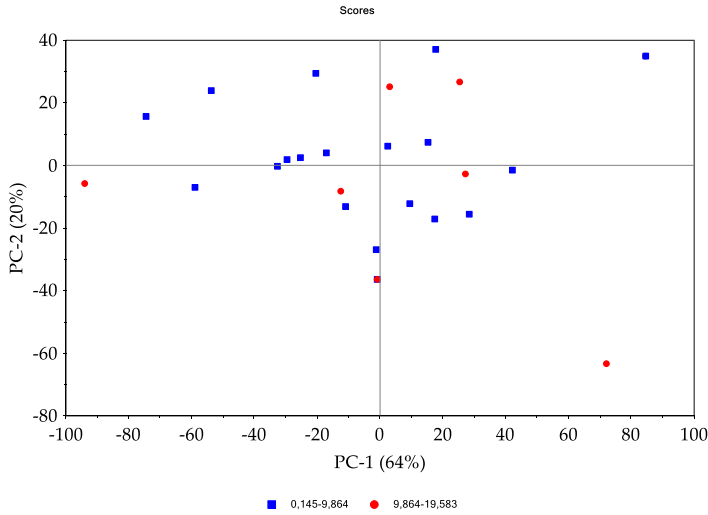


Figure 9.10: A score plot of a PCA model that shows the structure of sample distribution based on the concentration of elements of economic interest (Cu-Zn-Pb).

The samples were designated into ore and waste material types using 2% and 5% cut-off grades based on the concentration of the combined Cu—Zn—Pb concentration. Following this categorical data columns were generated in the data matrix. First, the measurements of the samples that show less than 2% of the combined Cu—Zn—Pb concentrations were considered as a waste and those samples with higher than 2% concentration was considered as ore. Likewise, in the second columns, the samples below 5% concentration were considered as waste, whereas those samples above 5% were considered as ore. Then the SVC model was applied using the Raman spectra as independent variables and the categorical column as a response variable. This was done two times, once for the 2% cut-off grade and then for the 5% cut-off grade. The results of the correct classification rate (based on the confusion matrix) of the SVC models for the 2% and 5% cut-off grades are presented in Tables 9.1 and 9.2, respectively. As shown in the Tables, 78% of the samples were correctly classified for the 2% cut-off grade (Table 9.1). On the other hand, the correct classification rate for the 5% cut-off grade was 59% (Table 9.2). However, both models predicted the materials into ore classes, this shows that the Raman spectra coupled with the SVC model could not differentiate the material into ore and waste classes instead all the samples were predicted as one class (ore). The observed difference of the correct classification rate was based on the number of samples in the ore class, the higher the number of ore samples the model tends to be more accurate. The SVC models with the polynomial and RBF kernel functions were assessed. However, comparable results were achieved using the different model parameters.

Table 9.1: The confusion matrix of the SVC (polynomial) prediction result for ore and waste classes based on 2% cut-off grade.

	Actual	Ore	Waste
Predicted		1	2
Ore	1	21	6
Waste	2	0	0
Correct classification rate			78%

Table 9.2: The confusion matrix of the SVC (polynomial) prediction result for ore and waste classes based on 5% cut-off grade.

	Actual	Ore	Waste
Predicted		1	2
Ore	1	16	11
Waste	2	0	0
Correct classification rate			59%

The result attained from the PLS-DA model shows that a relationship could be established between the Raman spectra and the material types based on the elemental concentrations. The score plot of the PLS-DA model for the classification of the ore and waste based on a 2% cut-off grade was presented in Figure 9.11. As shown in the figure, the plot shows a fairly good distinction among the classes with some overlaps observed with ore and waste materials. In addition, the correct classification rate that can be achieved using the PLS-DA for the classification of ore and waste based on a 2% cut-off was 81% (Table 9.3). On the other hand, the performance of the PLS-DA classification models declined when the cut-off grade was assigned as 5%. As shown in Table 9.4, the overall correct classification rate of the PLS-DA model for the 5% cut-off grade was 59%.

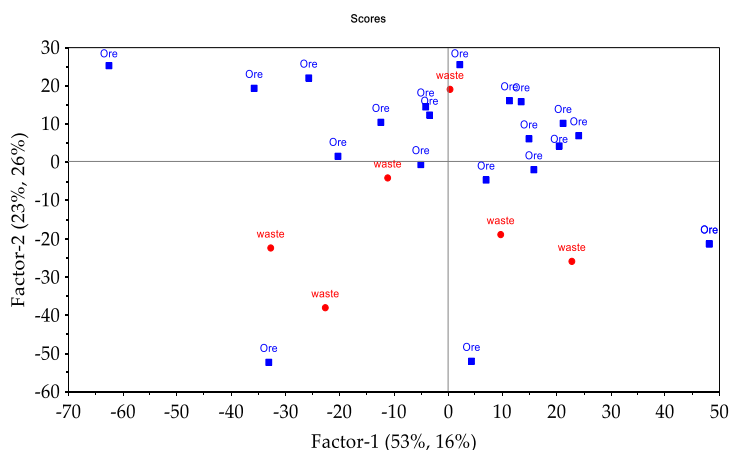


Figure 9.11: The score plot of the PLS-DA model for the prediction of ore and waste with 2% cut-off grade.

Table 9.3: The confusion matrix of the PLS-DA prediction result for the prediction of ore and waste classes based on 2% cut-off.

	Actual	Ore	Waste
Predicted		1	2
Ore	1	20	4
Waste	2	1	2
Correct classification rate			81%

Table 9.4: The confusion matrix of the PLS-DA prediction result for the prediction of ore and waste classes based on 5% cut-off.

	Actual	Ore	Waste
Predicted		1	2
Ore	1	13	8
Waste	2	3	3
Correct classification rate			59%

In the present study, the adoption of linear and non-linear multivariate techniques (PLS-DA and SVC) resulted in a comparable performance in terms of the classification of the materials into ore and waste. Both models exhibit a better classification of material for the lower cut-off grade (2%) than the 5% cut-off. The major difference between the PLS-DA and SVC models for the classification of the material into ore and waste at 2% cut-off is the PLS-DA was able to classify the waste material; however, the SVC could not classify any of the waste materials.

In general, the overall results show both the linear and non-linear techniques provided promising results. However, a strong correlation of the Raman spectra and the material types could not be established especially for separation of material with a 5% cut-off grade. One of the possible reasons for the lower performances of the classification models could be Raman is a mineralogical technique however in this study the ore and waste materials were determined based on the elemental concentration not based on the sourcing minerals concentrations (different minerals can source the same element). The other possible reasons could be the weaker Raman signals and the limited number of samples in the analysis. This analysis was performed using only 27 samples measurements and the samples exhibit high variability of materials (i.e., the concentration of the combined Cu—Zn—Pb ranges from 0.14 to 19, 45 wt.%). Better results could be possible with extended datasets and optimal signal enhancing techniques. Thus, further study is recommended to ensure the applicability of the technique for the classification of ore and waste materials at different cut-off grades.

9.4. CONCLUSIONS

In this work, the use of two Raman spectrometers with 532 nm and 785 nm excitation laser sources were investigated for the characterisation of polymetallic sulphide ore samples. The applicability of the Raman spectra for the identification of minerals and classification of materials into ore and waste were assessed using samples in three forms: rock, pellet and powder. The results reported in the preceding sections show that the 785 nm excitation laser source resulted in better Raman signals than the 532 nm laser source. The samples exhibit a strong fluorescence when excited with a 532 nm laser; thus; it limits the detection

of most of the minerals. The use of two Raman systems with 532 nm and 785 nm laser sources provided the flexibility to minimise the effect of unwanted fluorescence signal in the Raman spectra. Consequently, for the characterisation of the test case material, the preferred laser source is 785 nm. In addition, the Raman signals from the rock and pellet samples are better than the powder samples. The powder samples were highly influenced by fluorescence; as a result, robust Raman signals could not be recorded. The interpretation of the Raman spectra permits the identification of some of the test case minerals. The identified minerals using the 785 nm laser source Raman system include calcite, sphalerite, kaolinite, quartz, pyrite and siderite. The use of Raman spectra, coupled with the supervised classification techniques (SVC and PLS-DA) for the classification of ore and waste resulted in promising results. For example, for the classification of ore and waste material at a cut-off grade of 2%, the PLS-DA model resulted in a correct classification rate of 81%. However, the classification accuracy (59%) of the model lowered for the separation of the material at a higher (5%) cut-off grade. Thus, future study is recommended to ensure the applicability of the technique for the classification of ore and waste materials at different cut-off grades.

The use of Raman enabled the identification of most of the test case minerals and yielded promising results for the separation of ore and waste materials. The technique has a high potential not only in the identification of broad range minerals but also in permitting quantitative analysis and classification of materials in different deposit types. Besides, advances in Raman spectroscopy led to the development of rapid hand-held spectrometers that enable an analysis of materials in the field. Thus, the technique has a great potential for in-situ characterisation of materials in mining operations.

REFERENCES

- Bumrah, G. S. & Sharma, R. M. (2016). Raman spectroscopy – Basic principle, instrumentation and selected applications for the characterisation of drugs of abuse. *Egyptian Journal of Forensic Sciences*, 6(3), pp. 209-215. doi: 10.1016/j.ejfs.2015.06.001
- Buzatu, A., Buzgar, N., Damian, G., Vasilache, V. & Apopei, A. I. (2013). The determination of the Fe content in natural sphalerites by means of Raman spectroscopy. *Vibrational Spectroscopy*, 68, pp. 220-224. doi: 10.1016/j.vibspec.2013.08.007
- Chen, Z. P., Li, L. M., Jin, J. W., Nordon, A., Littlejohn, D., Yang, J., Zhang, J. & Yu, R. Q. (2012). Quantitative Analysis of Powder Mixtures by Raman Spectrometry: the influence of particle size and its correction. *Analytical Chemistry*, 84 (9), pp. 4088-4094. doi: 10.1021/ac300189p
- Chryssikos, G. D. & Gates, W. P. (2017). Chapter 4 - Spectral manipulation and introduction to multivariate analysis. In: W. P. Gates, J. T. Kloprogge, J. Madejová & F. Bergaya (Eds.), *Developments in Clay Science*, 1st ed., Elsevier, pp. 64-106.
- Escarate, P., Guesalaga, A. R., Albertini, V. R. & Bailo, D. (2010). Assessment of Three Spectroscopic Techniques for Rapid Estimation of Calcite in Copper Ore. In *IEEE Transactions on Instrumentation and Measurement*, 59(7), pp. 1911-1917.
- Foucher, F., Guimbretière, G., Bost, N. & Westall, F. (2017). Petrographical and Mineralogical Applications of Raman Mapping. In: K. Maaz (Ed.), *Raman Spectroscopy and Applications*, Intech Open, pp. 163-180.
- Gaft, M., Reisfeld, R. & Panczer, G. (2005). *Modern Luminescence Spectroscopy of Minerals and Materials*, 2nd ed., Springer, Cham, Switzerland.

- Griffith, W. (1975). Chapter 12 - Raman spectroscopy of terrestrial minerals. In: C. Karr (Ed.), *Infrared and Raman Spectroscopy of Lunar and Terrestrial Minerals*, Academic press, New York, USA, pp. 229-324.
- Haskin, L. A., Wang, A., Rockow, K. M., Jolliff, B. L., Korotev, R. L. & Viskupic, K. M. (1997). Raman spectroscopy for mineral identification and quantification for in situ planetary surface analysis: A point count method. *Journal of Geophysical research*, 102 (E8), pp. 19293-19306. doi: 10.1029/97je01694
- Heigl, N., Hodzic, A., Llusà, M., Tritthart, W., Reiter, F., Fraser, S. D., Laggner, P. & Khinast, J. G. (2012). Potential of Raman Spectroscopy for Evaluating Crushing Strength of Tablets. *Journal of Pharmaceutical Innovation*, 7(2), pp. 76-86. doi: 10.1007/s12247-012-9129-7
- Ho, D. M. L., Jones, A. E., Goulermas, J. Y., Turner, P., Varga, Z., Fongaro, L., Tomas, F. & Mayer, K. (2015). Raman spectroscopy of uranium compounds and the use of multivariate analysis for visualization and classification. *Forensic Science International*, 251, pp. 61-68. doi: 10.1016/j.forsciint.2015.03.002
- Kharbish, S. (2007). A Raman spectroscopic investigation of Fe-rich sphalerite: effect of Fe-substitution. *Physics and Chemistry of Minerals*, 34, pp. 551-558. doi: 10.1007/s00269-007-0170-x
- Li, Z., Deen, M. J., Kumar, S. & Selvaganapathy, P. R. (2014). Raman spectroscopy for in-line water quality monitoring--instrumentation and potential. *Sensors*, 14(9), pp. 17275-17303. doi: 10.3390/s140917275
- Mernagh, T. P. & Trudu, A. G. (1993). A laser Raman microprobe study of some geologically important sulphide minerals. *Chemical Geology*, 103(1), pp. 113-127. doi: 10.1016/0009-2541(93)90295-T
- Pani, S., Singh, S. K. & Mohapatra, B. K. (2016). Vibrational spectroscopic study for qualitative assessment of Mn-oxide Ore. *Resource Geology*, 66(1), pp. 12-23. doi: 10.1111/rge.12083
- Pellow-Jarman, M. V., Hendra, P. J. & Lehnert, R. J. (1996). The dependence of Raman signal intensity on particle size for crystal powders. *Vibrational Spectroscopy*, 12(2), pp. 257-261. doi: 10.1016/0924-2031(96)00023-9
- RRUFF. (2020). RRUFF sample data [Online]. Available: <https://rruff.info> [Accessed June 2020].
- Tuschel, D. (2016). Selecting an Excitation Wavelength for Raman Spectroscopy. *Spectroscopy*, 31(3), pp. 14-23.
- Uusitalo, S., Soudunsaari, T., Sumen, J., Haavisto, O., Kaartinen, J., Huuskonen, J., Tuikka, A., Rahkamaa-Tolonen, K. & Paaso, J. (2020). Online analysis of minerals from sulfide ore using near-infrared Raman spectroscopy, 51(6), pp. 978-988. doi: 10.1002/jrs.5859
- Wang, H., Mann, C. & Vickers, T. (2002). Effect of Powder Properties on the Intensity of Raman Scattering by Crystalline Solids. *Applied Spectroscopy*, 56, pp. 1538-1544.
- White, W. B. (1975). Chapter 13 - Structural interpretation of lunar and terrestrial minerals by Raman Spectroscopy. In: C. Karr (Ed.), *Infrared and Raman Spectroscopy of Lunar and Terrestrial Minerals*, Academic press, New York, USA, pp. 325-358.

IV

PERFORMANCE OF THE DATA FUSION APPROACHES

10

IMAGE AND POINT DATA FUSION FOR ORE–WASTE DISCRIMINATION

Data generalisation for the reduction of data volume in material characterisation

The previous chapters (Chapter 6, 7, 8 and 9) show the applicability of the individual techniques for the characterisation of material in the test case. The subsequent chapters (Chapter 10, 11 and 12) present the performance of the classification and prediction models after data fusion. This chapter presents an integrated image and point data fusion approach for the characterisation of material in polymetallic sulphide deposit using channel samples from the test case. The chapter compares the performance of the VNIR, SWIR, MWIR, and LWIR data models with the fused data model results for the discrimination of ore–waste materials.

Parts of this chapter have been published in:

Destá, F. & Buxton, M. (2020). Image and Point Data Fusion for Enhanced Discrimination of Ore and Waste in Mining. *Minerals*, 10(12), 1110. doi: 10.3390/min10121110

Sensor technologies provide relevant information on the key geological attributes in mining. The integration of data from multiple sources is advantageous in making use of the synergy among the outputs for the enhanced characterisation of materials. Sensors produce various types of data. Thus, the fusion of these data requires innovative data-driven strategies. In this study, the fusion of image and point data is proposed, aiming for the enhanced classification of ore and waste materials in a polymetallic sulphide deposit at 3%, 5% and 7% cut-off grades. The image data were acquired in the VNIR and SWIR regions of the electromagnetic spectrum. The point data cover the MWIR and LWIR spectral regions. A multi-step methodological approach was developed for the fusion of the image and point data at multiple levels using the supervised and unsupervised classification techniques. Several possible combinations of the data blocks were evaluated to select the optimal combinations in an optimised way. The obtained results indicate that the individual image and point techniques resulted in a successful classification of ore and waste materials. However, the classification performance greatly improved with the fusion of image and point data, where the K-means and SVC models provided acceptable results. The proposed approach enables a significant reduction in data volume while maintaining the relevant information in the spectra. This is principally beneficial for the integration of data from high-throughput and large data volume sources. Thus, the effectiveness and practicality of the approach can permit the enhanced separation of ore and waste materials in operational mines.

10.1. INTRODUCTION

The dynamic development of sensors resulted in high-end technologies that are rapid and efficient for the accurate characterisation of various types of materials. These technologies produce different types of data that are applicable to the analysis of materials in several disciplines. The two primary data types output from sensors are images (e.g., RGB images and hyperspectral images) and point data (e.g., infrared spectrum and Raman spectrum). Hyperspectral images can allow the simultaneous characterisation of minerals, geological structures and textural information. Moreover, portable point spectrometers also play a significant role in the rapid determination of mineralogical and geochemical data in mining. For example, a portable XRF system and a SWIR sensor are in use for the rapid in-situ analysis of materials (Malvern Panalytical, 2019, OLYMPUS, 2020). The two data types can provide valuable information on key geological attributes. Therefore, the integration of image and point data can significantly benefit mining by maximising the accuracy of material characterisation via the combined benefits from both data types.

Previous studies indicate that the fusion of hyperspectral images using different image fusion techniques resulted in improved performance in various geological and environmental studies. For example, the integration of the VNIR, SWIR and LWIR hyperspectral images using extracted spatio-spectral features resulted in greatly improved drill core mapping (Lorenz et al., 2019). Similarly, Feng et al. (2018) combined SWIR and LWIR hyperspectral image data for a better lithological mapping than with the individual techniques. More recently, Sun et al. (2020) showed that the fusion of hyperspectral images using the extracted spatio-spectral features resulted in the enhanced classification of land-use/land cover maps. In another study, Kruse, (2015) demonstrated an integrated analysis of the VNIR, SWIR and LWIR hyperspectral images for the improved mapping of geological units. In raw material characterisation, the VNIR, SWIR and LWIR are commonly utilised separately, and the integrated analysis of these technologies is very limited. Although few studies indicated the advantages of data fusion, such applications usually combine imageries to achieve enhanced classification maps or better resolution images. The integrated analysis of hyperspectral images is commonly performed by the concurrent analysis of data blocks after wavelength range-specific absorption features are extracted, or by combining the mapping results of the individual data blocks using

geologically directed logical operators (Kopačková and Koucká, 2017; Kruse, 2015). The other common fusion approach is a continuous wavelet analysis that combines wavelet scales spectral profiles of the data blocks (Feng et al., 2018). In a recent study, Lorenz et al. (2019) integrated VNIR, SWIR and LWIR data via images co-registration and spectral-spatial information fusion for enhanced drill core mineral mapping. However, the integration of multi-source and multi-scale data is still limited and requires novel fusion approaches for the integration of image-to-image, image-to-point or point-to-point spectral data.

In several studies, techniques have been developed to extract information using the diagnostic spectral features of minerals in the different wavelength regions of the infrared using both hyperspectral images and point measurements. However, such approaches become ineffective if, as in the case of sulphides, the minerals under study do not exhibit diagnostic features. Thus, in such cases, data-driven strategies that exploit the differences in the spectral responses of the minerals are required to extract knowledge from the infrared spectral data. Each sensor technology operates over a specific range of the electromagnetic spectrum and provides information on certain aspects of material properties. However, a single sensor might not offer a sufficiently comprehensive description of material composition. This study proposes a method of combining the hyperspectral images (VNIR and SWIR) with point spectrometer (MWIR and LWIR) data using machine learning techniques and data fusion approaches for the separation of sulphide ore from waste materials with no diagnostic absorption features of the sulphide minerals. To date, imaging and point infrared techniques have not been fused for the characterisation of material in polymetallic sulphide deposits. This gap in the current analytical methodology and the promising findings (Desta and Buxton, 2018; Desta et al., 2020) reported recently have motivated this study. Thus, the main aims of this study were (1) to assess the possibility of a fusion of hyperspectral images (VNIR and SWIR) and point (MWIR and LWIR) data for the discrimination of ore and waste materials at different cut-off grades using multivariate data analysis techniques and an endmembers weight-based data fusion approach, (2) to investigate the use of the generalised point spectra computed from hyperspectral image data (VNIR and SWIR) for the separation of ore and waste materials in a polymetallic sulphide deposit, and (3) to assess the improvements in the classification models after data fusion.

One of the main advantages of the developed methodological approach is that it dramatically minimises the data volume while maintaining most of the relevant information so as to enable ore and waste separation at different cut-off grades. This minimises the need for big data storage and high-performance computing systems for data processing. Thus, the approach is beneficial for the analysis of high-spatial and spectral resolutions data, as well as for high throughput data. The other advantage of the method is that it allows the establishing of a relationship between the spectral data of the different data blocks and the elemental concentration of the samples, thus permitting the classification of the materials at different cut-off grades. Besides this, the developed method relies on a data-driven approach, therefore does not require a prior specification or identification of minerals and elements.

10.2. DATASETS AND INSTRUMENTATION

Thirty-eight representative rock chip channel samples acquired from the mine face of the study block were used in this study. The samples were acquired from the ore and waste materials sourced at different locations of the mine face. Examples of some of the samples

are presented in Figure 10.1. The different lithotypes were sampled separately. Each sample was split into two, one part of the split powdered and the other half left as rock sample. The powdered samples were used to perform the MWIR and LWIR measurements and the chemical analysis. The VNIR and SWIR hyperspectral images were acquired using the half split rock chip samples. As described in Chapter 3, the VNIR and SWIR hyperspectral images were collected using the Specim's hyperspectral sensors. An Agilent 4300 FTIR analyser was used to acquire the MWIR and LWIR range spectral data. The data acquisition procedures followed for the collection of the hyperspectral images (VNIR and SWIR) and point data (MWIR and LWIR) are described in detail in Chapter 7 and Chapter 8, respectively. The samples were designated as ore and waste materials at 3%, 5% and 7% cut-off grades based on the concentration of the combined Pb—Zn elements. Consequently, the classification of ore—waste was performed for each cut-off grade, separately. The conventional geochemical technique ICP-MS was used to obtain the data that were employed in the validation of the ore—waste discrimination results.



Figure 10.1: Some of the analysed rock chip samples, (a) ore that consists of the sulphide minerals (e.g., galena, pyrite and sphalerite); (b) host rock—banded gneiss; and (c) the weathered material (e.g., clay minerals).

10.3. METHODS

As illustrated in Figure 10.2, the material discrimination approach developed as a part of the present study is a multi-step process that incorporates data conversion, data pre-processing, evaluation of possible combinations, modelling and model validation. The data conversion and pre-processing tasks (denoted as a green box in Figure 10.2) include the conversion of the pre-processed VNIR and SWIR hyperspectral image data into representative point spectra. The MWIR and LWIR data blocks were also pre-processed. Using the computed VNIR and SWIR representative spectra and the pre-processed MWIR and LWIR data, classification models were developed using the unsupervised and supervised classification techniques. The models were applied to the individual data blocks as well as to the multiple possible combinations of the four data blocks (Figure 10.2). The classification models were validated using the geochemical data. The details of each step are described below.

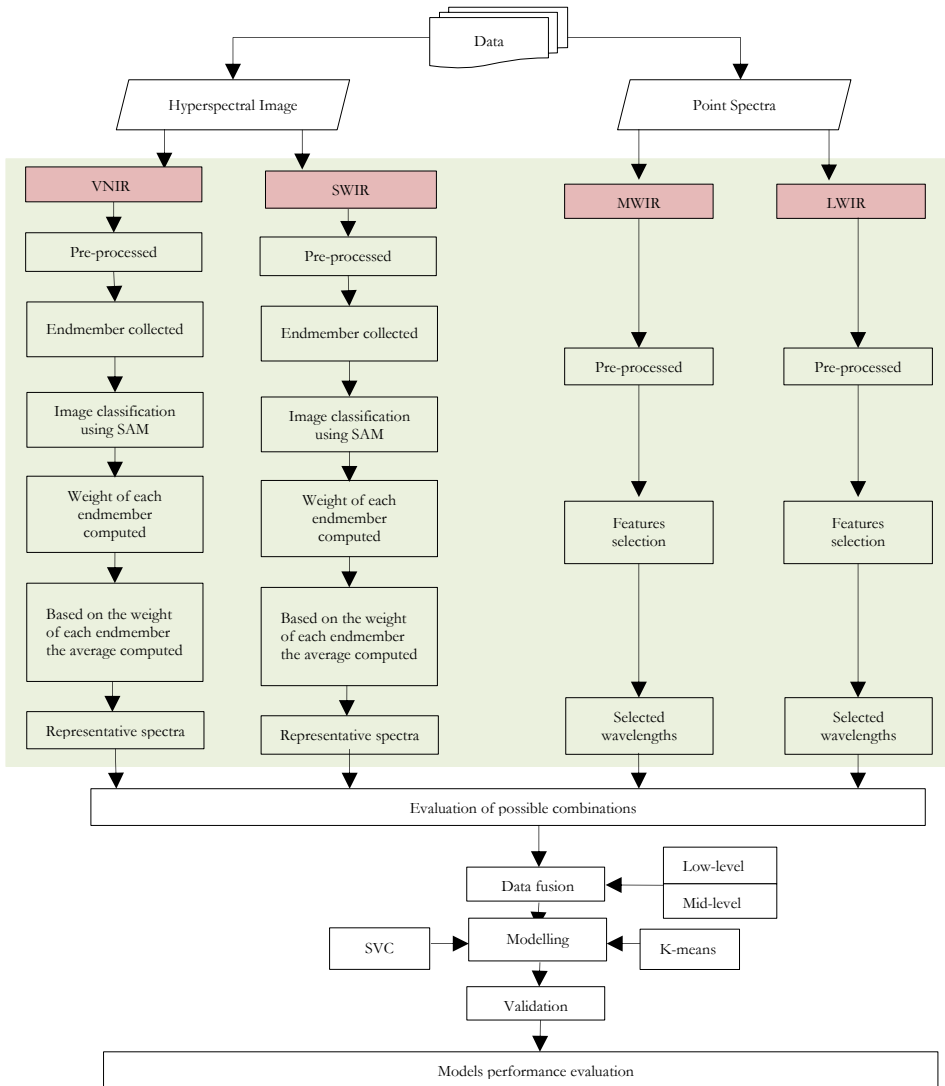


Figure 10.2: Workflow diagram showing the steps for the developed methodological approach in this study.

10.3.1. THEORETICAL CONCEPT FOR POSSIBLE IMAGE TO POINT DATA FUSION

Depending on the sensor data type and application, data fusion can be implemented using various approaches. For example, the integration of image and point data can be image-to-image, image-to-point or point-to-point. This study focuses on the integration of image and point data, but the integration of image-to-image was also assessed. Image and point data are multiscale and multiformat data that require data transformation (or other possible strategies) for use in the same data models. This should be done in such a way that the relevant information is retained while the data are converted to different data forms. In this study, three possible image and point spectroscopic data integration options were evaluated, and the preferred approach was implemented. The first approach transforms the

image data into point data by extracting the endmembers (i.e., spectrally unique pixels) of the image and computing the average without considering the weight of the endmembers. The results are spectra (point data), and so the representative spectra computed from the images and the collected point data can be fused. The second approach takes image and point measurements at the same locality, and fuses the two data types based on location (i.e., location-based fusion). This can be achieved by selecting target locations on the image and taking point measurements at those points. The third option converts the image data into point data by extracting the endmembers of the image and computes the average based on the weight of each endmember. This approach relies on the prominence of the endmembers and enables weight-based fusion. The benefits and limitations of the three possible approaches are presented in Table 10.1. In this study, the third option was preferred because it ensures representation based on the weight proportion of each endmember. The effect of weight-based averaging is comparable with point measurements since the latter relies on taking multiple measurements at different locations of the sample surface and averaging.

Table 10.1: Evaluation of some of the possible hyperspectral image and point spectroscopic data fusion options.

No.	Approach	Benefits	Limitations
1	Extract the endmembers and compute the average	It comprises all the unique spectra	<ul style="list-style-type: none"> • All endmembers get equal weight, and this is not the case in reality since some of the endmembers might exist in very few pixels • Underestimate the information from pixels with a higher count • Overestimate the signals from the pixels with a lower count • There might be information loss due to unclassified pixels • Averaging effect
2	Select target locations from the image and take point measurements at the same spots	The measurement targets the same spots	<ul style="list-style-type: none"> • The pixel size and point measurement techniques sensor view should match • It is possible to upscale or downscale the pixels size using resampling methods, but this requires complex implementation (and it is out of the scope of this study) • Positional accuracy might not enable same spot measurements
3	Consider the weight of each endmember to compute the representative spectrum	The proportion or weight of the abundance of the minerals will be taken into account	<ul style="list-style-type: none"> • Needs careful consideration of endmembers extraction • There might be information loss due to unclassified pixels • Averaging effect

Unlike hyperspectral imagers, point spectrometers capture spectral information at specific points on the material surface. Depending on the measuring surface of the sensors, the size of the point of observation (spot) varies. For example, an FTIR 4300 sensor offers different FOVs corresponding to the three interfaces: the diffuse reflectance sample interface has a 2 mm diameter, the ATR interface has a 1 mm diameter and the external reflectance has a 6 mm diameter (Agilent, 2020). Despite the variation in the measuring surface diameter (field of views—FOVs) of the sensors, point spectrometers provide a single spectrum. Therefore, multiple measurements are taken at the surface of the sample to ensure the measurements are representative. Thus, sample heterogeneity can determine the required number of point measurements per sample. More homogenous material requires fewer measurements, while the higher the heterogeneity, the more measurements are required. The point measurements do not necessarily provide spatially resolved data; instead, the spectral data can include spectral information from the co-existing mineral mixtures in the vicinity or within the FOV of the sensor. Therefore, the spectra from point spectrometers are mixed in most cases. In contrast, the image data, such as the hyperspectral imaging of rock chips or drill cores, covers all parts of the samples under the imaged scene. Therefore, the spectral information at each point of the sample surface is available. Some of the benefits and shortcomings of the image and point data types are summarised in Table 10.2.

Table 10.2: Some of the benefits and shortcomings of point and image data types in material characterisation.

Data Type	Pros.	Cons.
Image data	<ul style="list-style-type: none"> • Information all over the sample surface • Remote application possible • Suitable for the understanding of the spatial distribution of minerals • Allows simultaneous analysis of minerals, geological structures and textural information • Permits quantitative indication of mineralogical composition based on pixel count 	<ul style="list-style-type: none"> • High-data volume • Relatively lower resolution • Surface irregularities can cause difficulty in keeping all sample surface in focus
Point data	<ul style="list-style-type: none"> • Depending to the technology, more accurate data • Low-data volume • High spectral resolution • High dynamic range • High signal-to-noise ratio 	<ul style="list-style-type: none"> • Subjective in the way of selecting measurement points • Limited area coverage (spot measurement) • Needs actual contact with the sample

10.3.2. IMAGE DATA CONVERSION

The raw VNIR and SWIR hyperspectral images were pre-processed using the required pre-processing techniques. The spectrally unique endmembers were extracted from the pre-processed VNIR and SWIR images, separately, using the scatter plots and PPI technique. The details of the applied pre-processing and feature extraction techniques are described in Chapter 7. Some of the unique spectra were interpreted to identify minerals using the

available spectral libraries. However, there are also unidentified unique spectra, possibly due to factors such as mineral mixtures, physical matrix effects or weak spectral responses. The extracted endmembers (both the identified and unidentified unique spectra) were used to generate training sets (ROI). The ROI's were used to produce mineral maps that show the mineral distribution and pixel abundances using a SAM classifier. SAM is a rapid mapping tool, which is relatively insensitive to illumination effects and other spectral artefacts (Kruse et al., 1993). This technique is described in Chapter 3. The mineral maps produced show the locations and pixel abundances of each endmember. A pixel count was performed using the classified VNIR and SWIR images of each sample separately. The number of pixels of each endmember was used to compute the relative abundance of the identified and unidentified minerals. Following this, the weight of each endmember was used to calculate the final average spectrum of each sample. The mathematical equations for the conversion (representation) of the image data to a spectrum are shown below

$$y_i = \frac{100x_i}{w}, \quad (1)$$

$$T = \frac{\sum_{i=1}^n y_i}{k}, \quad (2)$$

where y denotes the proportion of an endmember in the sample, w is the total number of pixels of the image, x represents the endmembers (the identified and unidentified minerals), i is the number of endmembers, k is the total number of the endmembers, n represents the last endmember, and T is the average representative spectra of a sample.

As indicated in Table 10.2, both the image and point data have their advantages and limitations. Thus, the conversion of the image to point data is not because the point data is superior to the image data. Instead, for the combined analysis of the image and point data, one possible approach can be the converting of the two data types into the same data scale while maintaining the relevant spectral information from both data types. Consequently, data conversion was performed to transfer the hyperspectral image data of each sample into a representative spectrum. The representative spectrum represents the average of pure endmembers multiplied by their weight. The same procedure was followed to generate the VNIR and SWIR representative spectra separately.

The VNIR and SWIR sensors used in this study offer the same FOVs, such that a straightforward pixel-by-pixel co-registration of the two images is possible. However, this approach was not considered since the focus was the integration of the image and point data. Thus, the image data were converted to point representative spectra, and the usability of the transformed (generalised) data for the discrimination of ore and waste materials was assessed. In the proposed approach, two scenarios can be verified: (1) the usability of the images that were generalised into point data to still provide useful information, and (2) whether this approach permits the fusion of image (VNIR and SWIR) and point data (MWIR and LWIR) for the enhanced characterisation of materials.

10.3.3. POINT SPECTRAL DATA PRE-PROCESSING

The PCA model was applied to the MWIR and LWIR datasets. The scores plots of the PCA models were used to investigate the grouping structure (intra-sample relationships). The loading plot of the PCs was interpreted to reveal the wavelength regions with a large loading coefficient or the most variations. These wavelength regions are important variables

that contain more information. Consequently, the features, those containing information pertinent for the separation of ore and waste material, were independently extracted from the MWIR and LWIR data blocks. The extracted informative variables from the MWIR data are the wavelength ranges from 2.5 to 3.0 μm , 3.5 to 4.2 μm and 5.6 to 6.3 μm . Likewise, the ranges 7.3 to 7.8 μm , 10.8 to 11.5 μm , 13.6 to 14.0 μm and 14.5 to 15.0 μm were extracted from the LWIR data. Thus, the MWIR and LWIR data blocks consist of the extracted informative features from the two spectral regions. Prior to modelling, the two data blocks were pre-processed using smoothing (Gaussian filter smoothing), baseline correction and normalisation techniques. The MWIR and LWIR data used in this study are point measurements. As described in Chapter 8, sample heterogeneity was accounted for by collecting multiple spectra from each sample and computing the average. Therefore, the datasets (VNIR, SWIR, MWIR and LWIR) used in this work are based on average spectra that were calculated based on material variability.

10.3.4. DATA MODELLING

The multivariate analysis techniques used to develop the classification models are the K-means and SVC methods. Detailed descriptions of the K-means and SVC methods can be found in Chapter 4. One of the highly efficient, and the most commonly used, unsupervised classification methods, K-means with Euclidian distance was applied to examine any clustering in the spectral data. The K-means number of clusters was specified as two and clustering was independently generated for each individual and fused data block. The correct classification rate of each data block model was examined for the separation of ore and waste materials at the cut-off grades of 3%, 5% and 7%, separately. The classification results of the models and the reference values were used to compute the correct classification rate of the individual and fused data block models separately.

SVC is a supervised classification method, used to optimise separation between different classes or groups. The SVC classification type used in this work is C-SVR with a polynomial kernel function, as this kernel type can be utilised to model non-linear systems of varying complexity. The SVC is a supervised classification technique, thus prior to modelling, the samples were designated as ore or waste based on the concentration of the elements at the required cut-off grade. The data blocks with the material class information were used to develop the SVC models. The SVC model was validated using a LOOCV. LOOCV is one of the resampling (subsampling) procedures for the validation of models with a small dataset (Wong et al., 2015). In this work, the optimal model parameters (C and gamma) were optimised using a grid search approach. The correct classification rate of each left-out spectrum was calculated after selecting the optimal parameters. Finally, the average of the correct classification rate values of each iteration is reported as the performance of the classification model.

The performances of the K-means and SVC classification models were evaluated for the separation of ore and waste materials at the 3%, 5% and 7% cut-off grades using the individual as well as the fused datasets. Samples with a concentration below the cut-off grade are designated as waste, whereas those with a concentration above the cut-off grade are considered ore. This approach is beneficial in evaluating the usability of each technology for the separation of ore–waste at different thresholds. Thus, the applicability to both low- and high-grade deposits can be determined.

10.3.5. DATA FUSION AND VALIDATION

The integration of multi-source and multi-scale data can be realized at different levels using the various approaches. Data fusion enables multiplatform characterisation of the analysed samples by processing all the spectral signals from each sensor. It is therefore likely to improve classification results. The data fusion approaches adopted in this study are low-level, mid-level and multiple-level. The data fusion approaches in chemometrics are discussed in detail in Chapter 4. Multiple possible combinations of data blocks were explored to identify the optimal sensor combinations for the classification of the ore and waste materials at the indicated cut-off grades. These possible combinations include VNIR–SWIR, SWIR–MWIR, SWIR–LWIR, and VNIR–SWIR–MWIR–LWIR. First, separate models were developed using individual data blocks. Later, data fusion strategies were applied to the possible combinations of the data blocks. Therefore, the performances of the individual data blocks have also guided the choice of the possible combinations (i.e., data blocks with better classification results were mainly considered in the possible combinations options). The level of data fusion applied for the combination of the VNIR and SWIR data is mid-level since the integration is based on the extracted features (Figure 10.3). In this case, the important variables, the endmembers, were extracted using the approach mentioned above and the features from the two blocks were concatenated to form the final fused data block. On the other hand, a low-level fusion with feature selection was applied to integrate the MWIR and LWIR data blocks. In this approach, the pre-processed extracted informative variables of the MWIR and LWIR data were concatenated to form a fused data block. The two classifiers (K-means and SVC) were applied to the fused data.

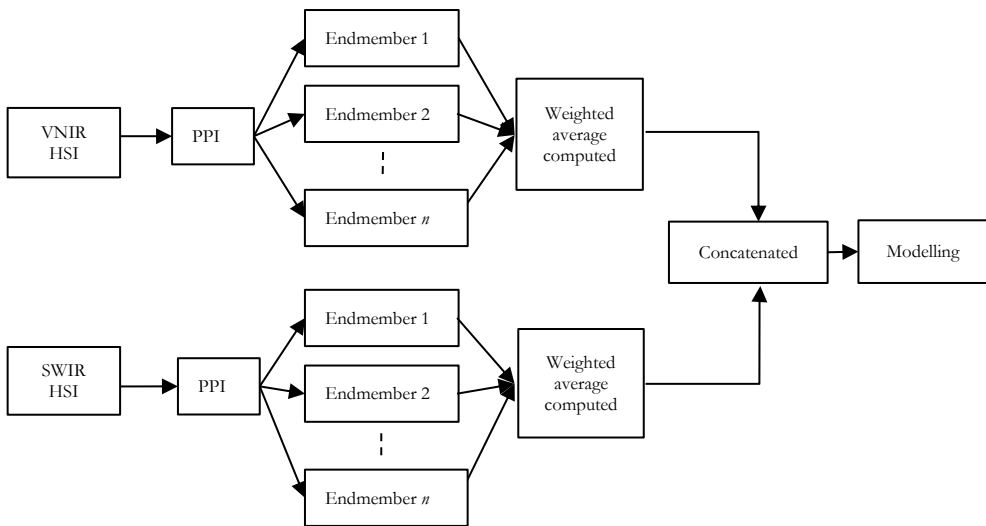


Figure 10.3: The steps for the fusion of the VNIR and SWIR data using a mid-level data fusion approach. HSI stands for hyperspectral image.

The fusion of image and point data requires integrating sensor data that have different scales and spatial resolutions. An optimal data fusion strategy is required to ensure data integrity while maximising the amount of relevant information that can be linked to material properties. In this study, the integration of the image and point data blocks was conducted

using a multiple-level fusion that incorporates both low-level and mid-level fusions. The extracted features of the VNIR and SWIR data, as well as the selected informative variables from the MWIR and LWIR data, were aligned and concatenated into a single matrix. Thus, the most relevant variables that explain most of the variations in the spectra were fused. Classification models were developed using the fused data blocks and the two classifiers (K-means and SVC). This approach offers the opportunity to explore the region from 0.4 to 15 μm of the electromagnetic spectrum. In most cases, the wider the wavelength range, the greater the amount of pertinent information.

The performances of the K-means and SVC models were assessed based on the correct classification rates calculated using confusion matrices. The true (reference) values in the computation are the geochemical data from the ICP-MS measurements. The correct classification rates were calculated for each individual and fused data block model at the indicated cut-off grades, separately. Subsequently, the classification accuracies of the individual data blocks and possible combinations were compared. The performances of the K-means and SVC models were optimised using the different pre-processing techniques (smoothing, baseline correction and normalisation) applied to the datasets. Thus, the results reported in this study are based on the preferred pre-processing techniques. Consequently, smoothing was applied to each data block, and the pre-processed data blocks were concatenated to form the fused data blocks used by the K-means model. The SVC models were developed after baseline correction was applied to each data block; the pre-processed data blocks were concatenated and normalised.

10.4. RESULTS AND DISCUSSION

This section consists of four parts. In the first part, the classification model results of the individual techniques for the separation of ore and waste materials using the unsupervised and supervised techniques are presented. In the second part, the results of the fused VNIR and SWIR data (i.e., image-to-image data fusion after data conversion) are presented. This section also compares the classification performances of the fused models with the individual data block models. In the third part, the ore and waste separation results after image and point data fusion are described in detail. In the last part, the potential benefits and possible limitations of the approach are discussed.

10.4.1. EXPLORATORY ANALYSIS

The concentrations of the combined Pb–Zn elements varied greatly among the analysed samples. The values ranged from 0.16 to 19.6 wt. % with a mean of 6.17 wt. %. The numbers of samples in the ore and waste classes at the three cut-off grades are indicated in Table 10.3. Figure 10.4 shows the PCA model score plots of the VNIR, SWIR, MWIR, and LWIR datasets patterns related to the ore and waste materials at the 3% cut-off grade. The plots show informative patterns (groupings) that are related to the combined Pb–Zn concentration. This indicates the possibilities for the use of the techniques in the separation of ore and waste materials in the analysed samples.

Table 10.3: Summary of the number of samples in the ore and waste classes at 3%, 5% and 7% cut-off grades.

Material	Number of samples		
	Cut-off 3%	Cut-off 5%	Cut-off 7%
Ore	23	18	15
Waste	15	20	23
Total	38	38	38

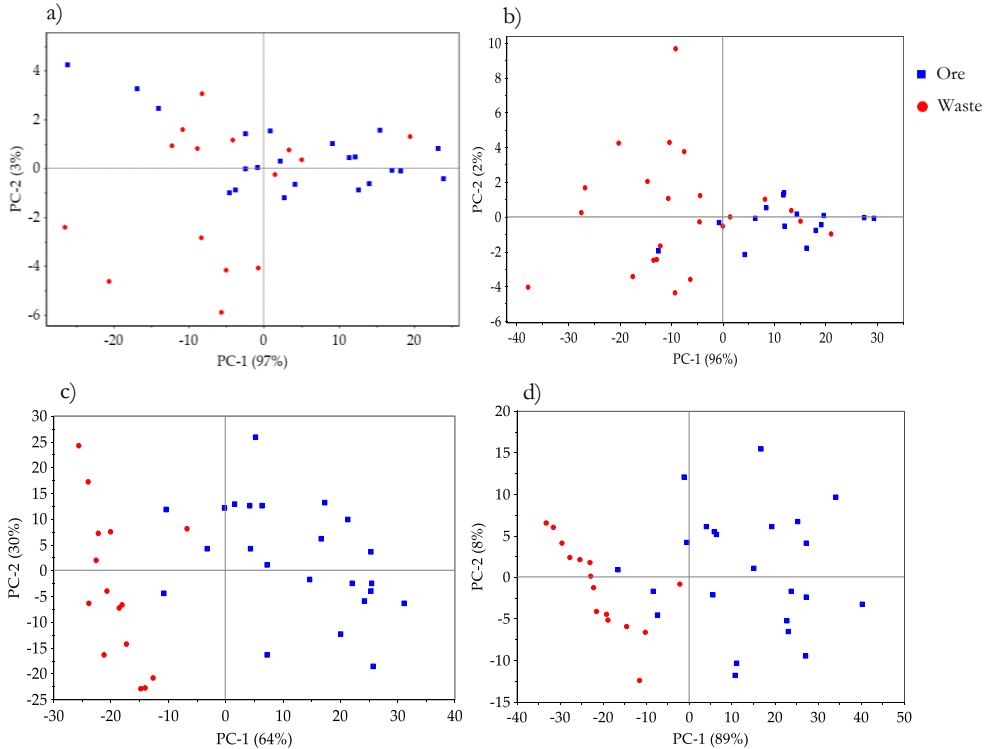


Figure 10.4: PCA model score plots of (a) VNIR; (b) SWIR; (c) MWIR; and (d) LWIR showing the patterns of the ore and waste materials at 3% cut-off grade.

10.4.2. THE INDIVIDUAL DATA BLOCKS MODELS

In Tables 10.4 and 10.5, the correct classification rates of the individual data blocks and the fused data models for the separation of ore and waste materials at the indicated cut-off grades are summarised. As shown in the tables, the performances of the classification models vary from technique to technique. For example, the achieved correct classification rate of the VNIR data K-means model for the separation of the materials at the 3% and 5% cut-off grades are 66% and 73.7%, respectively. The VNIR data have a narrower wavelength range than the other techniques, and the amount of relevant spectral information is limited. However, the technique yielded promising results. At the 3% cut-off grade, the classification rates acquired using the SWIR, MWIR and LWIR data K-means models are 76%, 94.7%,

and 92%, respectively. As can be seen from Table 10.5, the SVC classifier resulted in a very good classification performance for the segmentation of ore and waste using the SWIR, MWIR and LWIR data. Similar to the K-means classifier, the rates for the VNIR model are lower than the other models. Comparing the performances of the individual data block models for the separation of ore and waste in a polymetallic sulphide deposit, generally, the results acquired from the MWIR data model are superior to the results from the data models of other techniques (Tables 10.4 and 10.5). This is intriguing because the MWIR is an understudied region of the electromagnetic spectrum in raw material characterisation.

Table 10.4: Summary of the correct classification rates when a K-means classifier was applied to the individual and fused data blocks. The ore–waste classification rates for the three cut-off grades are indicated for each data model. The wavelength range indicates the operating wavelength range of the technologies.

Sensors	Wavelength (μm)	Correct Classification Rate (%)		
		3% Cut-off	5% Cut-off	7% Cut-off
VNIR	0.4–1.0	66	73.7	61
SWIR	1.0–2.5	76	79	81.6
MWIR	2.5–7.0	94.7	81.6	79
LWIR	7.0–15.0	92	90	87
VNIR–SWIR	0.4–2.5	76	79	81.6
SWIR–MWIR	1.0–7.0	90	92	90
SWIR–LWIR	1.0–2.5 and 7.0–15.0	90	84	81.6
MWIR–LWIR	2.5–15.0	92	84	81.6
SWIR–MWIR–LWIR	1.0–15.0	90	92	90
All	0.4–15.0	90	92	90

Table 10.5: Summary of the correct classification rates when the SVC classifier is applied to the individual and fused data blocks. The ore–waste classification rates for the three cut-off grades are indicated for each data model. The wavelength range indicates the operating wavelength range of the technologies.

Sensors	Wavelength (μm)	Correct Classification Rate (%)		
		3% Cut-off	5% Cut-off	7% Cut-off
VNIR	0.4–1.0	58	60.5	66
SWIR	1.0–2.5	73.7	60.5	81.6
MWIR	2.5–7.0	92	87	87
LWIR	7.0–15.0	92	76.3	73.7
VNIR–SWIR	0.4–2.5	81.6	79	84
SWIR–MWIR	1.0–7.0	95	90	87
SWIR–LWIR	1.0–2.5 and 7.0–15.0	92	90	76.3
MWIR–LWIR	2.5–15.0	92	90	84
SWIR–MWIR–LWIR	1.0–15.0	95	90	87
All	0.4–15.0	95	90	87

The MWIR and LWIR data models resulted in better performances at the lower cut-off grade than the higher cut-off grades. For example, the LWIR data K-means model yielded a 92% correct classification rate for the separation of the materials at the 3% cut-off grade; however, the classification performance of the model lowered to 87% for the separation of the materials at the 7% cut-off grade. The sulphide minerals exhibited strong spectral signals in the MWIR and LWIR; thus, even when they occur at a lower concentration, they can be detected and allow the classification of ore and waste materials at lower cut-off grades. The discrimination of the materials at lower cut-off grades addresses whether the sulphide minerals are in the samples or not. On the other hand, the separation of the ore and waste materials at mid-to-high cut-off grades requires detection of the sulphide minerals presence, as well as sufficient spectral difference among those samples having mid-to-high concentrations of the ore minerals. Therefore, when there is a limited spectral difference among the samples with the mid-to-high concentrations, the performances of the classification models at the higher cut-off grades can minimise. This is the likely reason for the observed relatively lower classification performances of the MWIR and LWIR data models at higher cut-off grades compared to lower cut-off grades.

The lower spectral difference among those samples having mid-to-high concentrations of the ore minerals is also evident from the descriptive analysis and the confusion matrices results. For example, the PCA plots of the LWIR data indicate better class separation at the 3% cut-off than the 7% cut-off grade. The confusion matrix also supports this; a higher cut-off grade means the majority of the misclassification is in signifying waste as ore. For example, at the 7% cut-off, all ore samples were correctly classified; however, some of the waste materials were misclassified as ore. The spectral difference between waste (lower concentrations) and ore (higher concentrations) materials is apparent (Figures 10.5). However, the signals from those samples with mid to high concentrations of the ore minerals show limited spectral variations. Extended datasets in the training model to better accommodate the spectral variation among the samples with mid to high concentrations could improve the performances of the classification models at higher cut-off grades. The excellent performance of the classification models at the lower cut-off grades suggests the usability of the techniques in economically suboptimal mining operations. A future work is recommended to find the optimal cut-off grade for the separation of the materials into ore and waste using the MWIR and LWIR technologies. It is also worth noting that the cut-off grade of a commodity varies due to fluctuations in the mined product prices and mining costs.

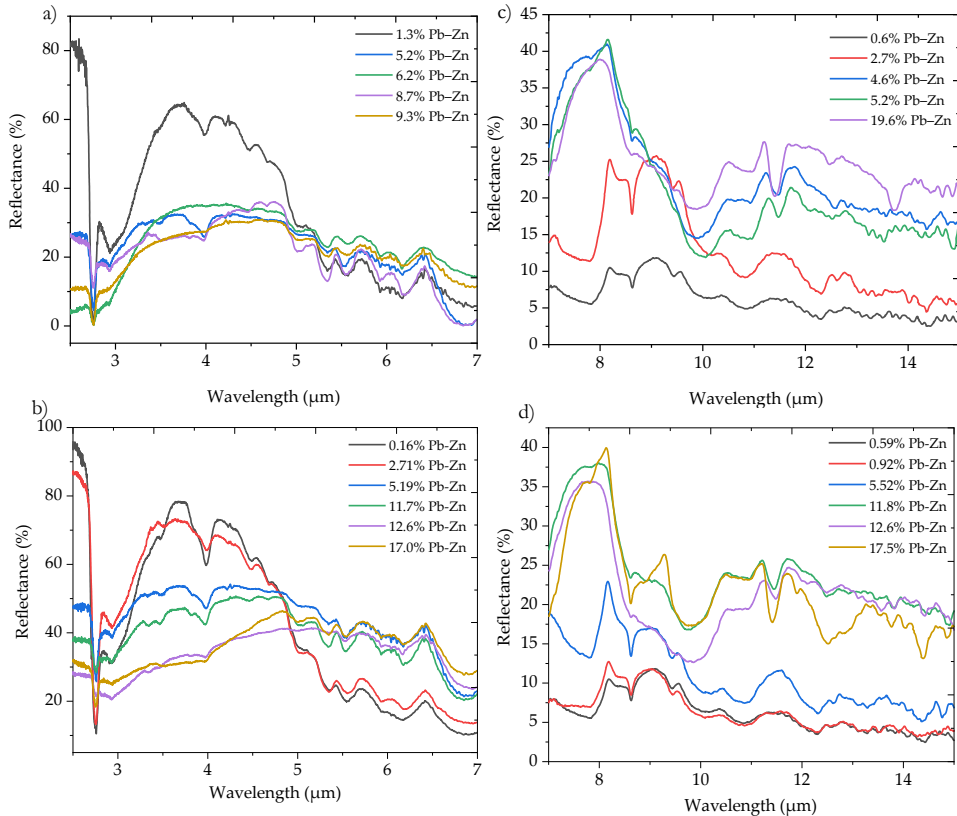


Figure 10.5: The spectra of some of the samples showing spectral variation based on the combined Pb–Zn concentration values in the ((a) & (b)) MWIR, and ((c) & (d)) LWIR regions of the infrared.

The VNIR and SWIR data models yielded better classification outcomes at a higher cut-off grade than the lower cut-off grade. The sulphide minerals exhibit very weak signals (low reflectance) in the VNIR and SWIR regions. When the minerals occur in lower concentrations, the signals even get weaker. This is likely the reason why the performances of the VNIR and SWIR data models lowered at the lower cut-off grade and yielded better classification results at higher cut-off grades. The data blocks of the VNIR and SWIR consist of extracted features, which tremendously minimised the data volume. Similarly, the MWIR and LWIR data blocks comprise the selected informative wavelengths. However, the extracted features from the four data blocks allowed the successful classification of ore and waste materials in the analysed samples. Overall, the individual techniques show good potential for the separation of ore and waste material at different cut-off grades, suggesting the presence of informative variables in each data block that can be linked to the ore and waste material properties. This could allow the use of these techniques for the separation of materials in different low-grade and high-grade deposits.

10.4.3. FUSION OF THE VNIR AND SWIR DATA

As described in Section 10.3.2, prior to modelling, the spectral features of the VNIR and SWIR image data were extracted using spectral unmixing algorithm. The fusion of the VNIR and SWIR data involves variable screening using a feature extraction technique. Thus,

it is considered a mid-level data fusion. This approach allowed the removal of non-informative variables while maintaining the relevant information in the spectra. As discussed in the previous section, both data blocks consist of the relevant information that can be linked to material properties (ore and waste materials in this case). Spectral plots of the ore and waste materials in the VNIR and SWIR regions can also support this (Figure 10.6). Thus, the fusion of the two data blocks benefited from the synergy between the individual datasets and resulted in a better separation of ore and waste material. For example, the fusion of the VNIR and SWIR data resulted in a remarkable improvement in the classification performance of the SVC models, suggesting the advantage of data fusion for the enhanced characterisation of materials (Table 10.5). When the K-means was applied to the fused VNIR and SWIR data block, the results were not necessarily improved compared to the individual techniques' data models (Table 10.4). However, the K-means clustering results of the two data block models resulted in better performances than the use of other algorithms, and could likely improve the results (this was also evident from the classification result of the SVC classifier). The fact that the image VNIR and SWIR data were converted to point data, integrated at the data level, and resulted in a better performance suggests the benefits and usability of the approach in material characterisation.

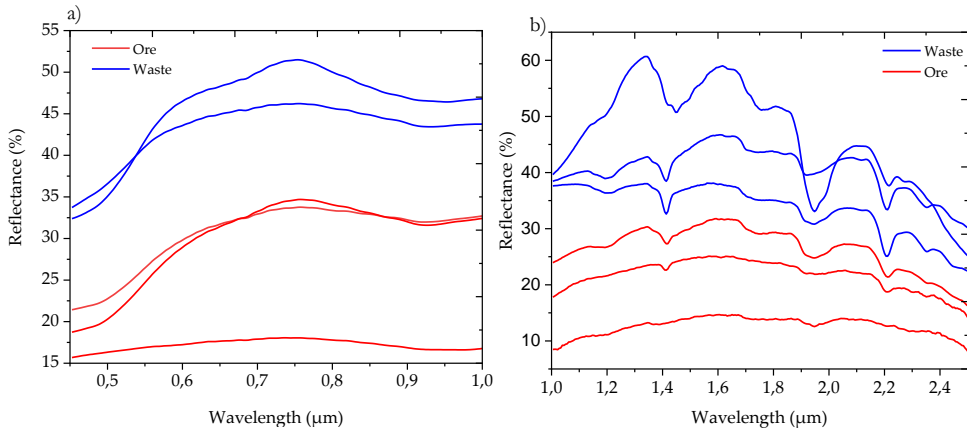


Figure 10.6: Representative spectra of samples that belong to ore and waste classes in the (a) VNIR and (b) SWIR wavelength regions.

The interpretation of the sulphide minerals using the VNIR and SWIR is challenging since the minerals do not exhibit particular absorption features in the regions. The VNIR allowed the identification of the ferric iron minerals (hematite and goethite), carbonates (siderites), and some of the sulphide minerals (such as pyrite and galena). However, the identification of the sulphides was not comprehensive since the minerals do not exhibit any absorption features. The minerals identified using the SWIR data include mica (muscovite), clay minerals (montmorillonite and illite), carbonates (siderite), tectosilicate (quartz), phyllosilicate (Mg + Fe chlorite), sulphide ores (with no particular absorption features), and a minerals mixture. The featureless nature of the sulphide minerals can be used to map the ore and waste regions of the analysed samples using the SWIR image data. This map can show the distribution and relative abundance of the minerals at the surface of samples. However, SWIR cannot be used to discriminate between the sulphide minerals, and the image data cannot be used to relate the spectral information to specific elemental

concentrations. Thus, it is challenging to indicate the ore and waste materials at different cut-off grades. The approach developed in this study allowed for establishing a relationship between the spectral data and the concentration of the elements of economic interest, and thus to classify the samples into ore and waste. This approach gives flexibility in analysing the spectra for various quantitative geochemical and mineralogical information. Therefore, it is efficient and has significant benefits in providing information about high-grade, medium-grade and low-grade areas in mining operations.

10.4.4. IMAGE AND POINT DATA FUSION

Imaging of the rock chips samples enables capturing the entire material composition at the surface of the sample. Examples of classified VNIR and SWIR images are shown in Figure 10.7. Depending on the spatial and spectral resolution of the imagers, imaging technologies can provide accurate and usable spectral information at every surface of the sample under the imaged scene. This allows the visualisation of the spatial distribution of minerals, and can also be used to estimate the relative abundances of minerals at the surface of the samples. However, the main drawback of hyperspectral images is the vast volume of data that require a large amount of computational power and data storage. Therefore, the proposed approach in this study is beneficial in minimising data volume by adopting a sequential features extraction and modelling approach. In addition to significantly minimising the volume of data, this approach allows the analysing of spectral data from multiple data sources operating over the wider range of the electromagnetic spectrum. An example of the representative spectra of ore and waste material across VNIR, SWIR, MWIR and LWIR is presented in Figure 10.8. This kind of approach permits the use of the relevant information in each spectral region to address the material property of interest. Overall, the integration of image and point data enables the integration of data of different scales and types.

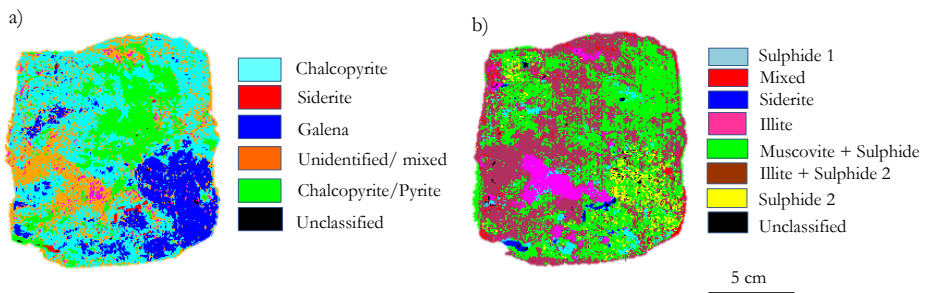


Figure 10.7: Examples of the classified images of (a) VNIR and (b) SWIR image acquired using the same sample.

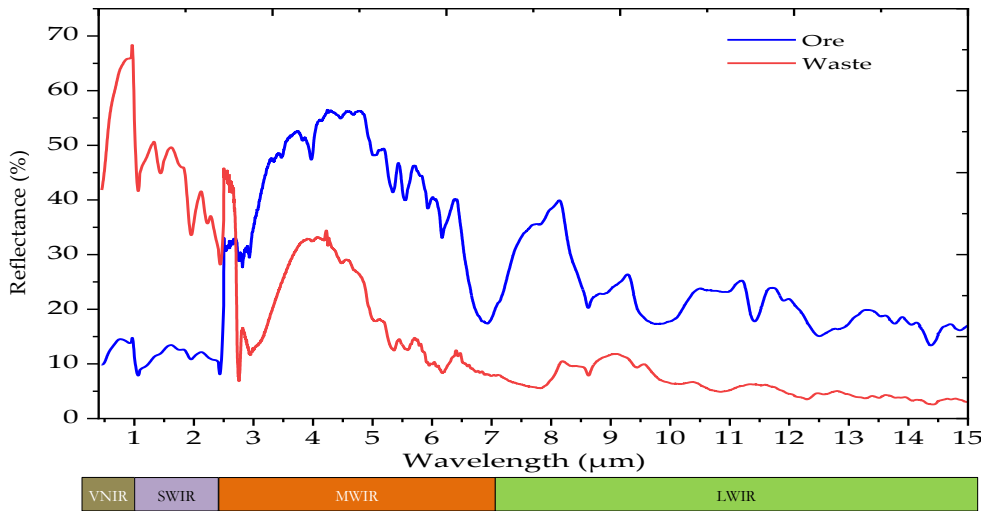


Figure 10.8: Representative spectra of the ore and waste materials across the VNIR, SWIR, MWIR and LWIR regions of the electromagnetic spectrum. The concentrations of the combined Pb–Zn in these ore and waste samples are 17.5 wt. % and 0.59 wt. %, respectively.

As shown in Tables 10.4 and 10.5, multiple possible combinations of the image and point data were evaluated using the K-means and SVC techniques. For example, the integration of the SWIR and MWIR data improved the correct classification rate of the SVC model at the 3% and 5% cut-off grades compared to the individual data models (Table 10.5). Likewise, the fusion of these two data blocks resulted in enhanced K-means classification rates at the 5% and 7% cut-off grades (Table 10.4). The integration of the VNIR, SWIR, MWIR and LWIR data blocks yielded better classification performance compared to those based on individual techniques. However, the classification performance of the fused four data blocks model did not show improvement over the fused SWIR and MWIR data model. This indicates the need for an optimised approach to identify the optimal combination or an alternative data fusion strategy. The likely reasons for not achieving improved results for the integration of the four data blocks compared to the results from the fused SWIR and MWIR data model could be the dominance of some of the data blocks or the occurrence of redundant information in the data blocks. Each data block resulted in good classification results and indicated the presence of relevant information in the spectra. Therefore, the result from the combination of the four data blocks might be maximised using alternative relevant information extraction techniques and classification models. The MWIR data model results show that MWIR technology alone can play a significant role in the discrimination of ore and waste in low-grade polymetallic sulphide deposits. However, looking at the overall performance trend of the two models (K-means and SVC), the results from fused data blocks models are better than those of the individual data blocks models for the classification of the materials at the indicated cut-off grades.

The classification of the materials at the three cut-off grades resulted in different model performances. For example, at the 3% cut-off grade, very good classification performances were achieved using the MWIR and LWIR data models (Tables 4, 5 and S7); however, at the higher cut-off grades, the performances of these individual data blocks models declined. The fusion of the data blocks for the classification of the materials at the three

cut-off grades resulted in improved classification performances compared to the outputs produced using the individual data blocks models. However, the difference in the performances of the models at the three cut-off grades suggests the importance of model calibration at the required threshold (in this case, cut-off grade).

Comparing the K-means and the SVC models, both models resulted in an improved classification rate for the fused data blocks compared to the individual datasets. Thus, the general performances of the models in showing the presence of relevant information in each data block, and the improved accuracies after data fusion, are comparable. Overall, the results of these models indicate the possibility of integrating image and point data for enhanced characterisation of materials in polymetallic sulphide deposits. These datasets have different scales and resolutions. The conversion of the image data into representative spectra allowed a significant reduction in data volume and permitted the fusion of the image data to point data for the enhanced separation of ore and waste materials in the analysed samples.

As discussed in Chapter 7, the distinct spectral features were used to identify some of the minerals in VNIR and SWIR data. However, the interpretation and identification of minerals using sensor output (spectra) are sometimes challenging for various reasons, such as the co-occurrence of minerals, the physical matrix effect, environmental influences (e.g., moisture) and a weak spectral response from some of the minerals. Thus, the identification of minerals using sensor outputs may result in an incomplete description of the minerals in the analysed samples. This shows the importance of understanding unidentified unique spectra using machine-learning techniques. Accordingly, the features extracted from the VNIR and SWIR data encompass both the identified spectrally pure mineral spectra and the unidentified (e.g., spectrally mixed) unique spectra. The unidentified unique spectra were also represented in the computation of the final spectra. Thus, the proposed approach is beneficial in providing a comprehensive description of mineral compositions in mining operations. The other advantage of the approach is the use of multiple data sources to permit enhanced classification results via the use of relevant information from each technique.

Feature selection requires highly efficient data reduction methods, as the aim is to retain only the most important variables in the model. In this work, the extraction of the endmembers from the VNIR and SWIR data, as well as feature selection using the MWIR and LWIR data, enabled the screening of the most informative variables for the separation of ore and waste materials. While the approach generalises the spectral information (i.e., the conversion of the image data), the generalised data allow for the efficient simplification and classification of materials at different cut-off grades. Thus, the developed methodology is effective in enhancing material characterisation with enormously reduced data volume.

In material characterisation, the techniques VNIR, SWIR and LWIR are commonly used for separate analysis. An integrated analysis of the techniques for enhanced characterisation is very uncommon. Of these limited applications, pixel location-based hyperspectral image fusion is now becoming popular, especially in remote sensing applications. However, this kind of approach is applicable to image-to-image fusion. The proposed approach in this study allows the integration of image and point data, remotely operated sensors with sensors that need actual contact, and data of different coverage, resolutions and scales. The approach further allows the holistic description of materials by providing the opportunity to explore a wider range of the electromagnetic spectrum. The classification accuracies achieved in this study show promise in terms of the separation of ore and waste materials

in polymetallic sulphide deposits using data sources that have different natures (i.e., image and point data). Therefore, this study can serve as a baseline for the integration of different forms of sensor outputs for the improved characterisation of materials in various deposit types.

10.4.5. THE OPPORTUNITIES AND LIMITATIONS OF THE APPROACH

The fusion of multiple sensors is challenging due to data complexity. The extraction of the features from data blocks and fusion helps simplify the data, make the classification results efficient, and can be maximised using optimal features selection methods. The proposed approach significantly minimised data volume while maintaining most of the relevant information in the spectra that can be related to material properties. For example, the average data size of an SWIR hyperspectral image of one of the rock samples used in this study was ~215 MB. However, the conversion of the hyperspectral image to the representative point spectrum reduced the data size to ~27 KB. This considerable reduction in data volume has implications for the requirements for data storage, data processing and visualisation. Thus, it can allow the analysis of high-spatial and -spectral resolution images from large datasets. This suggests the practicality of the approach for use in high-throughput active operational mines.

As discussed in Section 10.3.1 and Table 10.2, both the image and point data have the advantage that the integration of the two datasets likely maximises the benefits. For example, the image data represent all the information from the sample surface at the scene, where the point measurements might be subjected to a subjective decision on the selection of the measurement spots. However, depending on the technology, the point techniques can offer a higher signal-to-noise ratio than the image spectral data. Thus, the fusion of the two data types likely benefits from the synergy between them. The integration of image and point data can also be performed by the decomposition of the point spectra into pure components and the extraction of endmembers from image data. Thus, both datasets can have multiple spectra for each sample; however, such a kind of fusion requires optimal spectral decomposition algorithms and sophisticated data processing techniques.

The sulphide minerals exhibit limited spectral signals in the infrared region of the electromagnetic spectrum. However, the combined analysis of a wide range of infrared spectral data yielded better classification accuracies than the individual data block models. Thus, a combined analysis of these technologies likely results in the enhanced classification or prediction of materials in various deposit types. Moreover, the approach allows for correlating the concentration of the combined Pb and Zn to the spectral responses of the extracted or computed spectra of the VNIR, SWIR, MWIR and LWIR data. The interpretation of spectra might fail to identify all the minerals due to the mineral mixture or weaker signals of the minerals. However, the proposed approach enables the unidentified (unknown) unique spectra to be considered in the computation of the final spectra. Therefore, they are represented in the models based on their proportion.

The developed methodological approach has several potential benefits. For example, it simplifies data, enables the fusion of data from multiple platforms, reduces data volume, enhances classification accuracies, minimises information loss by including information from unidentified unique spectra, and can be used to relate the infrared spectra to quantitative elemental data. Besides, it is a data-driven approach that does not require a prior specification or identification of minerals and elements. Table 10.6 summarises some of the potential benefits and limitations of the proposed method. The limitations of the approach

include that the conversion of the image data into a single spectrum causes the loss of spatial information from the hyperspectral images. The other possible limitation is the loss of information related to the unclassified pixels. The former can be compensated by representing the pixels based on their proportion. The latter can be minimised by representing most of the unique spectra in the training dataset. Overall, this approach is a multi-step process that involves endmember extraction and image classification. Thus, it requires optimal feature extraction and classification techniques to minimise the error propagation in the final results.

Table 10.6: The potential benefits and limitations of the proposed methodological approach.

Benefits	Challenges
Significantly reduces data volume	Data conversion results in a loss of the spatial information (context) at the sample surface
Simplify data dimensions	Simplification or generalization of data might introduce uncertainty
Allow fusion of data having different scales, spatial and spectral resolutions (image and point)	Might cause error propagation
Do not require interpretation of each spectrum; rely on data-driven approaches	
Incorporate the unidentified unique spectra in the analysis, thus minimise the information gap	
Enable multi-sensors data analysis for enhanced classification of ore and waste materials	
Allow correlation of the infrared image and point spectral data to the elemental concentration at different cut-off grades	

The main contribution of this work is to integrate the hyperspectral image and point data using multivariate data analysis techniques and a data fusion approach. The different scales of observations from the image and point data sources were converted to form fused data blocks. The fused data blocks allowed the incorporation of the two data types into a single model for the enhanced separation of ore and waste materials in the analysed samples. Overall, the experimental results suggest the use of the developed methodological approach for the discrimination of ore and waste materials. Besides this, the use of the approach for the separation of the materials at lower cut-off grades suggests its potential applicability in sub-economical deposits. The proposed approach provides a versatile solution for the fusion of multiple sensor outputs in raw material characterisation. The analysed samples are highly variable and limited in number. Going forward, better classification results are possible with extended datasets that sufficiently represent the observed material variability. The successful practical implementation of the approach can lead to the pre-concentration of complex sulphide ore into a major classification of concentrated and less concentrated materials. This plays a significant role in ensuring energy efficiency in mineral processing. The developed method can be a baseline for the development of a framework for the spectral-spatial fusion of data from multiple sensors that have different scales of observation, spatial resolutions and spectral resolutions. Thus, it can play an essential role in the development of an optimally functioning process that informs decision-makers in real-time.

10.5. CONCLUSIONS

In this work, different scenarios were investigated to assess the use of integration of image and point data for the discrimination of ore and waste materials in polymetallic sulphide deposits using infrared technologies, namely:

- (1) the use of individual spectral regions (VNIR, SWIR, MWIR and LWIR);
- (2) the use of the computed representative spectra from the hyperspectral images (VNIR and SWIR);
- (3) potential for improvement in ore–waste discrimination accuracy by applying data fusion.

The experimental results reported in the preceding sections show that the representative spectra computed using the hyperspectral VNIR and SWIR images include relevant information that can be employed in ore–waste discrimination. Moreover, the fusion of the computed VNIR and SWIR spectra significantly improved the classification of ore and waste material in the analysed samples. At the 3% cut-off grade, the best achieved SVC model after fusion of the VNIR and SWIR resulted in a correct classification rate of 81.6%, whereas the results from the individual VNIR and SWIR data blocks at the same cut-off grade are 58% and 73.7%, respectively. At the 5% cut-off grade, the SWIR and MWIR data K-means models yielded correct classification rates of 79% and 81.6%, respectively. However, the fusion of the SWIR and MWIR data blocks improved the classification performance to 92%. Likewise, at the 7% cut-off grade, the fusion of the four data blocks improved the correct classification rate to 90%. Similarly, when the SVC model was applied to the fused four data blocks, the result improved to 95% for the classification of the material at the 3% cut-off grade. The multiple-level fusion of the four data blocks using both the K-means and SVC models resulted in improved classification performances compared to the individual data models. However, the achieved classification performances of the four data blocks models and the fused SWIR and MWIR data blocks are the same. This shows the need for an optimised data fusion approach to identify the optimal sensor combinations out of the possible options. Overall, the use of the individual data blocks coupled with K-means and SVC for the classification of ore and waste materials in the polymetallic sulphide deposit at the 3%, 5% and 7% cut-off grades resulted in good results. Moreover, the use of the data fusion strategy improved the model's classification ability relative to the results yielded by using individual techniques.

The developed workflow provides a versatile solution for the integration of hyperspectral imaging and point spectrometer data for use in material characterisation. The fusion of multi-source (VNIR, SWIR, MWIR and LWIR) spectral data with different spectral information significantly improved ore–waste discrimination at different cut-off grades. This novel methodology is very promising in minimising data volume and provides enhanced material characterisation. The results indicate the possibility and opportunities of the approach in material characterisation. Going forward, better results are possible with an optimised fusion of multiple data blocks for the quantitative and qualitative analysis of materials in various low-grade and high-grade deposits.

REFERENCES

- Agilent. (2020). FTIR Accessories - 4300 Handheld FTIR sampling accessories [Online]. Available: <https://www.agilent.com/en/products/ftir/ftir-accessories/4300-handheld-ftir-sampling-accessories> [Accessed May 2020].
- Desta, F. S. & Buxton, M. W. N. (2018). Chemometric Analysis of Mid-Wave Infrared Spectral Reflectance Data for Sulphide Ore Discrimination. *Mathematical Geosciences*, 51(7), pp. 877-903. doi: 10.1007/s11004-018-9776-4
- Desta, F., Buxton, M., & Jansen, J. (2020). Data Fusion for the Prediction of Elemental Concentrations in Polymetallic Sulphide Ore Using Mid-Wave Infrared and Long-Wave Infrared Reflectance Data. *Minerals*, 10(3), 235. doi: 10.3390/min10030235
- Feng, J., Rogge, D. & Rivard, B. (2018). Comparison of lithological mapping results from airborne hyperspectral VNIR-SWIR, LWIR and combined data. *International Journal of Applied Earth Observation and Geoinformation*, 64, pp. 340-353. doi: 10.1016/j.jag.2017.03.003
- Kopačková, V. & Koucká, L. (2017). Integration of Absorption Feature Information from Visible to Longwave Infrared Spectral Ranges for Mineral Mapping. *Remote Sensing*, 9(10), 1006. doi: 10.3390/rs9101006
- Kruse, F. (2015). Integrated visible and near infrared, shortwave infrared, and longwave infrared (VNIR-SWIR-LWIR), full-range hyperspectral data analysis for geologic mapping. *Journal of Applied Remote Sensing*, 9(1), 096005, doi: 10.1117/1.JRS.9.096005
- Kruse, F. A., Lefkoff, A. B., Boardman, J. W., Heidebrecht, K. B., Shapiro, A. T., Barloon, P. J. & Goetz, A. F. H. (1993). The spectral image processing system (SIPS)—interactive visualization and analysis of imaging spectrometer data. *Remote Sensing of Environment*, 44(2), pp.145-163. doi: 10.1016/0034-4257(93)90013-N
- Lorenz, S., Seidel, P., Ghamisi, P., Zimmermann, R., Tusa, L., Khodadadzadeh, M., Contreras, I.C. & Gloaguen, R. (2019). Multi-Sensor Spectral Imaging of Geological Samples: A Data Fusion Approach Using Spatio-Spectral Feature Extraction. *Sensors*, 19(12), 2787. doi: 10.3390/s19122787
- Malvern Panalytical. (2019). About ASD [Online]. Available: <https://www.malvernpanalytical.com/en/about-us/our-brands/asd-inc> [Accessed December 2019].
- OLYMPUS. (2020). Handheld XRF analyzers [Online]. Available: URL: <https://www.olympus-ims.com/en/xrf-xrd/xrf-handheld> [Accessed May 2020].
- Sun, G., Zhang, X., Jia, X., Ren, J., Zhang, A., Yao, Y. & Zhao, H. (2020). Deep Fusion of Localized Spectral Features and Multi-scale Spatial Features for Effective Classification of Hyperspectral Images. *International Journal of Applied Earth Observation and Geoinformation*, 91, 102157. doi: 10.1016/j.jag.2020.102157
- Wong, T. T. (2015). Performance evaluation of classification algorithms by k-fold and leave-one-out cross validation. *Pattern Recognition*, 48(9), pp. 2839-2846. doi: 10.1016/j.patcog.2015.03.009

11

DATA FUSION FOR SEMI-QUANTITATIVE ANALYSIS OF MINERALS

The previous chapter shows the use of data fusion for the separation of ore and waste materials in a polymetallic sulphide deposit. This chapter presents the use of data fusion approaches for semi-quantitative analysis of minerals in polymetallic sulphide ore using the MWIR and LWIR sensor technologies. The chapter compares two low-level data fusion approaches; one without features selection the other with feature selection for the prediction of mineralogical concentrations using PLSR, PCR and SVR algorithms. The analysis was performed using the channel, drill core and muck pile samples from the test case.

Parts of this chapter have been published in:

Desta, F., Buxton, M. & Jansen, J. (2020). Fusion of Mid-Wave Infrared and Long-Wave Infrared Reflectance Spectra for Quantitative Analysis of Minerals. *Sensors*, 20 (5), 1472. doi: 10.3390/s20051472

In this work, data fusion approaches for integrating datasets pertaining to the MWIR and LWIR spectral regions are proposed, aiming to facilitate more accurate prediction of SiO_2 , Al_2O_3 , and Fe_2O_3 concentrations in a polymetallic sulphide deposit. Two approaches of low-level data fusion were applied to these datasets. In the first approach, the pre-processed blocks of MWIR and LWIR data were concatenated to form a fused data block. In the second approach, a prior variable selection was performed to extract the most important features from the MWIR and LWIR datasets. The extracted informative features were subsequently concatenated to form a new fused data block. Next, prediction models that link the mineralogical concentrations with the infrared reflectance spectra were developed using PLSR, PCR and SVR analytical techniques. These models were applied to the fused data blocks as well as the individual (MWIR and LWIR) data blocks. The obtained results indicate that SiO_2 , Al_2O_3 , and Fe_2O_3 mineral concentrations can be successfully predicted using both MWIR and LWIR spectra individually, but the prediction performance greatly improved with data fusion; where the PLSR, PCR, and SVR models provided good and acceptable results. The proposed approach could be extended for online analysis of mineral concentrations in different deposit types. Thus, it would be highly beneficial in mining operations, where indications of mineralogical concentrations can have significant financial implications.

11.1. INTRODUCTION

Geometallurgical investigation links the geological and mineralogical characteristics to the metallurgical performance of an orebody. It is an important approach to optimise resource efficiency and reduce the technical risk associated with mining operations. The required information for geometallurgical applications is not limited to knowledge on the grades of valuable elements and their variability, but also extends to the gangue minerals, as their composition and volume also play a crucial role in ore processing. Extant studies highlight the importance of mineralogical information for the sustainability and energy efficiency of geometallurgical processes (David, 2013; Dominy et al., 2018). Ore minerals occur in veins, disseminated in the host rock and/or in pores with varying concentrations of other associated minerals such as silica, oxides and carbonates. The concentration of these minerals can be associated with the metallurgical behaviour of the ore minerals. Therefore, quantitative mineralogical information on the co-occurring minerals is one of the crucial parameters for the optimisation of ore processing.

Despite rapid advances in sensor technologies, there is still a demand for novel ideas to enable quantitative investigations of mineralogical compositions using sensor-derived data. In addition, in-situ application of sensor technologies requires portable and high-speed systems. Portable sensor technologies (such as XRF and SWIR) that provide geochemical or mineralogical data are available. However, most of the currently available sensor technologies are laboratory-based techniques. Owing to the growing interest in an accurate, in-situ and on-line quantitative analysis of minerals, infrared technologies coupled with advanced data analytics can be promising alternative tools.

Numerous previous studies indicate that infrared technologies can be utilised for the accurate identification of minerals. Such applications are usually qualitative. For example, near-infrared (NIR) sensors can provide accurate identification of clay minerals and rock-forming minerals (Spectral Evolution, 2019; Szalai et al., 2013), whereas SWIR is one of the most widely used infrared technologies for the identification of alteration minerals (Dalm et al., 2018; Sun et al., 2001). On the other hand, LWIR permits identification of rock-forming minerals, whereas far-infrared (FIR) can be used for the identification of rare earth minerals (Clark, 1999; Karr and Kovach, 1969). Characteristic features of the minerals have also been utilised to quantitatively relate variations in mineral concentrations. For example,

Hecker et al. (2012) estimated concentrations of rock-forming minerals using LWIR. Similarly, Mroczkowska-Szerszeń and Orzechowski (2018) used ATR-FTIR (attenuated total reflectance Fourier transform infrared) for semi-quantitative analysis of minerals in carbonate rocks. Palayangoda and Nguyen (2012), on the other hand, estimated mineral concentrations in oil shale using ATR-FTIR spectra combined with PCR method. In another study, Guatame-García and Buxton (2018) assessed the use of infrared spectroscopy for predicting the soluble Al_2O_3 content in calcined kaolin. Although few researchers indicated the potential for using infrared technologies in quantitative analysis of minerals, some authors also discussed the limitations of this approach. Specifically, Kaufhold et al. (2012) assessed the possibility of the use of infrared spectra for quantitative analysis of clay minerals and pointed out the mineral-specific challenges owing to instrument detection limit, availability of suitable reference and particle size. At present, infrared techniques are insufficiently used in quantitative analysis of minerals. Moreover, most of the existing studies in this field addressed the challenge for the development of reliable calibration models to predict mineral concentrations in complex mixtures. Consequently, there is a need for advanced data-driven approaches and spectral signal pre-processing techniques that can be incorporated into comprehensive calibration models, thus to achieve accurate estimation of mineral concentrations in different commodities.

As discussed in Chapter 4, fusing of different data sources enhances the reliability of prediction or classification models owing to the synergy among the incorporated datasets. Data fusion can be implemented in different ways and at different levels using various multivariate linear (e.g., PLSR) and non-linear (e.g., SVM) data analysis techniques (Borràs et al., 2015; Cocchi, 2019). Findings yielded by pertinent studies indicate that data fusion approaches can be highly beneficial for mineralogical applications (Chari et al., 2005; Khajehzadeh et al., 2017). However, at present, the application of data fusion for mineralogical investigations remains very limited.

To date, quantitative analysis of minerals in polymetallic sulphide ore samples using MWIR and LWIR spectra combined with data fusion methods has never been conducted. This gap in the current analytical methodology and the promising findings (Desta and Buxton, 2018; Desta et al., 2020) reported recently have motivated the present study. Its main aims are thus (1) to investigate the use of diffuse reflectance infrared (MWIR and LWIR) spectra for quantitative analysis of mineral mixtures in polymetallic sulphide ore samples, (2) to access the effect of different data pre-processing techniques on the prediction performance, (3) to assess the potential improvement in the prediction accuracies after data fusion, and (4) to evaluate the data fusion methods using linear (PLSR and PCR) and non-linear (SVR) multivariate regression techniques. The implemented low-level data fusion approaches are data fusion without feature selection (fusion of the entire variables in the MWIR and LWIR data blocks) and with feature selection (fusion of the extracted features of the two data blocks).

11.2. MATERIALS AND INSTRUMENTATION

11.2.1. MID-WAVE INFRARED AND LONG-WAVE INFRARED DATASETS

The study described in this paper is based on 58 representative rock samples collected from the test case site. The samples were obtained from the ore and waste materials, which are sourced from different locations. The collected samples were powdered, and measurements were performed using the Agilent portable 4300 FTIR sensor. The data

acquisition procedures followed for the collection of data are described in Chapter 8. Samples heterogeneity was accommodated by collecting multiple spectra from each sample. Depending on the observed variability within each sample, 7 to 10 measurements were collected, and the averages were subsequently computed for each sample. The acquired full-range FTIR dataset (covering the full wavelength span from 2.5 to 15.0 μm) were split into MWIR (2.5 to 7.0 μm) and LWIR (7.0 to 15.0 μm) spectral datasets. The full-range FTIR data were also analysed to compare the obtained results with the individual datasets and the data fusion outcomes. Therefore, the SiO_2 , Al_2O_3 , and Fe_2O_3 composition prediction accuracy obtained using the three datasets (namely full-range FTIR, MWIR, and LWIR) and the fused datasets pertaining to 58 samples are discussed and compared in the sections that follow.

11.2.2. CHEMICAL ANALYSIS

XRF is an established method for determining the major and minor elements constituting whole rock (SGS, 2019). As mentioned in Chapter 3, a conventional laboratory-based XRF was used to acquire mineralogical information on SiO_2 , Al_2O_3 , and Fe_2O_3 minerals. The quantitative mineralogical data obtained were employed in the validation of the developed methodological approaches.

11.3. METHODOLOGY

11.3.1. MULTIVARIATE ANALYSIS

As a part of the exploratory data analysis, PCA was performed. Quantitative prediction of mineral concentrations in the polymetallic sulphide ore samples was achieved using both linear (PLSR and PCR) and non-linear (SVR) techniques. A brief description of these multivariate techniques is given in Chapter 4. In this study, PCA was performed to reduce data dimension by generating new sets of variables PCs. It was applied to the individual datasets as well as to the fused spectral data. The scores and loading plots of the PCA models were used to investigate sample–variables relationships and the grouping structure (intra-sample relationships). The PLSR models were developed using both individual and fused data blocks. The dependent variables (the response) are mineral concentrations and the independent variables (the predictors) are the infrared spectra (e.g., MWIR and fused data blocks). The calibration datasets were used to develop the PLSR models and their predictive performance was validated using independent datasets (validation datasets). The PCR models were developed using the IR spectra (individual MWIR and LWIR, as well as fused data blocks) as the predictor and the mineral concentrations as the response variables. The singular value decomposition (SVD) algorithm was used to calculate the PCs of the PCR models. The weights of X variables and the Y variables were standardised.

For the implementation of SVR, three different kernel functions (RBF, sigmoidal, and polynomial) were examined and the optimal kernel function was selected based on the RMSE and R-squared values. As result, RBF kernel function was selected. RBF can be utilised to model non-linear systems of varying complexity. The SVM regression type used in this work is ϵ -SVR with RBF kernel function. The key model parameters for the specification of ϵ -SVR models are C value and epsilon (ϵ), as they respectively determine the trade-off between the training error and the model complexity (flatness), and control the width of the band where the cost of errors in the epsilon-intensive loss function is zero. The value of ϵ can thus affect the number of SVs used to construct the regression function.

The ϵ -SVR models developed as a part of this work use the infrared spectra (comprising the individual and fused datasets) as the input vector and mineral (SiO_2 , Al_2O_3 , and Fe_2O_3) concentrations as the response vector. As in SVM the values of the optimal model parameters are not known in advance, C and ϵ were optimised using grid search approach with a leave-one-out cross-validation.

11.3.2. MODEL PERFORMANCE ASSESSMENT

The performance of the prediction models was investigated using root mean square error of cross validation (RMSECV), the root mean square errors of prediction (RMSEP) and the coefficient of determination (R^2) of the prediction value. Lower statistical error terms (RMSECV and RMSEP) and higher predicted R^2 signify an improved predictive performance. In RMSECV, the error on test split is calculated using a cross-validation scheme; however, performance is based on the calibration cases. In this work, the RMSECV corresponds to the results of a LOOCV that prevents model over-fitting. The RMSECV was used to select the optimal number of PCs in the PLSR and PCR models, and to specify model parameters in SVR.

11.3.3. DATA PRE-PROCESSING

The undesired variation in the infrared data is removed to enhance the signal pertaining to the analytical information. The choice of data filtering techniques adopted for this purpose affects the outcome (Rinnan et al., 2009; Roussel et al., 2014). Therefore, DoE was developed considering MC and the signal correction methods, namely baseline correction, normalisation, SNV and smoothing (Gaussian filter smoothing) data pre-processing techniques. These methods were chosen, as the aim was to remove the most common artefacts from the infrared spectra (e.g., baseline shift). Detail descriptions of the pre-processing techniques are presented in Chapter 4.

11.3.4. DATA FUSION

The schematic diagram of the data fusion method adopted in this work is provided in Figure 11.1. As can be seen, the pre-processed datasets and the three multivariate techniques (PLSR, PCR, and SVR) were used for the realisation of low-level fusion of the MWIR and LWIR data blocks without feature selection and with feature selection (the grey and blue boxes of Figure 11.1, respectively). The methodological approaches applied for the implementation of the two data fusion approaches are described below.

11.3.4.1. LOW-LEVEL DATA FUSION WITHOUT FEATURE SELECTION

Depending on the dataset or detector, the amount and type of noise might differ across the infrared range. Therefore, pre-processing of the individual data blocks, separately, allows investigating and treating the various noise sources across the two infrared (MWIR and LWIR) wavelength ranges, independently. In the low-level fusion without feature selection approach, the individual pre-processed reflectance spectra acquired from the MWIR and LWIR data sources were concatenated into a single matrix, as shown in the grey box of Figure 11.1. Therefore, four fused data blocks were generated, corresponding to the application of four pre-processing techniques (SNV, normalise, baseline, and smoothing) to the individual data blocks (MWIR and LWIR). The fused data blocks were used to develop the prediction models using PLSR, PCR, and SVR algorithms, as shown in Figure 11.1. The

models were developed using the training (calibration) datasets and were subsequently validated using the independent (validation) datasets.

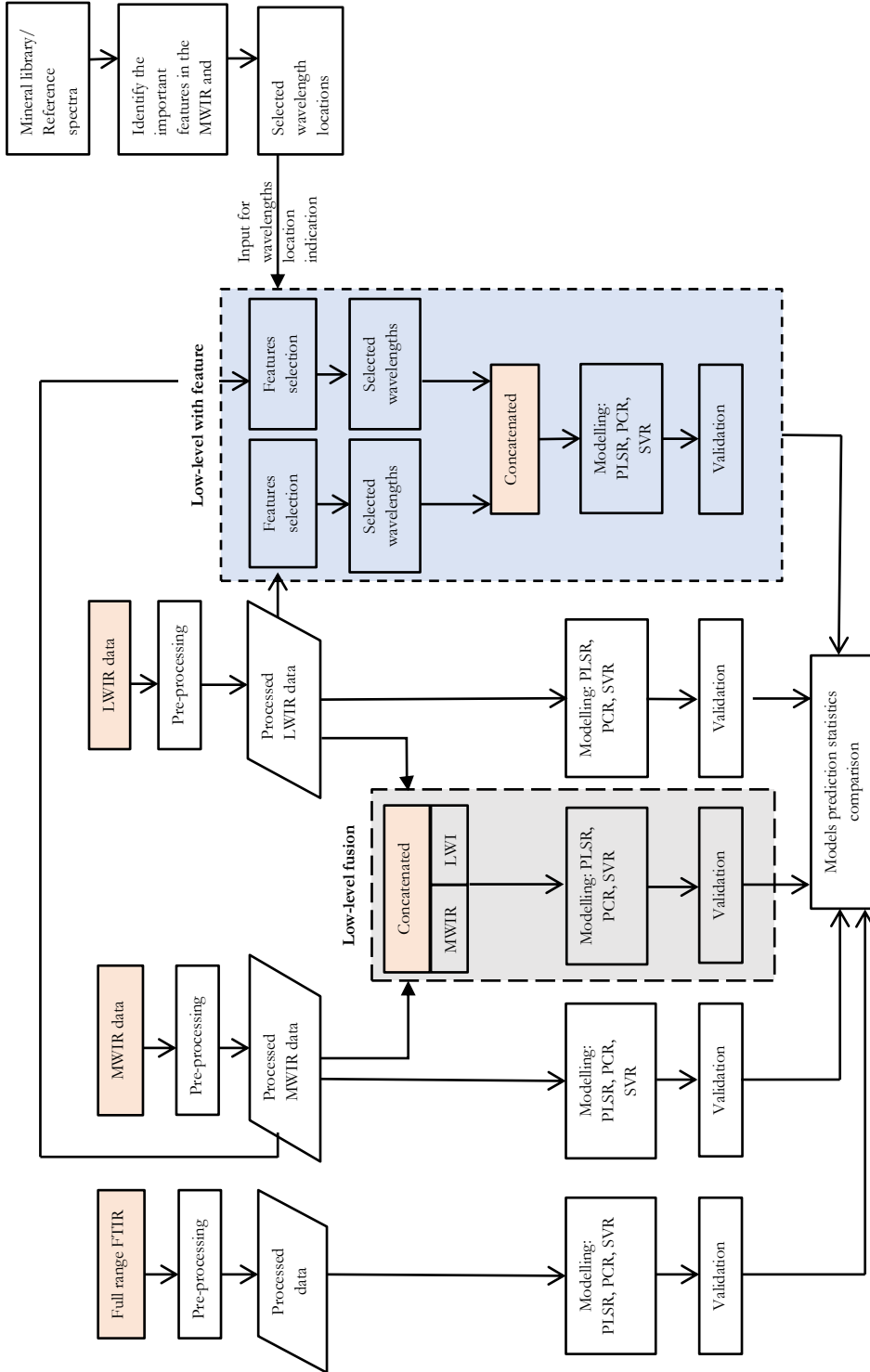


Figure 11.1: Workflow diagram depicting the steps of the low-level fusion (1) without feature selection (the grey box) and (2) with feature selection (the blue box).

11.3.4.2. LOW-LEVEL DATA FUSION WITH FEATURE SELECTION

Unlike low-level fusion, mid-level data fusion requires features reduction, which is achieved through variable screening, and thus allows all non-informative variables to be removed in the feature selection step. The mid-level fusion requires a modelling step for the extraction of the informative features. However, the feature selection method deployed in this study was not based on models' outputs. Thus, the approach is not a standard mid-level fusion where modelling is involved for the extraction of the important variables. Therefore, it is referred to as a low-level fusion with feature selection.

In the low-level fusion with feature selection approach, informative features (in this case, those that contain information pertinent for the prediction of mineral compositions of interest) were independently extracted from the MWIR and LWIR data blocks. The variable selection or feature extraction technique used in this study is based on the reference spectra of the minerals from the well-established mineral spectral libraries. Feature selection requires highly efficient data reduction methods, as the aim is to retain only the most important variables in the model. The mineral libraries show the infrared reflectance spectra of the (relatively pure) minerals and were used to identify the wavelength locations of the spectral features corresponding to the functional groups of the target minerals (e.g., Si–O). In this work, the hypothesis for the low-level fusion with feature selection implementation is that variables that correspond to the main spectral features are the most informative for the prediction of mineral concentrations. Therefore, variable screening was performed based on a prior knowledge-based approach.

The pre-processing techniques described in Section 10.3.3 were applied on the individual datasets prior to variable screening. Subsequently, the important variables (relevant information related to the chemical composition) were retrieved from both MWIR and LWIR pre-processed data blocks separately. The extracted features from the two data blocks were aligned and concatenated into a single matrix. Therefore, the most relevant variables that explain most of the variations in the spectra were fused and mean centred. Prediction models were developed using the fused data blocks comprising of the extracted features and the three multivariate regression techniques (PLSR, PCR, and SVR). The workflow of the low-level fusion with feature selection approach is presented in the blue box of Figure 11.1.

11.3.4.3. INDIVIDUAL DATASETS

The prediction models were developed using the individual data blocks (MWIR and LWIR) and the three aforementioned analytical techniques (PLSR, PCR, and SVR). The Y (response) variables are the concentrations of the minerals (SiO_2 , Al_2O_3 , and Fe_2O_3). A series of models were developed using the pre-processed MWIR and LWIR data separately. The prediction performance of each model was evaluated using independent validation datasets. Next, performance of the prediction models based on the fused datasets was compared with that of the models developed using individual data blocks (MWIR and LWIR). In the present study, the MWIR and LWIR spectral data were acquired using a single instrument (physically integrated system). Thus, to assess the performance of the full-range FTIR data model with the fused and individual data blocks, prediction models were developed using the full-range FTIR data. The main difference between the full-range FTIR data and the low-level fusion is the later pre-processed the individual datasets separately and concatenated. Whereas, the former considers both ranges (the MWIR and LWIR) in the pre-processing stage. The low-level fusion approach is useful in treating different forms of

noise in the spectra data block by data block. Finally, the prediction performances of the models developed using the individual techniques, the full-range FTIR and the two low-level data fusion approaches were assessed based on the RMSECV, RMSEP, and R^2 values.

11.3.5. CALIBRATION AND VALIDATION DATASETS

The 58 samples that were analysed were divided into calibration and validation subsets using a random sample selection algorithm, which was first applied to the MWIR dataset. The randomly selected samples were assigned into the calibration and validation datasets of the full-range FTIR and LWIR datasets. The same procedure was followed for the three datasets (Si_2O_3 , Al_2O_3 , and Fe_2O_3) to ensure that all models related to each mineral utilise the calibration and validation datasets comprising of the same samples. The calibration dataset consisted of 43 sample measurements and the validation dataset included 15 remaining measurements. To allow a direct model comparison, the same split was maintained in the calibration and validation datasets of the individual data blocks (MWIR and LWIR), the full-range FTIR dataset, and the fused datasets. In this study, all the analyses were performed using the Unscrambler and R software.

11.4. RESULTS AND DISCUSSION

11.4.1. SPECTRAL FEATURES OF THE MINERALS

Typical MWIR and LWIR spectra of nearly pure SiO_2 , Al_2O_3 , and Fe_2O_3 are shown in Figure 11.2. In the MWIR region, the Al_2O_3 spectrum exhibits significant features at 2.9 μm , 3.97 μm , 4.75 μm , and 6.28 μm wavelengths. In the LWIR region of the SiO_2 spectrum, stretching vibration modes can be seen in the 8–10 μm and 12–14 μm regions due to Si-O stretching. Fe_2O_3 spectrum similarly shows prominent spectral features (peaks) at 3.45 μm , 3.97 μm , 5.57 μm , and 6.76 μm . The spectra pertaining to the three minerals show important features (prominent peaks) that are caused by the molecular vibration of the functional groups of each mineral. Therefore, it is likely that the mineral concentrations can be related to the reflectance value of each sample's spectrum.

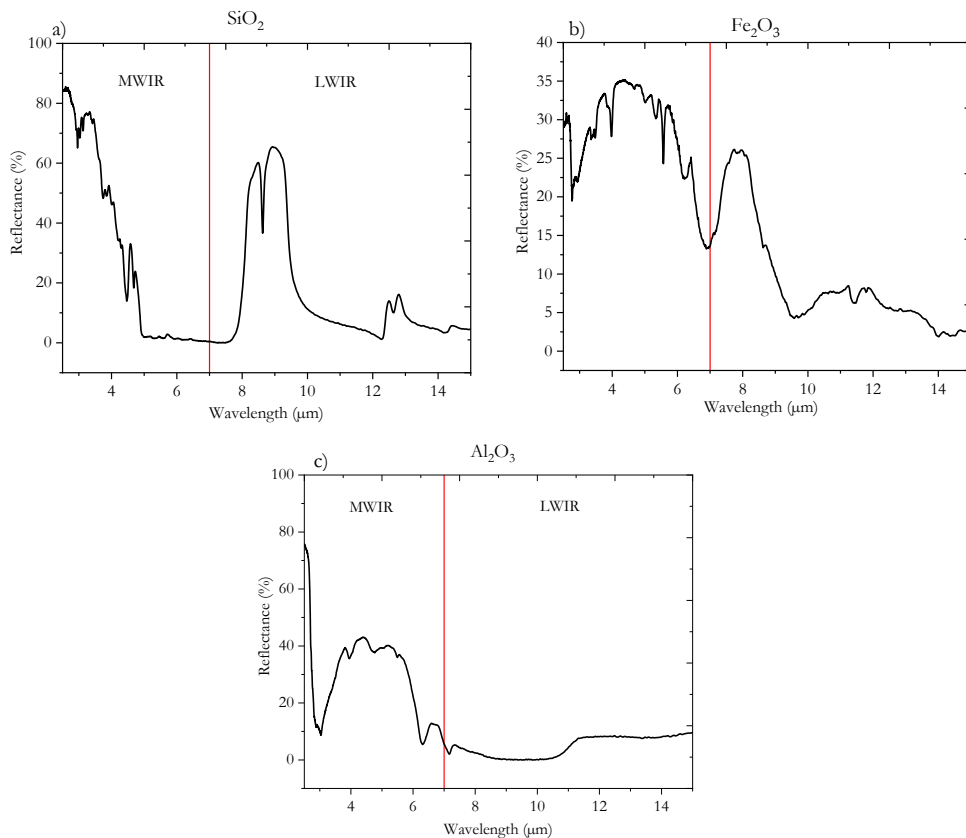


Figure 11.2: The mid-wave infrared (MWIR) and long-wave infrared (LWIR) reflectance spectra of (a) SiO₂; (b) Fe₂O₃; and (c) Al₂O₃ (Source: NASA, 2019).

11.4.2. EXPLORATORY ANALYSIS

Mineral concentrations varied greatly among the analysed samples, as the Fe₂O₃ value ranged from 3.03 to 59.9 wt% with a mean of 24.61, whereas the SiO₂ value ranged from 1.66 to 84.1 wt% with a mean of 41.28 wt%, and 0.06–15.9 wt% (M = 4.22 wt%) was obtained for Al₂O₃. Figure 11.3 shows the PCA model score plots of the full-range FTIR data for the SiO₂, Fe₂O₃, and Al₂O₃ datasets. The plots provide information on the potential patterns that are related to the mineral's concentration.

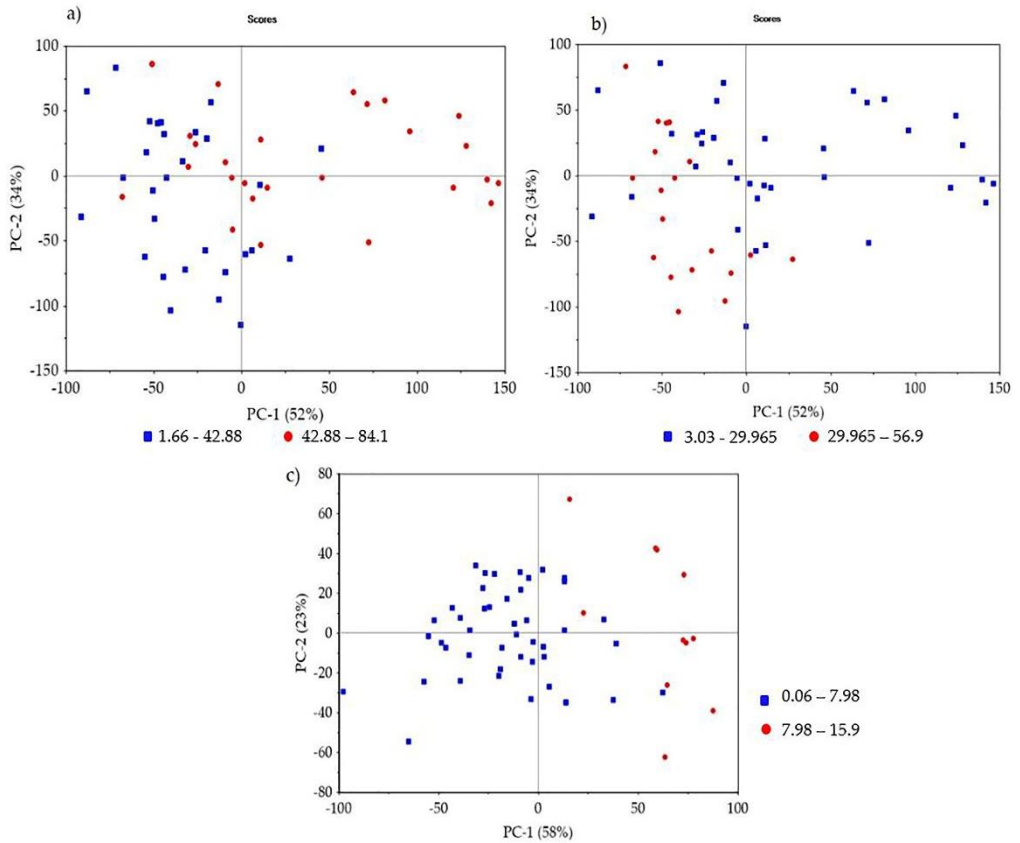


Figure 11.3: PCA model score plots of (a) SiO₂; (b) Fe₂O₃; and (c) Al₂O₃ concentrations categorized into two ranges (the concentrations are expressed in wt %).

11.4.3. MWIR AND LWIR DATA MODELS

In Tables 11.1–11.3, the calibration and prediction statistics of the five datasets for Fe₂O₃, SiO₂, and Al₂O₃ prediction, respectively, are summarised. The prediction models were developed once each dataset has been subjected to the data pre-processing techniques mentioned in Section 10.3.3. However, the prediction performance of the data models declined after SNV filtering and not showed significant improvement after data smoothing. Therefore, the tabulated data indicate model performance after normalisation and baseline correction have been applied to the datasets.

It is evident that a more accurate prediction was obtained by applying the data pre-processing techniques to MWIR, LWIR, and full-range FTIR datasets. For example, for Al₂O₃ prediction using PLSR, the normalised MWIR data model resulted in an improved performance than the raw MWIR data model (Table 11.3). Similarly, the prediction performance of both PCR and SVR models improved after data pre-processing (Tables 11.1–11.3). For all three models (PLSR, PCR, and SVR) used to predict Fe₂O₃ and SiO₂, the error terms declined and the R² value improved after MWIR data normalisation. Likewise, the LWIR data models developed using the three algorithms (PLSR, PCR, and SVR) exhibited improvement after data pre-processing. For example, for the prediction of

SiO₂ concentration, the normalised LWIR data model showed a remarkable improvement than the raw LWIR data model (Table 11.2).

As can be seen from the results reported in Table 11.1–11.3, normalisation of the infrared data resulted in remarkable improvement in the performance of all models, suggesting presence of undesired intensity variations in the spectra caused by multiplicative effects. On the other hand, not all data filtering techniques necessarily improved model performance, as was the case for the SNV filtering technique, irrespective of the dataset or multivariate regression method (PLSR, PCR, or SVR) used. This is most likely due to the minimal effects of light scattering and particle size in the infrared spectra of the analysed samples. Combination of the pre-processing techniques were analysed for the prediction of the mineral's concentration, however, the prediction performances of the models were not improved, thus the results are not included in this paper.

It is also evident that the prediction performance of models based on MWIR and LWIR data depends on the mineral type. For example, LWIR-based models outperform those utilising MWIR data in the quantification of the SiO₂ concentration (Table 11.2). Conversely, MWIR data models yielded more accurate Al₂O₃ concentration prediction (RMSEP = 1.86, R² = 0.85) than those based on LWIR (RMSEP = 2.14, R² = 0.8), as shown in Table 11.3. It is likely that prediction accuracy is linked to the amount of spectral information (relevant spectral features) in the infrared dataset. For example, as shown in Figure 11.2 and discussed in Section 10.4.1, the Al₂O₃ spectrum contains more informative spectral features in the MWIR region than in the LWIR region. Conversely, the SiO₂ spectrum shows a greater number of prominent spectral features in LWIR than in the MWIR region (Figure 11.2), thus resulting in superior prediction of SiO₂ concentration by the model based on LWIR data.

Table 11.1: Statistical summary of the PLSR, PCR, and SVR models for the prediction of Fe₂O₃. The concentrations of Fe₂O₃ in the analysed samples were in the range of 3.03–59.9 wt%.

Datasets/ Fusion method	Pre- processing	PLSR		PCR		SVR	
		RMSEP	R ²	RMSEP	R ²	RMSEP	R ²
MWIR	Raw	6.18	0.78	7.88	0.64	5.50	0.81
	Normalise	4.53	0.88	4.97	0.86	3.95	0.90
	Baseline	5.02	0.86	4.01	0.91	6.39	0.77
LWIR	Raw	7.32	0.69	5.97	0.80	4.78	0.85
	Normalise	4.51	0.88	5.34	0.84	4.57	0.87
	Baseline	7.50	0.68	5.79	0.81	5.26	0.84
Full-range	Raw	6.05	0.79	5.2	0.84	4.71	0.87
	Normalise	3.68	0.92	3.95	0.91	3.40	0.93
	Baseline	4.29	0.89	4.03	0.91	4.86	0.87
Low-level	Normalise	3.30	0.94	3.36	0.94	3.16	0.95
	Baseline	4.57	0.88	3.87	0.91	4.94	0.84
Low-level with the selected features	Normalise	4.22	0.90	4.44	0.89	4.34	0.89
	Baseline	5.18	0.85	5.76	0.81	7.34	0.69

Table 11.2: Statistical summary of the PLSR, PCR, and SVR models for the prediction of SiO₂. The concentrations of SiO₂ in the analysed samples were in the range of 1.66–84.1 wt%.

Datasets/ Fusion method	Pre- processing	PLSR		PCR		SVR	
		RMSEP	R ²	RMSEP	R ²	RMSEP	R ²
MWIR	Raw	7.95	0.87	8.22	0.86	10.30	0.74
	Normalise	7.77	0.88	8.80	0.84	8.47	0.86
	Baseline	8.40	0.86	7.38	0.89	9.89	0.82
LWIR	Raw	12.8	0.67	9.69	0.81	9.13	0.83
	Normalise	6.12	0.92	6.50	0.91	6.56	0.90
	Baseline	9.13	0.83	9.06	0.83	8.74	0.85
Full-range	Raw	6.95	0.90	7.55	0.88	9.14	0.86
	Normalise	6.42	0.92	7.16	0.90	7.52	0.90
	Baseline	7.19	0.90	8.44	0.86	9.08	0.83
Low-level	Normalise	5.96	0.93	7.17	0.90	6.85	0.90
	Baseline	7.66	0.88	8.56	0.85	8.69	0.89
Low-level with the selected features	Normalise	6.40	0.92	6.06	0.93	6.77	0.91
	Baseline	8.30	0.86	8.37	0.86	10.10	0.81

Table 11.3: Statistical summary of the PLSR, PCR, and SVR models for the prediction of Al₂O₃. The concentrations of Al₂O₃ in the analysed samples were in the range of 0.06–15.9 wt%.

Datasets/ Fusion method	Pre- processing	PLSR		PCR		SVR	
		RMSEP	R ²	RMSEP	R ²	RMSEP	R ²
MWIR	Raw	2.16	0.79	2.05	0.81	1.69	0.86
	Normalise	1.86	0.85	1.92	0.84	1.93	0.83
	Baseline	2.11	0.80	1.99	0.82	1.68	0.88
LWIR	Raw	2.47	0.73	2.59	0.70	2.3	0.77
	Normalise	2.09	0.80	2.03	0.82	1.86	0.85
	Baseline	2.29	0.76	2.71	0.75	1.83	0.84
Full-range	Raw	2.02	0.82	1.99	0.82	1.75	0.87
	Normalise	2.02	0.82	1.99	0.82	1.9	0.85
	Baseline	2.15	0.79	1.82	0.85	1.69	0.87
Low-level	Normalise	1.95	0.83	2.06	0.81	1.83	0.86
	Baseline	2.06	0.81	2.13	0.80	1.68	0.88
Low-level with the selected features	Normalise	1.40	0.91	1.48	0.90	1.79	0.86
	Baseline	1.82	0.85	1.77	0.86	1.59	0.89

As shown in Figure 11.2, the pure minerals show spectral features in both MWIR and LWIR regions. However, the spectrum of each sample also includes information pertaining to the complex matrix of sulphide minerals, making identification of each individual component challenging. For this reason, in this work, three multivariate analysis techniques (PLSR, PCR, or SVR) were adopted, confirming that semi-quantification of the minerals in a polymetallic sulphide ore samples was possible using individual MWIR and LWIR datasets.

This is an interesting finding, since the MWIR region of the electromagnetic spectrum is rarely used in lithological material characterisation.

11.4.4. LOW-LEVEL FUSION WITHOUT FEATURE SELECTION

In low-level data fusion, data integration occurs in the initial stages of the analytical data flow, after proper pre-processing (Cocchi, 2019). Thus, mineral concentration prediction based on this approach is highly influenced by the choice of pre-processing techniques. In the present study, as shown in Table 11.1, a better prediction of Fe_2O_3 concentration (RMSEP = 3.31, $R^2 = 0.94$) was achieved using the PLSR model when the normalised MWIR and LWIR data blocks were fused than when these datasets were treated with SNV (RMSEP = 4.76, $R^2 = 0.87$). Moreover, the SVR model resulted in a better prediction of Fe_2O_3 after normalisation (RMSECV = 3.90, RMSEP = 3.16, $R^2 = 0.95$) relative to that yielded by the PLSR or PCR models (Table 11.1 and Figure 11.4).

Similarly, enhanced SiO_2 prediction was achieved after the normalised MWIR and LWIR data blocks were fused compared to the outputs produced using other pre-processing techniques (Table 11.2). For the prediction of Al_2O_3 , low-level fusion of normalised MWIR and LWIR data blocks resulted in a better prediction than when the data blocks were treated with the other data filtering techniques (Table 11.3 and Figure 11.5). These findings confirm the need for adopting DoE in the selection of most optimal data filtering techniques.

As noted in Section 10.2.1, the MWIR and LWIR datasets were acquired using a single-sensor FTIR spectrometer. This allowed the performance of models based on the full-range FTIR data (which includes both MWIR and LWIR datasets) to be assessed and compared to the low-level fusion results. The findings revealed that the prediction models applied to the dataset formed by low-level fusion are superior to the full-range FTIR data models. For example, for the prediction of Fe_2O_3 , the optimal PLSR model after low-level fusion has an RMSEP = 3.3 and R^2 value of 0.94, compared to RMSEP = 3.68 and $R^2 = 0.92$ obtained for the full-range FTIR (Table 11.1). Similarly, using low-level fusion for the prediction of SiO_2 and Al_2O_3 concentration is superior to the results obtained using the full-range FTIR data (Table 11.2 and 11.3). This might be due to the different amount of noise in the MWIR and LWIR wavelength regions that require independent pre-processing of the two data blocks. Even though these improvements are not statistically significant, the results suggest data fusion as a better and comparative option for a combination of multiple sensors. This is an interesting point, since the physical integration of multiple sensors into a single platform is challenging and expensive, in terms of practical implementation. Thus, for a combination of multiple data sources, data fusion can be considered as an economic and practical alternative option.

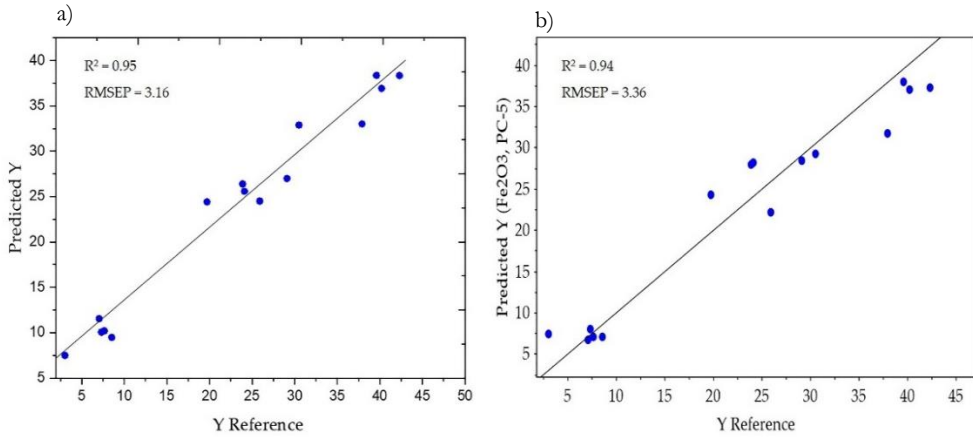


Figure 11.4: (a) SVR; and (b) PCR regression results for the predicted vs. actual Fe_2O_3 concentration after applying low-level fusion on the normalised MWIR and LWIR data blocks.

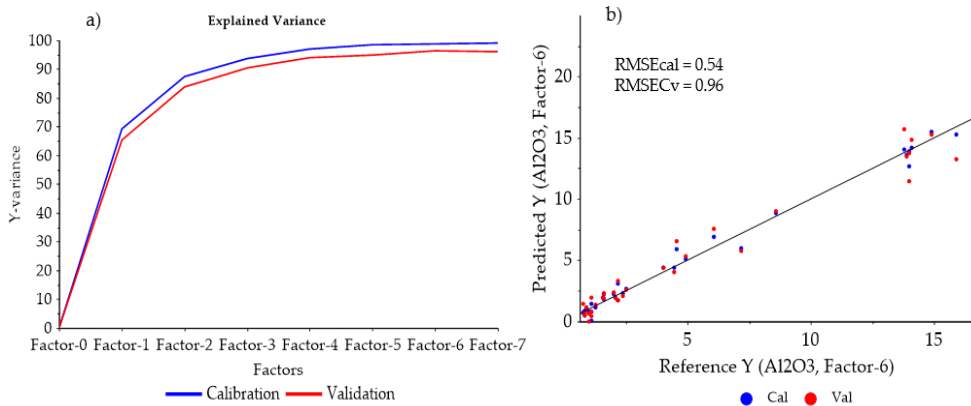


Figure 11.5: PLS regression results based on the dataset formed by low-level fusion of the normalised MWIR and LWIR data blocks for predicting Al_2O_3 concentrations (a) the explained variance (b) the predicted vs. actual concentration for the calibration (RMSEcal) and cross-validation (RMSECV) models.

11.4.5. LOW-LEVEL DATA FUSION WITH FEATURE SELECTION

In this study, the extracted informative variables from the two data blocks are indicated in Table 11.4. The prediction of Al_2O_3 concentration using PLSR and the low-level fusion with the selected features after data normalization, significantly improved compared to applying the models to datasets subjected to low-level fusion without feature selection as well as the full-range FTIR data models (Table 11.3). Similarly, after low-level fusion with the selected features, enhanced Al_2O_3 prediction performance was observed for models based on the PCR and SVR (Table 11.3). These findings indicate that the feature selection approach was able to capture most of the important variations in the spectral data. In addition, by excluding the irrelevant information, feature selection method enhanced the prediction performance of the Al_2O_3 models.

Table 11.4: The wavelength range of the features related to SiO_2 , Al_2O_3 , and Fe_2O_3 mineral composition extracted from the MWIR and LWIR reflectance datasets.

Minerals	MWIR wavelength (μm)	LWIR wavelength (μm)
	2.85–3.10	7.00–7.29
Al_2O_3	3.83–5.73, 6.20–6.40	10.50–11.40
	2.78–2.92, 3.38–3.5, 3.92–4.03, 5.0–5.10	7.00–7.20, 7.74–8.05, 9.38–10.00
Fe_2O_3	5.30–5.39, 5.53–5.69, 6.15–6.31, 6.76–7.00	11.30–11.6, 13.90–14.10, 14.40–14.60
SiO_2	3.65–4.93	8.00–10.00, 12.00–13.00

The SiO_2 and Fe_2O_3 prediction models after the selected features fusion were better than the individual datasets models (Table 11.1, 11.2, and Figure 11.6). However, low-level fusion without feature extraction resulted in a better Fe_2O_3 and SiO_2 concentration prediction relative to the extracted features fusion (Table 11.1 and 11.2). This is likely due to the fact that not all relevant information was retained in the extracted spectra of the minerals. Therefore, alternative feature extraction techniques (e.g., multivariate curve resolution-MCR) can likely improve the fusion results.

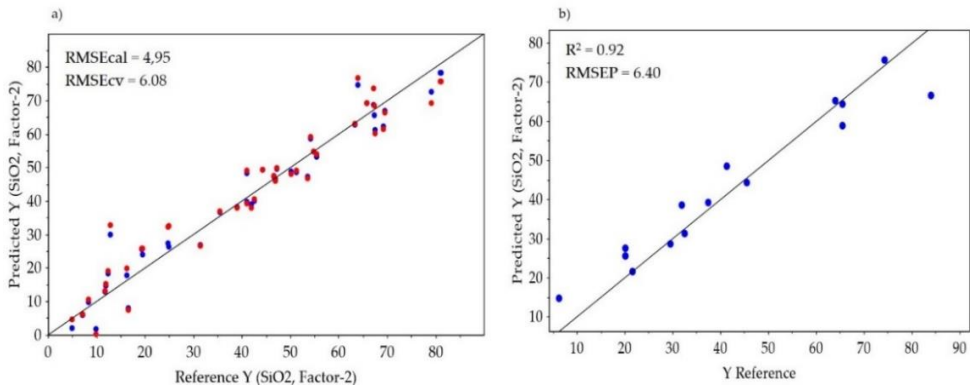


Figure 11.6: PLS regression of predicted vs. actual SiO_2 concentration after the selected features fusion of the normalised MWIR and LWIR data blocks (a) for calibration and cross-validation; and in (b) the prediction model.

The main advantage of feature selection (variable screening) is that non-informative variation can be removed in the variable screening step, potentially enhancing the prediction accuracy. The rapid advances in sensor technologies allow generation of multi- and megavariate data. These datasets can be utilised in data-driven approaches. Nonetheless, high data volume remains a significant challenge for both data processing and storage. Therefore, data volume reduction without loss of information is always preferable. This can be achieved using multivariate data analysis techniques and data fusion approaches. For example, in this work, when variable screening was performed prior to the implementation of the low-level data fusion, data volume reduction from 79% to 58% was achieved. Specifically, for the prediction of Fe_2O_3 and Al_2O_3 concentration 21% and 40% of the variables (data) were

used, respectively, in the prediction models to retain the important information while enhancing prediction accuracy.

11.4.6. DATA FUSION VS. INDIVIDUAL SENSORS

Despite the fact that infrared technologies are mainly used for qualitative analysis of materials, the results obtained in this work show the potential of the individual techniques (MWIR and LWIR) for quantitative analysis of minerals in polymetallic sulphide ore samples. Moreover, data fusion both with and without feature selection yielded better prediction performance compared to those based on individual techniques and the full-range FTIR data models (Table 11.1–11.3). This is likely due to the fact that the fused data blocks use the synergy between the two data blocks (MWIR and LWIR). In addition, extraction of the informative variables maximises the relevant information (related to the concentration of the minerals) in the fused data models. Therefore, data fusion is a preferred approach for quantitative analysis of minerals.

It is also worth noting that some of the models based on individual (MWIR and LWIR) datasets yielded more accurate prediction than did models based on the full-range FTIR dataset. For example, applying models based on PLSR, PCR, and SVR on the LWIR data resulted in enhanced SiO₂ prediction compared to the full-range FTIR model (Table 11.2). This indicates the importance of extracting the informative variables from the two datasets prior to modelling, which was achieved in this work by adopting data fusion.

Data fusion allows handling different forms of uncertainties (e.g., different forms of noise) prior to modelling and is thus very useful approach for both classification and prediction problems analysis using various classification or regression algorithms. Its main benefits are enhanced prediction accuracy, lower uncertainty, enhanced availability of information, and holistic description of materials under investigation. Moreover, the physical integration of sensors requires complex and expensive system design. Therefore, data fusion is a promising alternative for enhanced characterisation of materials in mining operations using multiple sensors.

11.4.7. COMPARISON OF THE PROPOSED MODELS

In the present study, adoption of linear and non-linear multivariate techniques (PLSR, PCR, and SVR) resulted in comparable performance in terms of prediction of the minerals concentrations. Particularly, the PLSR and PCR results are similar. The major difference was obtaining the higher number of factors (PCs) for PCR. In general, the overall results show both the linear and non-linear techniques provided good and acceptable results. Therefore, for the given datasets, moderate effects of the choices of models (linear or non-linear models) were observed.

11.4.8. BENEFITS AND LIMITATIONS OF THE PROPOSED APPROACH FOR MINING APPLICATIONS

The results reported in this work demonstrate that MWIR and LWIR spectral ranges capture information relevant for predicting mineral concentrations in polymetallic sulphide ore samples. While data fusion appears to enhance model prediction accuracy, it may be difficult to apply to data obtained from multiple sources. A further potential challenge stems from the large data matrix produced by data concatenation, as this is likely to cause both computational and data storage issues. However, fusion of the extracted informative

variables minimises the data volume using variable screening and was shown in this work to yield enhanced or comparable prediction performance. This is an interesting finding, since it shows the potential of the proposed approach for integration of multiple data sources (such as SWIR or Raman spectra) without generating a large data matrix after concatenation.

Quantified mineralogical information is crucial for elucidating the variability within a deposit, and can benefit in geometallurgical characterisation (e.g., different minerals have different flotation properties), controlling ore grade, defining blasting parameter requirements, and ensuring product quality. Thus, it can be highly valuable for maximising the potential economic benefit of mining operations. Currently, quantitative analysis of minerals is conducted using XRD or automated scanning electron microscopy (ASEM), both of which are laboratory-based techniques. Thus, infrared systems coupled with data fusion approaches can be considered as complementary techniques to achieve rapid determination of mineral concentrations. Overall, the prediction accuracies achieved in this study are sufficient for rapid in-situ indication of mineral concentrations in polymetallic sulphide ores using a portable system. Therefore, the availability of the portable instruments combined with the promising results of this study supports the practicality of the proposed approach for online in-situ analysis of minerals.

11.5. CONCLUSIONS

In this work, different scenarios were investigated to assess their influence on the prediction of SiO_2 , Al_2O_3 and Fe_2O_3 concentrations in polymetallic sulphide ore samples using infrared reflectance spectra, namely:

- (1) the use of individual spectral regions (MWIR and LWIR);
- (2) the effect of different data pre-processing techniques on the prediction performance;
- (3) potential for improvement in prediction accuracy by applying low-level and low-level with feature selection data fusion approaches;
- (4) comparative benefits of applying linear (PLSR and PCR) and non-linear (SVR) multivariate analysis techniques.

The results reported in the preceding sections show that both MWIR and LWIR datasets include relevant information that can be employed in determining mineral concentrations. Moreover, data fusion significantly improved model prediction accuracy. Models incorporating both the linear and non-linear multivariate techniques (PLSR, PCR, and SVR) resulted in comparable performance. The choice of the data pre-processing techniques was shown to exert significant influence on the model output. For the prediction of Al_2O_3 , the best-performing model was achieved using PLSR and the low-level fusion of the extracted features after data normalisation (RMSEP = 1.4, $R^2 = 0.91$). The PLSR model better predicted Fe_2O_3 in polymetallic sulphide ore after low-level fusion of normalised MWIR and LWIR data blocks (RMSEP = 3.3, $R^2 = 0.94$). Finally, the best prediction of SiO_2 concentration was achieved by the PLSR model after normalised data blocks were subjected to low-level fusion (RMSEP = 5.96, $R^2 = 0.93$). Overall, both the linear and non-linear techniques provided good and acceptable results. Although the acquired prediction accuracies are lower than those of the standard laboratory-based techniques, the proposed method is suitable for rapid in-situ indication (semi-quantification) of mineralogical concentrations along the mining value chain.

The fact that the use of the extracted features significantly reduced the data volume and resulted in promising results suggests a great potential of applying data fusion to data obtained from multiple sources. Our future work will focus on extending the data fusion framework for integration of additional data sources (e.g., SWIR and Raman) to achieve a holistic description and improved quantification of minerals in different deposit types using the synergy among the different data sources. This will be beneficial for improving resource efficiency in the mining industry.

REFERENCES

- Borràs, E., Ferré, J., Boqué, R., Mestres, M., Aceña, L. & Busto, O. (2015). Data fusion methodologies for food and beverage authentication and quality assessment - a review. *Analytica chimica acta*, 891, pp. 1-14. doi: 10.1016/j.aca.2015.04.042
- Chari, S. K., Fanning, J. D., Salem, S. M., Robinson, A. L. & Halford, C. E. (2005). LWIR and MWIR fusion algorithm comparison using image metrics. *Proceedings of the Infrared Imaging Systems: Design, Analysis, Modeling and Testing XVI*, Orlando, USA, pp. 16-26.
- Clark, R. N. (1999). Chapter 1 - Spectroscopy of Rocks and Minerals, and Principles of Spectroscopy. In: A.N. Rencz (Ed.), *Remote Sensing for the Earth Sciences, Manual of Remote Sensing*, John Wiley & Sons, Hoboken, New York, pp. 3-58.
- Cocchi, M. (2019). Chapter 1 - Introduction: Ways and Means to Deal with Data from Multiple Sources. In: M. Cocchi (Ed.), *Data Handling in Science and Technology*. Elsevier, pp. 1-26.
- Dalm, M., Buxton, M. W. N. & van Ruitenbeek, F. J. A. (2018). Ore–Waste Discrimination in Epithermal Deposits Using Near-Infrared to Short-Wavelength Infrared (NIR-SWIR) Hyperspectral Imagery. *Mathematical Geosciences*, 51, pp. 849-875. doi: 10.1007/s11004-018-9758-6
- David, D. (2013). Geometallurgical guidelines for miners, geologists and process engineers – discovery to design. *Proceedings of the Second AusIMM International Geometallurgy Conference*, Melbourne, Australia, pp. 129-132.
- Desta, F. S. & Buxton, M. W. N. (2018). Chemometric Analysis of Mid-Wave Infrared Spectral Reflectance Data for Sulphide Ore Discrimination. *Mathematical Geosciences*, 51, pp. 877-903. doi: 10.1007/s11004-018-9776-4
- Desta, F. S., Buxton, M. W. N. & Jansen, J. (2020). Data Fusion for the Prediction of elemental concentrations in polymetallic sulphide ore using Mid-wave infrared and Long-wave infrared reflectance data. *Minerals*, 10(3), 235. doi: 10.3390/min10030235
- Dominy, S. C., O'Connor, L., Parbhakar-Fox, A., Glass, H. J. & Purevgerel, S. (2018). Geometallurgy—A Route to More Resilient Mine Operations. *Minerals*, 8 (12), 560. doi: 10.3390/min8120560
- Guatame-Garcia, A. & Buxton, M. (2018). Prediction of Soluble Al₂O₃ in Calcined Kaolin Using Infrared Spectroscopy and Multivariate Calibration. *Minerals*, 8, 136. doi: 10.3390/min8040136
- Hecker, C., Dilles, J. H., van der Meijde, M. & van der Meer, F. D. (2012). Thermal infrared spectroscopy and partial least squares regression to determine mineral modes of granitoid rocks. *Geochemistry, Geophysics, Geosystems*, 13(3), 3021. doi: 10.1029/2011GC004004

- Karr, C. & Kovach, J. J. (1969). Far-infrared spectroscopy of minerals and inorganics. *Applied Spectroscopy*, 23, pp. 219-223. doi: 10.1366/000370269774380932
- Kaufhold, S., Hein, M., Dohrmann, R. & Ufer, K. (2012). Quantification of the mineralogical composition of clays using FTIR spectroscopy. *Vibrational Spectroscopy*, 59, pp. 29-39. doi: 10.1016/j.vibspec.2011.12.012
- Khajehzadeh, N., Haavisto, O. & Koresaar, L. (2017). On-stream mineral identification of tailing slurries of an iron ore concentrator using data fusion of LIBS, reflectance spectroscopy and XRF measurement techniques. *Minerals Engineering*, 113, pp. 83-94. doi: 10.1016/j.mineng.2017.08.007
- Mroczkowska-Szerszeń, M. & Orzechowski, M. (2018). Infrared spectroscopy methods in reservoir rocks analysis - semi-quantitative approach for carbonate rocks. *Nafta-Gaz*, 11, pp. 802-812. doi: 10.18668/NG.2018.11.04
- NASA. (2019). ECOSTRESS spectral library [Online]. Available: <https://speclib.jpl.nasa.gov/library> [Accessed September 2019].
- Palayangoda, S. S. & Nguyen, Q. P. (2012). An ATR-FTIR procedure for quantitative analysis of mineral constituents and kerogen in oil shale. *Oil Shale*, 29, pp. 344-356. doi: 10.3176/oil.2012.4.05
- Rinnan, Å., van den Berg, F. & Engelsen, S. B. (2009). Review of the most common pre-processing techniques for near-infrared spectra. *TRAC-Trends in Analytical Chemistry* 28, pp. 1201-1222. doi: 10.1016/j.trac.2009.07.007
- Roussel, S., Preys, S., Chauchard, F. & Lallemand, J. (2014). Chapter 2 - Multivariate Data Analysis (Chemometrics). In: C. P. O'Donnell, C. Fagan & P. J. Cullen (Eds.), *Process Analytical Technology for the Food Industry*. Springer, New York, USA, pp. 7-59.
- SGS. (2019). X-Ray Fluorescence [Online]. Available: <https://www.sgs.com/en/mining/analytical-services> [Accessed November 2019].
- Sun, Y., Seccombe, P. K. & Yang, K. (2001). Application of short-wave infrared spectroscopy to define alteration zones associated with the Elura zinc-lead-silver deposit, NSW, Australia. *Journal of Geochemical Exploration*, 73(1), pp. 11-26. doi: 10.1016/S0375-6742(01)00167-4
- Szalai, Z., Kiss, K., Jakab, G., Sipos, P., Belucz, B. & Németh, T. (2013). The use of UV-VIS-NIR reflectance spectroscopy to identify iron minerals. *Astronomische Nachrichten*, 334(9), pp. 940-943. doi: 10.1002/asna.201211965

12

DATA FUSION FOR THE INDICATION OF ELEMENTAL CONCENTRATIONS

Chapter 10 and 11 show the use of data fusion for the discrimination of ore–waste and semi-quantitative analysis of minerals, respectively. This chapter presents the use of data fusion for the prediction of elemental concentrations in polymetallic sulphide ore using the MWIR and LWIR technologies. The chapter compares the use of low- and mid-level fusions for the indication of the elemental concentrations. It also compares the performances of the individual data models with the fused data models. The analysis was performed using the channel, drill core and muck pile samples from the test case.

Parts of this chapter have been published in:

Destá, F., Buxton, M. & Jansen, J. (2020). Data Fusion for the Prediction of Elemental Concentrations in Polymetallic Sulphide Ore Using Mid-Wave Infrared and Long-Wave Infrared Reflectance Data. *Minerals*, 10(3), 235. doi: 10.3390/min10030235

In this work, a PLSR model was used for the prediction of elemental concentrations using the mineralogical techniques MWIR and LWIR combined with data fusion approaches. In achieving the study objectives, the usability of the individual MWIR and LWIR datasets for the prediction of the concentration of elements in a polymetallic sulphide deposit was assessed, and the results were compared with the outputs of low- and mid-level data fusion methods. Prior to low-level data fusion implementation, data filtering techniques were applied to the MWIR and LWIR datasets. The pre-processed data were concatenated and a PLSR model was developed using the fused data. The mid-level data fusion was implemented by extracting features using principal PCA scores. As the models were applied to the MWIR, LWIR, and fused datasets, an improved prediction was achieved using the low-level data fusion approach. Overall, the acquired results indicate that the MWIR data can be used to reliably predict a combined Pb–Zn concentration, whereas LWIR data has a good correlation with the Fe concentration. The proposed approach could be extended for generating indicative element concentrations in polymetallic sulphide deposits in real-time using infrared reflectance data. Thus, it is beneficial in providing elemental concentration insights in mining operations.

12.1. INTRODUCTION

The increasing availability of complex multivariate data yielded by sensor technologies permits qualitative and quantitative data analysis for material characterisation. Multivariate data are hard to understand by visual inspection and intuition. Thus, data-driven models are required to derive study-specific insights from large datasets. Qualitative and quantitative geochemical data can be acquired using the elemental techniques such as LIBS, XRF and ICP-MS. On the other hand, technologies that provide qualitative, quantitative and semi-quantitative mineralogical information include infrared, Raman and XRD. Numerous researchers deployed the geochemical techniques for the analysis of elements in different applications. For example, elemental analysis using LIBS system is used in the multi-elemental analysis of iron ore deposit (Death et al., 2008; Khajehzadeh et al., 2017), mineral exploration (Cuñat, 2008; Harmon et al., 2019; Lemièrre and Uvarova, 2019), major elemental analysis (Boucher et al., 2015), and metal contaminant analysis (Wainner et al., 2001; Yamamoto et al., 1996). XRF systems are widely used in elemental analysis of various deposit types, such as in iron ore characterisation (Alov et al., 2010; Khajehzadeh et al., 2017), in the elemental composition analysis of highly organic-rich sediments (Kern et al., 2019), and the exploration of komatiite-hosted nickel sulphide deposits (Le et al., 2014). Despite the availability of well-established geochemical methods, a single sensor might not provide a sufficiently comprehensive description of a material composition. For example, materials often comprise more than the elements of economic interest. However, due to complex mineral mixtures, most of the analytical techniques are not able to detect the complete range of elements in mineral deposits. Thus, it is necessary to utilise strategic sensor combinations to improve accuracy and availability in raw material characterisation. Moreover, the use of mineralogical techniques (e.g., infrared) for the indication of elemental concentration can be beneficial for the simultaneous analysis of elements and minerals in various deposit types.

As discussed in Chapter 3, the infrared wavelength range is divided into different regions, and the choice of the infrared region depends on the type of minerals under investigation. Mineralogical techniques (MWIR and LWIR) have not been previously employed for the indication of element concentrations in polymetallic sulphide ore. This gap in the current analytical approaches and the promising findings reported recently (Desta and Buxton, 2018) have motivated the present study. The objective of this investigation was twofold: to develop prediction models that indicate the elemental concentration in

polymetallic sulphide ore using the mineralogical techniques (i.e., MWIR and LWIR reflectance spectral data) separately, and to assess the improvements in the predictive models using low-level and mid-level data fusion approaches.

12.2. MATERIALS AND INSTRUMENTATION

12.2.1. MATERIALS

One hundred and seventeen representative samples were acquired from the test case area. These samples included 62 channel samples acquired from the mine face, 45 samples that were systematically collected from eight drill cores each having a length of approximately 2 to 3 m, as well as 10 muck pile samples collected after blasting part of the mine face (Figure 12.1). The collected samples were powdered and the measurements were performed using the powdered samples.

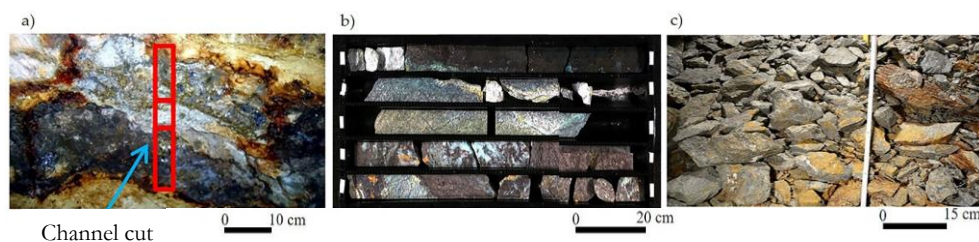


Figure 12.1: Images of (a) the mine face showing a channel cut with different intervals (the red boxes); (b) drill core samples; and (c) muck pile samples.

12.2.2. MWIR AND LWIR DATASETS

The Agilent 4300 FTIR analyser was used to acquire reflectance spectral data using the collected 117 samples. The instrument set-up and data acquisition procedures followed for the acquisition of data are described in Chapter 8. To accommodate the samples' heterogeneity, multiple spectra (7 to 10 measurements) were collected from each sample and the averages were computed. Three sub-datasets were prepared prior to modelling: the full FTIR data (excluding the range from 1.9 to 2.5 μm), the MWIR (2.5 to 7 μm) data, and the LWIR (7 to 15 μm) data.

12.2.3. CHEMICAL ANALYSES

Conventional data acquisition techniques XRF and ICP-MS were used to obtain the data that were used as response variables and in the validation of the element concentrations prediction results. The datasets of Pb, Zn, and Cu comprised XRF and ICP-MS measurements performed using 117 samples. The analysis of As, Fe, Mg, and Ca was performed using the ICP-MS technique and 89 samples. In this study, the number of samples analysed using the FTIR analyser was 117. All 117 samples were analysed for Cu, Pb, and Zn. However, 89 out of the 117 samples were analysed for Fe, As, Ca, and Mg. Therefore, the same samples were used; however, the number of samples used to analyse the elements differed. Therefore, the Cu, Pb, and Zn dataset consisted of 117 sample measurements whereas the Fe, As, Ca, and Mg dataset consisted of 89 sample measurements. Due to their co-occurrence, Pb and Zn are mainly mined simultaneously. Thus, Pb and Zn were combined (the concentrations of the two elements were summed) in

this study. The analysis results pertaining to 117 powder samples of Cu and the combined Pb–Zn and 89 powder samples of Fe, As, Ca, and Mg are discussed in the sections that follow.

12.3. METHODOLOGY

Prediction of elemental concentration in polymetallic sulphide ore using MWIR and LWIR reflectance spectra requires an integrated methodology. Therefore, the methodological approach developed as a part of the present study comprises a multi-step process that commences with data exploration, followed by data pre-processing and data fusion, and culminates with data modelling and model validation (Figure 12.2). The unscrambler software was employed for the analysis. The data exploration task includes outlier detection and data splitting (i.e., into calibration and validation datasets). In the present study, data pre-processing was performed using different data filtering techniques. The pre-processed data were subsequently used to develop a series of calibration and prediction models for MWIR and LWIR datasets separately. The low-level (the red box in Figure 12.2) and mid-level (the green box in Figure 12.2) data fusion approaches were implemented using the concatenated pre-processed MWIR and LWIR data blocks, and the features extracted from the two data blocks, respectively. All prediction models were validated using independent datasets. The use of the individual datasets and the fused dataset for the prediction of element concentrations in polymetallic sulphide ore was evaluated and compared. Each of these steps is described in detail below.

12.3.1. DATA EXPLORATION

PCA models were developed using the full-range FTIR data. Potential outliers were identified using Hotelling's T^2 of the PCA model with the critical limit (p-value) of 5%. Therefore, the 95% confidence ellipse was included in the score plots of the PCA models to reveal potential outliers (i.e., data points located outside the ellipse contour). Potential outliers were further investigated using the influence plot. The pattern of the spectral data with respect to the elemental concentration was assessed using PCA. The proportion of the variance in the y-variable (the quantitative elemental data) that is predictable from the x-variables (full-range FTIR reflectance spectra) was computed using PLSR and each target element, separately. Elements that showed a weak linear relationship with the spectral data (a coefficient of determination less than 0.4) were excluded from further analysis.

12.3.2. DATA SPLITTING

For the combined Pb–Zn dataset, the full-range FTIR, MWIR, and LWIR datasets, each containing 113 samples, were split into calibration (72 measurements) and validation (35 measurements) subsets using a random sample selection algorithm. To encompass the entire variability domain and allow for direct model comparisons, the same split was maintained in the calibration and validation datasets pertaining to the three data blocks. The same procedure was followed for the Fe dataset to obtain calibration (64 measurements) and validation (23 measurements) datasets.

12.3.3. PRE-PROCESSING

Data from different sensors should be treated based on the specific characteristics of the spectral data and the ultimate goal of data analysis in order to remove undesired

variations (e.g., instrumental artefacts) (Roussel et al., 2014). Accordingly, prior to modelling, the data matrices were treated with normalization, baseline correction, MC, SNV, and smoothing (Gaussian filter smoothing). MC was performed in combination with each pre-processing technique.

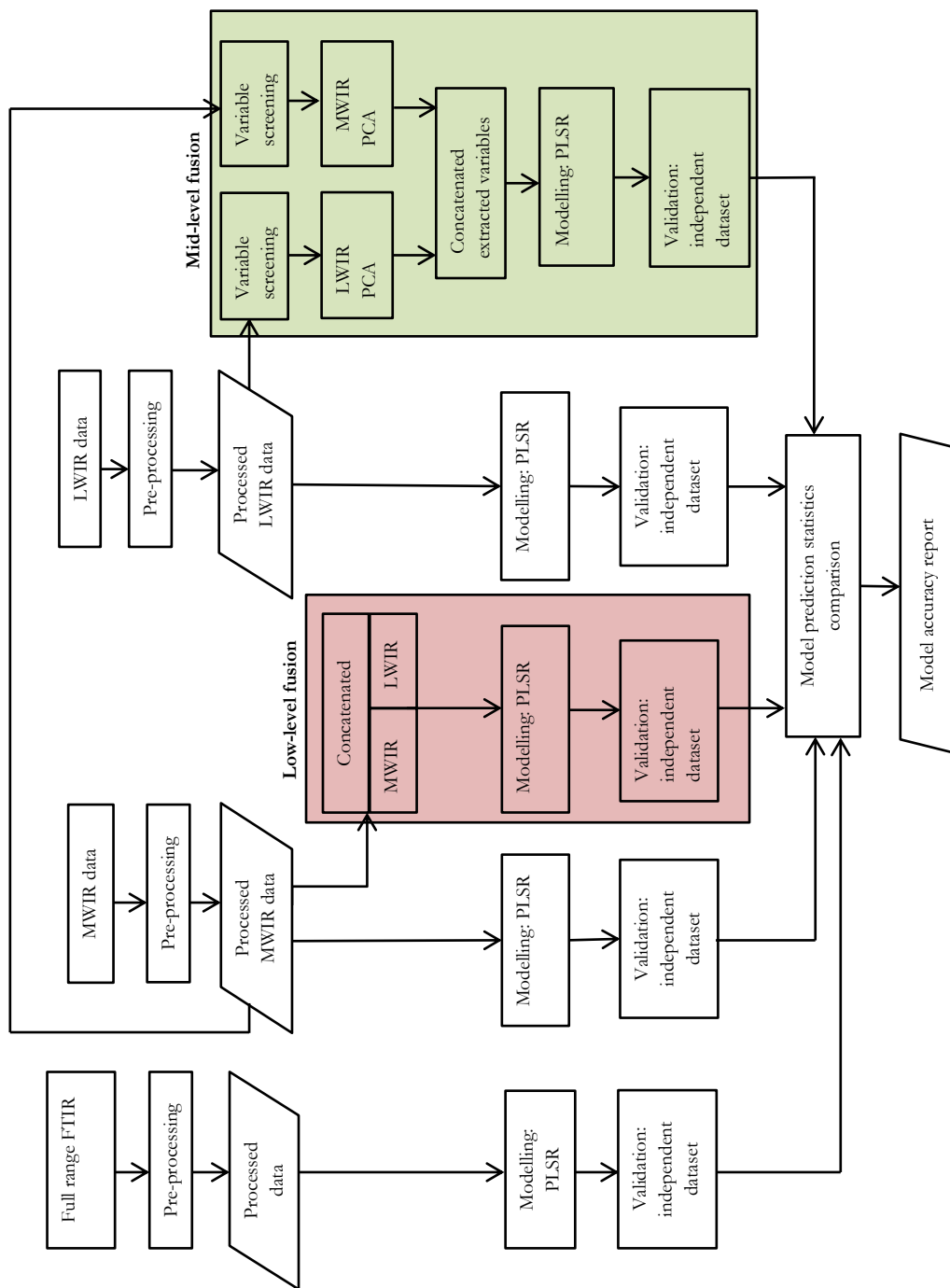


Figure 12.2: A workflow diagram depicting the steps of the research approach.

12.3.4. PREDICTION MODELS

In this study, PLSR models were developed using the infrared spectral data as explanatory variables (X) and the concentration of elements as response variables (Y). Models were developed for the prediction of each element concentration, separately. Thus, the usability of the infrared spectra for the prediction of the individual element under investigation was assessed. A series of PLSR models were developed using the pre-processed data. The models were developed using calibration datasets and the performance of the models was validated using independent datasets (validation datasets). The predictive performance of the models was evaluated in terms of statistical error terms (RMSECV and RMSEP) and the coefficient of determination (R^2) of the prediction values. RMSECV is calculated on the test split using a 10-fold cross validation. The optimum number of PLS factors was determined using the RMSECV values. RMSEP represents the prediction error based on a comparison of real cases not used to make the model with reference values (in this case, an independent dataset). Consequently, RMSEP indicates how well the model built using calibration data performs when applied to unknown cases. R^2 denotes the strength of the linear relationship between the response and predictor variables. When R^2 is computed using the validation samples it signifies a model's predictive ability. Improved predictive performance is associated with a lower value of statistical error terms (RMSECV and RMSEP) and a higher predicted R^2 .

12.3.5. MWIR AND LWIR DATA MODELS

PLSR models were developed using the MWIR and LWIR reflectance spectral data separately. A series of models was developed using the pre-processed MWIR data after applying the aforementioned data-filtering techniques. Similarly, a series of prediction models was developed using the pre-processed LWIR data. The prediction performance of each model was evaluated using independent datasets. The predictive performances of MWIR and LWIR data models for the prediction of elemental concentrations were compared.

12.3.6. LOW-LEVEL DATA FUSION

Potential correlations between wavelengths in different infrared ranges (e.g., MWIR and LWIR) require data fusion to capture latent information that cannot be extracted by analysis of individual data blocks separately. In low-level data fusion, the way in which the data matrices from different sources are concatenated, normalised, and scaled, and the variation in variable magnitude, potentially have a profound effect on model performance in terms of both prediction and classification. For the choice of the optimal model, a “systematic approach” is recommended to understand the effect of the pre-processing techniques on model accuracy (Engel et al., 2013). The pre-processed data from the MWIR and LWIR data blocks were concatenated to form a series of new data blocks. The unified (fused) data were mean-centred and a single model that provides the final elemental concentration prediction was developed (indicated by the red box in Figure 12.2). The PLSR models were developed using calibration datasets and were validated using the independent datasets. The pre-processing techniques applied to the datasets prior to modelling resulted in different model performances. Thus, the optimal pre-processing method was selected by comparing the performance of the prediction models using RMSECV, RMSEP, and R^2 values.

For data blocks based on a different measurement scale, low-level fusion may require additional pre-processing (e.g., block scaling with log scaling, root square scaling) of data blocks to compensate for the scale differences. However, as the MWIR and LWIR data blocks were obtained by adopting the same measuring scale (reflectance value in the 0–100 range), the chance of one technique being dominant was very low. The MWIR and LWIR data considered in the present study were acquired using a single instrument. Therefore, to fully elucidate the importance of the low-level fusion approach, the performance of the predictive models based on the full-range FTIR data and low-level fusion results was compared.

12.3.7. MID-LEVEL DATA FUSION

Mid-level data fusion consists of feature extraction from the signals pertaining to each data block (Cocchi, 2019). In this study, a PCA model was used to extract important variables from the MWIR and LWIR data (Figure 12.2). The most informative variables that explain most of the variations in the spectral data were extracted from the results yielded by the PCA models developed using the two data blocks. These extracted features were fused to develop a final model. Prior to conducting PCA, different data pre-processing techniques (discussed in Section 12.3.3) were applied. The number of PCs that explain most of the total variance in the data was chosen based on the minimum RMSECV value. The scores of the extracted PCs were concatenated to build a final fused data block of the calibration datasets. Similarly, the same procedures were followed to build the validation datasets separately. The fused data block was mean-centered and a prediction model was developed using PLSR (the green box in Figure 12.2). The new variable blocks formed matrices of the elemental concentration and PC scores that were used in the models as response and explanatory variables, respectively. Finally, the performance of the models developed using low-level and mid-level data fusion approaches was compared.

12.4. RESULTS AND DISCUSSION

This section consists of seven parts. In the first two, the exploratory data analysis results and the results of the MWIR and LWIR prediction models are presented. In the subsequent two parts, the results of the low-level and mid-level data fusion for the prediction of element concentrations are described in detail. In the remaining three parts, the comparisons of the adopted approaches, assessment of infrared spectra usability for prediction of elemental concentrations, and benefits and limitations of the current approach for in-situ applications are discussed, respectively.

12.4.1. EXPLORATORY DATA ANALYSIS AND PRE-PROCESSING

Descriptive statistics were used in the present study to describe and summarize the basic features of the elemental concentrations in the analysed samples (Table 12.1). The results reported in Table 12.1 indicate that the samples exhibit high variability in elemental concentrations. This likely stems from the sample collection strategy, whereby the ore zone region and waste (host rock and weathered) material were obtained to ensure material representativity (Figure 12.3). However, variability was also observed within the ore material.

Table 12.1: Summary statistics of elemental concentrations (in wt.%) in the analysed samples.

Statistics	Fe	Cu	As	Mg	Ca	Pb–Zn
Mean	13.72	0.1	0.27	0.25	0.69	6.43
Std Deviation	10.45	0.12	0.46	0.21	0.56	5.87
Min	2.30	0.002	0.006	0.03	0.08	0.04
Median	10.22	0.08	0.13	0.22	0.52	5.08
Max	40.00	0.9	2.44	1.4	3.33	30.32

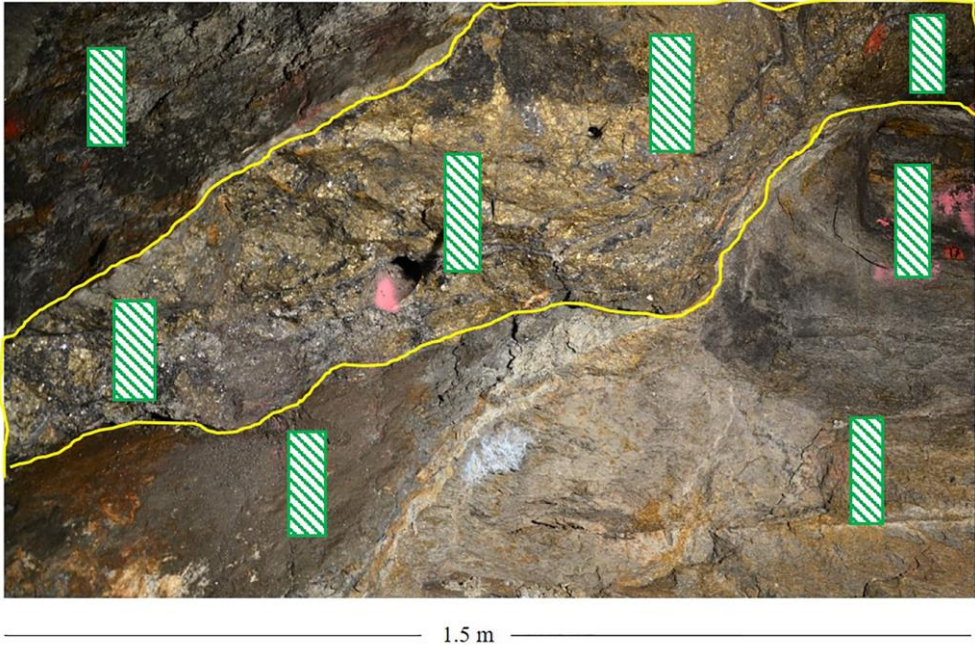


Figure 12.3: A mine face photograph that shows the location of some of the channel samples (the green boxes). The yellow line shows the boundaries of the ore zone.

As shown in Table 12.2, the use of the infrared spectra for the prediction of the As, Cu, Ca, and Mg concentrations resulted in lower R^2 values (<0.4). Therefore, these elements were excluded from further analysis. Conversely, Fe and the combined Pb–Zn concentration showed a strong association (linear relationship) with the infrared reflectance data. Therefore, the analysis results presented in this and the subsequent sections focus on Fe and the combined Pb–Zn only. The lower relationships of As, Cu, Ca, and Mg with the infrared reflectance spectra are likely attributed to the lower concentration of the sourcing minerals in the samples that resulted in a lower spectral signal. It is also possible that the concentration of the sourcing minerals was below the detection limit of the instrument, or that the spectral signals of the sourcing minerals in the infrared reflectance spectra were very weak.

Table 12.2: Coefficient of determination values for the prediction of each target element using the full-range FTIR reflectance spectra and partial least squares regression (PLSR).

Element	As	Ca	Mg	Cu	Fe	Pb–Zn
R ²	0.07	0.2	0.19	0.35	0.80	0.81

Figure 12.4 shows the PCA model score plots of the full-range FTIR data for Fe and the combined Pb–Zn datasets. The plots provide information on the potential patterns that are related to elemental concentration. As shown in Figure 12.4, elemental concentrations (Fe and the combined Pb–Zn) were categorized into three ranges. The plots further reveal the presence of patterns that can be related to the elemental concentration. Potential outliers were identified. As a result, two outliers were excluded from the Fe dataset, whereas four outliers were excluded from the combined Pb–Zn dataset.

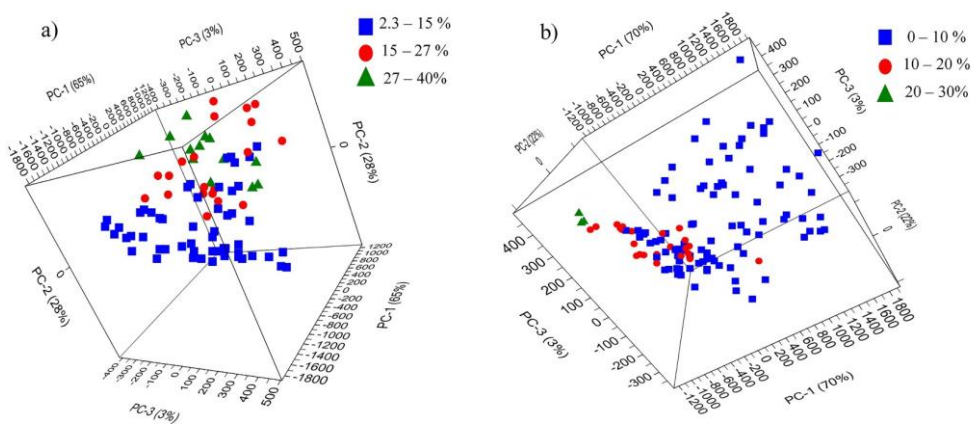


Figure 12.4: Principal Component Analysis (PCA) model score plots of (a) the Fe concentration categorized into three ranges; and (b) the combined Pb–Zn concentration categorized into three ranges (the concentrations are expressed in wt.%).

12.4.2. MWIR AND LWIR DATASETS

As shown in Table 12.3, the model based on the MWIR dataset yields a better Fe prediction, with the RMSEP of 4.80 and the R² value of 0.69, after data normalization. Compared with the model performance based on raw MWIR data (the RMSEP of 5.63 and the R² of 0.58), data filtering using normalization improved the results. Likewise, the model developed using the normalised LWIR data resulted in RMSEP = 3.38 and R² = 0.85, which is a remarkable improvement relative to the RMSEP = 4.59 and the R² = 0.72 obtained using the raw LWIR data. Therefore, for Fe prediction, data normalization resulted in a better prediction performance for both MWIR and LWIR models. This shows that the removal of the undesired intensity variation in the spectra caused by multiplicative effects enhances the signals from the Fe-bearing minerals. Comparing the two datasets in terms of Fe prediction, the LWIR data model is superior to the MWIR model. The Fe-bearing minerals include oxides (e.g., hematite, goethite), carbonates (e.g., siderite), sulphides (e.g., pyrite, chalcopyrite), and silicates (pyroxene, olivine). LWIR is suited for rock-forming mineral and carbonate identification (Clark, 1999; Hecker et al., 2012; Terracore, 2018). This

is likely one of the reasons for the better prediction of Fe concentration based on the LWIR relative to MWIR data. The other possible reason is the presence of certain minerals that have a good correlation with both infrared spectra and Fe concentration but do not contain Fe. For example, minerals formed as a result of retrogressive mineralization during hydrothermal events have a high chance of correlation.

Model performance in terms of predicting the combined Pb–Zn concentration using MWIR and LWIR data is summarised in Table 12.4. The model based on the MWIR data yielded a better prediction after the data were treated using baseline correction (RMSEP = 2.23 and $R^2 = 0.83$). The model prediction accuracy obtained using raw MWIR data was lower than that based on the pre-processed data (RMSEP = 2.46 and $R^2 = 0.80$). The prediction accuracy of the model based on the LWIR data treated using baseline correction is reflected in RMSEP = 3.25 and $R^2 = 0.65$. As shown in Table 12.4, a better prediction was attained using the LWIR data subjected to baseline correction. A combination of the pre-processing techniques was analysed for the prediction of both Fe and the combined Pb–Zn concentrations. However, the prediction performances of the models were not improved; thus, the results were not included in this paper.

Comparing the model performance in terms of the combined Pb–Zn concentration prediction, the model based on the MWIR data is superior to that using the LWIR data. The primary mineral sources of Pb and Zn in the test case deposit are galena and sphalerite, respectively. This is one of the likely reasons for a better prediction of the combined Pb–Zn concentration using the MWIR data than the LWIR data. For example, sphalerite has a lower reflection pattern in the spectral data in the 2.33–3.78 μm range and at 14.9 μm (NASA, 2017). Similarly, for galena, higher reflection points are found in the MWIR region (Figure 12.5). Therefore, the amount of spectral information (signals) in the MWIR dataset is greater (more pronounced) than in the LWIR dataset, resulting in a superior combined Pb–Zn concentration prediction yielded by the model based on MWIR data.

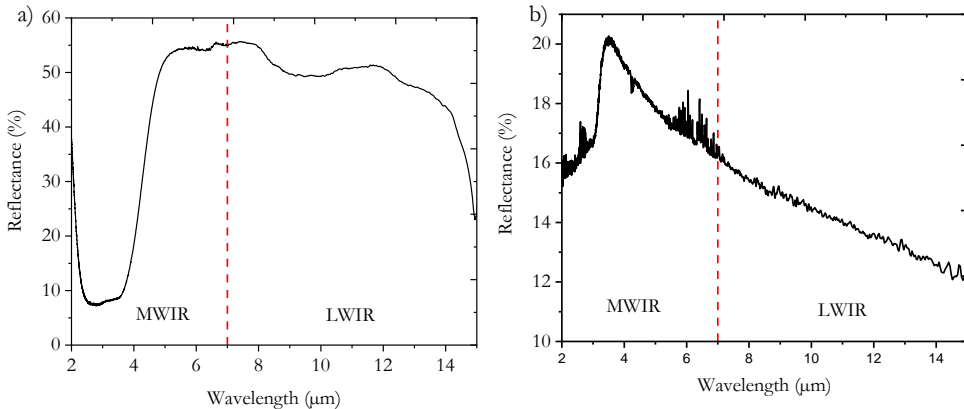


Figure 12.5: Reflectance spectra of (a) sphalerite and (b) galena (source: NASA, 2017).

The elemental concentration prediction results yielded by the MWIR and LWIR models show that the infrared technique is capable of indicating the concentration of elements in polymetallic sulphide ore semi-quantitatively. The infrared technique is a mineralogical technique that provides information on the functional groups of minerals. Thus, elemental

information cannot directly be derived from the infrared spectra. However, the acquired results show that an indicative elemental concentration can be estimated using multivariate techniques without directly examining the fingerprint of individual elements in the infrared spectral signals. The results of the present study indicate that MWIR data are a promising candidate for prediction of combined Pb–Zn concentrations. Thus, MWIR has great potential for use in material characterisation.

The models developed using MWIR and LWIR data explained the variations in the Y-variables (concentration of elements) from the variations in the X-variables (reflectance spectral data), and resulted in acceptable prediction model accuracies. The model based on the MWIR data yielded a better prediction of the combined Pb–Zn concentration than that based on the LWIR data, whereas the Fe concentration was more accurately predicted using LWIR rather than MWIR data. Based on the available spectral libraries (e.g., the NASA mineral library), the sulphide minerals showed weak spectral features in the MWIR and LWIR spectral data. Such weak spectral information (signal) is insufficient for a direct interpretation or mineral fingerprinting, especially when target minerals are present in a mixture (co-occurring with other minerals). Moreover, the infrared sensors provide mineralogical information but cannot directly identify the elements in the spectral signal. However, such information can be extracted using multivariate data analysis techniques.

12.4.3. LOW-LEVEL DATA FUSION

Table 12.3 shows a summary of the Fe prediction model performance when applied to the individual data blocks, full-range FTIR data, and low-level data fusion results. As shown in Table 12.3 and Figure 12.6, better model performance was achieved using low-level data fusion (RMSEP = 2.71 and $R^2 = 0.90$) after the normalised data blocks based on the MWIR and LWIR datasets were fused.

As described in Section 12.2.2, the MWIR and LWIR datasets were acquired using a single-sensor FTIR spectrometer, which allowed for the performance of models based on the full-range FTIR data (which include both MWIR and LWIR datasets) to be assessed and compared to the low-level fusion results. This was done to test whether the low-level data fusion approach yielded superior results to those based on the full-range data. Though the performance of the prediction models based on the full-range FTIR data was better than that obtained using the individual datasets (Tables 12.3 and 12.4), the prediction performance acquired from the low-level data fusion (after data block normalization) was superior to that acquired from the full-range FTIR data model. Similarly, the combined Pb–Zn prediction using a low-level data fusion was better than the results obtained using the individual and the full-range FTIR data (Table 12.4).

Table 12.3: Summary of the predictive performances of MWIR, LWIR, full-range FTIR, and low-level data fusion models for Fe concentration prediction.

Filtering	Statistics	MWIR	LWIR	Full Range	Low-Level
Raw data	RMSECV	3.76	4.54	3.75	
	RMSEP	5.63	4.59	3.87	
	R ²	0.58	0.72	0.80	
SNV	RMSECV	3.57	3.96	3.89	3.81
	RMSEP	5.49	4.13	4.43	4.12
	R ²	0.60	0.77	0.74	0.77
Normalise	RMSECV	3.46	3.51	2.88	2.71
	RMSEP	4.80	3.38	3.18	2.71
	R ²	0.69	0.85	0.87	0.90
Baseline	RMSECV	4.27	4.87	3.80	3.85
	RMSEP	5.73	4.20	4.50	4.11
	R ²	0.56	0.77	0.73	0.77
Gaussian	RMSECV	3.93	4.35	3.09	2.97
	RMSEP	5.47	4.44	3.40	3.43
	R ²	0.60	0.74	0.84	0.84

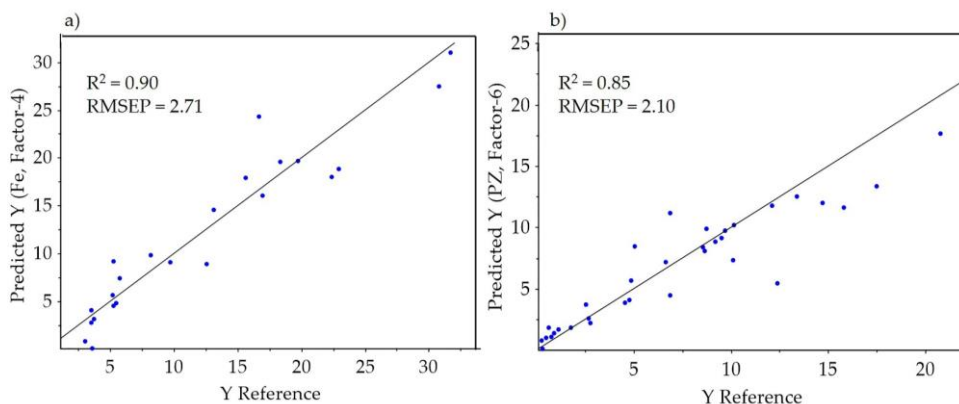


Figure 12.6: Predicted versus actual (a) Fe concentration values (wt.%); (b) the combined Pb–Zn concentration values (wt.%) computed using a low-level data fusion approach.

The portable full-range FTIR sensor is an example of a physically integrated MWIR and LWIR sensor. This is an interesting achievement of the current advancement of infrared technologies. The performance of the prediction models based on the full-range FTIR data was better than that obtained using the individual datasets. However, the results of this study suggest data fusion to be a better and comparative option for a combination of multiple sensors. Moreover, the physical integration of multiple sensor technologies into a single platform is challenging and, in terms of practical implementation, it is expensive. Therefore, for the integration of multiple data sources, such as short-wave infrared (SWIR), Raman, and LWIR data (provided each sensor technology has its own advantages in providing useful information), data fusion can be considered to be an economic and practical alternative option.

Table 12.4: Summary statistics of the predictive performances of MWIR, LWIR, full-range FTIR, and low-level data fusion models for the combined Pb–Zn concentration prediction.

Filtering Techniques	Statistics	MWIR	LWIR	Full Range FTIR	Low-Level Fusion
Raw data	RMSECV	1.97	2.94	2.04	
	RMSEP	2.46	3.48	2.37	
	R ²	0.80	0.60	0.81	
SNV	RMSECV	2.37	3.65	2.41	1.96
	RMSEP	3.11	3.39	2.79	2.86
	R ²	0.68	0.62	0.74	0.73
Normalise	RMSECV	1.87	3.32	1.88	1.90
	RMSEP	2.33	3.28	2.19	2.24
	R ²	0.82	0.64	0.84	0.83
Baseline	RMSECV	2.09	3.04	2.07	1.89
	RMSEP	2.23	3.25	2.32	2.10
	R ²	0.83	0.65	0.82	0.85
Gaussian	RMSECV	2.04	3.15	2.09	1.98
	RMSEP	2.34	3.34	2.28	2.27
	R ²	0.82	0.63	0.83	0.83

The Fe and the combined Pb–Zn concentrations yielded by the low-level data fusion approach were highly affected by the choice of pre-processing technique. This is in line with the recommended “systematic approach” (Engel et al., 2013). The normalization of the two data blocks prior to data fusion resulted in a better prediction of Fe concentration, whereas baseline correction resulted in a better model prediction for the combined Pb–Zn concentration. The MWIR and LWIR data considered in this study were acquired using a single instrument, thus ensuring that the data scale difference is not an issue. However, treating the noise in the two data blocks separately and fusing the pre-processed data blocks enhanced the prediction performance of the PLSR models.

In low-level data fusion, as the name suggests, data integration occurs at the bottom of the analytical data flow. Indeed, this strategy implies that the matrices describing the individual blocks, after proper pre-processing, are concatenated to build a fused data block, which is then processed by the desired chemometrics technique. Suppose X denotes an $m \times n$ matrix of independent variables, where m is the number of samples and n is the number of MWIR and LWIR wavelengths together. Y ($m \times p$) is the matrix of dependent variables, where p denotes the elements to be predicted. The purpose is to train a model estimating the concentration of the elements in each polymetallic sulphide ore sample through the matrix of the measured spectra. The problem is formulated by constructing input (X) and output (Y) matrices. For example, the combined MWIR and LWIR reflectance for 89 samples is formed as X (89 7190) and the matrix of outputs for Fe will be Y (89 1). As the fusion occurs at the level of the original data matrices, the resulting data block will typically contain a very high number of variables. Consequently, the main drawback of this strategy is that the increase in information obtained by adding one or more blocks of data to describe

the sample may not compensate for irrelevant variability introduced by the addition of the same blocks.

The PLSR model developed using the fused data blocks simultaneously considers the MWIR and LWIR measurements, due to which it takes advantage of having a greater number of informative explanatory variables to perform the elemental concentration prediction with better accuracy than that achieved by the models based on individual data blocks. Low-level fusion is conceptually simple to implement and the acquired results are superior to those yielded when using individual techniques. However, the prediction performance of the individual MWIR and LWIR data models also resulted in a good prediction potential for Fe and the combined Pb–Zn concentration. It is possible that the same minerals were measured in both datasets or the minerals were highly correlated to each other due to their co-occurrence in the deposit. However, the improvement of the predictive model after low-level data fusion implies that, as there is unique spectral information in both datasets, combining the two data blocks results in better prediction performance.

12.4.4. MID-LEVEL DATA FUSION

Feature selection is an important step in mid-level data fusion implementation. Hence, an attempt was made to ensure proper coverage of the existing variation in the reflectance spectra data. For example, for the prediction of the combined Pb–Zn concentration using the MWIR data treated with baseline correction, four PCs that explain 98% of the variance in the data were chosen. Similarly, five PCs that explain 97% of the variation in the data were chosen for the LWIR data treated with baseline correction. These PCs (four from the MWIR data block and five from the LWIR data block) were concatenated to generate the fused data matrix. Using the newly generated variable data matrices, final elemental concentration prediction models were developed by adopting PLSR.

As shown in Table 12.5, for the prediction of the combined Pb–Zn concentration, better model performance was achieved (RMSEP = 3.05 and $R^2 = 0.69$) after baseline correction. For the Fe concentration prediction, a better model was achieved after the normalised data block features were fused (RMSEP = 5.09 and $R^2 = 0.65$). The acquired prediction performance of the models for estimation of the combined Pb–Zn concentration was good. However, model performance in terms of predicting the Fe concentration was lower (RMSEP = 5.09). Overall, the performance of the prediction models after mid-level data fusion was lower than that of the models employing individual techniques. Nonetheless, the acquired results are promising and can likely be improved by adding more data to the calibration dataset (thus to fully capture the high variability between the samples) or by considering other feature selection techniques.

Table 12.5: Summary of the low-level and mid-level data fusion model performance in terms of prediction accuracy of Fe and the combined Pb–Zn concentration. The total number of selected PCs shows the number of selected PCs from the PCA models of the MWIR and LWIR data.

Element	Data Pre-Processing Technique	Statistics	Low-Level Fusion	Total No. of Selected PCs	Mid-Level Fusion	Factors for the Model after Mid-Level
Pb–Zn	Normalise	RMSECV	1.90	7	2.37	2
		RMSEP	2.24		3.12	
		R ²	0.83		0.68	
	Baseline	RMSECV	1.89	9	2.09	2
		RMSEP	2.10		3.05	
		R ²	0.85		0.69	
Fe	Normalise	RMSECV	2.71	7	2.87	2
		RMSEP	2.71		5.09	
		R ²	0.90		0.65	
	Baseline	RMSECV	3.67	7	5.08	4
		RMSEP	4.58		5.67	
		R ²	0.72		0.57	

In the mid-level data fusion approach, data reduction using variable screening is a prerequisite. The data volume of the combined MWIR and LWIR datasets and the new data matrices generated from the extracted features have a significant difference. The combined MWIR and LWIR datasets contain 7190 variables, whereas the new data blocks generated from the extracted features included only seven to nine variables, depending on the amount of the explained variance from the score results of the PCA models. With feature extraction methods, the important information (informative variables in the spectral data) is retained using fewer variables than in the original data blocks (MWIR and LWIR datasets). This is an interesting point, since a large data volume (megavariate or multivariate data) may lead to several computational challenges and, due to the development of high-throughput instrumentation, complex datasets are increasingly becoming available.

The reflectance infrared data likely contains a certain amount of noise (e.g., caused by instrument imprecision and/or measurement errors) and, in some instances, may include irrelevant information in the spectra (data that are unrelated to elemental concentrations). Therefore, treating the datasets with the data filtering techniques mentioned above improved the prediction accuracy of the models developed as a part of this study. Irrelevant information can also hinder the predictive ability of the available information; in this case, extracting the important variables can result in better prediction.

12.4.5. DATA FUSION VERSUS INDIVIDUAL SENSORS

The prediction model performance based on the individual MWIR and LWIR datasets is favorable in terms of the elemental concentration (Fe and the combined Pb–Zn concentration) prediction accuracy. Owing to the fact that these mineralogical techniques are mainly used for qualitative analysis of mineralogical information, the results obtained in this study are encouraging, indicating that the potential of these techniques, especially the

MWIR data, should be explored further, since it is the least-utilised region of the infrared spectrum. The approach presented in this study is a data-driven approach as a part of which the hidden information in the spectral signal is transformed into a quantitative indication of elemental concentration.

Comparing the performance of the prediction models based on the individual techniques with the data fusion results, an improved prediction accuracy was achieved using a low-level data fusion approach. Low-level data fusion enhanced the reliability of the prediction models by increasing the prediction performance and minimising the uncertainty implicit in each individual technique. Data fusion is effective in identifying the correlations and the similarities/differences (common and distinctive information) among different variables. However, if applied to correlated or noisy data blocks, data fusion might not necessarily improve model performance (Forshed et al., 2017). In some cases, unnecessary information can also hinder model performance, due to which a better prediction can be achieved from individual data blocks than from the fused dataset.

The prediction performance of the models after low-level data fusion was superior to that yielded by the mid-level data fusion models. This is likely due to the fact that the original information from both data blocks (MWIR and LWIR) is maintained in low-level fusion, making it potentially more accurate. In mid-level data fusion, PCA potentially failed to describe all-important variations in the data. However, this issue can be overcome by considering other data decomposition methods, such as MCR-ALS or independent component analysis (ICA). Review studies (Borràs et al., 2015) indicate that there is no preferred level of data fusion, as the choice is always application-dependent.

12.4.6. USE OF INFRARED REFLECTANCE SPECTRA FOR INDICATION OF ELEMENTAL CONCENTRATION

Understanding the spatial variability in elemental concentration is crucial for the effective extraction of minable products in mining operations. The data-driven approach proposed in this study provides an insight into the quantifiable elemental concentrations in polymetallic sulphide ore using infrared reflectance data. PLSR was used to relate the concentration of elements of interest with complex high-dimensional infrared data to reveal hidden information in the spectra. Low-level data fusion resulted in better predictive performance of models than could be attained using models based on the individual techniques. This is likely due to the fact that the two data blocks (MWIR and LWIR) contain different chemical information that can be linked to the description of the sourcing minerals containing elements of interest. In addition, the comparable predictive performance of the MWIR and LWIR data models likely indicates the occurrence of similar chemical information as well. Therefore, the two techniques are complementary to each other.

The performance of the prediction models utilizing the MWIR, LWIR, and fused datasets indicates that prediction improves with higher Fe concentration in the samples. This is likely due to the fact that a higher Fe concentration in the samples results in a better spectral signal of the Fe sourcing minerals in the datasets. Thus, a better linear relationship can be established with the infrared spectra. Conversely, for the combined Pb–Zn concentration prediction, a lower concentration of these elements was better described by the models. However, the higher the Pb–Zn concentration in the samples, the lower its description by the models, likely due to higher reflectance variation, as more samples are needed in the calibration data to obtain a better description by the models.

In mineralogical or elemental investigations, identification of as many minerals or elements as possible in the material is advantageous to finding indirect proxies of target minerals and understanding the requirements for mineral processing. However, material characterisation is a multi-step process that involves addressing different issues at different levels. The entire process, which is comprised of data generation, analysis, information extraction, and the depth of information (or scope of material characterisation), is illustrated in Figure 12.7. Nowadays, most sensors produce high-throughput multivariate or megavariate data. The raw data is complex, making it challenging to interpret and handle the megavariate data obtained from different sources. Therefore, there is a need for machine learning methods, such as chemometrics, for data-driven understanding of the complex datasets. Using multivariate techniques, the hidden information in spectral data can be transformed into useful information, such as key geological parameters (elemental, mineralogical, and textural data) in mining operations. However, based on the information level that can be acquired from the sensor signals, the depth of information or the amount of information that can be generated differs. The depth of information or scope of material characterisation from the bottom up can be organised into (i) detection (determines the presence of materials in the entity under investigation), (ii) discrimination (separates materials into similar groups based on the signals in the spectral data), (iii) identification (determines the fingerprints of individual entities), and (iv) quantification (determines the quantity of materials).

Thus, quantification of the composition of a material under investigation is at a higher level of the material characterisation or information extraction process. Quantification can be achieved after identification of a unique identity of a material in the acquired spectra, or it can be achieved indirectly by developing prediction models based on the correlation between the spectral signal and the entity under investigation (e.g., elemental concentration). In the present study, the use of MWIR and LWIR data for semi-quantification of elemental concentration was analysed. The prediction accuracies acquired from the fused data or individual datasets were very good. The achieved results should be termed 'semi-quantification', since the acquired RMSEP was not as low as would be expected for exact prediction. However, the achieved RMSEP gives a very good indication of the elemental concentration in the samples and can be used to indicate high-, medium-, and low-mineralization zones in mining operations. In addition, a lower RMSEP can be achieved using more data in the calibration datasets. One of the advantages of the use of infrared data for the indication of elemental concentration stems from the fact that the infrared data can be further analysed to acquire mineralogical information simultaneously. Thus, infrared can be considered to be a complementary technique to technologies that provide elemental information (e.g., XRF or LIBS).

Overall, the prediction accuracies acquired in this study show promise in terms of semi-quantification of elemental concentrations in polymetallic sulphide ore samples using data sources that have historically been used for mineral identification only. Therefore, this study can serve as a baseline to show a framework for the implementation of data fusion using multiple data sources and various classification or regression algorithms.

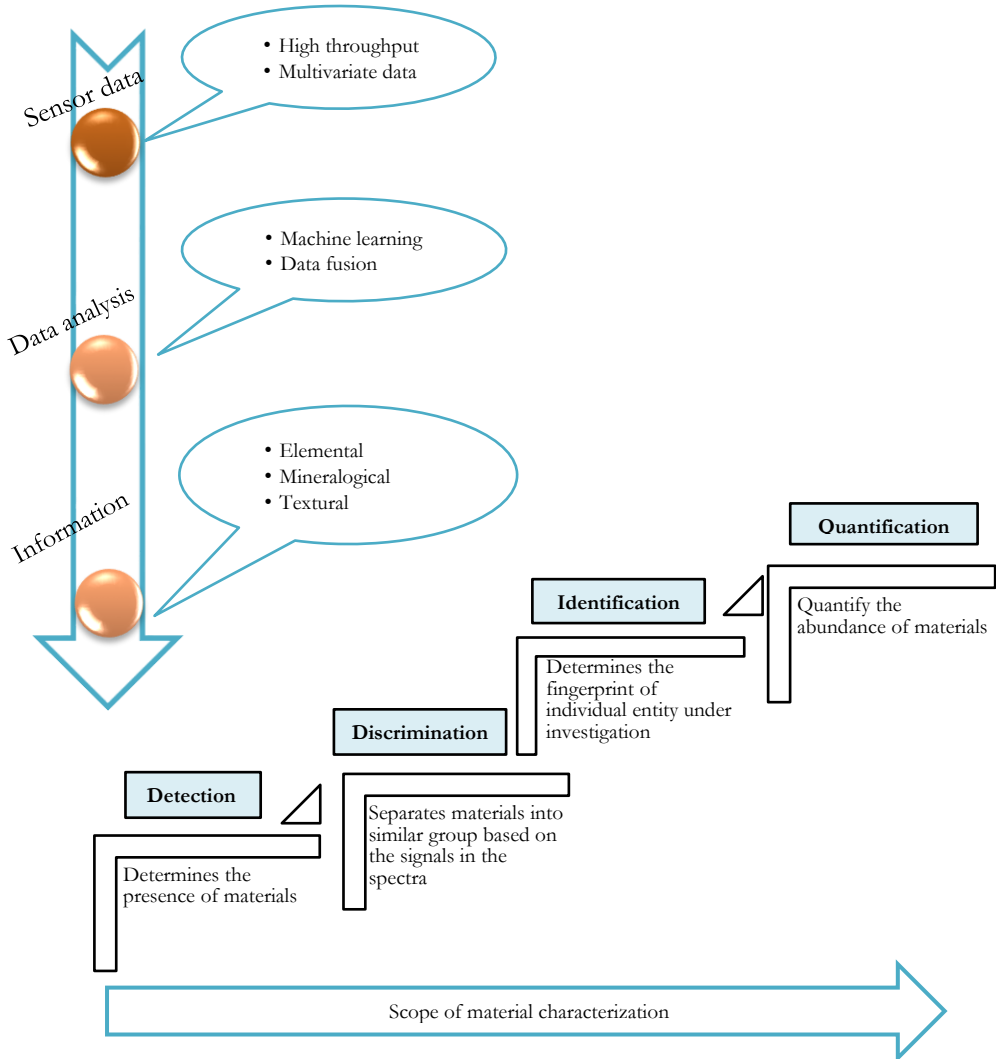


Figure 12.7: A schematic diagram illustrating the process of knowledge generation from sensor data and the level of information.

12.4.7. OPPORTUNITIES AND LIMITATIONS FOR IN-SITU APPLICATION

Owing to current technological advancement, rapid and non-destructive sensor technologies are feasible for mineral and mining applications. These technologies produce high-throughput megavariable datasets. As a result, understanding and interpreting the sensor data directly might not be possible. This leads to computational challenges in analysing the megavariable data and generating knowledge based on fast fingerprinting approaches in order to automate a material characterisation process. Therefore, as illustrated in Figure 12.7, knowledge generation from sensor-derived data requires advances in analytics using machine-learning techniques. The approach presented in this study enables semi-

quantification of elemental concentrations using infrared spectra and data fusion. The reflectance infrared spectra were linearly correlated to the elemental concentrations in polymetallic sulphide ore. Data fusion resulted in improved model prediction accuracies and lower detection errors (uncertainty) than the individual datasets. This is likely due to jointly analysing data blocks from different sensors, which allowed us to capture the latent information that would not be extracted by analysing each data block individually.

Data fusion is mainly a data-driven approach in which the preferred level of data fusion depends on the nature of the data. Low-level fusion is conceptually simple, uses a single model, and can capture correlations between variables contained in different blocks. The disadvantages of the low-level data fusion are the high data volume (high variable to sample ratio) and the possible predominance of one data source over the others. The concerns stemming from a high data volume can be resolved using mid-level data fusion. For example, data reduction via feature selection (the scores in this case) in mid-level data fusion reduced the data dimensionality tremendously in the present study. Comparing the number of variables used in the two levels of data fusion, the mid-level data fusion used $\sim 0.14\%$ of the data volume required for low-level fusion. Thus, feature extraction in mid-level fusion reduces data dimensionality (in this case by $\sim 99.86\%$), which significantly minimises the time required for computational analysis. The disadvantage of mid-level data fusion is that it requires the development of many models prior to fusion (each dataset must be reduced) and there is a need for an ultimate variable screening method. Therefore, the choice of the preferred level of data fusion is dependent on the performance of prediction or classification models and their applications, and should thus be made using a “systematic” approach.

Polymetallic sulphide ore characterisation using infrared spectra considers weak infrared features, complex matrices due to the presence of multiple sulphide minerals and other associated minerals, peak overlaps, and additional variability that results from physical and chemical weathering. Therefore, the need to reveal the hidden information in infrared spectra related to the material of interest mandates the use of multivariate analysis (e.g., integration of data blocks from multiple sensors). Elemental concentration indication into low-, medium-, and high-mineralization zones is advantageous for elemental spatial variability mapping in ore grade control applications. The proposed framework can be extended to simultaneous fingerprinting of the mineralogical information and elemental concentration indication (measurements of concentrations of valuable elements) in order to achieve comprehensive quantitative analysis.

The in-situ application of elemental concentration indication using an infrared spectra and data fusion approach is highly advantageous. However, to achieve this aim in practice, a robust system design and an integrated principled tool that integrates efficient data collection, processing, and knowledge generation is necessary. Going forward, automated material characterisation is possible with a robust system design (exemplified by a portable and ruggedized system) and efficient software (test-case-specific mineral libraries) that can be developed using a combined sensor signal. As currently available sensor technologies measure different aspects of material properties, information acquired from each technique likely adds to a holistic description of materials. The application presented in this study was based on a point technique (FTIR spectrometer data), which yields information at a specific point. However, a correlation model can be developed using image data yielded by other sensor technologies, such as hyperspectral imagery or RGB imaging, to predict the elemental concentration in unmeasured areas (to extend the coverage).

12.5. CONCLUSIONS

This study developed prediction models for the indication of elemental concentration in polymetallic sulphide ore using infrared reflectance spectra. Different factors that possibly influence the performance of the prediction models were used to formulate testing scenarios: (1) the usability of the individual datasets (MWIR and LWIR) for the prediction of the elemental concentrations; (2) the effect of the different data pre-processing techniques on the prediction performance; and (3) the potential for improvement in prediction accuracy by applying low-level data fusion and mid-level data fusion.

The results reported in the preceding sections show that both MWIR and LWIR datasets include relevant information that can be related to the concentrations of the elements. Comparing the best-performing models, the prediction performance of the MWIR model after baseline correction (RMSEP = 2.23 and $R^2 = 0.83$) for the combined Pb–Zn elemental concentration prediction was superior to that obtained using LWIR data (RMSEP = 3.25 and $R^2 = 0.65$). On the other hand, the LWIR-based model after data normalization predicted the Fe concentration (RMSEP = 3.38 and $R^2 = 0.85$) better than the MWIR-based model (RMSEP = 4.80 and $R^2 = 0.69$). The MWIR is the least-explored region of the electromagnetic spectrum for mineralogical applications. However, the results yielded by this study show the potential of this technique for material characterisation. The use of a low-level data fusion strategy improved the model predictive ability relative to the results yielded by using individual techniques. After the low-level fusion, the best-achieved model performance for the prediction of the combined Pb–Zn concentration was RMSEP = 2.10 and $R^2 = 0.85$ and for the prediction of the Fe concentration was RMSEP = 2.71 and $R^2 = 0.90$. The performance of the prediction models after the mid-level fusion was lower than that of the models employing individual techniques. However, the acquired results are promising and can likely be improved by adding more data to the calibration dataset (thus to fully capture the high variability between the samples) or by considering other feature extraction techniques.

Overall, the low- and mid-level data fusion approaches proposed in this study showed promising results. The outcomes suggest that the approach has a great potential to be extended for the integration of more complex data from a range of sensor technologies, due to the fact that each sensor technology has its own advantages in providing useful information. Prediction or indication of elemental concentration using mineralogical techniques (infrared data) is useful to understand compositional properties, both in terms of mineralogy and geochemistry. The individual techniques (MWIR and LWIR) exhibit a great potential for use in elemental concentration characterisation in sulphide ore, and the model performance can be improved using data fusion. This study is a baseline for future research that involves multiple sensor integration aimed at developing predictive models that can estimate elemental concentrations in different types of deposits. We recommend enhancing the current work using data from other sensors.

REFERENCES

- Aloy, N. V., Volkov, A. I., Usherov, A. I., Ishmets'ev, E. N. & Usherova, E. V. (2010). Continuous X-ray fluorescence analysis of iron ore mixtures in the production of agglomerate. *Journal of Analytical Chemistry*, 65(2), pp. 169-173. doi: 10.1134/s1061934810020127
- Borràs, E., Ferré, J., Boqué, R., Mestres, M., Aceña, L. & Busto, O. (2015). Data fusion methodologies for food and beverage authentication and quality assessment - a review. *Analytica chimica acta*, 891, pp. 1-14. doi: 10.1016/j.aca.2015.04.042
- Boucher, T. F., Ozanne, M. V., Carmosino, M. L., Dyar, M. D., Mahadevan, S., Breves, E. A., Lepore, K. H. & Clegg, S. M. (2015). A study of machine learning regression methods for major elemental analysis of rocks using laser-induced breakdown spectroscopy. *Spectrochimica Acta Part B: Atomic Spectroscopy*, 107, pp. 1-10. doi: 10.1016/j.sab.2015.02.003
- Clark, R. N. (1999). Chapter 1 - Spectroscopy of Rocks and Minerals, and Principles of Spectroscopy. In: A.N. Rencz (Ed.), *Remote Sensing for the Earth Sciences, Manual of Remote Sensing*, John Wiley & Sons, Hoboken, New York, pp. 3-58.
- Cocchi, M. (2019). Chapter 1 - Introduction: Ways and Means to Deal with Data from Multiple Sources. In: M. Cocchi (Ed.), *Data Handling in Science and Technology*. Elsevier, pp. 1-26.
- Cuñat, J., Fortes, F., Cabalín, L., Carrasco, F., Simón, M. & Laserna, J. (2008). Man-portable laser-induced breakdown spectroscopy system for in-situ characterisation of karstic formations. *Applied Spectroscopy*, 62, pp. 1250-1255.
- Death, D. L., Cunningham, A. P. & Pollard, L. J. (2008). Multi-element analysis of iron ore pellets by Laser-induced Breakdown Spectroscopy and Principal Components Regression. *Spectrochimica Acta Part B, Atomic Spectroscopy*, 63(7), pp. 763-769. doi: 10.1016/j.sab.2008.04.014
- Desta, F. S. & Buxton, M. W. N. (2018). Chemometric Analysis of Mid-Wave Infrared Spectral Reflectance Data for Sulphide Ore Discrimination. *Mathematical Geosciences*, 51, pp. 877-903. doi: 10.1007/s11004-018-9776-4
- Engel, J., Gerretzen, J., Szymańska, E., Jansen, J. J., Downey, G., Blanchet, L. & Buydens, L. M. C. (2013). Breaking with trends in pre-processing? TrAC Trends in Analytical Chemistry, 50, pp. 96-106. doi: 10.1016/j.trac.2013.04.015
- Forshed, J., Idborg, H. & Jacobsson, S. (2007). Evaluation of different techniques for data fusion of LC/MS and ¹H-NMR. *Chemometrics and Intelligent Laboratory Systems - Chemometr Intell Lab Syst*, 85, pp. 102-109. doi: 10.1016/j.chemolab.2006.05.002
- Harmon, R. S., Lawley, C. J., Watts, J., Harraden, C. L. & Somers, A. M., Hark, R. R. (2019). Laser-Induced Breakdown Spectroscopy—An Emerging Analytical Tool for Mineral Exploration. *Minerals*, 9 (12), 718. doi: 10.3390/min9120718
- Hecker, C., Dilles, J. H., van der Meijde, M. & van der Meer, F. D. (2012). Thermal infrared spectroscopy and partial least squares regression to determine mineral modes of granitoid rocks. *Geochemistry, Geophysics, Geosystems*, 13(3), 3021. doi: 10.1029/2011GC004004
- Kern, O. A., Koutsodendris, A., Mächtle, B., Christanis, K., Schukraft, G., Scholz, C., Kotthoff, U. & Pross, J. (2019). XRF core scanning yields reliable semi-quantitative data on the elemental composition of highly organic-rich sediments: Evidence from

- the Füramoos peat bog (Southern Germany). *Science of the Total Environment*, 697, 134110. doi: 10.1016/j.scitotenv.2019.134110
- Khajehzadeh, N., Haavisto, O. & Koresaar, L. (2017). On-stream mineral identification of tailing slurries of an iron ore concentrator using data fusion of LIBS, reflectance spectroscopy and XRF measurement techniques. *Minerals Engineering*, 113, pp. 83-94. doi: 10.1016/j.mineng.2017.08.007
- Lemière, B. & Uvarova, Y. A. (2019). New developments in field-portable geochemical techniques and on-site technologies and their place in mineral exploration. *Geochemistry: Exploration, Environment, Analysis*, 20(2), pp. 205-216. doi: 10.1144/geochem2019-044
- Le Vaillant, M., Barnes, S. J., Fisher, L., Fiorentini, M. L. & Caruso, S. (2014). Use and calibration of portable X-Ray fluorescence analysers: application to litho-geochemical exploration for komatiite-hosted nickel sulphide deposits. *Geochemistry: Exploration, Environment, Analysis*, 14(3), pp. 199-209. doi: 10.1144/geochem2012-166
- NASA. (2017). ECOSTRESS spectral library [Online]. Available: <https://speclib.jpl.nasa.gov/library> [Accessed September 2017].
- Roussel, S., Preys, S., Chauchard, F. & Lallemand, J. (2014). Chapter 2 - Multivariate Data Analysis (Chemometrics). In: C. P. O'Donnell, C. Fagan & P. J. Cullen (Eds.), *Process Analytical Technology for the Food Industry*, Springer, New York, USA, pp. 7-59.
- Terracore. (2018). The Geospectral Image [Online]. Available: www.terracoregeo.com [Accessed December 2018].
- Yamamoto, K. Y., Cremers, D. A., Ferris, M. J. & Foster, L. E. (1996). Detection of Metals in the Environment Using a Portable Laser-Induced Breakdown Spectroscopy Instrument. *Applied Spectroscopy*, 50(2), pp. 222-233. doi: 10.1366/0003702963906519
- Wainner, R., Harmon, R., Miziolek, A., McNesby, K. & French, P. (2001). Analysis of environmental lead contamination: Comparison of LIBS field and laboratory instruments. *Spectrochimica Acta Part B*, 56, pp. 777-793. doi: 10.1016/S0584-8547(01)00229-4

V

EPILOGUE

13

DISCUSSION

This chapter discusses the key findings in the dissertation and indicates the links between the research objectives and the results. The chapter also discusses the implications of the results and indicates the opportunities and limitations of the use of sensor technologies and data fusion in mining operations.

13.1. SYNTHESIS

This research assessed the potential benefits and opportunities of data fusion for improved accuracy, availability, predictability and quantification in raw material characterisation than can be achieved using the individual sensor technologies. Multiple sensor technologies, namely RGB imaging, VNIR, SWIR, MWIR, LWIR, and Raman spectroscopy, coupled with multivariate analysis techniques and data fusion approaches, were explored to inform about the geological attributes that are important in mining operations. The positive outcomes of the use of the individual techniques guided the development of innovative methodological approaches for the integration of multi-scale and multi-source sensor data. The study provides a brief overview of the use of sensors and data fusion for material characterisation at different levels. Thus, it can contribute to the current need for enhanced material characterisation to enable effective process control, decision-making and sustainability in the mining sector.

The value of the use of sensor technologies in mining is diverse. For example, permit the production of reproducible data that can be validated via independent measurements, allow rapid and non-destructive analysis, enable the provision of comprehensive descriptions of materials, and permit a repeatable analysis using new analytical methods at a late stage. Therefore, sensors can play a vital role to achieve efficiency in the mining process. In mining, the required information from sensor data is not limited to grade control applications. Nevertheless, information on co-occurring minerals or elements is also essential to identify indirect proxies of elements or minerals of interest, define requirements in mineral processing, specify blasting parameters, and environmental monitoring of toxic material. Moreover, information on rock fragmentation, ore geometry and ore versus waste materials are also crucial information for efficient mining. Consequently, the geological attributes investigated in this research were mineralogy, geochemistry, ore geometry, ore–waste discrimination, and rock fragmentation (summarised in Table 13.1).

Technology-driven physical separation of materials into ore and waste can lead to the realisation of sensor-based sorting in mining. Sensor-based sorting permits the dry separation of ore and waste materials and pre-concentrating the ore for further processing. Thus, it offers potential economic and environmental benefits by eliminating the waste from the subsequent steps of mineral processing. For the separation of ore and waste materials, a prior determination of the economic cut-off grade is required. Cut-off grades are essential to determine the economic feasibility and life of a mining project. The determination of economic cut-off grades requires a feasibility study that takes in to account different factors such as commodity market value, depth of the deposit, and location of the mine. Therefore, the technological assessment for the use of ore–waste separation requires the evaluation of the usability at different cut-off grades. Subsequently, in this study, the technological assessment for the separation of ore–waste considered different cut-off grades. The technologies assessed for the separation of ore and waste in the analysed samples are VNIR, SWIR, MWIR, LWIR and Raman spectroscopy (Table 13.1). The applied methodological approaches and results of the ore–waste discrimination are presented in Chapters 7, 8, 9 and 10.

The identification and mapping of minerals are essential information in any geological studies. Accurate information on the distribution and occurrence of minerals is significant input for mine development, resource extraction and environmental studies. The use of sensor technologies can allow automatic identification and mapping of minerals. In this

study, the use of RGB imaging and hyperspectral images (VNIR and SWIR) were assessed for the identification and mapping of minerals at the mine face and in drill core samples, respectively. Besides, Raman spectroscopy was used to identify some of the minerals in the case study site, this is discussed in Chapter 9. The potential use of RGB imaging for the mapping of minerals, delineation of ore-geometry, fragmentation analysis, and target domain definition was assessed in Chapter 6. In Chapter 7, the results of the VNIR and SWIR techniques for the identification and mapping of minerals are presented. Quantitative mineralogical and geochemical information has substantial benefits along the mining value chain, such as in resource model updating and mineral processing. In this study, the applicability of infrared technologies that are commonly used for mineralogical studies was assessed for the prediction of elemental concentrations. The techniques used for semi-quantitative analysis of minerals and elements are MWIR and LWIR, as discussed in Chapters 11 and 12, respectively.

The use of sensor combinations for improved semi-quantitative analysis of minerals and elements were assessed using MWIR and LWIR data. In addition, a data fusion approach was developed and implemented to integrate hyperspectral images (VNIR and SWIR) and point spectral data (MWIR and LWIR) for the discrimination of ore and waste materials. The data fusion approach developed and implemented in this study allowed fusing of the data blocks at different levels, as discussed in Chapters 10, 11 and 12. The test scenarios investigated in this work are summarised in Table 13.1. The table restates the specific objectives of the use of each technology and the combined sensors to investigate the material properties that define the key geological attributes. It also outlines the levels of data fusion and fused data types that are relevant for model specifications.

Table 13.1: Summary of the use of individual techniques and the combined sensors for the characterisation of materials at different levels.

Sensors		Use of the technologies	
Individual sensor technologies	RGB imaging		<ul style="list-style-type: none"> • Mineral mapping • Fragmentation analysis • Ore geometry delineation • Target domain definition
	VNIR hyperspectral imaging		<ul style="list-style-type: none"> • Mineral identification • Ore–waste discrimination
	SWIR hyperspectral imaging		<ul style="list-style-type: none"> • Mineral identification • Ore–waste discrimination
	MWIR		<ul style="list-style-type: none"> • Indication of elemental concertation • Indication of mineralogical concertation • Ore–waste discrimination
	LWIR		<ul style="list-style-type: none"> • Indication of elemental concertation • Indication of mineralogical concertation • Ore–waste discrimination
	Raman		<ul style="list-style-type: none"> • Mineral identification • Ore–waste discrimination
Sensor combinations using the data fusion approach			
Fused data types	Fused technologies	Levels of data fusion	Use of sensors
Data fusion	Point data to point data fusion	MWIR and LWIR	<ul style="list-style-type: none"> • Low-level fusion • Low-level with feature extraction • Mid-level fusion <ul style="list-style-type: none"> • Indication of elemental concertation • Indication of mineralogical concertation
	Image to image fusion	VNIR and SWIR	Mid-level fusion Ore–waste discrimination
	Point data to image data fusion	VNIR, SWIR, MWIR and LWIR	Multiple-level fusion Ore–waste discrimination

The subsequent sections discuss the key findings in this work pertaining to the research objectives. The first section synthesises and evaluates the use of the technologies for the characterisation of materials in mining. The section also discusses the use of each technique for the characterisation of the polymetallic sulphide deposit. In the subsequent parts, the implications of the key findings and opportunities for the use of sensors and data fusion in mining operations are discussed. The chapter also demonstrates how the approach fits within the real-time material characterisation framework, identifies software and hardware requirements, and defines the gaps and limitations of the application of sensors and data fusion in mining.

13.2. THE USE OF THE INDIVIDUAL TECHNIQUES FOR MATERIAL CHARACTERISATION

Deposit type defines the material properties that are relevant to sensor measurements. For example, it determines the composition, grain size, texture and porosity of a material. Thus, assessment of the applicability of sensors for the characterisation of a particular deposit type is essential. In this work, the use of the above-mentioned technologies resulted in the successful characterisation of a polymetallic sulphide deposit at different information levels. The results from each technology are discussed in the corresponding chapters. In the subsequent sections, summaries of the usability assessment of the techniques are discussed. Moreover, the applicability and viability of the sensors in both open-pit and underground mines were synthesised and evaluated using a SWOT (strengths, weaknesses, opportunities, and threats) analysis (Table 13.2).

13.2.1. RGB IMAGING

RGB imaging can allow the characterisation of material based on visual appearance (colour difference). This can enable the mapping of minerals if there is a colour contrast among them. RGB imaging is a surface technique that measures the exposed surface of a material; thus, surface weathering might affect the classification results. However, imaging relatively soon after a new blast can minimise the effect of surface weathering. The presence of water on the mine face is the other challenge that might affect the reflectance value. Conversely, calibration of the classification algorithm with a training dataset that contains water can minimise this effect. In this study, the use of the technique allowed mapping of minerals, delineation of ore geometry and fragmentation analysis. It was also deployed for the definition of target domains (i.e., the indication of the mineralised zone) thus to define the locations of the collected samples (Figure 13.1). The minerals in the test case mainly have medium-to-coarse grains. This is advantageous for the mapping of the minerals using an RGB sensor since having larger grain sizes likely minimise the effect of the mineral mixture in each pixel. The use of the technique for mapping of minerals in fine-grained and mixed materials could be challenging since the sizes of the grains might be too small to be detected from the RGB image data. However, the type of mineralisation also determines the applicability of the technique. For example, for disseminated mineralisation in smaller pores, the detection of the ore minerals might be difficult due to mineral mixtures, surface irregularities and limitation related to sensitivity capability of the technique. The other important consideration for the use of the technique in material characterisation is the data acquisition procedure. For example, the variation in illumination at mine faces might lead to the misclassification of mineral types that maintaining constant illumination throughout the mine face is essential.

Overall, the results of this study suggest the potential use of the technique for the mapping of visually distinct minerals remotely in a polymetallic sulphide deposit. Besides, imaging of a mine face after consecutive blasts can provide information on how material changes with depth. However, for volumetric information, other approaches, such as geophysical techniques, are required. The geological conditions, the data acquisition process and the sensitivity of sensors determine the usability of the technique for mapping of minerals in different deposit types. Some of the potential benefits and limitations of the technique are discussed in Table 13.2.

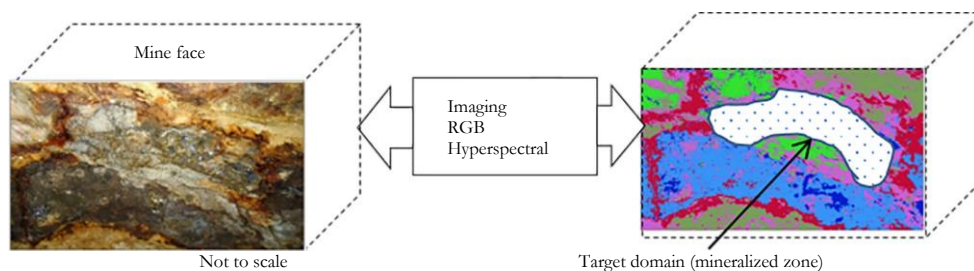


Figure 13.1: Schematic sketch that shows the potential use of the imaging techniques to define target domains for point analysis.

13.2.2. VISIBLE AND NEAR-INFRARED

The VNIR signals are a response to the molecular electronic transition process produced by changes in the position of electrons from one energy level to a higher energy level (Hunt, 1977; Clark, 1999). The VNIR radiation is characterised by high-energy compared to other infrared radiation; thus, it can excite electrons and induce electronic transitions. The energy change associated with the electronic transition can be used to determine the molecular properties of some of the minerals. The spectral features in the VNIR are generally broad and relatively weaker. However, they are characteristic to identify some of the minerals such as the Fe oxides (Hunt, 1977). In this study, the VNIR hyperspectral images were analysed to identify some of the test case minerals and separate the ore from the waste. The identified minerals were the Fe oxides (e.g., hematite) and some of the sulphides (e.g., pyrite). The previous study by Bolin and Moon, (2003) indicated the potential of VNIR to estimate sulphide minerals percentage in drill core samples. The study showed the use of the technique for mapping sulphide minerals versus other minerals (e.g., serpentinised olivine and augite minerals). In this work, the VNIR spectral data were used to distinguish among some of the sulphide minerals based on their spectral response pattern (intensity and shape). However, the sulphide minerals were not identified in some of the samples likely due to the lower concentrations of the minerals or mineral mixture. The technique can detect and identify some of the sulphide minerals but it requires careful analysis and validation since the sulphides do not show any particular absorption features.

The spectral information in the VNIR data enabled the classification of ore and waste materials in the polymetallic sulphide deposit. The classification model performance of the VNIR data is lower than that of the SWIR, MWIR and LWIR data models. This is likely due to the limited amount of relevant spectral information in the VNIR data than the other infrared regions. However, the achieved classification rate using the VNIR data model alone is promising to indicate ore and waste materials in a polymetallic sulphide deposit. Overall, the technique can provide crucial information in material characterisation. Point spectrometers and hyperspectral imagers that operate in the VNIR wavelength range are available from multiple suppliers, such as Specim's VNIR sensor and Headwall's Nano-Hyperspec® (Specim, 2019, Headwall, 2020). The potential applicability, coupled with the state-of-the-art instrumental availability indicates the possible use of the technology in the mining industry. Some of the potential benefits and limitations of the technique are discussed in Table 13.2.

Table 13.2: SWOT analysis for the usability of sensor technologies for the characterisation of polymetallic sulphide deposits in underground mining operations.

Technology	Strength	Weakness	Opportunities	Threats
RGB Imaging	<ul style="list-style-type: none"> • Good for qualitative analysis • Semi-quantification is possible with pixel count • Rapid data processing • Can be used in colour detection and shape recognition (ore-geometry) • Can be used for fragmentation/textural analysis • No actual contact is required/ can be used for remote application • Non-destructive • Non-intrusive • High spatial resolution • No sample preparation needed 	<ul style="list-style-type: none"> • Surface technique • The information is limited to 3 bands • Lower reflection • Minerals having the same colour cannot be differentiated 	<ul style="list-style-type: none"> • Light sources can be optimised • Improved signal processing/Image processing techniques available • Applicable for visually distinct minerals • Most advanced technology • Ruggedized systems available • Small size: ideal for embedding and surface mounting • Potential for mineral/lithological mapping • Indirect proxy for mineralogy/grade • Low-cost • Multiple suppliers 	<ul style="list-style-type: none"> • Variable operating conditions • Can be affected by surface impurities • Surface roughness affects the measurements • Dust affects the measurements
VNIR	<ul style="list-style-type: none"> • Good for qualitative and semi-quantitative analysis • Can be used to distinguish between some of the sulphide minerals • Imaging techniques do not require actual contact with samples • Non-destructive • Good for mapping of iron oxides and REEs • No sample preparation needed 	<ul style="list-style-type: none"> • The narrow the wavelength range the limited the information • Surface technique • Detects fewer minerals • Exhibit broad spectral features 	<ul style="list-style-type: none"> • Developments are dynamic and advancing rapidly • Potential for sensor-based sorting • Well established technology • Rapid data acquisition (in seconds) • Remote application possible • Multiple suppliers available • Passive systems available • Relatively low power requirements 	<ul style="list-style-type: none"> • Environmental influence (such as water and dust) can affect in-situ measurements • Mineral mixtures affect the results • Least commonly used for quantitative analysis • Calibration difficult

Technology	Strength	Weakness	Opportunities	Threats
SWIR	<ul style="list-style-type: none"> • Can be used for sulphide ore and waste discrimination using the approach described in Chapter 7 • Can be used for identification of associated minerals • Imaging techniques - do not require actual contact with the samples • Can be used for textural and mineralogical analysis • Applicable for the characterisation of a wide range of minerals e.g., alteration minerals, sulphates and REEs • No sample preparation needed • Provide sharp spectral features 	<ul style="list-style-type: none"> • Processing and handling of the large volumes of the image data • Surface technique • Can be affected by matrix effect 	<ul style="list-style-type: none"> • Developments are dynamic and advancing rapidly • Most advanced technology in terms of technological development and availability of well-established mineral library • Portable instruments are available and emerging • Image and point data can be acquired • Rapid technique • Multiple suppliers available • Nano scale spatial resolution • Remote application possible • Relatively low power requirements 	<ul style="list-style-type: none"> • Environmental influence (such as water and dust) can affect in-situ analysis • Least commonly used for quantitative analysis
MWIR	<ul style="list-style-type: none"> • Can be used for sulphide ore discrimination • Spectra showed a very good correlation with Fe, the combined Pb_Zn, SiO₂, Al₂O₃, Fe₂O₃ • Detection limit ~0.01 % • No sample preparation needed 	<ul style="list-style-type: none"> • Least explored region • Lack of well documented mineral library • Surface technique • Mainly provide broad features 	<ul style="list-style-type: none"> • The least explored region of the IR but with a good potential • Portable instrument already available • Hyperspectral imager is developed • Relatively low power requirements • Passive systems available 	<ul style="list-style-type: none"> • No commercial system for mineral identification • Robust system is required for underground (harsh environment) application
LWIR	<ul style="list-style-type: none"> • Can be used for discrimination of sulphide ore and waste • Can be used for identification of rock forming minerals • Spectral signal has a good correlation with some of the test case elements thus can be used for elemental prediction • Detect a wide range of minerals e.g., silicates and carbonates • Detection limit~0.01 % 	<ul style="list-style-type: none"> • Surface technique 	<ul style="list-style-type: none"> • Good potential for mining applications • Advanced technology • Point and imaging spectrometers are emerging • Portable instruments are available • Remote application possible • Relatively low power requirements • Passive systems available 	<ul style="list-style-type: none"> • Robust system is required for underground (harsh environment) applications • Camera need robust housing (e.g., water and dust proof)

Technology	Strength	Weakness	Opportunities	Threats
Raman	<ul style="list-style-type: none"> • Detect a wide range of minerals • Detect some of the sulphide minerals • Enriched spectral libraries • No sample preparation needed • Non-destructive 	<ul style="list-style-type: none"> • Detection limit (ppm level detection is not attainable) • Weak in intensity compared to Infrared • Raman signal has a very low correlation with the elemental concentration of the test case materials • Surface technique 	<ul style="list-style-type: none"> • Mobile units available • Both imaging and point techniques are available • Provides complementary information to infrared • High spatial resolution (< 1µm) • Ruggedized system available • Not interfered by water • Rapid technique (few seconds) • Remote analysis is possible 	<ul style="list-style-type: none"> • Sensitive to vibration and dust • Conflict with fluorescent minerals • Intense laser radiation can destroy the sample or cover the Raman spectrum • Due to weak scattering it provides the best result under complete darkness

13.2.3. SHORT-WAVE INFRARED

The absorption of the infrared radiation in the SWIR-MWIR-LWIR ranges causes vibration of molecules that trigger a change in the dipole moment as the bonds expand and contract. The molecular bonds and the mass of the elements in the molecule determine the frequency and intensity of the vibration (Clark, 1999). However, not all minerals absorb infrared radiation. For example, the metals in the sulphide minerals exhibit higher reflectance, and the minerals do not absorb the infrared light in the VNIR, SWIR, MWIR and LWIR wavelength regions (Bolin and Moon, 2003; Clark et al., 1993). Therefore, the sulphide minerals do not show diagnostic absorption features in the infrared wavelength region (AusSpec, 2008). In this study, the featureless nature of the minerals in the SWIR spectra was used as a characteristic value to discriminate ore and waste materials. This suggests the potential of the technique for the separation of materials without particular absorption features, instead using the spectral reflectance difference of the minerals. The required infrared radiation to change the energy of the molecule from one state to another (vibrational transitions) differs since the structure of molecular bonds are different. For example, the SWIR range infrared radiation induces vibration in the molecules of most of the alteration minerals. Therefore, these minerals exhibit characteristic diagnostic features in the SWIR region. However, infrared radiation in the VNIR range could not evoke vibration in the molecules of these minerals. Moreover, the absorption peaks within the SWIR region is usually sharper compared to the absorption peaks in the VNIR.

The SWIR technique is sensitive to the determination of functional groups within a material since different functional groups absorb the SWIR light at particular wavelengths. The absorption of the functional groups at certain wavelengths is characteristics for the corresponding molecules thus, used to fingerprint minerals. Consequently, the SWIR data allowed the identification of some of the minerals such as muscovite, montmorillonite, siderite, quartz, and mineral mixtures in the case study site. In SWIR, the difference in grain size and mineral contents in the sample can change the reflectance value and absorption features depth of the spectra (Zaini et al., 2012). In this study, the VNIR and SWIR

measurements were performed using drill core and rock samples having mainly medium-to-coarse grains minerals. Generally, the finer the grain size the higher the reflected light due to volume scattering (Clark, 1999; Zaini et al., 2012). However, minerals with finer grains and smaller quantities might not be detected using the VNIR and SWIR imaging techniques because they are too small grains and mixed with other co-occurring minerals. Therefore, co-occurring minerals can dominate the spectral response. This is especially more problematic for those minerals that produce weak spectral features.

Overall, SWIR is a well-established technology with enriched mineral libraries such as the USGS and TSG mineral spectral databases (AusSpec, 2008; Clark et al., 2003). Moreover, portable and high-speed SWIR technologies emerged recently from multiple suppliers such as Malvern Pananalytical and Specim (Malvern Pananalytical 2020; Specim, 2019). Thus, with integrated hardware and a comprehensive spectral database, the technique has excellent potential for automated material characterisation in different deposit types. Besides, the SWIR imagers can permit remote or ground-based applications for mine face mapping in open-pit or underground mines. Some of the potential benefits and limitations of the technique are discussed in Table 13.2.

13.2.4. MID-WAVE INFRARED

As discussed in section 13.2.3, sulphide minerals do not absorb MWIR radiation due to their molecular structure. Thus, fingerprinting of the minerals using MWIR is challenging. However, the sulphide minerals show variation in their reflection values at different wavelength locations. The variation in reflectance value is not constant; instead, it varies within the MWIR range. For example, the MWIR spectra show variation in the reflectance value based on the concentration of the combined Pb–Zn in the wavelength ranges from 2.5 to 2.6 μm and 3.5 to 4.0 μm (Figure 10.5). The sourcing minerals of the elements (galena and sphalerite in the case study site) exhibit a spectral pattern in these ranges (NASA, 2018). This is the likely reason for the observed variation in the spectra according to the concentration of the elements. In this work, the spectral variations in the reflectance value were used to perform a semi-quantitative analysis of elements and minerals. With this approach, the MWIR data provided sufficient information and showed great potential for semi-quantitative analysis of minerals and elements, and the separation of ore–waste materials. Besides, minerals such as epidote and alunite exhibit broad spectral features in the region that the technique can be used for the identification of some minerals.

Water has absorptions in the infrared regions. For example, water absorbs MWIR light within the range from 2.6 μm to 3.1 μm due to H–O–H symmetrical and asymmetrical stretching vibrations (Aines and Rossman, 1984). The effect of water in the MWIR spectra was not investigated in this study. However, the measurements were carried out under a similar condition within a short time interval in the laboratory. The applicability of the MWIR for the characterisation of polymetallic sulphide deposit is an interesting finding since this region of the electromagnetic spectrum is not well studied for application in raw material characterisation. There has been limited instrumental development, but recent advancement of the technology has resulted in portable imaging and point MWIR spectrometers. For example, FLIR, Specim, SphereOptics, and TELOPS developed rapid, sensitive and lightweight MWIR spectrometers (FLIR, 2019; Specim, 2019; SphereOptics, 2020; TELOPS, 2020). The potential usability of the technique, coupled with the current technological advances, likely permits its use in raw material characterisation. Some of the potential benefits and limitations of the technique are discussed in Table 13.2.

13.2.5. LONG-WAVE INFRARED

LWIR is mainly used for the characterisation of rock-forming minerals such as silicates and carbonates (Lorenz et al., 2018). The non-diagnostic or minimal spectral information of silicate minerals in the VNIR and SWIR data makes LWIR a good alternative for the characterisation of these minerals. In this study, the use of LWIR data models resulted in successful discrimination of ore and waste in a polymetallic sulphide deposit. This was achieved due to the spectral differences between the minerals of the ore and waste materials. The LWIR reflectance data were also analysed for the prediction of the concentration of elements and minerals in the analysed samples. The achieved promising results for the determination of both elemental and mineralogical concentrations indicate the possibility for simultaneous semi-quantitative analysis of minerals and elements in mining.

The spectral response can vary depending on material characteristics such as grain size and surface roughness (Clark, 1999; Rost et al., 2018; Zaini et al., 2012). In the LWIR region, the band positions of some minerals (e.g., calcite and dolomite) can also change according to their grain sizes (Zaini et al., 2012). In this study, the MWIR and LWIR measurements were performed using powder samples (fine grains) and rock samples (having relatively larger grain sizes). The powder sample measurements resulted in better-infrared signals than that of the rock sample measurements. Several factors could be attributed to the observed difference. For example, measurement using fine-grained material is advantageous in maximising the amount of light reflected in infrared measurements. The other possible reason is that the irregularities at the rock sample surface can inhibit all the reflected light to reach the detector of the sensor. This is because of the gap created between the sensor tip and the sample surface due to surface roughness that could allow reflected light to escape before reaching the detector. Therefore, the signal from rough surface measurements could be lower. It is also important to note that powder samples are homogenised material whereas the analysed rock samples are heterogeneous in nature. This could also cause spectral differences. Investigation of the differences in model results according to the grain sizes is out of the scope of this work. However, the physical and chemical matrix can influence spectral responses and this is discussed in detail in Section 13.6.1.

LWIR is commonly used in the field of remote sensing (e.g., satellite data) and laboratory measurements. The technique has excellent potential for use in ground-based close-range remote sensing of mine faces. Both imaging and point spectrometers are available from multiple suppliers such as Agilent, Corescan, FLIR, and Specim (Agilent, 2017; Corescan, 2019; FLIR, 2019; Specim, 2019). Some of the potential benefits and limitations of the technique are discussed in Table 13.2.

13.2.6. RAMAN SPECTROSCOPY

Raman spectra were collected using two excitation laser sources of 532 nm and 785 nm. The identified minerals using Raman include calcite, sphalerite, kaolinite, marcasite, pyrite and siderite. Some of the sulphide minerals such as galena do not exhibit a well-defined Raman peak due to their structural symmetry and distinct metallic characteristics (Mernagh and Trudu, 1993). This is the likely reason for galena not being identified in the analysed samples. Comparing the two excitation laser sources, the spectra signal (Raman peaks) from the 785 nm is superior to that obtained with the 532 nm laser for the characterisation of the polymetallic sulphide deposit. This is likely because longer excitation wavelengths give less fluorescence than shorter excitation wavelengths (Bumrah and Sharma, 2016; Gaft et al.,

2005). The other possible reason could be that the opaque (non-transparent) nature of the sulphide minerals needs lower energy (higher wavelength) laser sources to penetrate deeper into the samples than high-energy (low wavelength) laser sources (Tuschel, 2016). Thus, higher wavelength laser sources provide better Raman signals for non-transparent minerals.

The Raman spectra were also analysed for the separation of ore and waste in polymetallic sulphide ore samples. Promising ore and waste classification results were achieved using the PLS-DA model at a lower cut-off grade (2%). The overlapping of peaks, weak peak intensity and the fluorescence effect are the main challenges in Raman spectroscopy. Overlapping peaks can be resolved using spectral decomposition algorithms such as MCR-ALS. Adaptive signal-processing techniques can allow enhancing the signals of the Raman spectra. The fluorescence effect can be minimised by considering longer excitation wavelengths since the laser photon could not have enough energy to excite molecular fluorescence. The other method to avoid the effect of fluorescence emission is to consider a time-gated Raman spectroscopy. The Raman and fluorescence signals can be separated in a temporal domain. The lifetime of Raman scattering is shorter than the fluorescence process since the later involves real electronic excited states. Thus, time-gated Raman spectroscopy can be used to collect the Raman signal during the short laser pulses, and the fluorescence emission can be rejected during the measurement process (Edwards, 2005; Kgler and Heilala, 2020; Yaney, 1976).

Raman spectroscopy is a well-established technique that has good potential for the analysis of a wide range of minerals. The current state of the technology supports a hand-held and portable instrumentation permitting in-situ measurements. For example, Agilent's portable Raman system, BWTEK's i-Raman® Plus and Spectral solutions' Raman imager (Agilent, 2020; BWTEK, 2020; Spectral solutions, 2020). However, on-line analysis of materials requires a deposit-specific mineral library that takes into account the heterogeneity (variability of materials). Raman is very well known as a point spectroscopy. However, Raman hyperspectral imagers are now available from different suppliers. For example, WITec provides high-speed sensitive microscope Raman Imagers and Photon provide an ultrafast Raman hyperspectral imager: RIMA™ (Photon, 2020; WITec, 2020). Table 13.2 shows some of the benefits and limitations of the technique.

13.2.7. COMPARISON OF TECHNIQUES

As presented in Table 13.2, each technique has its benefits and drawbacks for the characterisation of raw materials in mining. For example, water has intense absorptions in the infrared, whereas Raman is not affected by water. Infrared (SWIR, MWIR and LWIR) and Raman are vibrational techniques that involve changes in vibrational modes of molecules in a different manner. In infrared spectroscopy, the photon energy interacts with a molecule to change its dipole moment and result in infrared absorption. Conversely, the Raman effect is observed when the vibration mode of molecules causes changes in the polarizability of molecules. Thus, the Raman effect is weak that results from an inelastic scattering process whereas, infrared has stronger spectral signals that result from absorption of light by vibrating molecules. Unlike infrared spectroscopy, which is limited to infrared frequencies, Raman spectroscopy can use a monochromatic light source in UV, visible and near-infrared ranges to generate the Raman effect. This gives the opportunity to measure using a high-intensity laser.

The infrared techniques are capable of identification, quantification and classification of most minerals. However, quantitative and classification analysis using the infrared requires

a well-calibrated model with mineralogical concentration values quantified by a primary technique, such as XRD or XRF. XRD is flexible in the quantification of minerals and can provide relatively more accurate results than infrared. In addition, it is capable of identifying a wide range of minerals, including the sulphides. Conversely, the main advantage of the infrared techniques over the XRD is the availability of portable and rapid systems that enable in-situ and on-line analysis of materials. For example, rapid VNIR systems, which operate over a conveyor belt to determine mineralogy, are available. The other advantage of infrared systems is that they offer lower detection limits than XRD. For example, the detection limit for XRD is 1 - 3 wt%; whereas, infrared systems such as FTIR spectrometer has a detection limit of 0.01 wt%.

Some of the technologies can collect both point and image data. For example, SWIR data can be acquired using a point spectrometer (Malvern Panalytical, 2018) or a hyperspectral imaging spectrometer (Specim, 2019). The advantage of the hyperspectral imaging systems over the point spectrometers include, the former offer wider area coverage and the spatial resolution of most of the imagers is better than that of the point spectrometer. For example, one spot size that is measured by an ASD sensor covers 10 mm whereas; the Specim OWL hyperspectral camera has a spatial resolution of 48 μm (Malvern Panalytical, 2018 and Specim, 2019). High-resolution images likely minimise the matrix effects due to the likely chance of finding pure minerals and can result in better mineralogical information. Pixel-by-pixel classification of hyperspectral images is advantageous to understand the distribution pattern of the constituent minerals. It also allows semi-quantification of the abundance of the minerals based on pixel count. For example, georeferencing and mosaicking of the RGB images provided a comprehensive view of mineral distribution over the imaged mine face surface. On the other hand, point spectrometers offer high spectral resolution and high signal spectral data; however, unlike the image data, they lack spatial reference. Thus, point measurements require precise positioning to provide a spatial context. This can be achieved by projecting the measurement points on the surface (e.g., at the mine face). Overall, each technology has its advantages and shortcomings: thus, sensor combinations can allow enhanced and holistic characterisation of materials using multiple techniques.

13.2.8. POLYMETALLIC SULPHIDE DEPOSITS AND SENSOR TECHNOLOGIES

The sulphide minerals are the major sources of metals and are the most important group of ore minerals (Richards, 1998; Vaughan, 2021; Vaughan and Corkhill, 2017). The minerals occur in all rock types; except for dissemination in certain sedimentary rocks; they occur concentrated in ore deposits or mineralised zones filling the geological structures such as veins and fractures (Richards, 1998). The metals that occur most commonly in sulphide minerals include Cu, Zn and Pb. The sulphide-bearing deposits are also the sources of various precious metals such as Au, Ag and Pt. Sulphide minerals have a significant economic and environmental importance that understanding the compositional information using sensor technologies is crucial. Most of these minerals exhibit properties such as electrical conductivity, striking colour, emissivity, low hardness and high specific gravity. These properties are subject to measurement using various sensor technologies. For example, a thermal infrared camera can be used to measure the emissivity of metals (FLUKE, 2020). Most of the sulphide minerals show colour differences, so the RGB imaging can be used to map the minerals. Attributed to the higher specific gravity of the sulphide minerals, the DE-XRT can also be a potential technique for the separation of ore

and waste materials based on their density differences. Metals have high reflectivity, due to this; metal ores are not commonly analysed using infrared reflectance technologies. However, the results of this research indicate the potential use of the infrared techniques for the characterisation of base metal enriched ores. This is a promising result for future applications of infrared technologies for the characterisation of sulphide-bearing deposits. Besides, information on the base metals can also be used as indirect proxies for information on precious metals. For example, galena is the most important ore of Pb and an important source of Ag. Thus, the quantitative analysis of Pb in the sample can indirectly indicate the amount of Ag present.

13.3. SENSOR DATA AND DATA QUALITY

Sensor technologies are as valuable as the data they can produce, so ensuring quality is fundamental for any sensor application (McGrath and Scanaill, 2013). Consequently, the quality of the sensor outputs was investigated using the data quality parameters: accuracy, completeness, consistency and precision. Table 13.3 summarises the assessed data quality parameters for each sensor data and data model. The other data quality parameter evaluated in this study was noise in the spectra; different signal correction methods were applied to minimise the effect of noise and this is discussed in the subsequent chapters. The reliable use of sensor derived data is not only limited to the quality of data that is produced by sensors; instead, it also depends on the quality control procedure that ensures the integrity of all the factors involved in the process. Therefore, ensuring quality also requires a well-defined quality control procedure that regulates the sampling protocol, data collection process, data analysis methods, and interpretation of results.

Table 13.3: Summary of the assessed data quality parameters for each sensor output.

Technology	Data quality parameters			
	Accuracy	Completeness	Consistency	Precision
RGB Imaging	<ul style="list-style-type: none"> Compared with field verification and high quality pictures taken with closer distance Measured with correct classification rate 	<ul style="list-style-type: none"> Full pixel information on the entire image, full coverage of the study site (e.g., the defined mine face) 	<ul style="list-style-type: none"> The consistency was checked using the geological map and RGB image taken using LIDAR 	<ul style="list-style-type: none"> Multiple images were acquired from each image acquisition stand and compared
VNIR	<ul style="list-style-type: none"> The accuracy was assessed using the XRD results as true value or reference (for mineral identification) Assessed using XRF and ICP-MS (for ore-waste discrimination) 	<ul style="list-style-type: none"> Missing pixel values were assessed using NaN search algorithm Full coverage of the target imaged area 	<ul style="list-style-type: none"> Compared with XRD and SWIR results 	<ul style="list-style-type: none"> Repeated measurements were taken and compared
SWIR	<ul style="list-style-type: none"> The accuracy was assessed using the XRD results as true value or reference (for mineral identification) Visual inspection using the RGB image Assessed using XRF and ICP-MS (for ore-waste discrimination) 	<ul style="list-style-type: none"> Missing pixel values were assessed using NaN search algorithm Full coverage of the target imaged area 	<ul style="list-style-type: none"> Compared with XRD, Raman and VNIR results 	<ul style="list-style-type: none"> Repeated measurements were taken and compared
MWIR	<ul style="list-style-type: none"> Assessed using XRF, XRD and ICP-MS data Measured with correct classification rate Prediction models performance 	<ul style="list-style-type: none"> No missing values Dataset completeness (the availability of each analysed sample spectrum) 	<ul style="list-style-type: none"> Compared with XRD, VNIR and SWIR results 	<ul style="list-style-type: none"> Repeated measurements were taken and compared
LWIR	<ul style="list-style-type: none"> Assessed using XRF, XRD and ICP-MS data Measured with correct classification rate Prediction models performance 	<ul style="list-style-type: none"> No missing values Dataset completeness (the availability of each analysed sample spectrum) 	<ul style="list-style-type: none"> Compared with XRD, VNIR and SWIR results 	<ul style="list-style-type: none"> Repeated measurements were taken and compared

Technology	Data quality parameters			
	Accuracy	Completeness	Consistency	Precision
Raman	<ul style="list-style-type: none"> Validated using XRD The classification models performance assessed using ICP-MS data 	<ul style="list-style-type: none"> No missing values Dataset completeness (the availability of each analysed sample spectrum) 	<ul style="list-style-type: none"> Compared with XRD, VNIR, SWIR and LWIR results 	<ul style="list-style-type: none"> Repeated measurements were taken and compared

13.4. DATA FUSION AND ANALYTICS

13.4.1. THE USE OF DATA FUSION

Data fusion permits the simultaneous analysis of data blocks of different nature and integrates various kinds of information about the same entity. It reduces the uncertainties by combining data from multiple sources. Therefore, it is a useful approach for the classification and prediction problems. In this study, the use of a low-level fusion of the MWIR and LWIR data for the prediction of the elemental concentration of the combined Pb–Zn and Fe resulted in better performance than that of the individual techniques. Similarly, the low-level fusion of the extracted features from the MWIR and LWIR resulted in predictions of mineralogical concentrations enhanced over those generated from the individual data models. Achieving improved prediction using extracted features is an appealing approach since it allows the reduction of data volume while maintaining the relevant information. For the prediction of the mineralogical concentrations, the low-level fusion with feature extraction approach required prior knowledge for the extraction of important variables using the already existing well-established mineral libraries. Thus, the applied features selection method was not based on the outputs of models. The standard mid-level data fusion approach instead requires features extraction through a modelling step. The low-level fusion with the feature extraction approach reduced the data volume, was able to capture most of the informative variables and resulted in enhanced prediction performances. Therefore, this approach has great potential for the analysis of mineralogical information using multiple sensors.

The spectra of the analysed samples show variation based on the concentration of the Al_2O_3 , SiO_2 and Fe_2O_3 minerals (Figures 13.2 and 13.3). Likewise, the reflectance value of the samples shows variation based on the concentration of the minerals over the key wavelength regions extracted in the low-level fusion with feature extraction approach (Figure 13.3). This is in-line with the achieved semi-quantitative mineralogical analysis results of the individual and fused data models. Commonly, quantitative analysis of minerals using infrared becomes complicated in regions where mineral signals overlap (Bou-Orm et al., 2020). In this study, a combined approach using absorption depth and reflectance values were used to relate the relevant spectral information to the concentration of the minerals.

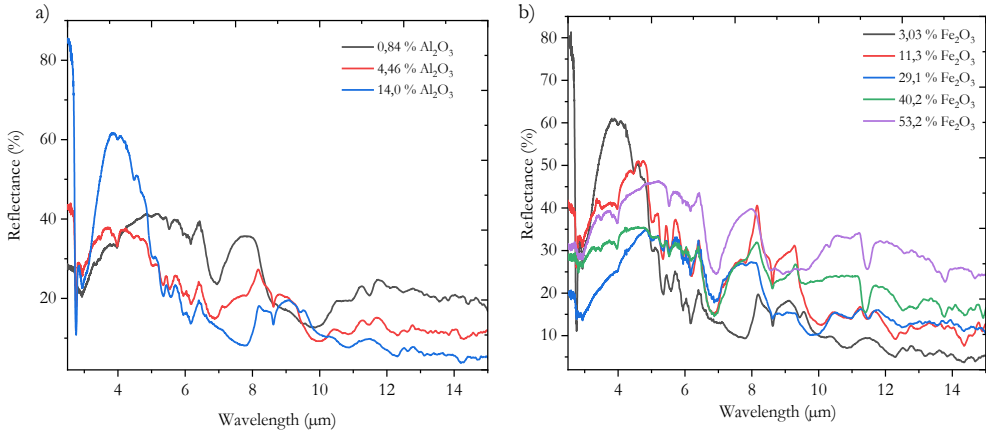


Figure 13.2: The spectra of some of the samples showing a variation in the spectral response based on the concentration of (a) Al_2O_3 , and (b) Fe_2O_3 minerals.

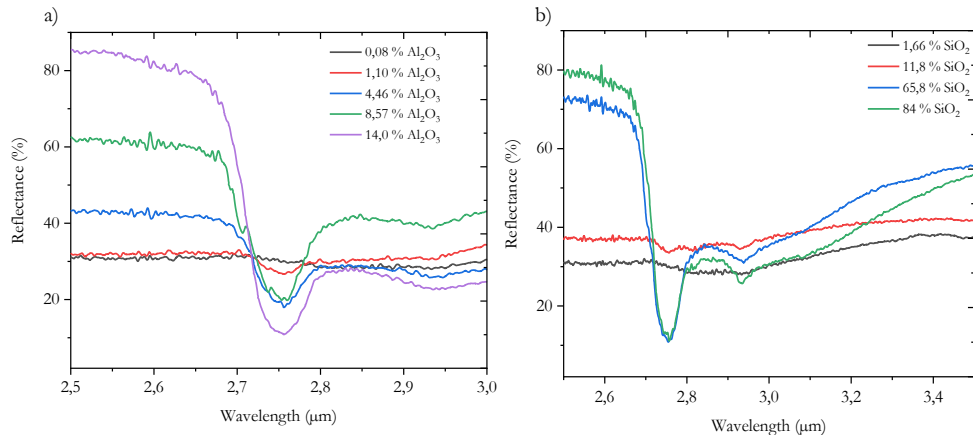


Figure 13.3: The spectra of some of the samples in the wavelength region of 2.5 to 2.75 μm , which shows the variation of reflectance value, based on the concentrations of the minerals (a) Al_2O_3 , and (b) SiO_2 .

Data fusion is a multidisciplinary technique that involves multiple fields. Numerous researchers (Castanedo, 2013; Cocchi, 2019; Khaleghi et al., 2013) discuss the various approaches of data fusion in different disciplines. Despite the discrepancy in the fusing of different data sources together, data fusion is aimed at increased accuracy, increased availability, reduced uncertainty and rapid analysis. However, not all data fusion approaches result in enhanced material characterisation. For example, as discussed in Chapter 12, for the prediction of the combined Pb–Zn concentration using the MWIR and LWIR data, the prediction model performances of the fused data blocks after mid-level data fusion is lower than that of the individual models. This is likely because the extracted variables (PCA components) could not fully capture the variation in the data. Nonetheless, the acquired results are promising and can likely be improved by considering other feature selection techniques such as MCR-ALS.

The results of the low-level fusion approach suggest that fusing data blocks from multiple sources could likely result in enhanced prediction and classification models

performances. However, low-level data fusion might cause a high data volume issue and the possible predominance of one data source over the others that feature-level fusion with variable screening might be preferred in some applications. Conversely, mid-level fusion requires the development of an ultimate model for the extraction of relevant information (Cocchi, 2019). Therefore, each level of fusion has advantages and disadvantages that a systematic approach is required to find the optimal level of fusion in different applications. Studies also indicated that the preferred level of data fusion is always application dependent (Borràs et al., 2015; Khaleghi et al., 2013).

The integration of image and point data is advantageous to make use of the combined effect between the two data types; the image data covers an extended area whereas the point data is more accurate for most of the sensor outputs but covers a smaller area. The different scale of observations and resolutions of the image and point data brought to the same data scale for enhanced separation of ore and waste materials in the analysed samples. The image data was converted to representative spectra using endmember selection techniques and the developed methodological approach. This approach is beneficial for data simplification, data volume reduction, classification accuracy enhancement and relating the geochemical data to infrared image data. The method is data-driven that does not require a prior specification or identification of minerals and elements. As the experimental results show, enhanced classification accuracies were achieved by the integration of the SWIR (image data) and MWIR (point measurement) data than the individual techniques. The fusing of the VNIR, SWIR, MWIR and LWIR data blocks also resulted in enhanced classification accuracies than that of the individual techniques. However, the result from the integration of the four data blocks is comparable to the fusion results of the SWIR and MWIR data blocks solely. This shows the need for an optimised approach for the selection of the optimal sensor combination. Overall, the results from the integration of image and point data suggest the use of the approach for enhanced characterisation of materials in different deposit types.

The results of this study indicate that data fusion is a promising approach for enhanced material characterisation. The developed methodology can enable rapid analysis of materials in near real-time using a fused sensors signal and the inherent material properties. However, the actual implementation of data fusion for rapid analysis of materials in mining requires advanced instrumentation and comprehensive tools. Such an efficient integrated intelligence system is not currently available or operationally implemented. However, it is a key enabler for a holistic overview and accurate analysis of material along the mining value chain.

13.4.2. MODELS IN DATA FUSION

Multivariate analysis techniques were used to assess the usability of each sensor and the comparative merits of the combined data for the characterisation of a polymetallic sulphide deposit. For the prediction of the mineralogical concentrations, linear and non-linear multivariate techniques (PLSR, PCR, and SVR) resulted in comparable performances. Therefore, for the given datasets, only moderate effects of the choices of models (linear or non-linear models) were observed. In regression models, the relationship between the predictor and response variables can be linear or non-linear. This relationship is dependent on the nature of the data. Understanding of the relationship between the predictor and response is crucial to maximise the performances of the classification or prediction models. Researchers in various fields indicate that the use of the linear or the non-linear models for the same application may outperform one another or may result in comparable model

performances. For example, Khosravi et al., (2017) indicated that for the prediction of arsenic content in soil samples using VNIR spectra, the performance of the SVR model was superior to the PCR and PLSR models. Likewise, Shi et al., (2015) showed the superiority of the SVR model to the PLSR model for the prediction of elements in sedimentary rocks using LIBS data. In contrast, Boucher et al. (2015) compared the performances of the linear and non-linear models for the prediction of major elements in igneous and meta-igneous rocks using LIBS data, and their results show that the linear models resulted in better prediction performances than the non-linear models.

The classification models applied in this study include unsupervised (K-means) and supervised techniques (e.g., SVC and PLS-DA). The classification accuracies achieved using these techniques is acceptable for the separation of ore and waste materials at different cut-off grades. In this work, the level of data fusion or the data fusion strategy is more influential than the model choice. However, there is a small difference in the performances of the models, meaning that model choice might have a significant influence on the characterisation of materials in other deposit types. Generally, the results of this study and previous studies suggest that the preferred model depends on the nature of the data. Thus, future application of models for the prediction or classification of different material types requires optimisation of the response and predictor relationship.

13.4.3. OPPORTUNITIES WITH FUSING OF DATA

Combination of sensors has an advantage over a single sensor in providing improved accuracy, improved precision, reduced uncertainty and holistic description of materials (Bi et al., 2015; Doeswijk, 2011; Kruse, 2015; Morors et al., 2010; Moros and Laserna, 2015; Rajalakshmi and Chamundeeswari, 2014; Sjoqvist, 2015; Westa and Resminib, 2009). As discussed in Chapter 4, a combination of sensors can be implemented using different approaches, such as physical integration of sensors and data fusion. The former requires a complicated and expensive system design to be implemented in practice. For example, a physical combination of sensors that operate remotely and sensors that need physical contact to the surface of the sample requires a complex solution. Moreover, the portability of the integrated system might be challenging to achieve. On the other hand, data fusion allows handling data with diverse natures such as data with different scales of observation, data that are acquired with actual contact and remote sensors, data on various material properties (e.g., reflectance and Raman scattering) and data with varying strengths of signals. Therefore, for the combination of multiple sensors, data fusion can be an economical and practical alternative option.

Most minerals show certain spectral information in different regions of the electromagnetic spectrum. The fusing of the data from these regions likely results in an enhanced analysis of the minerals since each region can provide new information to the models. Moreover, data from multiple sources can also offer different sorts of information such as mineralogical, geochemical and textural information. Thus, simultaneous analysis of multiple data blocks can likely enhance the results and enable the comprehensive description of materials. However, data fusion might not necessarily result in the improved characterisation of material under certain conditions. These conditions include the presence of highly correlated data blocks, lack of relevant information in one or more of the data blocks, high dominance of one or more of the data blocks, use of suboptimal variable screening techniques, a shortfall in relevant data scale conversions and incompetence of the modelling algorithms. Therefore, a successful application of data fusion requires meeting

certain conditions. Some of the requirements for the selection of appropriate sensors and data analytics to realise the benefits of data fusion are provided in Figure 13.4.

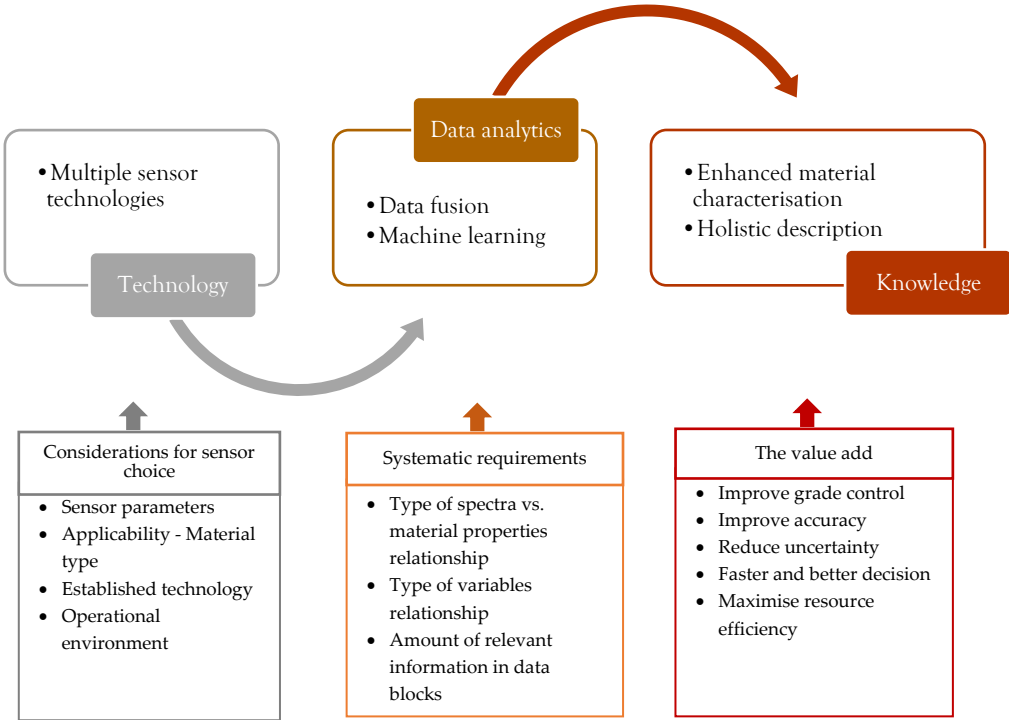


Figure 13.4: Some of the requirements for the selection of appropriate sensors and data analytics for improved spectroscopic characterisation of raw materials.

There is an ever-increasing interest in a near-complete description of materials using multi-sensor data across diverse areas of application. One such application is a mining operation. A comprehensive view of materials in mining applications is advantageous to understand the requirements in mineral processing, find indirect proxies of minerals of economic interest, provide mineralogical information to the resource model, and convey safety information. Near-complete description materials can be achieved using a data fusion approach. In general, data fusion in mining operations enables effective grade control, improves process control, minimises handling of waste or zero-value material and allows automation. Therefore, it can significantly support effective decision-making and play an essential role in ensuring resource efficiency.

Advances in technology have resulted in multiple state-of-the-art sensors that produce high-throughput multi- and megavariable data. The high frequency and high data volume impose a challenge for the computational analysis and understanding of the sensor outputs. Therefore, advances in data analytics are required to generate knowledge from complex data. Data fusion is one of the approaches that provide the opportunity to use the synergy among the different data sources. It can permit an understanding of the contribution of the relevant information that is common among the data blocks and unique to individual data

blocks. The fusing of data at different levels allows an assessment of the different abstraction levels and associated uncertainties to enable improved accuracy, improved availability, and reduced uncertainty.

Sets of sensor solutions that are applicable to material characterisation are available. Each technology measures several aspects of material properties at different depths of penetrations and scales. Figure 13.5 shows some of the potential sensor solutions applicable to mining and the possible benefits of data fusion. These suggested technological solutions can provide information on the key geological attributes. Moreover, the benefits of the use of the technologies can be maximised via integration of data outputs using scalable data fusion algorithms. Maximised results do not necessarily require the integration of data from several sources: the optimal combination can be selected in an optimised way. This way, the complexity that might arise because of the fusing of multiple sensors can be minimised.

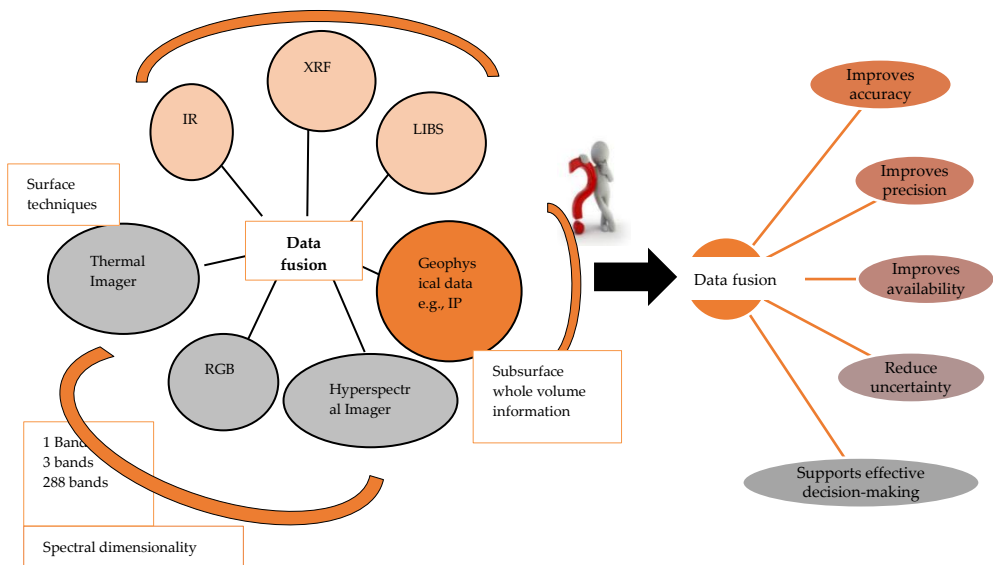


Figure 13.5: Some of the potential sensors and benefits of data fusion in mining.

13.4.4. CHALLENGES IN DATA FUSION

The majority of the challenges in data fusion arise from the varied data types and the diversity of sensor technologies (Khaleghi et al., 2013; Wongthongtham et al., 2017). For example, sensors produce data with different observation scales and resolutions. This might pose a challenge when fusing data from multiple sensors. Therefore, data fusion need to address the issue related to the differences in observation scale and resolution. In Figure 13.6, the data types, scales and resolutions of the data used in this study are shown as an example. The integration of these data types requires upscaling or downscaling resampling approaches and logical reasoning based on the nature of the material and data types. The other challenge is related to data volume: depending on the technology, some of the sensors (e.g., hyperspectral imagers) produce a large volume of data. In some cases, redundant data on the same target from different sources increases the confidence of the analysis. In other

cases, model performances can be enhanced by removing redundant and non-relevant information in the spectra. Therefore, to resolve the issue of data volume and remove redundant information, variable screening techniques are a good option. Some of the data fusion challenges and the corresponding possible solutions are summarised in Table 13.4.

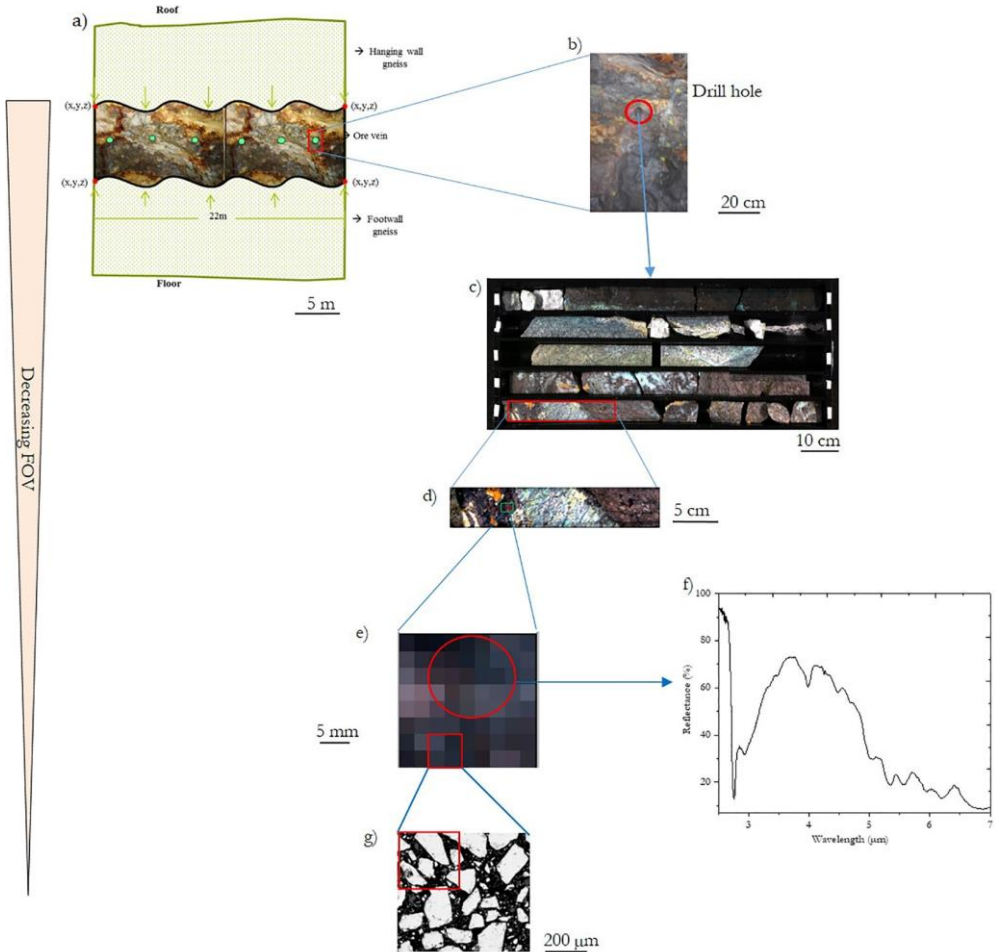


Figure 13.6: The FOV and scales of the different sensor technologies used in this work (a) RGB image of a mine face, (b) a drill hole having a 5 cm diameter—the hole in the red circle, (c) drill core, (d) a drill core having a length of 35 cm, the green box shows the imaged area, (e) SWIR hyperspectral image having a pixel size of 0.28 mm (the red square), (f) MWIR spectra taken at a spot indicated by the red circle, and (g) a thin section image taken using an optical microscope.

Table 13.4: Some of the possible challenges of data fusion and proposed solutions.

	Issues	Solutions
Data quality	Low signal to noise ratio \ noisy data	<ul style="list-style-type: none"> Data pre-processing techniques that can enhance signals can be considered, data blocks need to be processed separately
	Sensor data can have measurement errors	<ul style="list-style-type: none"> Data quality assessment should be performed
	Data redundancy	<ul style="list-style-type: none"> Variable screening techniques can filter relevant information and reduce the effect
	Presence of outliers	<ul style="list-style-type: none"> Outlier detection can be performed for the individual and fused datasets
Data volume	High data volume	<ul style="list-style-type: none"> Data pre-processing and variable screening techniques can minimise data volume
Sensor diversity	Sensors signal with different response or intensity	<ul style="list-style-type: none"> Consider data scaling techniques (e.g., block scaling techniques)
	High data correlation between data blocks	<ul style="list-style-type: none"> Consider other technologies that have low correlation or extract the uncorrelated relevant information
	Data from multiple sensors have different resolution thus impose challenge for data fusion	<ul style="list-style-type: none"> The data fusion approach needs to consider data upscaling or downscaling techniques and consider logical reasoning that takes into account material type and data type
Others	Reliability of the data fusion results	<ul style="list-style-type: none"> Validate the data fusion results using reference standards
	Computational power - depending on the data types and volume data fusion tasks might be computationally expensive	<ul style="list-style-type: none"> The effect can be minimised by considering data filtering and relevant variable extraction techniques or divide the steps in data fusion and perform parallel analysis
	Software scalability - processing power and database might not be expanded to accommodate high throughput in online analysis	<ul style="list-style-type: none"> Scale-up data storage Consider scalable computing infrastructure for the parallel analysis of the different steps in data fusion

13.5. IMPLICATIONS OF THE RESULTS

As discussed in Chapter 12, the level of information that can be generated from sensor data differs. Sensors can be used for the detection, identification, discrimination or quantification of materials. These levels of information can be linked to the geological attributes that are crucial in mining such as mineralogy, geochemistry, ore geometry, ore-waste discrimination, and rock fragmentation. The subsequent sections discuss the significance of the results of this study to mining.

13.5.1. IDENTIFICATION OF MINERALS

Identification of minerals is crucial to understand the material composition in any geological investigations. Numerous researchers studied the spectroscopies of minerals and indicated the wavelength regions of the functional groups of specific minerals that possess diagnostic features (Clark, 1983; Clark, 1999; Clark et al., 2003; Lyon, 1965; Hunt et al., 1971; RRUFF, 2020). Mineral libraries and published works were used to identify various minerals using the VNIR, SWIR, LWIR and Raman sensor technologies. For example, the minerals identified using the VNIR spectral data were the iron oxides (e.g., hematite and magnetite) and some of the sulphide minerals (e.g., pyrite). The SWIR was used to identify the hydroxyl-bearing dioctahedral silicates (e.g., kaolin, montmorillonite, and muscovite clays) and carbonates (e.g., calcite, dolomite). The LWIR reflectance spectra were utilised to identify the silicates (e.g., quartz) and carbonates. The minerals identified using the Raman spectroscopy include sulphides (e.g., sphalerite and pyrite), carbonates (e.g., calcite and siderite), and layered silicates (e.g., kaolinite). In addition, the RGB imaging was successfully used to map visually distinct minerals such as galena/sphalerite, quartz/calcite, pyrite/chalcopyrite, and the oxidized minerals.

In this study, the interpretation of the spectra from the different sensors enabled the identification of various kinds of minerals. However, the identification of minerals might not be complete due to several factors, such as influence from the matrix effect, weaker spectral responses and the fluorescence effect (AusSpec, 2008; Kafle, 2020). For example, depending on the composition of a mixture, the wavelength locations of the diagnostic features of minerals can shift. As shown in Figure 13.7, the Raman peak position of pyrite shifts in pyrite samples collected from the three localities. Therefore, holistic description of material compositions is challenging to achieve. This drives the need for data-driven approaches to find relationships between spectral data and material properties. Establishing and understanding these relationships are useful for transforming the hidden aspect of the spectra into crucial information. This approach can contribute to a better description of the required details of material compositions.

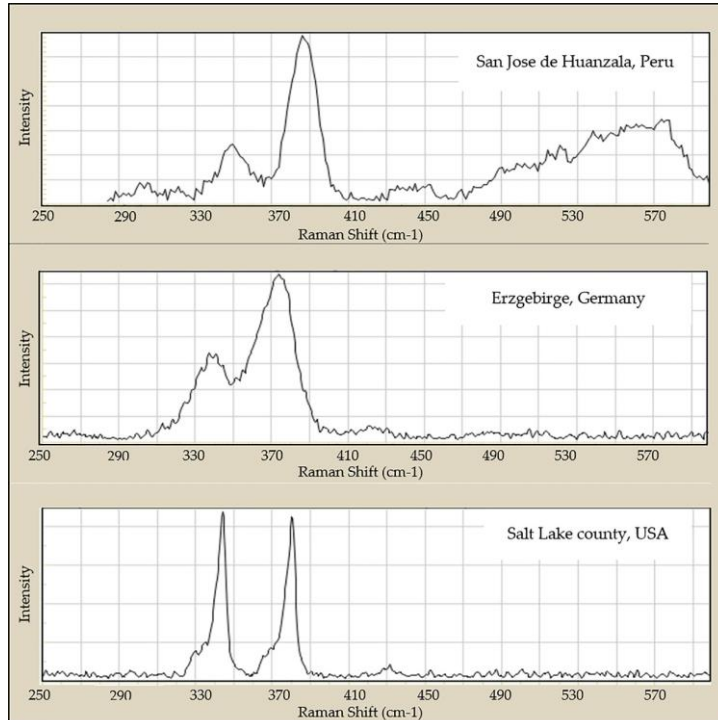


Figure 13.7: The Raman spectra of pyrite from three different sample localities (Source: RRUFF, 2020).

13.5.2. ORE–WASTE DISCRIMINATION

In mining, waste material is excavated to reach the ore. The amount of waste material that needs to be removed depends on the nature, location and geometry of the ore body. Besides, the mining method, and the stability and composition of the host rocks determine the waste volume. The higher the waste volume, the higher the financial implications for material transport, handling and processing. This shows the need for efficient methods to separate the ore from the waste as early as possible in the mining process. The waste material can be rejected, and the waste volume reduced early in the extraction and mineral processing phases. For example, the ore–waste boundary can be indicated during mineral mapping at the mine face, and sensor-based sorting can allow the pre-concentration of ore and rejection of waste material prior to mineral processing.

Ore–waste discrimination is one of the key processes in the extraction, material transport and mineral processing. The successful separation of ore and waste material relies on the sensor technology and the software tool that sorts the material into ore and waste streams. Minerals occur in association with other minerals, which makes the identification or quantification of each mineral a challenge. Therefore, materials are designated as ore if they contain the minerals or elements of economic interest above the determined cut-off grade or considered to be waste if the commercially worthless material dominates. Therefore, the separation of the ore material is advantageous in minimising the material transport cost incurred during material handling. Moreover, removing waste material prior to mineral processing reduces the energy and water requirements of each tonne of ore

concentrate produced and minimises the time required for processing (Buxton and Benndorf, 2013; Lessard et al., 2014; Wills and Finch, 2016). Therefore, it has a tangible contribution to maximise the recovery and resource efficiency in mining.

In this study, ore and waste materials were segmented using imaging and point technologies: VNIR, SWIR, MWIR, LWIR and Raman. The individual data blocks, coupled with the supervised and non-supervised classification techniques, resulted in an acceptable classification rate. The use of data fusion strategy improved the models classification ability relative to the results yielded by using the individual techniques. The sulphide minerals exhibit very weak features in infrared spectra, which made identification of the minerals in the sulphide ore challenging. However, in this study, it has been demonstrated that without direct fingerprinting of the sulphide minerals, the economically valuable material can be distinguished from the zero-value material using data-driven approaches. This indicates the potential of the technologies for future sensor-based sorting applications.

13.5.3. SEMI-QUANTITATIVE ANALYSIS OF MINERALS AND ELEMENTS

Quantitative mineralogical and geochemical information is crucial for the understanding of the material compositions at a higher-level. For example, along with other conditions such as the accessibility and extent of the ore zone, quantitative geochemical data are used to determine the economic feasibility of a deposit. However, for most of the sensor outputs, quantitative analysis of minerals and elements are challenging to achieve. Therefore, sensor technologies such as infrared, Raman and XRD are commonly used for qualitative analysis of minerals. In this study, the data-driven approaches enabled the definition of a relationship between the infrared spectra and the concentrations of SiO_2 , Fe_2O_3 and Al_2O_3 minerals for semi-quantitative analysis of minerals in the polymetallic sulphide ore. Pure minerals are difficult to find in nature and in mixed spectra identification of each mineral is challenging, so this result is very promising. The characteristic of ore have direct implications for metallurgical behaviour; it determines the grinding capacity, mineral hardness and flotation behaviour. Therefore, the gangue minerals can be used to define the ore types. For example, for iron ore, silicate gangue minerals can be used to define the ore types. Likewise, the semi-quantitative information on SiO_2 , Fe_2O_3 and Al_2O_3 is essential in understanding the requirements of mineral processing.

Geochemical data play an essential role in supporting effective-decision making in mining operations. The multi-elemental geochemical analysis is commonly carried out using elemental technologies such as XRF and LIBS. Depending on the working principle of these technologies, signals are generated, and the spectral signals are related to qualitative or quantitative elemental data. In other words, the fingerprints in the spectra are interpreted to determine the elemental compositions of material. The infrared spectra provide information on the functional groups of molecules. Thus, it is a mineralogical technique. The elemental information cannot directly be observed in infrared spectra. The mineralogical information in the infrared spectra can identify which minerals are the source of the elements. In this study, robust correlations were observed between the infrared spectra (MWIR and LWIR) and the elements of economic interest (the combined Pb–Zn and Fe concentrations). Elemental techniques provide information on the geochemistry; however, the sourcing minerals of the elements could not be derived from the spectra. Knowledge of minerals is beneficial for resource modelling and in understanding the requirements for mineral processing. The results of this study suggest the potential use of the technologies for simultaneous semi-quantitative analysis of mineralogical and elemental information. The

analysis was performed using a rapid and portable system; thus, it can allow on-line in-situ characterisation of materials. This is beneficial in maximising the efficiency of mining.

The performance of the MWIR model for the prediction of the combined Pb–Zn, Fe₂O₃ and Al₂O₃ concentrations is superior to the LWIR model, but Fe and SiO₂ concentrations were better predicted using the LWIR model than the MWIR data model. This indicates that adequate spectral signals of the combined Pb–Zn, Fe₂O₃ and Al₂O₃ exist in the MWIR than in the LWIR. Likewise, in the LWIR region, the amount of information related to Fe and SiO₂ is superior to that in the MWIR region. These findings are in line with the available spectral information related to the minerals and the presumed source minerals of the elements (Kokaly et al., 2017; NASA, 2019). Despite the difference in the prediction performances of the MWIR and LWIR models, the results of the quantitative analysis of the minerals and elements reveal the presence of relevant spectral information in the two regions.

Overall, geochemical data are commonly used in mining operations; however, chemical analysis alone cannot ensure efficiency in the mining process. For example, both geochemistry and mineralogy can define the ore grade; nevertheless, in mineral processing, the mineralogy determines the recovery rate. Likewise, dry separation of ore and waste materials ensures resource efficiency. Information on rock fragments is crucial in defining requirements in blasting parameters and mineral processing. This shows the need for comprehensive information to enable effective process control and optimisation in mining.

13.6. FEASIBILITY OF THE USE OF SENSORS AND DATA FUSION FOR MATERIAL CHARACTERISATION IN MINING

In mining, sensors can be used for different applications—for example, sensors for machine performance monitoring, collision avoidance and material characterisation. Sensors for material characterisation can be utilised along the mining value chain, to provide usable data on several aspects of material properties. The technical and economic feasibility of the use of sensors and data fusion for material characterisation in mining relies on various viability measures. These viability criteria include sensor robustness, portability, sensitivity, accuracy, data acquisition speed, operational costs, purchasing cost, data transmission availability, high throughput data capability, low-power technology and the availability of a well-calibrated tool for automatic determination of material composition. Recent advances in sensor technology and data analytics, coupled with the enormous opportunities from internet and wireless networking, suggest the feasibility of the use of sensors and data fusion in mining operations. This integrated solution should be operated economically with reliable technical performance. Thus, the economic viability of the use of sensors and data fusion requires a cost-benefit analysis.

13.6.1. SENSOR-BASED MATERIAL CHARACTERISATION

Material characterisation along the mining value chain is increasingly reliant on new sensor technologies that operate from satellites, drones, field-based and drill-core logging systems. Sensor-based material characterisation is crucial in providing continuous (or near real-time) data on the essential geological attributes (e.g., mineralogy and geochemistry). The key performance indicators for the use of sensor technologies in mining operations include better grade accuracy, better availability, enhanced ore–waste separation, and automated

results. Therefore, sensor-derived rapid and accurate information along the mining value chain is advantageous for effective grade control, process optimisation and effective-decision making in mining operations (Figure 13.8).

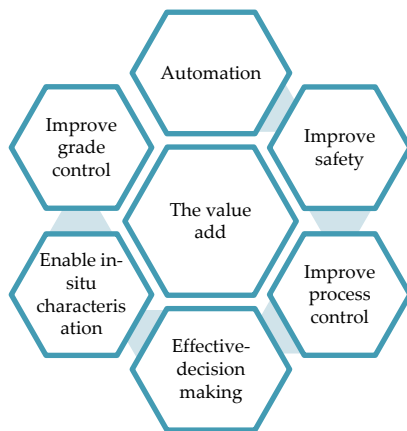


Figure 13.8: Some of the values of the use of sensors in mining operations.

Some of the specific findings of this research that potentially indicate the benefits and feasibility of the use of sensors and data fusion are discussed below:

- RGB imaging enabled mineral mapping, ore zone delineation and fragmentation analysis using in-situ measurements in an underground mine. An RGB sensor is a simple technique that is capable of providing mineralogical insights, structural information, and a semi-quantitative indication of ore/waste ratio in deposits with visually distinct minerals. Lightweight, rapid, high-resolution and robust RGB cameras are available from multiple manufacturers. This technology has great potential for in-situ mapping of mine faces in underground and open-pit mines. However, in-situ measurements in harsh environments require optimal compensation techniques for enhanced results.
- Infrared technologies were successfully used to semi-quantify metals in polymetallic sulphide ore samples. The infrared spectra can simultaneously be used for the identification and quantification of minerals.
- The successful discrimination of ore–waste materials using the SWIR, MWIR and LWIR indicates the potential use of these technologies in the dry separation of ore and waste materials. The pre-upgrading or dry separation of ore and waste minimises the extraction and ore processing costs (Buxton and Benndorf, 2013; Lessard et al., 2014; Wills and Finch, 2016). Thus, it is beneficial in maximising efficiency in mining operations.
- In material characterisation, the MWIR is the least-explored region of the electromagnetic spectrum due to limited instrumental development in the past. Recently, significant development of novel MWIR technologies has been undertaken by different manufactures. The very promising results obtained in this research, coupled with the dynamic development of MWIR sensors, establish the

high potential of this technique for rapid and accurate characterisation of materials in mining.

- This research was conducted using a block of ~ 22 m long and ~ 2 m high. The measurements were taken in-situ at the mine face and in a laboratory using the collected samples. One of the possible mechanisms to scale-up the approach into a larger area in operational mines could be by the integration of image and point data. Image data provide information over a wider area with a relatively small amount of time compared to the point measurements. The point measurements have an advantage in providing a certain amount of specific information (e.g., elemental concentrations). The image data and the point data can be linked using the methodological approach developed in this study or based on the geographic locations. However, to connect the two data types based on location, it is crucial to take into account the positional uncertainty, the spatial resolution of the sensors, and the material variability. Therefore, the measurement can be performed within certain very small areas to incorporate the positional uncertainty. The point measurements in the defined small area can be linked to the image data in that same area to develop a correlation model. The learned relationship can be used to predict the quantitative elemental or mineralogical information at unmeasured locations. Therefore, an established correlation of the point measurements with the image data at each location can be used to predict the quantitative information at unmeasured locations. Moreover, the established relationship could be used to indicate mineralised zones such as low-grade, medium-grade and high-grade regions.
- Fusing the different data blocks enhanced the classification and prediction models performances relative to the results yielded by using individual techniques. The physical integration of multiple sensor technologies into a single platform is challenging and, in terms of practical implementation, it is expensive. Therefore, data fusion can be the ultimate alternative option for the combination of multiple sensors.
- Data fusion techniques can reduce data volume. In this work, the developed methodological approach for fusing of the image and point data allowed a significant reduction of data volume, while maintaining the most relevant information. One of the main issues for the use of sensors in operational mines is the high data volume resulting from the high material throughput. Several factors determine data volumes such as the data frequency, spatial resolution, spectral resolution, spatial extent of the study site, and the nature of the data. For example, the higher the spatial or spectral resolution, the higher the data volume. However, higher resolutions yield better information that the effort should not be on minimising the spatial or spectral resolutions; instead, the strategies should focus on reducing data volume using data analysis techniques. One such approach is the use of features extraction techniques. Multiple variable screening techniques are available, such as parallel factor analysis (PARAFAC) and MCR (Cocchi, 2019). However, the ultimate method depends on the nature of the data.

The nature of the deposit defines the properties of the material that are relevant to sensor measurements. Deposit types are typified by composition, grain size, crystallinity,

and the likes. These properties can cause spectral variations; for example, grain size influences the amount of light reflected and absorbed (Clark, 1999; Hapke, 2012; Zaini et al., 2012). Larger grains have a greater internal path where photons may be absorbed than smaller grains. Therefore, reflectance usually decreases as the grain size increases in the VNIR and SWIR spectra (Clark, 1999). This indicates the importance of understanding the material variability to accommodate the variations caused by the chemical and physical matrix effects. The chemical effects are related to the composition of materials (e.g., mineral associations). Whereas, the physical matrix effects are caused by material properties attributable to grain size, water content, surface texture, as well as textural and porosity changes. The size of a spot measured by a point spectrometer or the spatial resolution of an image can also determine the degree of the chemical matrix effects. The smaller the spot (measurement) size, or the smaller the pixel size of an image, the lower the matrix effect. For example, Figure 13.9 shows an electron microprobe analyser (EPMA) image taken using one of the samples. The red circle shows a spot size for a point measurement using an FTIR. The identified minerals at the indicated spot using the EPMA include galena, pyrite, feldspar, quartz, and mica, whereas the point measurement provides a mixed spectrum, which combines the spectra of all these minerals. Spectral data can be complex in nature, and fingerprinting of most of the minerals in the mixture is challenging. One of the potential approaches to minimise the chemical matrix effect is the use of data-driven approaches that make use of multivariate analysis techniques and data fusion. For example, decomposition techniques can separate a mixed spectrum into (nearly) pure components. This can provide a better insight to understand material compositions.

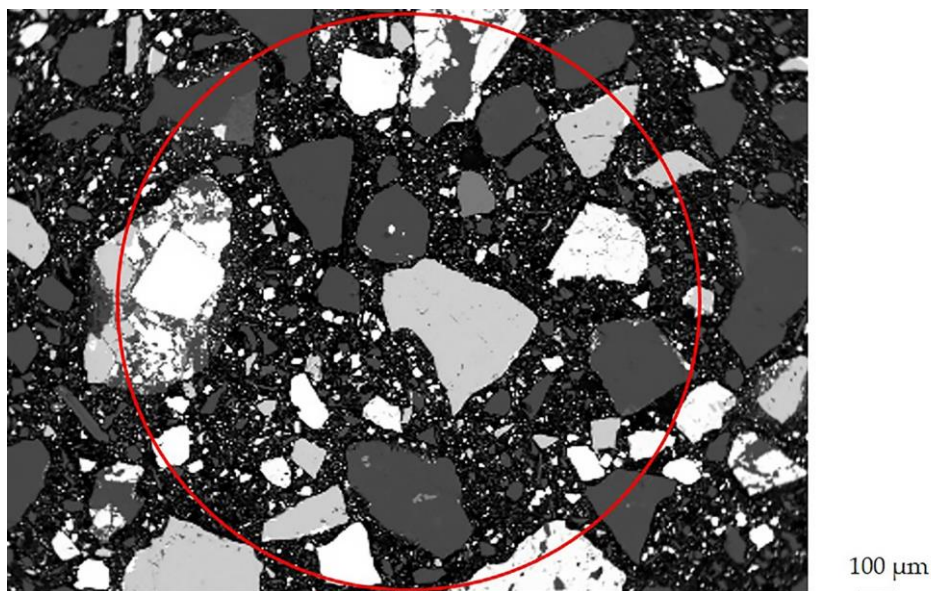


Figure 13.9: A microscope image of one of the analysed samples showing the different mineral grains within the red circle, where the red circle indicates a spot size (~ 2 mm) of a point measurement (for example, a spot for measurement using an FTIR spectrometer).

The use of the explored techniques and the developed methodological approaches for the characterisation of materials in other deposit types might require different

considerations. One such consideration is the customisation of the technologies via optimised sensor parameter specifications. For example, in this study, the 785 nm excitation laser source resulted in better Raman spectra than the 532 nm excitation laser source. Likewise, the diffuse interface resulted in a better FTIR signal than the ATR interface. However, the use of the techniques in other deposits might require a different specification. Use of the developed methods for the characterisation of materials in other deposit types might require different levels of data fusion and alternative features extraction techniques. However, the developed general framework of the data fusion concept provides a versatile solution for use on various deposit types.

Sensor derived information could be generated throughout the mining value chain such as at the mine face, using drill cores and blast hole logging, over conveyor belts, and at muck pile sites. This is valuable in generating consistent and accurate on-line data throughout the mining process. Advances in sensor technologies have resulted in simplified designs and low-cost systems. In the near future, it is likely that even lower cost systems will emerge. Portable, rapid and flexible systems are already available from multiple suppliers. This ensures maximised use of sensors in mining applications. However, due to economically marginal deposits, deeper mines and complex geology, there is still a need to define and develop improved technology that can address current and future mining challenges.

13.6.2. PROSPECT FOR AUTOMATED (REAL-TIME) ANALYSIS OF MATERIAL

Real-time accurate data is crucial for rapid resource model updating, mine operational planning and decision-making. It offers opportunities for cost savings and increases mineral recovery rates through optimised process control and effective-decision making. Real-time material characterisation requires rapid data acquisition, automated data processing and rapid return of results. This requires an advanced platform that integrates hardware and high-performance computing software systems. The development of such integrated systems could enable the generation of on-line data along the mining value chain such as for face mapping, drill core logging and ore sorting applications. Material flow at potential sensor installation sites along the mining value chain can be categorised into static and dynamic sites. Static sites are sites with a relatively slow movement of materials such as the mine face, drill core logging and muck piles, whereas dynamic sites are those sites with a rapid flow of materials (e.g., conveyor belt). For example, the required real-time response of material characterisation at the mine face might be in the order of a few hours to a few days while conveyor applications could be in the order of milliseconds, and sometimes microseconds depending on the conveyor belt speed. Therefore, real-time material characterisation at the potential sensor mounting sites along the mining value chain has different time requirements.

In this research, the prediction and classification calibration models developed using the individual and fused data blocks resulted in the successful prediction and classification of the unknown spectra. Likewise, for visually distinct minerals, mineral mapping using RGB imaging can provide automated, reproducible and objective results. Therefore, well-calibrated prediction and classification models can allow the automation of the material characterisation process. Besides, better results are possible with test case-specific calibration models since they likely capture the material variability in each deposit type. Moreover, the identification of minerals can be automated using mineral search algorithms and test case-specific mineral libraries (Lorenz et al., 2018). Some of the technologies are

already in use for on-line analysis of materials. For example, RGB imaging is currently being used in sorting of visually distinct materials (TOMRA, 2017) and NIR systems are used for sorting of materials over the conveyor belt (Mahlangu et al., 2016; Robben and Wotruba, 2019). There is an excellent opportunity for the use of sensor technologies for automated characterisation of material in mining operations.

13.6.3. IN-SITU CHARACTERISATION OF MATERIALS

The operational environment is one of the key criteria for the use of sensors in in-situ measurements. For example, some environments require ruggedized systems due to the harsh environmental conditions; others such as conveyor belt applications require sensors capable of rapid data acquisition. In-situ use of sensor technologies requires portable, ruggedized and high-speed systems. Rapid in-situ determination of material properties saves the time previously needed for the shipment of samples to conventional laboratories and the turn-around time necessary for the analysis. Thus, it has a tangible contribution to effective process control in mining operations. In some circumstances, the operational environment, coupled with the nature of deposit, can determine sensors applicability. For example, sulphide minerals and metals heat faster than other minerals. The underground mine environmental condition can cause the self-heating of sulphide ores because of the ambient exothermic oxidation reactions such as pyrite oxidation. Therefore, thermal cameras can likely provide useful information for mapping the sulphide minerals in underground mines.

Environmental factors (e.g., dust and moisture) and surface weathering likely influence in-situ sensor measurements, requiring optimal compensation techniques. This is discussed in the next chapter. Moreover, surface weathering is a common issue in underground mines. An example of surface weathering which occurred at the mine face is shown in Figure 13.10. Most of the available sensors are surface technologies that provide information on the topmost part of the sample surface. The depth of penetration varies from technology to technology. For example, an FTIR spectrometer with a diffuse interface can penetrate from 200 to 700 μm into the sample (Agilent, 2017). However, these penetration depths are not deep enough to provide information under the weathered surface. Consequently, mine face measurements should be done at freshly exposed surfaces (e.g., immediately after a new blast) to minimise the effect of weathering. Understanding of the alteration assemblages resulted from minerals weathering is crucial in the interpretation and analysis of the spectral data. However, for estimation of the mineable products, relying only on surface measurements can underestimate or overestimate the reserve. Therefore, surface measurements should be combined with subsurface information to provide minerals distribution in 3D.



Figure 13.10: A picture that shows surface oxidation at the mine face in an underground mine.

The recent advances in sensor technologies resulted in innovative development of rapid, sensitive, and lightweight sensor systems, for example, the FTIR analyser by Agilent and the ruggedised Raman systems by StellarNet (Agilent, 2017; StellarNet, 2019). This shows the high potential of the techniques for in-situ characterisation of materials. However, for underground applications, most sensor systems still require a protective shield or robustness. Lightweight sensors can potentially be embedded into a single platform to acquire data simultaneously in in-situ measurements. Then the data from multiple sensors can be integrated using data fusion approaches. Therefore, the recent advances and future developments in the field of sensor technology coupled with advances in data analytics (e.g., data fusion) can potentially lead towards the practical implementation of partially or fully automated in-situ material analysis in mining operations.

Overall, the use of sensors and data fusion can allow in-situ automated material characterisation in mining. However, the technical and economic feasibility needs to be investigated. The technical feasibility involves assessment of the hardware, software and other technical requirements. The hardware design requirements include portability, robustness, and rapid data acquisition speed, while the software requirements include the availability of comprehensive mineral libraries and high computational power. The economic feasibility of the use of sensors in mining operations depends on different factors such as the cost of the sensor technologies, the quality of the data, the price of the mined product on the market, the efficiency of the sensor technology, the nature of the deposit, the ore to waste ratio and the operational costs. Thus, future practical implementation of in-situ automated material characterisation requires economic feasibility assessment, system robustness, comprehensive test case-specific well-calibrated models, and a principled integrated tool for efficient data collection, processing and knowledge generation.

13.7. OPPORTUNITIES AND LIMITATIONS

The technologies explored in this study provided useful information on the key geological attributes at different levels. Moreover, the use of data fusion resulted in increased availability and enhanced accuracy in material characterisation. This suggests the practicality and efficiency of the use of sensors and data fusion for material characterisation in mining. Going forward, better results are possible with extended datasets that address material variability, optimal variable screening techniques, novel signal processing methods and an optimised fusion of multiple sensors at different levels. This is beneficial in maximising

resource efficiency and can contribute to ensuring sustainability in mining. However, a cost-benefit analysis is required to assess the economic feasibility in operational mines. In this section, the prospect and societal significance of the use of sensor technologies and data fusion in mining are discussed. In addition, the possible shortcomings of the research are identified and presented to propose a direction for future studies. Additional recommendations for future research directions are outlined in the next chapter.

13.7.1. INTERNET OF THINGS (IOT)

The use of sensors in mining plays an essential role in the digital transformation of mining. Sensor data and advanced data analytics are the main components of the realisation of the Internet of things (IoT) in the mining industry. IoT is a system that connects computing devices, machines, and internet to collect, transfer and analyse data for addressing specific needs (Atzori et al., 2010, Chehri et al., 2019, Xiaosan, et al., 2018). The implementation of IoT in several industries has resulted in improved productivity and safety. Recent studies indicated the potential benefits of IoT in mining operations for the optimisation of the performance of mining equipment and mineral processing plants (Chehri et al., 2019, Mining Technology, 2020). IoT in mining, become the current and future active area of research that is highly dependent on sensors and advanced data analytics to inform about the geological and metallurgical properties of raw materials.

13.7.2. SOCIETAL RELEVANCE

The transformation into clean energy and electrification drives base metal demand into the future. Currently, there is a growing demand for metals to use in renewable energy and battery technologies (VISIUAL Capitalist, 2018). This could lead to the extraction of low-grade ore, mining in geologically complex regions or deeper mines. In the near future, economically marginal deposits will become industrially viable. These more challenging environments require advanced integrated software (data analytics) and sensor technologies. This work investigates the applicability of sensor technologies and data fusion concepts for the characterisation of materials in a low-grade or sub-economic deposit.

The approach developed here potentially realises resource efficiency through the promotion of dry separation of ore from waste, the ability to extract currently sub-economic “waste”, the automation of the material characterisation process and the provision of information that is more accurate, available and precise. For example, with enhanced dry separation of ore from waste, only value-containing material will be extracted and processed. This minimises water and energy requirements in mineral processing, and reduce waste volume. Moreover, selective mining (i.e., extraction focused on the target domains) can also reduce waste volume. This target domains or areas of interest can be defined using imaging technologies. The other potential benefit of the developed approach in this research is that it leads to automated systems that minimise human exposure risk to dust and hazardous materials during material extraction.

Much of the sustainability and energy efficiency of mineral extraction and processing is driven by the knowledge of the composition of materials such as mineralogy and geochemistry (Sterling and Johnson, 2010). Therefore, enhanced or improved characterisation of materials benefits the realisation of resource efficiency and supports sustained economic growth. This work is a baseline for the future development of focused solutions that deliver tangible contributions to resource efficiency through sensor technologies and data analytics. However, the achieved enhanced material characterisation

can potentially lead to resource efficiency and contribute to sustainability to ensure societal relevance.

13.7.3. LIMITATIONS

The results achieved in this research are very promising and imply potential practical applications in the mining sector. The explored technologies, coupled with the developed methodological approaches, were applied to the characterisation of materials in a polymetallic sulphide deposit. However, this approach might not offer universal applicability for all deposit types. The variability of the spectral responses of minerals does not only vary from deposit to deposit. Indeed, the same deposit can show geological variations (e.g., mineral mixtures) attributed to the geological formation and settings. The use of the methodological approaches of this work to other deposits might require an optimised procedure for recalibration of models, features extraction and sensor customisation based on the material type. Sensor measurements are vulnerable to different environmental factors, including temperature, humidity, vibrations and dust. These environmental factors are more pronounced in in-situ applications than in laboratory measurements. As discussed in previous chapters, most of the sensor measurements were performed in the laboratory: the use of sensor technologies for in-situ applications will require optimal compensation techniques for enhanced sensor responses. Nevertheless, the key findings and essential values of this work rely on the developed methodological approaches for enhanced characterisation of materials at different levels (e.g., semi-quantification and classification). In mining, the approaches can be adapted to various applications in different deposit types. The versatility of the data fusion approach developed in this work can allow the integration of multi-scale and multi-source data into a single model. Moreover, the ore–waste discrimination assessments were made based on different cut-off grades, indicating that the approach can accommodate the change on the cut-off value to some degree. This flexibility also permits the evaluation of the approaches in low-grade and high-grade deposits. Nevertheless, the practical implementation of the results of this work in actual operational mines requires a techno-economic assessment to compare the associated costs and benefits.

REFERENCES

- Agilent. (2017). FTIR Compact & Portable Systems [Online]. Available: <http://www.agilent.com/en/products/ftir/ftir-compact-portable-systems/4300-handheld-ftir> [Accessed February 2017].
- Agilent. (2020). Raman spectroscopy [Online]. Available: <https://www.agilent.com/en/products/raman-spectroscopy> [Accessed on April 1 2020].
- Aines, R. D. & Rossman, G. R. (1984), Water in minerals? A peak in the infrared. *Journal of Geophysical Research*, 89(B6), pp. 4059-4071, doi: 10.1029/JB089iB06p04059
- Atzori, L., Iera, A. & Morabito, G. (2010). The Internet of Things: A survey. *Computer Networks*, 54(15), pp. 2787-2805. doi: 10.1016/j.comnet.2010.05.010
- AusSpec. (2008). G-MEX Spectral interpretation field manual (3 ed.). AusSpec International Ltd.

- Bi, Y., Zhang, Y., Yan, J., Wu, Z., & Li, Y. (2015). Classification and Discrimination of Minerals Using Laser Induced Breakdown Spectroscopy and Raman Spectroscopy. *Plasma Science and Technology*, 17(11), pp. 923-927. doi: 10.1088/1009-0630/17/11/06
- Bolin, B. J. & Moon, T. S. (2003). Sulfide detection in drill core from the Stillwater complex using visible/near-infrared imaging spectroscopy. *Geophysics*, 68(5), pp. 1561-1568. doi: 10.1190/1.1620630
- Borràs, E., Ferré, J., Boqué, R., Mestres, M., Aceña, L. & Busto, O. (2015). Data fusion methodologies for food and beverage authentication and quality assessment - a review. *Analytica chimica acta*, 891, pp. 1-14. doi: 10.1016/j.aca.2015.04.042
- Boucher, T. F., Ozanne, M. V., Carmosino, M. L., Dyar, M. D., Mahadevan, S., Breves, E. A., Lepore, K. H. & Clegg, S. M. (2015). A study of machine learning regression methods for major elemental analysis of rocks using laser-induced breakdown spectroscopy. *Spectrochimica Acta Part B: Atomic Spectroscopy*, 107, pp. 1-10. doi: 10.1016/j.sab.2015.02.003
- Bou-Orm, N., AlRomaihi, A. A., Elrmeithi, M., Ali, F. M., Nazzal, Y., Howari, F. M. & Al Aydaros, F. (2020). Advantages of first-derivative reflectance spectroscopy in the VNIR-SWIR for the quantification of olivine and hematite. *Planetary and Space Science*, 188, 104957. doi: 10.1016/j.pss.2020.104957
- Bumrah, G. S. & Sharma, R. M. (2016). Raman spectroscopy – Basic principle, instrumentation and selected applications for the characterisation of drugs of abuse. *Egyptian Journal of Forensic Sciences*, 6(3), pp. 209-215. doi: 10.1016/j.ejfs.2015.06.001
- Buxton, M. & Benndorf, J. (2013). The use of sensor derived data in optimization along the mine-value-chain: An overview and assessment of techno-economic significance. *Proceedings of the 15th International ISM Congress, Aachen, Germany*, pp. 324-336.
- BWTEK. (2020). Portable Raman Spectrometers [Online]. Available: <https://bwtek.com> [Accessed April 2020].
- Castanedo, F. (2013). A Review of Data Fusion Techniques. *The Scientific World Journal*, 2013(6), 704504. doi: 10.1155/2013/704504
- Chehri, A., Ouahmani, T. E. & Hakem, N. (2019). Mining and IoT-based Vehicle Ad-hoc Network: Industry opportunities and innovation. *Internet of Things*, 100117. doi: 10.1016/j.iot.2019.100117
- Clark, R. N. (1983). Spectral properties of mixtures of montmorillonite and dark carbon grains: Implications for remote sensing minerals containing chemically and physically adsorbed water, *Journal of Geophysical Research*, 88(B12), pp. 10635-10644, doi: 10.1029/JB088iB12p10635.
- Clark, R. N. (1999). Chapter 1 - Spectroscopy of Rocks and Minerals, and Principles of Spectroscopy. In: A. N. Rencz (Ed.), *Remote Sensing for the Earth Sciences: Manual of Remote Sensing*, John Wiley & Sons, Hoboken, New York, pp. 3-58.
- Clark, R. N., Swayze, G. A., Gallagher, A. J., King, T. V. V. & Calvin, W. M. (1993). The U. S. Geological Survey, Digital Spectral Library: Version 1: (0.2 to 3.0 μm). Open File Report 93-592. Available online: <http://pubs.er.usgs.gov/publication/ofr93592>
- Clark, R. N., Swayze, G. A., Wise, R. K., Livo, E., Hoefen, T. M., Kokaly, R. F. & Sutley, S. J. (2003). USGS Digital Spectral Library splib05a, Open-File Report 2003-395. Available online: <http://pubs.er.usgs.gov/publication/ofr03395>

- Cocchi, M. (2019). Chapter 1 - Introduction: Ways and Means to Deal with Data from Multiple Sources. In: M. Cocchi (Ed.), *Data Handling in Science and Technology*. Elsevier, pp. 1-26.
- Corescan. (2019). Automated mineralogy and texture [Online]. Available: <http://www.corescan.com.au> [Accessed December 2019].
- Doeswijk, T. G., Smilde, A. K., Hageman, J. A., Westerhuis, J. A. & van Eeuwijk, F. A. (2011). On the increase of predictive performance with high-level data fusion. *Analytica Chimica Acta*, 705(1-2), pp. 41-47. doi: 10.1016/j.aca.2011.03.025
- Edwards, H. G. M. (2005). Modern Raman spectroscopy—a practical approach. *Journal of Raman spectroscopy*, 36, pp. 835-835. doi: 10.1002/jrs.1320
- FLIR. (2019). Handheld Thermal Cameras [Online]. Available: <https://www.flir.eu/browse/industrial/handheld-thermal-cameras/> [Accessed November 2019].
- FLUKE. (2020). Infrared technology. Emissivity – Metals [Online]. Available: <https://www.flukeprocessinstruments.com> [Accessed April 2020].
- Gaft, M., Reisfeld, R. & Panczer, G. (2005). *Modern Luminescence Spectroscopy of Minerals and Materials*, 2nd ed., Springer, Cham, Switzerland.
- Hapke, B. (2012). Chapter 5 - Single-particle scattering: Perfect spheres. In: B. Hapke (Ed.), *Theory of Reflectance and Emittance Spectroscopy*, Cambridge University Press, Cambridge, England, pp. 66-99.
- Hauff, P. (2008). An overview of VIS-NIR-SWIR field spectroscopy as applied to precious metals exploration. Spectral International Inc., Arvada, USA.
- Headwall. (2020). Hyperspectral sensors [Online]. Available: <https://www.headwallphotonics.com> [Accessed March 2020].
- Hunt, G. R. (1977). Spectral signatures of particulate minerals in the visible and near infrared. *Geophysics*, 42, pp. 501-513. doi: 10.1190/1.1440721
- Hunt, G.R., Salisbury, J.W. & Lenhoff, C.J. (1971). Visible and near-infrared spectra of minerals and rocks. III. Oxides and hydroxides. *Modern Geology*, 2, pp. 195-205.
- Kafle, B. P. (2020). Chapter 8 - Raman spectroscopy. In: B.P. Kafle (Ed.), *Chemical Analysis and Material Characterization by Spectrophotometry*, Elsevier, pp. 245-268.
- Kgler, M. & Heilala, B. (2020). Time-gated Raman spectroscopy a review. *Measurement Science and Technology*, 32(1), 012002. doi: 10.1088/1361-6501/abb044
- Khaleghi, B., Khamis, A., Karray, F. O. & Razavi, S. N. (2013). Multisensor data fusion: A review of the state-of-the-art. *Information Fusion*, 14(1), pp. 28-44. doi: 10.1016/j.inffus.2011.08.001
- Khosravi, V., Doulati Ardejani, F. & Yousefi, S. (2017). Spectroscopic-based assessment of the content and geochemical behaviour of arsenic in a highly heterogeneous sulphide-rich mine waste dump. *Environmental Earth Sciences*, 76(13), 459. doi: 10.1007/s12665-017-6793-4
- Kokaly, R. F., Clark, R. N., Swayze, G. A., Livo, K. E., Hoefen, T. M., Pearson, N. C., Wise, R. A., Benzel, W. M., Lowers, H. A., Driscoll, R. L. & Klein, A. J. (2017). USGS Spectral Library Version 7(1035). Available online: <http://pubs.er.usgs.gov/publication/ds1035>
- Kruse, F. (2015). Integrated visible and near infrared, shortwave infrared, and longwave infrared (VNIR-SWIR-LWIR), full-range hyperspectral data analysis for geologic mapping. *Journal of Applied Remote Sensing*, 9(1), 096005, doi: 10.1117/1.JRS.9.096005

- Lahat, D., Adalı, T. & Jutten, C. (2015). Multimodal Data Fusion: An Overview of Methods, Challenges, and Prospects. *Proceedings of the IEEE*, Vol. 103, pp. 1449-1477.
- Lessard, J., de Bakker, J. & McHugh, L. (2014). Development of ore sorting and its impact on mineral processing economics. *Minerals Engineering*, 65, pp. 88-97. doi: 10.1016/j.mineng.2014.05.019
- Lorenz, S., Kirsch, M., Zimmermann, R., Tusa, L., Möckel, R., Chamberland, M. & Gloaguen, R. (2018). Long-Wave Hyperspectral Imaging for Lithological Mapping: A Case Study. *Proceedings of International Geoscience and Remote Sensing Symposium – IGARSS: IEEE*, Valencia, Spain, pp. 1620-1623.
- Lyon, R. J. P. (1965). Analysis of rocks by spectral infrared emission (8 to 25 microns). *Economic Geology*, 60(4), pp. 715-736. doi: 10.2113/gsecongeo.60.4.715
- Mahlangu, T., Moemise, N., Ramakokovhu, M. M., Olubambi, P. A., & Shongwe, M. B. (2016). Separation of kimberlite from waste rocks using sensor-based sorting at Cullinan Diamond Mine. *Journal of the Southern African Institute of Mining and Metallurgy*, 116(4), pp. 343-347. doi: 10.17159/2411-9717/2016/v116n4a7.
- Malvern Panalytical. (2019). About ASD [Online]. Available: <https://www.malvernpanalytical.com/en/about-us/our-brands/asd-inc> [Accessed December 2019].
- Malvern Panalytical. (2020). ASD QualitySpec® Trek Portable Spectrometer [Online]. Available: <https://www.malvernpanalytical.com/en/products/product-range/asd-range> [Accessed April 2020].
- McGrath, M. J. & Scanail, C. N. (2013). Chapter 2 - Sensing and Sensor Fundamentals. In: M.J. McGrath & C.N. Scanail (Eds.), *Sensor Technologies: Healthcare, Wellness, and Environmental Applications*. Apress, Berkeley, CA, pp. 15-50.
- Mernagh, T. P. & Trudu, A. G. (1993). A laser Raman microprobe study of some geologically important sulphide minerals. *Chemical Geology*, 103(1), pp. 113-127. doi: 10.1016/0009-2541(93)90295-T
- Mining Technology. (2020). How the Internet of Things is transforming Australian mining [Online]. Available: <https://www.mining-technology.com> [Accessed May-2020].
- Moros, J. & Javier, L. J. (2015). Unveiling the identity of distant targets through advanced Raman-laser-induced breakdown spectroscopy data fusion strategies. *Talanta*, 134, pp. 627-639. doi: 10.1016/j.talanta.2014.12.001
- Moros, J., Lorenzo, J. A., Lucena, P., Miguel Tobaría, L. & Laserna, J. J. (2010). Simultaneous Raman Spectroscopy–Laser-Induced Breakdown Spectroscopy for Instant Standoff Analysis of Explosives Using a Mobile Integrated Sensor Platform. *Analytical Chemistry*, 82(4), pp.1389-1400. doi: 10.1021/ac902470v
- NASA. (2018). ECOSTRESS spectral library [Online]. Available: <https://speclib.jpl.nasa.gov/library> [Accessed May 2018].
- Photon. (2020). RIMATM The fastest Raman imaging system [Online]. Available: <http://www.photonetc.com> [Accessed April 2020].
- Rajalakshmi, S. & Chamundeeswari, V. V. (2014). Mapping of mineral deposits using image fusion by PCA approach. *Proceedings of International Conference on Computer Communication and Systems - ICCCS14: IEEE*, Chennai, India, pp. 024-029.
- Richards, J. P. (1998) Sulfide minerals. In: C. P. Marshall & R. W. Fairbridge (Eds.), *Encyclopedia of Geochemistry*. Springer, Dordrecht, Netherlands, pp. 605-605.
- Robben, C. & Wotruba, H. (2019). Sensor-Based Ore Sorting Technology in Mining—Past, Present and Future. *Minerals*, 9(9), 523. doi: 10.3390/min9090523

- Rost, E., Hecker, C., Schodlok, M. & van der Meer, F. (2018). Rock sample surface preparation influences thermal infrared spectra. *Minerals*, 8(11), 475. doi: 10.3390/min8110475
- RRUFF. (2020). RRUFF sample data [Online]. Available: <https://rruff.info> [Accessed June 2020]
- Shi, Q., Niu, G., Lin, Q., Xu, T., Li, F. & Duan, Y. (2015). Quantitative analysis of sedimentary rocks using laser-induced breakdown spectroscopy: comparison of support vector regression and partial least squares regression chemometric methods. *Journal of Analytical Atomic Spectrometry*, 30(12), pp. 2384-2393. doi: 10.1039/C5JA00255A
- Sjöqvist, A., Arthursson, M., Lundström, A., Estrada, E. C., Inerfeldt, A. & Lorenz, H. (2015). An innovative optical and chemical drill core scanner. *Scientific Drilling*, 19, pp. 13-16. doi: 10.5194/sd-19-13-2015
- Specim. (2019). Spectral Cameras [Online]. Available: <https://www.specim.fi/spectral-cameras> [Accessed October 2019].
- Spectral solutions. (2020). Raman spectrometry [Online]. Available: <https://www.spectrasolutionsinc.com> [Accessed April 2020].
- SphereOptics. (2020). Multispectral infrared Cameras (MWIR and LWIR) [Online]. Available: <https://sphereoptics.de/en/product/multispec-ir-cams/> [Accessed April 2020].
- StellarNet. (2019). Spectrometers [Online]. Available: <https://www.stellarnet.us> [Accessed October 2019].
- Sterling, D. & Johnson, G. (2010). Identifying opportunities to reduce the consumption of energy across mining and processing plants. *Proceedings of the 21st World Energy Congress (WEC-2010)*, Montreal, Canada, pp. 1633-1644.
- TELOPS. (2020). MWIR [Online]. Available: <https://www.telops.com/products/high-speed-cameras/mwir-cameras> [Accessed April 2020].
- Tuschel, D. (2016). Selecting an Excitation Wavelength for Raman Spectroscopy. *Spectroscopy*, 31(3), pp. 14-23.
- TOMRA. (2017). Mining Sorting Equipment [Online]. Available: <https://www.tomra.com/en/sorting/mining/sorting-equipment> [Accessed March 2019].
- Vaughan, D. J. (2021). Mineralogy: Sulphides. In: D. Aldereton & S.A. Elias, *Encyclopaedia of Geology*, 2nd ed., Elsevier, pp. 395-412.
- Vaughan, D. J. & Corkhill, C. L. (2017). Mineralogy of Sulfides. *Elements*, 13, pp. 81-87. doi: 10.2113/gselements.13.2.81
- VISIUAL Capitalist. (2018). The Base Metal Boom: The Start of a New Bull Market? [Online] Available: <https://www.visualcapitalist.com/base-metal-boom> [Accessed April 2020].
- Westa, M. S. & Resminib, R. G. (2009). Hyperspectral imagery and LiDAR for geological analysis of Cuprite, Nevada. *Proceedings of SPIE on Defense & Security, Algorithms and Technologies for Multispectral, Hyperspectral, and Ultraspectral Imagery XV*, Vol. 7334, Orlando, USA.
- Wills, B. A. & Finch, J. A. (2016). Chapter 14 - Sensor-based Ore Sorting. In: B.A. Wills & J.A. Finch (Eds.), *Wills' Mineral Processing Technology*, 8th ed., Butterworth-Heinemann, Boston, USA, pp. 409-416.

- WITec. (2020). Raman Imager [Online]. Available: <https://www.witec.de/products/raman-microscopes/alpha300-r-confocal-raman-imaging> [Accessed April 2020].
- Wongthongtham, P., Kaur, J., Potdar, V. & Das, A. (2017). Big Data Challenges for the Internet of Things (IoT) Paradigm. In: Z. Mahmood (Ed.), *Connected Environments for the Internet of Things: Challenges and Solutions*. Springer, Cham, Switzerland, pp. 41-62.
- Xiaosan, G., Shuai, S., Haiyang, Y., Gang C. & Xiaoping L. (2018). Smart Mine Construction based on Knowledge Engineering and Internet of Things. *International Journal of Performability Engineering*, 14(5), pp. 1060-1068. doi: 10.23940/ijpe.18.05.p25.10601068
- Yaney, P. P. (1976). The pulsed laser and gated detection in Raman spectroscopy – a survey of the spectra of common substances including studies of adsorbed benzene. *Journal of Raman Spectroscopy*, 5(3), pp. 219-241. doi: 10.1002/jrs.1250050304
- Zaini, N., Van der Meer, F. & Van der Werff, H. (2012). Effect of Grain Size and Mineral Mixing on Carbonate Absorption Features in the SWIR and TIR Wavelength Regions. *Remote Sensing*, 4(4), pp. 987-1003. doi: 10.3390/rs4040987

14

CONCLUSIONS AND RECOMMENDATIONS

The last chapter of the dissertation presents a brief overview of the general conclusions. It also provides few recommendations for future work to further improve and automate the classification and prediction of material attributes.

14.1. CONCLUSIONS

14.1.1. THE USE OF SENSOR TECHNOLOGIES

Sensor technologies can provide information on the geological attributes along the mining value chain. These geological attributes include mineralogy, geochemistry, ore geometry, ore–waste ratio and texture. In mining, accurate data on the geological attributes are crucial for updating resource models, definition of requirements in mineral processing, effective grade control, improved ore quality control and effective decision-making. Therefore, the use of sensors benefits mining operations in achieving resource efficiency.

The increasing advances in sensor technology have resulted in greater availability of sensor data for a wide range of applications. One such application is the characterisation of raw materials in mining operations. In this study, sensor technologies were utilised to extract knowledge about the key geological attributes of polymetallic sulphide deposit. Technologies namely RGB imaging, VNIR, SWIR, MWIR, LWIR and Raman spectroscopy were investigated. Using the sensor outputs, a direct fingerprinting of minerals and indirect data-driven approaches were implemented to generate information on the key geological attributes. The indirect data-driven approaches were implemented by defining the relation between the spectral data and material properties. This approach greatly benefited the realization of indirect characterisation of materials without a direct fingerprinting or interpretation of the spectra.

This contribution demonstrated that sensor techniques could be utilised for discrimination of ore and waste, identification of mineral, mapping of minerals, and semi-quantitative analysis of minerals and elements. Each technology resulted in the successful characterisation of materials, although at different levels. For example, the RGB imaging technique was successfully used for mineral mapping and ore geometry delineation. The VNIR and SWIR techniques are good for the identification of minerals and ore–waste discrimination. Likewise, the MWIR and LWIR technologies are efficient for the discrimination of ore and waste material, quantification of minerals (SiO_2 , Fe_2O_3 and Al_2O_3) and semi-quantification of the combined Pb–Zn and Fe. Moreover, the Raman technique was used for the identification of some of the minerals in the analysed samples. Therefore, the use of the sensor technologies enabled effective characterisation of the polymetallic sulphide deposit. This indicates the potential benefits of the use of sensors in mining operations.

Overall, the techniques provided crucial information required to understand material composition (e.g., ore mineralogy) and can be considered as complementary techniques. The results are promising and the technologies are efficient for automated characterisation of materials in mining operations. However, owing to the current and future mining challenges, exemplified by economically marginal deposits, deeper mines and complex geology, there is still a need to define and develop improved technologies and tools that can automate the accurate characterisation of materials in mining operations. The observed rapid advancement and dynamic development of the technologies assure the emergence of high-end state-of-the-art sensor technologies that are capable of rapidly providing accurate data. However, practical use of sensors along the mining value chain still requires sensors that gather high throughput data, sensors that provide greater data quality, robust technologies that withstand the harsh environmental conditions and rapid techniques that provide data in real-time.

14.1.2. DATA FUSION IN MATERIAL CHARACTERISATION

The use of sensor combinations should aim to maximise the accuracy of models by minimising the uncertainty related to the models' performance. Accordingly, the use of data fusion allowed for improved predictability and classification of materials. In this study, data fusion was implemented at three levels: low-level, low-level with feature selection and mid-level. The fused datasets were used to develop classification and prediction models. The models were used for ore–waste discrimination and semi-quantitative analysis of minerals and elements. The results showed that the fusion of the MWIR and LWIR data resulted in better classification and prediction models than the individual sensor techniques. Likewise, fusion of the VNIR and SWIR spectral data resulted in better classification of ore and waste material than the individual sensor techniques. The fused data results illustrate that integrated analysis provides enhanced prediction accuracy than the use of individual data sources. Even though acceptable results were acquired from the use of the individual sensor technologies, the results from the fused data models were superior.

Overall, data fusion resulted in improved accuracy, improved availability, increased sensitivity and reduced uncertainty. Thus, it is an effective strategy for a comprehensive description and an enhanced material characterisation. Going forward, better results are possible with extended datasets, multiple sensors data fusion and optimal variable screening techniques. Furthermore, a tool that correlates the combined sensor signals to material properties can be developed using advanced artificial intelligence. This is beneficial for the automation of the material characterisation process in mining operations. The approach can be used throughout the mining value chain (e.g., in mineral exploration, extraction and processing) and would significantly enhance productivity and efficiency in mining.

14.1.3. GENERAL CONCLUSIONS

The use of sensor technologies coupled with data analytics has enabled the determination of material properties that are relevant to the primary components of economic interest (e.g., Pb and Zn) and the gangue minerals (e.g., SiO_2) in the polymetallic sulphide deposit. The key findings of this study demonstrate:

- the use of infrared technologies for the characterisation of polymetallic sulphide ore,
- the use of RGB imaging for mapping of mine face in-situ in an underground mine,
- the use of MWIR (the least explored region of the electromagnetic spectrum) for ore–waste discrimination, and as an indication of elemental and mineralogical concentrations,
- the integration of image and point data for ore–waste discrimination and
- the use of data fusion for improved material characterisations in mining applications.

The results from the use of the individual techniques indicate the feasibility of utilizing sensors in mining. Data fusion improved the classification and prediction performance of the models. The merits of data fusion include improved accuracy, improved availability, reduced uncertainty, and automation. Thus, data fusion techniques can lead to effective grade control and process control (e.g., minimising the handling of zero-value waste material) and effective optimisation of mineral processing in mining operations.

This study contributed to the development of an effective and efficient tool for automated characterisation of materials applicable to mining operations. The success of this study suggests the significant potential of sensors and data fusion for enhanced material characterisation in polymetallic sulphide deposits. The fact that the investigated techniques are well-established (or matured) techniques ensures the potential of the developed methodology for rapid practical implementation. Moreover, the developed methodology can be implemented for use in other deposit types and in different disciplines, such as in environmental studies (modelling of contaminants in air or water), mine waste characterisation (modelling of hazardous minerals/elements in the waste) and secondary recovery studies.

The growing global demand for metals and the declining ore grades urges advances in sensor development and data analytics to allow fast and effective characterisation of ore-bearing rocks. This study can be considered as a baseline for the future development of sensor technologies and tools that could enable automated characterisation of materials in the in-situ analysis. Such an innovative approach is not currently commercially available or operationally implemented, but is a key enabler for a holistic overview and enhanced mineral extraction and processing. The success of this experiment suggests possible data fusion applications in future mining operations, such as automation of mine face mapping and core logging. Going forward, automated material characterisation is possible with a robust system design (exemplified by the portable and ruggedized system) and efficient software (test case-specific mineral libraries) that can be developed using combined sensor signals. Moreover, with integrated software and hardware systems, sensor technologies can be impeded on machinery or robots to provide online information in unsafe underground mines. This is beneficial for ensuring safety by minimising the exposure to hazardous materials and unstable ground conditions while maintaining the mining process. Overall, the approach can contribute to sustainability in mining via reduction of waste volume, less energy consumption (as a result of dry ore-waste separation) and automation. Thus, it can potentially offer short- and long-term economic, social and environmental benefits.

14.2. RECOMMENDATIONS FOR FUTURE WORK

This dissertation presents promising results of the use of sensors and data fusion for enhanced material characterisation in mining operations. It shows great potential for the utilisation of sensor outputs coupled with data analytics for improved accuracy, improved availability and effective decision-making. However, further researches are required to advance the developed methodological approaches to a higher level of maturity (or readiness). Some interesting new research directions that potentially lead to maximised benefits and practical implementation of automated on-site analysis of materials in operational mines are outlined below. The proposed potential research directions were formulated based on the actual existing limitations and open questions that are related to sensor-based material characterisation in mining operations. Practical implementation of the proposed approach benefits from research and development in six key areas: (a) further experiments to assess the use of the methods in different geological settings, (b) additional experiments to optimise the data fusion approach, (c) tools for automation, (d) sensor design and development, (e) mechanisms to minimise the effect of environmental factors on sensor measurements, and (f) extending the approach into material characterisation in three-dimensional (3D) subsurface environments.

14.2.1. FURTHER EXPERIMENTS IN DIFFERENT GEOLOGICAL SETTINGS

The use of sensor technologies and the developed methodological approaches presented in this work resulted in promising outcomes for the characterisation of materials in polymetallic sulphide deposit. However, deposit types define the properties of a material that are relevant for sensor measurements that future work is required to assess the usability in multiple geological settings. Applicability assessment in different deposit types could consider

- a complete understanding of how the properties of various deposit types affect the usability of the techniques and developed methodologies,
- the use of each technique for the characterisation of materials at different levels (e.g., detection, classification and quantification), and
- usability for the classification of materials at different cut-off grades, thus to assess the applicability in low- and high-grade deposits.

Besides, the implementation of the developed methodologies in the polymetallic sulphide deposits could also benefit from future works that address the below-mentioned points:

- assess the techno-economic viability of the developed approaches for the separation of ore-waste and quantitative analysis of minerals and elements in operational mines. An efficient implementation might be limited by the environmental factors influence on sensor measurements, classification/prediction algorithms accuracy and sensor efficiency in performing in different material mixtures,
- use of the developed methodologies with extended datasets in the calibration models is recommended to better accommodate the variabilities of materials in the deposit, and improve the performances of the models,
- assessment of the methods for the simultaneous analysis of the geological parameters (e.g., quantitative analysis of minerals and elements) using the same prediction models and datasets is beneficial to generate information contemporarily,
- valuation of the developed approach in an operational environment, and
- evaluation of the applicability of the developed methods in other polymetallic sulphide deposit with different mineral mixtures and complexity is valuable to ensure the inclusiveness of the approaches in addressing properties of a material in wide-ranging compositional variations.

14.2.2. ADDITIONAL EXPERIMENTS TO OPTIMISE THE DATA FUSION APPROACH

The data fusion approaches presented in this dissertation resulted in promising results for enhanced characterisation of materials. The study focused on the application of low-level and mid-level data fusion approaches. Because most sensor outputs are complex and different by nature, a practical implementation of the methods requires an optimised approach. Optimisation of the approach could consider

- the different levels of data fusion (e.g., high-level),
- different fusion algorithms that can define the linear or non-linear relationships,
- different pre-processing techniques (e.g., block scaling and auto-scaling) depending on the nature of the data,

- integration of various sensor outputs into a fused data block likely results in high data volume, which can be computationally expensive; therefore alternative information screening techniques could be considered to maintain the relevant spectral information,
- further study of multiple sensor technologies to identify the optimal sensor combination options.

The optimised results can lead to the development of a tool that identifies material properties based on the fused sensor signals. Therefore, the proposed approach could be extended to characterise materials in real-time using multiple sensor outputs.

The low- and mid-level data fusion approaches proposed in this study showed promising results for semi-quantitative analysis of elemental and mineralogical information. The individual techniques (MWIR and LWIR) exhibit high potential for use in semi-quantification of the minerals and elements; however, the results acquired from the data fusion processes are superior to the results obtained using data models of individual techniques. This outcome suggests that the data fusion approach has a great potential to be extended for the integration of more complex data from a range of sensor technologies, owing to the fact that each sensor technology has its advantages in providing useful information. This study is a baseline for future research that involves multi-sensor integration aimed at developing predictive models that can estimate elemental and mineralogical concentrations in different types of deposits. We recommend enhancing the current work by using data from multiple sensors such as Raman and LIBS in an optimised way.

For sensor combinations, data fusion is a more economical and practical alternative option than the physical integration of multiple sensors into a single platform. However, in terms of the practical implementation of data fusion, a techno-economic assessment is required to evaluate the feasibility of the approach in mining operations. Therefore, a future study is recommended to assess the techno-economic benefits of the fusion of multiple sensor outputs. Such an assessment should take into account various factors such as portability of sensor technologies, the robustness of technologies for in-situ applications, the efficiency of the resulting classification or prediction models, the throughput of material and data, the market trend and price of commodities, cost related to the initial investment for instrument purchase, installation and maintenance and the limitations related to environmental influences of sensor measurements.

14.2.3. TOOLS FOR AUTOMATION

Automation of the material characterisation process requires integrated hardware and software systems with high-performance computing power. The hardware requirements are discussed in section 14.2.1. Software capability is the other key factor for automated determination of material properties using sensor-derived data. Currently, the software related issues include lack of well-established comprehensive mineral spectral database systems (SDBS), lack of well-calibrated models for automated characterisation of materials, and limitations related to the computing power of software and operating systems. Therefore, to achieve automation in material characterisation and maximise the benefits of the use of sensors for effective, prompt decision-making in mining operations, it is highly recommended that tools be developed that have high-performance (high-throughput)

computing power, efficient spectral matching algorithms, comprehensive SDBS, and efficient platform designs.

A combination of the emergent technologies could accelerate the accurate and automated analysis of materials in different applications, such as ore–waste discrimination or quantitative analyses of minerals. Automated characterisation of materials using the combined sensor signals requires a software tool that links the material properties to the fused sensor signals. Such a software tool requires comprehensive SDBS, a platform that integrates data of a different nature, efficient spectral matching algorithms, and data processing and visualisation methods. The associated hardware must also have high-performance (high-throughput) computing power.

14.2.4. SENSOR DESIGN AND DEVELOPMENT

The primary limitations of most sensor technologies for use in mining include lack of system robustness, portability, rapid data acquisition speed, higher detection limits, affordability and optional sensor parameters to retune sensor specifications. These factors are crucial for the use of sensor systems in operational mines (e.g., open pit or underground mines). Future sensor developments or sensor design plans could consider these factors to develop the ultimate solutions that address each of the outlined concerns. For example, system robustness can be ensured via a ruggedized system design that has a protective shield or other technological alternatives. Currently, some lightweight sensor technologies are emerging. However, most of the well-matured technologies are still laboratory-based, and integrated portable and robust systems are very limited. Therefore, the size of the sensor systems should also be taken into account in the sensor development plan. To ensure the use of sensors along the mining value chain, the data acquisition speed of the sensor system is a key aspect. The different potential sensor installation sites along the mining value chain require different data acquisition speeds. For example, the use of sensors for sorting of material on a conveyor belt requires sensors that provide data within microseconds. This shows the need for sensor systems with rapid data acquisition speed. The other limitation of the use of sensors for the characterisation of material is the detection limit of the sensor systems. The detection limit is a very crucial issue, especially when dealing with low-grade ore that is more likely to be encountered in most of the future mining operations. The high cost of the sensor systems is also one of the reasons for the limited use of sensors in mining. Therefore, cost-effective solutions (inexpensive sensors) could be proposed. The other important factor is provision for optional sensor parameters to retune sensor specifications; i.e., to configure sensor set-up and optimise measurements according to the commodity type. Therefore, addressing these factors during sensor development (sensor design) could encourage exploitation of sensor technologies in operational mines, thus achieving improved process control and effective decision-making.

14.2.5. COPING WITH THE ENVIRONMENTAL FACTORS ON SENSOR MEASUREMENTS

The development of new and improved coping strategies is crucial to grand challenges that affect the quality of sensor outputs (data). Sensor measurements are vulnerable to different environmental factors, including temperature, humidity, vibration and illumination. These environmental factors influence the sensors' operability, measurement results (spectral data) and sample behaviour (e.g., weathering and saturation). The effect is much more pronounced in in-situ applications than in laboratory conditions. Therefore, to

ensure online in-situ analyses of materials in different environmental conditions, coping strategies are recommended to compensate or minimise the effect of the environmental factors on the analysis results. The possible coping strategies include developing pre-processing algorithms that correct the noise caused by the environmental influences, simulation of measurements with different moisture content, models calibration considering certain levels of the influences, and development of new innovative illumination correction algorithms. The effect of the environmental factors on the sensor system can be minimised or controlled with a ruggedized system design that tolerates a certain level of vibration, moisture and dust. These approaches potentially lead to improved data quality and generate usable data along the process, thus maximises the benefits of the use of sensor systems in mining operations.

14.2.6. EXTENDING THE APPROACH INTO SUBSURFACE (3D) INFORMATION

The investigated sensor technologies are surface techniques that provide information at the upper measured surface of the analysed samples. However, volumetric information is crucial for the understanding of mineral composition within a sample, quantification of the reserves and prediction of geological conditions in advance of the mining face. The implantation of sensors that provide 3D (volumetric) information can potentially be beneficial for the understanding of the extent of the mineralized zones and useful geological structures that influence the mineralization and that incur stability (safety) (e.g., identification of faults, openings, and aquifers). Thus, the geophysical techniques having greater depth penetration can be a potential candidate to support the resource estimation and prediction conditions in advance of extraction at the mining surface. The potential geophysical sensing methods that could be explored include electrical resistivity, magnetic sensors, gravity, induced polarization (IP), and ground-penetrating radar. For example, electrical resistivity measures how strongly a material resists the flow of electric current. Most minerals (including some of the sulphides) vary in their electrical resistivity property and exhibit different resistivity values. Thus, electrical methods could allow material characterisation in mining and can be used in combination with the surface techniques (e.g., infrared) to provide better insight on the material under study. However, the value of resistivity of a material is influenced by different factors such as the presence of a porous structure and joints that the use of the electrical resistivity in material characterisation should investigate and account for the variation caused by such factors. The other example is IP that measures the chargeability of materials (i.e., how well materials hold charges). The chargeability of materials depends on different factors, such as mineral types and grain size. The minerals that are the most chargeable include sulphide minerals and clay-rich materials. Therefore, IP can be used for the detection and delineation of mineralized zones, and this can be applied along the mining value chain, for example, during exploration and extraction (e.g., mine face mapping). However, discrimination of mineral types based on chargeability alone could not be sufficient since the effect from other factors such as grain size can influence measurements. Thus, a combination of this method with sensor measurement can likely lead to the enhanced characterisation of material in 3D.

Accordingly, it would be advantageous to explore the combination of the geophysical methods with sensor technologies for material characterisation, to maximise the synergy among the surface and volumetric techniques for improved information in 3D, over a wider area. The integration can be performed using geographic coordinates or data fusion based on locations. Thus, transferring the current 1D point measurements and 2D mine face

images into a 3D framework requires a state-of-the-art software platform that integrates sensor systems, data processing and visualisation of spatially constrained data of a different nature. If a good relationship is established between sensor measurements and the geophysical sensor, for example, at mine face or drill hole analysis, the learned relationship (calibration model) can be used to predict information at unmeasured areas. Advances in ground geophysical techniques coupled with this proposed approach can be beneficial for the indication of the mineralised zones within specific depths over a wider area and prediction of geological conditions in advance of the mining face. Thus, it provides support for effective planning in the mining process.

SPATIALLY CONSTRAINED DATA

In this study, spatially constrained compositional data were generated using geographic coordinates from the LIDAR technique. This was performed using the ArcGIS, Datamine Studio RM and RiSCAN PRO software platforms. However, future work is required to develop a self-contained software platform that integrates the LIDAR data, the image classification tool, and prediction models in a 3D environment. Such a platform can integrate 1D (point measurements), 2D (image data) and 3D (geographic coordinates) data to permit accurate results with lower positional uncertainties. Thus, it is beneficial to generate spatially constrained compositional data (such as mineral maps and geochemical information) along the mining process.

PUBLICATIONS

JOURNAL PAPERS

4. **Destá, F.** & Buxton, M. (2020). Image and Point Data Fusion for Enhanced Discrimination of Ore and Waste in Mining. *Minerals*, 10(12), 1110. doi: 10.3390/min10121110
3. **Destá, F.**, Buxton, M. & Jansen, J. (2020). Fusion of Mid-Wave Infrared and Long-Wave Infrared Reflectance Spectra for Quantitative Analysis of Minerals. *Sensors*, 20(5), 1472. doi: 10.3390/s20051472
2. **Destá, F.**, Buxton, M. & Jansen, J. (2020). Data Fusion for the Prediction of Elemental Concentrations in Polymetallic Sulphide Ore Using Mid-Wave Infrared and Long-Wave Infrared Reflectance Data. *Minerals*, 10(3), 235. doi: 10.3390/min10030235
1. **Destá, F.S.** & Buxton, M.W.N. (2018). Chemometric Analysis of Mid-Wave Infrared Spectral Reflectance Data for Sulphide Ore Discrimination. *Mathematical Geosciences*. 51(7), pp. 877-903. doi: 10.1007/s11004-018-9776-4

CONFERENCE PROCEEDINGS AND PRESENTATIONS

6. **Destá, F.** & Buxton, M. (2020). Sensing and data fusion for material characterization in mining. Booklet of the new challenges in the mineral raw materials industry: safety, digitalisation, technology & innovation workshop, organized by the cluster Portugal mineral resources and INESC TEC, online workshop, pp. 19-20. Available online: <http://www.strongmar.eu/site/new-challenges-in-the-mineral-raw-materials-industry-120>
5. **Destá, F.S.** & Buxton, M. W. N. (2019). Evaluation of sensor technologies for on-line raw material characterisation in "Reiche Zeche" underground mine - outcomes of RTM implementation. Proceedings of the Real Time Mining - 2nd International Raw Materials Extraction Innovation Conference, Freiberg, Germany, pp. 32-48.
4. **Destá, F. S.** & Buxton, M. W. N. (2018). Automation in sensing and raw material characterization - a conceptual framework. Proceedings of the 2018 IEEE/RSJ International Conference on Intelligent Robots and Systems (IROS), Madrid, Spain, pp. 1501-1506. **(Peer reviewed)**
3. **Destá, F.** & Buxton, M. (2018). Sensing and data fusion for raw material characterization. 22nd General Meeting of the International Mineralogical Association (IMA 2018), August 2018, Melbourne, Australia.
2. **Destá, F.**, Buxton, M., van der Werff, H. & Dalm, M. (2018). Real-Time Mining: Sensors for materials characterization. Proceedings of the use of robotics and automation for mineral prospecting and extraction conference, Bled, Slovenia, pp. 43-45.

1. **Desta F.S.** & Buxton M.W.N. (2017). The use of RGB Imaging and FTIR Sensors for Mineral mapping in the Reiche Zeche underground test mine, Freiberg. Proceedings of the Real-Time Mining International Raw Materials Extraction Innovation Conference, Amsterdam, the Netherlands, pp. 103-127.

OTHER PUBLICATIONS

3. **Desta, F.** & Buxton, M. (2019). Sensor data in Mining. Geobrief -2019-7 - KNGMG Magazine, pp. 20-23. Available online: <http://www.kngmg.nl/wp-content/uploads/2019/11/geobrief-2019-7.pdf>
2. **Desta, F.** & Buxton, M. (2018). Mapping minerals with sensor technologies. Delft university of technology, Story of science, Available online: <https://www.tudelft.nl/en/ceg/research/stories-of-science/mapping-minerals-with-sensor-technology>
1. Dalm, M., Buxton, M., Guatame-Garcia, L.A., **Desta, F.S.** & van Ruitenbeek, F. (2017). A review of sensors applicable to real-time raw material characterisation in mining. Book publication (In preparation).

MSc. AND BSc. THESES AND PROJECTS RELATED TO THIS RESEARCH

3. van Nie, D. (2019). The influence of environmental conditions on the use of sensor technologies for in-situ material characterization - A review. BSc. thesis, Delft University of Technology.
2. Van Erp, H., Krijn, J. & Knops, S. (2019). Influence of sample moisture content on measurements using a handheld FTIR spectrometer. MSc. project, Delft University of Technology.
1. Hanemaaijer, T. (2017). The applicability of Raman spectrometry for characterization of sulphide ore. MSc. project, Delft University of Technology.

